GENERATION AND OPTIMIZATION OF PICOSECOND OPTICAL PULSES FOR USE IN HYBRID WDM/OTDM NETWORKS

A THESIS FOR THE DEGREE OF DOCTOR OF PHILOSOPHY

Presented to

Dublin City University (DCU)

by

Prince M. Anandarajah
B. Eng., M. Eng., MIEE, SMIEEE

School Of Electronic Engineering
Dublin City University

Research Supervisor
Dr. Liam Barry

June 2003

APPROVAL

Name: Prince Anandarajah

Degree: Doctor of Philosophy

Title of Thesis: Generation and Optimization of Picosecond Optical Pulses for Use in Hybrid WDM/OTDM Networks

Examining Committee:

Ms. Jennifer Bruton (Dublin City University)
Chair

_____

Prof. John Dudley (Université de Franche-Comté)
External Examiner

_____

Dr. Pascal Landais (Dublin City University)
Internal Examiner

_____

Dr. Liam Barry (Dublin City University)
Supervisor

Date Approved: _____

DECLARATION

I hereby certify that this material, which I now submit for assessment on the programme of study leading to the award of Doctor of Philosophy is entirely my own work and has not been taken from the work of others save an to the extent that such work has been cited and acknowledged within the text of my work.

ID No.: 98971190

Signed: P. M. Mwandagali

Date: 08/07/2003

DEDICATION

To my Appa, Amma, Ola and Julia.

Curiosity kindles the flame
Quest for knowledge fans it
Resolve and guidance fuels it
Research gives it the glow
The flame radiates and illuminates
The road to success

ACKNOWLEDGEMENT

When closing an important chapter in life, one looks back and savours the moments of achievement, happiness and sadness. Each such moment brings to mind the incidents and people associated with these events in one way or another. When the time comes to move on, the heart fills with gratitude and a desire to reciprocate their generosity.

First and foremost, my special thanks goes to my supervisor, Dr. Liam Barry for his guidance and constructive advice. Without his professional assistance, the completion of this project would not have been possible. His patience and understanding, until the last lap of this work, are virtues that have been a blessing. I hope that someday I would get an opportunity to repay all the kindness he has shown.

I am also highly indebted to my parents who always encouraged me on any endeavour I took. Not only did they lay the foundation in building up my life but have also helped in putting every brick in place. The support they gave from childhood, both morally and financially, has brought nothing but happiness. The dedication and sacrifices they have made towards the education of their children would keep us ever in their debt.

Thanks are also due to my brother, Dr. Allen Anandarajah for encouraging me to ride on the highway of knowledge.

Mere words cannot express the gratitude I owe to the person who stood by my side, ably assisted me and spurred me on. My wife, colleague and friend in life, whose love, encouragement and understanding paved most of the way to the completion of this work.

I owe a lot to Frank Smyth (FS services) who assisted me whenever the "Gates of Microsoft" obstructed me. I would also like to thank my friends and colleagues Paul Maguire, Brendan Kennedy, Damien O'Rourke and Antonia Dantcha for all their assistance.

I would be failing in my duty if I do not acknowledge all the assistance and help provided by the technicians in the Electronic Engineering department.

Thanks are also due to my good friends Valentin Muresan, Gabriel Muntean, Kalaiarul Dharmalingam and Sekar Parthasarathy with whom I have shared a lot of the lighter moments during the past few years. Unfortunately it is difficult to list everyone who played a role in one way or another in bringing my work to fruition. Nevertheless they will always be in my thoughts.

Finally I would like to thank God for his countless blessings and for bringing all these people into my life.

ABSTRACT

The burgeoning demand for broadband services such as database queries, home shopping, video-on-demand, remote education, telemedicine and videoconferencing will push the existing networks to their limits. This demand was mainly fueled by the brisk proliferation of Personal Computers (PC) together with the exceptional increases in their storage capacity and processing capabilities and the widespread availability of the internet. Hence the necessity, to develop high-speed optical technologies in order to construct large capacity networks, arises. Two of the most popular multiplexing techniques available in the optical domain that are used in the building of such high capacity networks, are Wavelength Division Multiplexing (WDM) and Optical Time Division Multiplexing (OTDM). However merging these two techniques to form very high-speed hybrid WDM/OTDM networks brings about the merits of both multiplexing technologies.

This thesis examines the development of one of the key components (picosecond optical pulses) associated to such high-speed systems. Recent analysis has shown that RZ format is superior to conventional NRZ systems as it is easier to compensate for dispersion and nonlinear effects in the fibre by employing soliton-like propagation. In addition to this development, the use of wavelength tunability for dynamic provisioning is another area that is actively researched on. Self-seeding of a gain switched Fabry Perot laser is shown to one of the simplest and cost effective methods of generating, transform limited optical pulses that are wavelength tunable over very wide ranges. One of the vital characteristics of the above mentioned pulse sources, is their Side Mode Suppression Ratio (SMSR). This thesis examines in detail how the pulse SMSR affects the performance of high-speed WDM/OTDM systems that employ self-seeded gain-switched pulse sources.

LIST OF ACRONYMS

Amplified Spontaneous Emission	ASE
Bit Error Rate	BER
Code Division Multiplexing	CDM
Continuous Wave	CW
Conventional Band	C-Band
Cross Phase Modulation	CPM
Dispersion Compensating Fibre	DCF
Dispersion Shifted Fibre	DSF
Distributed Feedback	DFB
Electrical Time Division Multiplexing	ETDM
Electro-Absorption	EA
Erbium Doped Fibre Amplifier	EDFA
External Cavity Laser	ECL
Fabry-Perot	FP
Fibre To The Home	FTTH
Four Wave Mixing	FWM
Frequency Division Multiplexing	FDM
Gain Switched Laser Diode	GSLD
Group Velocity Dispersion	GVD
Intensity Modulation-Direct Detection	IM-DD
Inter Symbol Interference	ISI
International Telecommunications Union	ITU
Mach Zehnder Modulator	MZM
Mode Partition Noise	MPN
Non Return-to-Zero	NRZ
Non-linear Optical Loop Mirror	NOLM
Open Systems Interconnect	OSI
Optical Carrier	OC

Optical Delay Line	ODL
Optical Fabry-Perot Tunable Filter	OFPTF
Optical Spectrum Analyzer	OSA
Optical Time Division Multiplexing	OTDM
Photonic Design Automation	PDA
Polarization Controller	PC
Polarization Mode Dispersion	PMD
Pseudo Random Binary Sequence	PRBS
Pulse Length Ratio	PLR
Pulse Pattern Generator	PPG
Return-to-Zero	RZ
Self Phase Modulation	SPM
Self Seeded Gain Switched	SSGS
Semiconductor Mode Locked Laser	SMLL
Semiconductor Optical Amplifier	SOA
Side Mode Suppression Ratio	SMSR
Standard Single Mode Fibre	SSMF
Stimulated Brillouin Scattering	SBS
Stimulated Raman Scattering	SRS
Sub-Carrier Multiplexing	SCM
Synchronous Digital Hierarchy	SDH
Synchronous Optical Networks	SONET
Synchronous Transport Module	STM
Terahertz Optical Asymmetric Demultiplexer	TOAD
Time Bandwidth Product	TBWP
Tunable Bragg Grating	TBG
Very Large Scale Integration	VLSI
Virtual Photonics Incorporated	VPI
Wavelength Division Multiplexing	WDM

TABLE OF CONTENTS

LIST OF TABLES

LIST OF FIGURES

INTRODUCTION

Limitations on the overall capacity of optical communications systems will be encountered in the future due to the ever growing demand for broadband services. Thus it will become necessary to develop optical technologies that can handle these extremely high capacities given the huge available bandwidth of the fiber transmission medium. However, in a basic optical communication system comprising a laser transmitter, an optical fiber transmission medium, and a receiver, the capacity is essentially limited by the speed of the available electronics (e.g.: modulation speed of transmitter). To overcome this limitation, it is necessary to use optical multiplexing techniques. This thesis deals with high-speed optical communication systems, using technologies such as Wavelength Division Multiplexing (WDM) and Optical Time Division Multiplexing (OTDM). In order to design optical systems, which can handle data transmission at ultra high bit rates (excess of 100 Gb/s on each wavelength channel) it is vital to use short optical pulses to represent the data signals. In addition to the optical pulses being ultra short (in order to maximize the data rate) they also have to be spectrally pure.

Since the development of transform-limited optical pulse sources with wavelength tunability, short pulsewidths and high repetition rates are extremely important for use in future high speed communication systems, especially in applications such as WDM, OTDM, Hybrid WDM/OTDM and soliton systems, the main body of work in this thesis thus deals with the generation of such optical pulses and their performance in high speed optical communication systems.

Prominence was given to one of the simplest and most reliable techniques available to generate high quality wavelength tunable single mode optical pulses, which involves the self-seeding of a gain-switched (SSGS) Fabry Perot (FP) laser. Our experimental results present the generation of transform limited pulses using the self-seeding technique. Timing jitter and frequency chirp, two of the major problems associated with gain switching, are reduced by using this technique. The maximum repetition rate at which optical pulses can be generated is another limitation of the gain switching technique. It is

essentially due to the limited bandwidth of the laser diode. Using strong external injection, we demonstrate how pulses can be generated at repetition rates up to 20 GHz, which is far beyond what would be possible with the laser's inherent bandwidth of 8 GHz. Another technique, which was experimentally investigated, involved pulse shaping using an external modulator.

In addition the work also examines performance issues associated with the use of the developed pulse sources in high-speed optical systems. One of the important characteristics of SSGS pulse sources is the Side Mode Suppression Ratio (SMSR). A variation in the SMSR of the pulse sources, as the wavelength is tuned, could ultimately affect their usefulness in optical communication systems. We initially demonstrated how this SMSR variation greatly affected the noise induced on a single 2.5 GHz pulse source as the pulse propagated through optical fibre and an optical filter. We then investigated this effect in a multi channel system (WDM) where the variation of SMSR of other sources brings about cross channel interference due to mode partition noise, on the filtered channel. Simulations were carried to support the experimental findings described above, and also to investigate these effects in an eight-channel WDM system employing SSGS pulse sources.

Final simulations involved the building of a hybrid WDM/OTDM system. Four channels each at rates of 10 Gb/s were multiplexed together in the temporal domain (aggregate bit rate of 40 Gb/s on a single wavelength channel). Multiplexing was then carried out in the wavelength domain by putting together four different wavelengths (aggregate bit rate of 160 Gb/s). The major aim behind this was to vary the pulsewidth and channel spacing in order to explore how to optimize the system parameters for a hybrid WDM/OTDM system.

The thesis is divided into six chapters and its layout is as follows:

Chapter 1: An introduction to optical communication systems. A comparison of photonic networks and electrical networks is made. Attention is focused on the merits and demerits of lightwave communication systems.

Chapter 2: Two of the techniques, Optical Time Division Multiplexing (OTDM) and Wavelength Division Multiplexing (WDM), used in satisfying the phenomenal hunger and greed for bandwidth and speed, are introduced. High-speed networks (Hybrid WDM/OTDM), incorporating both technologies giving greater flexibility and strength, are also discussed in this chapter.

Chapter 3: This section deals with the methods of generation of short optical pulses suitable to be used in high-speed optical communication systems. One of such techniques being gain-switching is discussed in detail since this was the most beneficial method that was used in this work. Another aspect that is considered involves ways of overcoming the impairments brought about by these techniques. Investigation into pulse shaping as a method of pulse generation is also carried out in this section

Chapter 4: This chapter focuses on performance issues associated with the usage of self-seeded gain switched pulse sources in WDM lightwave systems. Experimental results ranging from a single to a four-wavelength channel WDM system using SSGS pulses are presented here. Examination of parameters such as side mode suppression ratios, their variation and its effects on such pulse sources is the main theme of discussion here. Simulations were carried out in order to verify the experimental results.

Chapter 5: The simulations carried out here are based on two key system parameters of a hybrid WDM/OTDM system. The problems associated with arbitrary selection of the pulsewidth and the spectral spacing is highlighted. Verification of an optimum value to obtain satisfactory system performance and efficiency is investigated.

Chapter 6: Conclusions.

Chapter 1 - Optical Telecommunication Networks

1.1 Why optical networking?

This section provides an insight into the present state and future prospects for telecommunication networks. The need for transmission capacity is increasing faster than Moore's law[1], mainly due to the growth of internet traffic in recent years. One of the challenges here is to design systems that can offer more capacity without resulting in higher costs. The Time Division Multiplexing (TDM) approach, realized in electronic circuitry of ever increasing speed and complexity, is slowly beginning to prove incompetent. The ineffectiveness comes about because of the fact that the required job cannot be done as cost efficiently as the optical approach [1]. Advances in photonic technologies have made, bit rates of 2.5 Gb/s, 10 Gb/s and 40 Gb/s over many kilometres of single mode fibre, a reality [2]. The reasons and motivations behind the thinking that the optical approach will be the way of the future, arises from the fact that fibre has the ability to satisfy the growing demand for the following criteria.

1.1.1 Growing demand for bandwidth

The demand for bandwidth per user has taken many forms but currently the major contributing factor towards this is the World Wide Web (WWW). This mode of PC usage is likely to have a deep and permanent significance and has undergone a marked acceleration to a factor of eight per year [3]. The Napster craze is just one such example, marking the opening of many more of such floodgates. Such an increase looks even more daunting when the access times of the web user are taken into account. If sessions are to get shorter, from the current standard of milliseconds or seconds, the peak bit rate per user has to increase. Hence in anticipation of such increases copper of any form, even coaxial, clearly offers only temporary relief. Wireless being the other long-term technology option available, has insufficient bandwidth, even as cell sizes become quite small. The total bandwidth of radio that is currently being used on our planet is small (~25GHz) in comparison to what each strand of fibre could offer. Radio and mobile communications will continue to play an important role. Even copper would not

[1] Number of transistors on an IC would double every year.

completely disappear but it has been predicted that only optical communications could provide the capacity needed for a truly broadband future [4]. The competition from coaxial cables for the last mile access[2] will persist until the installation of fibre and cost of optical components becomes cheaper [5].

1.1.2 Performance

Radio and copper use complex modulation formats and source coding (compression) etc. in order to maintain a satisfactory error performance. However fibre has the intrinsic capability to drive the error rate to arbitrarily low levels using link budget improvements alone. The reason for this is due to the large bandwidth available thereby leading to simple schemes such as On-Off Keying (OOK). Furthermore effects such as electrical cross talk and impulse noise are avoided due to the fact that moving photons do not interact, as do moving electrons.

1.1.3 Protocol transparency

Protocol transparency is achieved when the path, all-optical or not, offers the flexibility of requiring the end users to understand each other only, rather than obey the network protocol. Protocol variegation is one of the biggest inhibitors to the flexibility and growth of the information industry [6]. In order to enforce stability and uniformity universal standards such as OSI have been introduced. Unfortunately most of them have failed mainly due to new innovations and also due to serving providers (customers) proving reluctant to scrap their existing facilities. Lightpaths in optical networks provide end-to-end service transparently with no buffering or logic in between.

1.1.4 Reliability and maintainability

Electronic networks have evolved to become structures of great logical complexity. This brings together with it the major disadvantage of many failure modes as well as diagnostic complexity. Even VLSI circuits could be pushed into unreliable territory when moved to high bit rates. In comparison optical networks are much simpler and mostly make use of passive components. The major points of failure associated with this type of networks involve optical amplifiers and electronically actuated switches.

---

[2] Fibre to the Home (FTTH).

1.1.5 Ease of use

Optical fibres even when covered with protective coatings are much smaller, lighter and more flexible than their corresponding copper cables. This makes them ideal for signal transmission within difficult environments [7].

1.1.6 Attenuation

Fibres fabricated today have very low losses (0.2 dB km^{-1}) in comparison to copper conductors. The low loss makes them ideal for long haul communication systems, as it allows the use of very large repeater spacing. Since it determines the maximum transmission distance, attenuation is one of the most important parameters of the transmission medium. The attenuation of a fiber determines the light wavelength that could be used for transmission. In the attenuation profile we can distinguish three regions with the minimum losses (transmission windows). The most exploited window with its centre wavelength of 1550 nm, is due to the existence of optical amplifiers that operate within this region of frequencies.

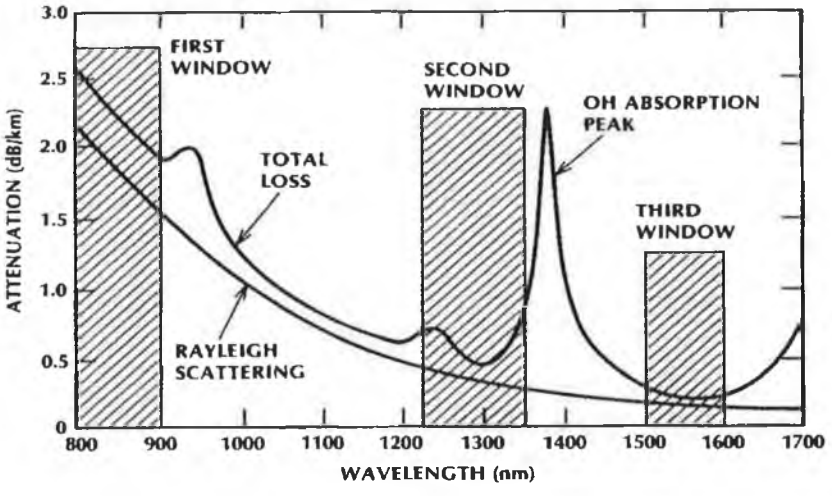

Figure 1-1: Attenuation profile for a silica glass fibre.

1.2 Limits

In view of all the advantages mentioned above, the use of fibre optic technology in communication networks looks very straightforward and promising. However, there are many technical hindrances and barriers to overcome. As of today, most commercial single channel rates are stuck at 10 Gb/s while a few operate at 40 Gb/s. Even such

transmission speeds threaten to choke the electronic processing side of the networks. Even though the race to augment the fibre content in the world's networks has started, the deployment of many technologies will take a while since they are currently at experimental level in laboratories rather than being ready to be slotted into racks as commercially ready equipment [8].

1.2.1 Limits imposed by capacity

The increase in channel bit rates places very high demands on opto-electronic devices such as the transmitter and receiver. The major factors limiting the speed involve the carrier and photon lifetimes, diffusion of carriers, drift transit time in the depletion region and the capacitance of the depletion region [9]. Apart from the transmitter and receiver, opto-electronic repeaters are also limited by bandwidth. The major theme of discussion here is that the electronics must be replaced. The worldwide backbone of electronic based telephone switches constitute today's principal architecture of inter exchange carriers. As such these switches have two major drawbacks. One being the speed at which they operate and second that they are based on circuit switching [10, 11].

1.2.2 Limits imposed by dispersion

The transmission speed of light through fibre varies due to the wavelength and propagation mode and such an effect is generally known as dispersion. Even though the differences in speed might be slight, the accumulation over distance makes it a substantial force to be dealt with. It is a major limiting factor in optical communications systems with an imposing effect on transmission bandwidth. There are four types of dispersion: modal dispersion arising from fibre transmission properties, material dispersion arising from variations in glass refractive index with wavelength, waveguide dispersion arising from the fibre's waveguide structure, and polarization mode dispersion arising from the transmission of two orthogonal polarization modes through single mode fibres.

1. Modal dispersion (multi-path dispersion)

Modal Dispersion arises from the fact that different electromagnetic (EM) modes propagate at different speeds and is highest in step index multi-mode fibres. This problem

could be overcome by the use of graded-index fibre by gradually reducing the refractive index from core to cladding.

2. Material dispersion

When an EM wave interacts with bound electrons of a dielectric (e.g. silica), the medium response in general depends on the optical frequency ω. This property, referred to as material dispersion, manifests itself through the frequency dependence of the refractive index $n(\omega)$ [12]. Essentially, what this means is that different spectral components of an optical pulse travel at different speeds given by the group velocity v_g as in equation 1-1.

$$v_g = \frac{d\omega}{d\beta} \qquad \textbf{Equation 1-1}$$

In mathematical terms (equation 1-2), the effects of fibre dispersion are accounted for by expanding the mode propagation constant β in a Taylor Series about the centre frequency ω_0:

$$\beta(\omega) = n(\omega)\frac{\omega}{c} = \beta_0 + \beta_1(\omega - \omega_0) + \frac{1}{2}\beta_2(\omega - \omega_0)^2 + \ldots\ldots \qquad \textbf{Equation 1-2}$$

The two constants introduced above that we are most interested in are β_1 and β_2.

$$\beta_1 = \frac{1}{v_g} \qquad \textbf{Equation 1-3}$$

$$\beta_2 = \frac{\omega}{c}\frac{d^2 n}{d\omega^2} \qquad \textbf{Equation 1-4}$$

The pulse envelope moves at the Group Velocity v_g. Hence, we use the term Group Velocity Dispersion (GVD) to describe β_2. GVD may lead to the broadening of data signals in optical systems. This broadening of the pulse means that each pulse can start to overlap with its neighbours, eventually becoming indistinguishable at the receiver output. Such a phenomenon is known as inter-symbol interference (ISI).

It is important to note that β_2 is zero for $\lambda \approx 1.27\mu m$ and becomes negative for longer wavelengths. For the case where $\beta_2 > 0$, the fibre is said to exhibit normal dispersion. In

the normal dispersion regime, the higher frequency components of the propagating optical pulse will travel slower than the lower frequency components. For the case where $\beta_2 < 0$, the fibre is said to exhibit anomalous dispersion. In the anomalous dispersion regime, the lower frequency components of a pulse travel slower than the higher frequency components. Figure 1-2 shows a plot of the variation of β_2 with wavelength.

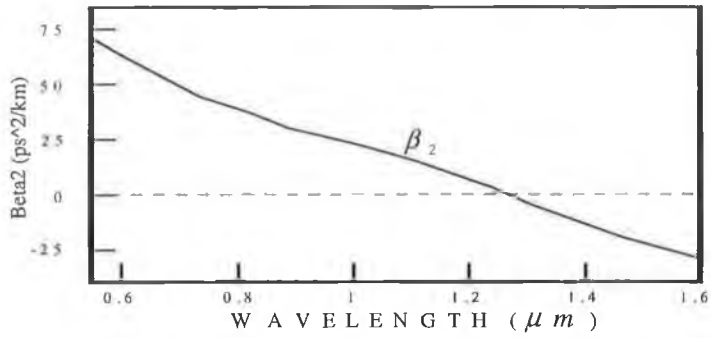

Figure 1-2: Variation of β_2 with wavelength

Figure 1-3 (a) and (b) show the shift in frequencies and the chirp[3] for the normal dispersion and anomalous dispersion regimes respectively.

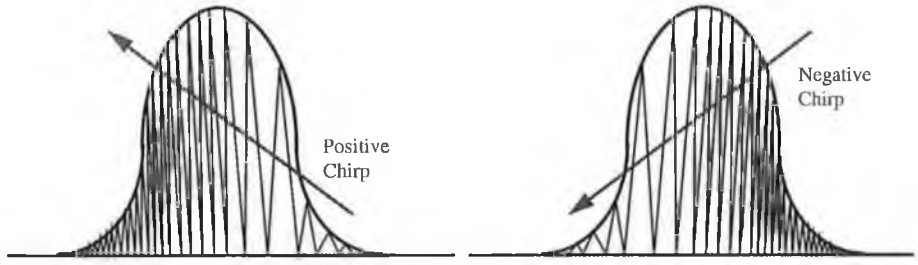

Figure 1-3: (a) Normal Dispersion (b) Anomalous Dispersion

It is important to remember that chromatic dispersion affects pulses in the time domain (dispersion induced broadening) and in the frequency domain the phase of the spectrum is changed.

3. Waveguide dispersion

Waveguide dispersion arises when the optical signal is not confined completely within the core of the fibre. The effect of waveguide dispersion is much smaller than material

[3] The change in instantaneous frequency across the pulse is known as frequency chirp.

dispersion, but may vary the overall value of β_2. We use the dispersion parameter D, which is related to β_2 by:

$$D = -\frac{2\pi c}{\lambda^2}\beta_2 \qquad \textbf{Equation 1-5}$$

The contribution of waveguide dispersion to D depends on the fibre design parameters such as the core radius a and the core-cladding index difference Δ. This feature can be used to shift the zero dispersion wavelength λ_D in the vicinity of 1.55 μm where the fibre loss is minimum. Such fibres are known as 'Dispersion-Shifted' fibre [13].

Material and waveguide dispersion combine to make up chromatic dispersion. The actual pulse spreading depends not only on the inherent dispersion and distance but also on the range of wavelengths transmitted. Therefore even though the dispersion parameter of the fibre might be given, the actual amount of chromatic dispersion depends on the spectral width of the light source. Dispersion can be a serious concern at 10 Gb/s per channel where bit intervals are 100 ps. However compensation for chromatic dispersion at such bit rates is readily achievable. Higher bit rates (such as 40 Gb/s) would have smaller bit slots (25 ps time slot). It also means that the spectral width associated with such signals would be much larger. Hence such systems would be more prone to dispersion effects. The added complexity arises from the small bit slot, which leaves little tolerance for chromatic and polarization mode dispersion effects.

4. Polarization Mode Dispersion (PMD)

Even a single mode fibre is not truly single mode since it could support two degenerate modes that are dominantly polarized in two orthogonal directions [13]. When light is transmitted down an optical fibre, the power between the two principal states of polarization is periodically exchanged. Under ideal conditions where the fibre exhibits a perfect cylindrical cross section, both components would travel at the same speed. However, manufacturing defects (causes mechanical imperfections) or small fluctuations in material anisotropy (due to stress) of the fibre result in the mode propagation constant (β) being slightly different for the modes polarized in the x and y directions. This property is referred to as modal birefringence. The mechanical deviations in the cross

section of the fibre affect each of the polarizations independently and differently, causing a relative displacement between the components at the end of the fibre[4]. This displacement causes the spreading of the original pulse and is known as Polarization Mode Dispersion (PMD) [14, 15].

Generally PMD exhibits a non-deterministic property, varying with short and long term effects such as seasonal and diurnal temperature variations, vibrations etc. This makes it very hard to compensate for PMD. The severity of this effect depends on both the fibre and the bit rate. A 40 Gb/s signal with a 25 ps bit slot is much more susceptible to such impairments than a 10 Gb/s signal which has a 100 ps bit slot.

1.2.3 Limits imposed by fibre nonlinearities

Nonlinearity can also be a limiting factor in optical transmission systems. The response of silica fibre (which is a dielectric material) to light becomes nonlinear for intense electromagnetic fields. Fundamentally, the origin of nonlinear response is related to anharmonic (i.e. not harmonic) motion of bound electrons under the influence of an applied field. This is also referred to as the Kerr effect [12, 13].

Most of the nonlinear effects in optical fibres originate from nonlinear refraction. Nonlinear refraction refers to the intensity dependence of the refractive index. In the case of GVD (discussed previously), the frequency dependence of the refractive index was noted. However in the case of nonlinearity, the intensity dependence of the refractive index must also be considered. This intensity dependence of the refractive index coefficient leads to many nonlinear effects. The two main nonlinear effects are Self-Phase Modulation (SPM) and Cross-Phase Modulation (XPM) [16].

1. Self-Phase Modulation (SPM)

SPM refers to the self-induced phase shift experienced by an optical pulse during its propagation in optical fibres. The effects of SPM can be seen during propagation, where the phase of an optical field changes by a certain amount. This phase shift in turn causes a

[4] Hence the sum of vectors results in the spreading of the pulse.

positive chirp, resulting in an instantaneous increase in the frequency across the pulse from its leading edge to its trailing edge [17].

SPM is responsible for spectral broadening of ultrashort pulses. It is also responsible for the existence of optical solitons in the anomalous dispersion regime ($\beta_2 < 0$) of fibres.

2. Cross-Phase Modulation (XPM)

Cross-Phase Modulation refers to the nonlinear phase shift of an optical field induced by a co- propagating field at a different wavelength. An important characteristic of XPM is that, for equally intense optical fields, the contribution of XPM to the nonlinear phase shift is twice that compared with SPM [18].

1.3 Multiplexing techniques used in high capacity networks

As the demand for bandwidth continues to grow, driven by the massive increase in internet usage, so will the necessity to have communications networks that can handle very high data rates. The use of optical fiber networks is the clear choice for such systems given the huge available bandwidth of the fiber transmission medium. However, in a basic optical communication system comprising a laser transmitter, an optical fiber transmission medium, and a receiver, the capacity is essentially limited by the speed at which light can be modulated at the transmitter. To overcome this limitation, due to the speed of available electronics, it is necessary to use optical multiplexing techniques such as Wavelength Division Multiplexing (WDM) and Optical Time Division Multiplexing (OTDM). A basic overview of these technologies follows in the forthcoming section. Two other multiplexing technologies that are used in the electrical domain but are applicable to the optical domain as well are also cited within the same section.

1.3.1 Wavelength Division Multiplexing (WDM)

The technology of combining many different wavelengths onto one single fibre is known as Wavelength Division Multiplexing (WDM). Conceptually WDM is the same as Frequency Division Multiplexing (FDM) in microwave radio and satellite systems. The spacing in both technologies is very important. The key features of an optical WDM system are:

1. Capacity upgrade: If each wavelength can support a few gigabits per second (Gb/s), then WDM can increase the capacity of fibre network dramatically.
2. Transparency: Each channel may carry different transmission formats and is one of the key features provided by WDM.
3. Wavelength routing: The use of wavelength sensitive optical routing devices enables the design of networks and switches. Wavelength routed networks use the actual wavelength of the signal as the intermediate or final address.

1.3.2 Optical Time Division Multiplexing (OTDM)

Compared to WDM networks, OTDM networks are still in their infancy, partly due to the primitive and expensive nature of the required devices. Furthermore the fact that it destroys protocol transparency[5] and exacerbates synchronization problems[6], intensifies its problems especially when it competes with the already established WDM technology. There are two types of OTDM networks.

1. Bit interleaved OTDM (Figure 1-4) is similar to WDM in that the access nodes share many small channels operating at a peak rate that is a fraction of the media rate.

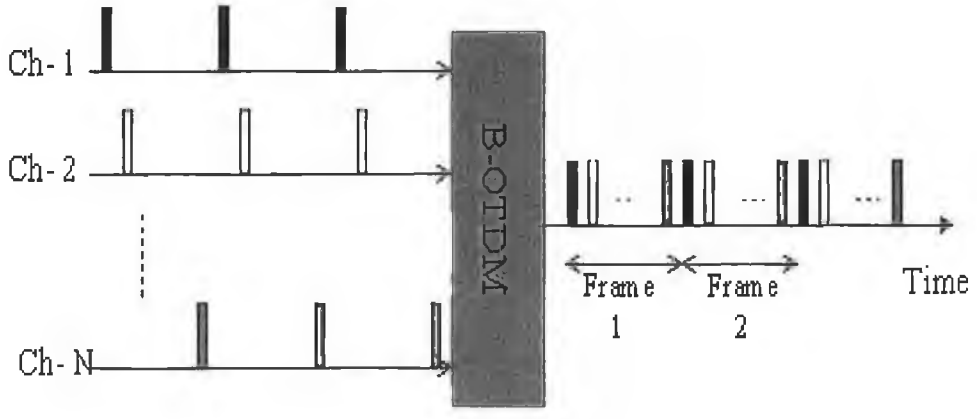

Figure 1-4: Bit interleaved OTDM communication system

For instance the channel rates could vary from 100 Mb/s to 1 Gb/s, whereas the time multiplexed media rate could be around 100 Gb/s. In the process of bit interleaving, a laser source produces a regular stream of very narrow Return to Zero (RZ) pulses at a

[5] Dictates the framing format.
[6] Timing has to be accurate due to the interleaving process.

certain repetition rate (B). This rate corresponds to the bit rate of the electronic data tributaries feeding the system. An optical splitter then divides the pulse train in to N separate streams (channels). Each of these channels is then individually modulated by an electrical tributary data source at a bit rate (B). The modulated outputs are delayed individually by different fractions of the clock period, and are then interleaved through an optical combiner to produce an aggregate bit rate of NxB.

2. In time slotted OTDM (also called packet interleaving) [19], the access nodes share one fast channel, which is capable of sending burst rates at 100 Gb/s. Slotted OTDM networks are fundamentally different from bit-interleaved OTDM and WDM systems. Time is partitioned into slots containing tens-of-thousands of bits and each access node is capable of bursting data into these slots at the ultrafast channel rate (100 Gbs). One of the striking attributes of theses type of networks is that they are able to provide a truly flexible bandwidth on demand service for high or low rate access to users. The basic operation of a time slotted OTDM system is shown in Figure 1-5.

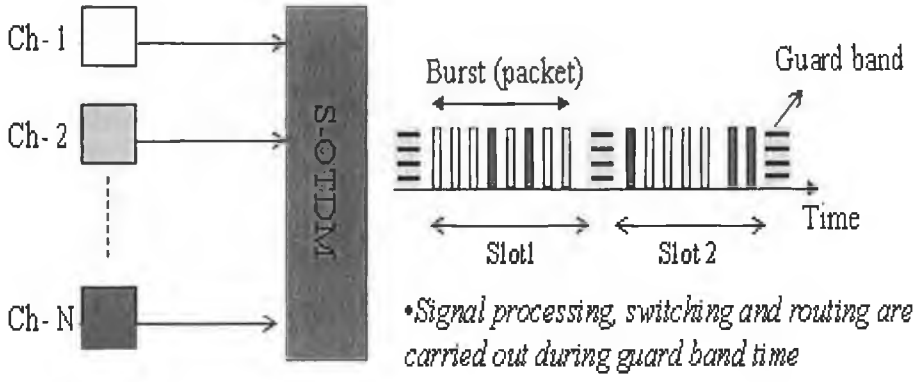

Figure 1-5: Time slotted OTDM communication system

1.3.3 Sub-Carrier Multiplexing (SCM)

Currently Sub-Carrier Multiplexing (SCM) [20, 21] is mainly utilized in cable TV, radio and satellite applications. Recently it has been considered in optical systems as a means of optimizing the bandwidth usage[7]. Initial operation in SCM involves different data channels being up-converted to various Intermediate Frequencies (IF). The IF acts as the

[7] Bandwidth Efficient Modulation (BEM) and/or Single Side Band (SSB) modulation schemes are used.

sub-carrier in optical SCM systems. The up-converted signal is then multiplexed in the frequency domain before being used to modulate the carrier (light) by means of direct or external modulation. A block diagram of an SCM transmitter reflecting the operational principle explained above is shown in Figure 1-6.

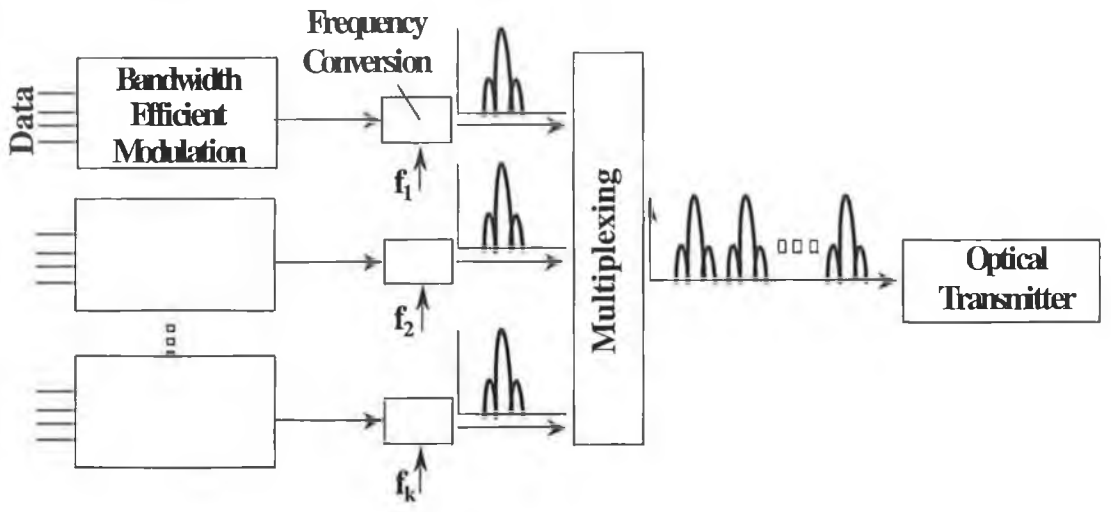

Figure 1-6: Schematic of a SCM transmitter

At the receiver, the desired channel is acquired by mixing the composite signal with the appropriate IF. Final filtering rejects the unwanted components in the down-converted signal.

1.3.4 Code Division Multiplexing (CDM)

Code Division Multiplexing (CDM) [22, 23] is one of the spread spectrum techniques. 3G mobile systems are based on this technology. The main principle of operation involves each user being assigned a different code. The signal is spread over a wide spectrum (within a allocated bandwidth) due to mixing the data with the assigned code, which is at a higher chip rate (bit rate). At the receiver, the incoming signal is once again mixed with the code. Since all the codes are orthogonal (resulting in minimal interference), at the output only the desired signal is obtained. The operational principle is extended in order to carry this scheme over to the optical domain (OCDM) [24].

1.3.5 Comparative analysis

One of the major advantages with WDM over OTDM is that it is a mature technology and is currently being widely used in commercial networks (backbones). Another

attractive feature with WDM is that they are transparent to the protocol being used. On the other hand OTDM is much more spectrally efficient and uses just one source or transmitter. The contrasts between the two technologies are tabulated and shown in Table 1-1.

WDM	OTDM
Multiple wavelength (Multiple sources)	Single wavelength (Single source)
Reaching an advanced stage of development	Immature technology
Protocol transparent	Dictates framing format
-	Synchronization problems

Table 1-1: WDM vs OTDM

The capacity of optical fibre communication system has grown exponentially over the past fifteen years or so. The evolution of this growth is shown in Figure 1-7 [25].

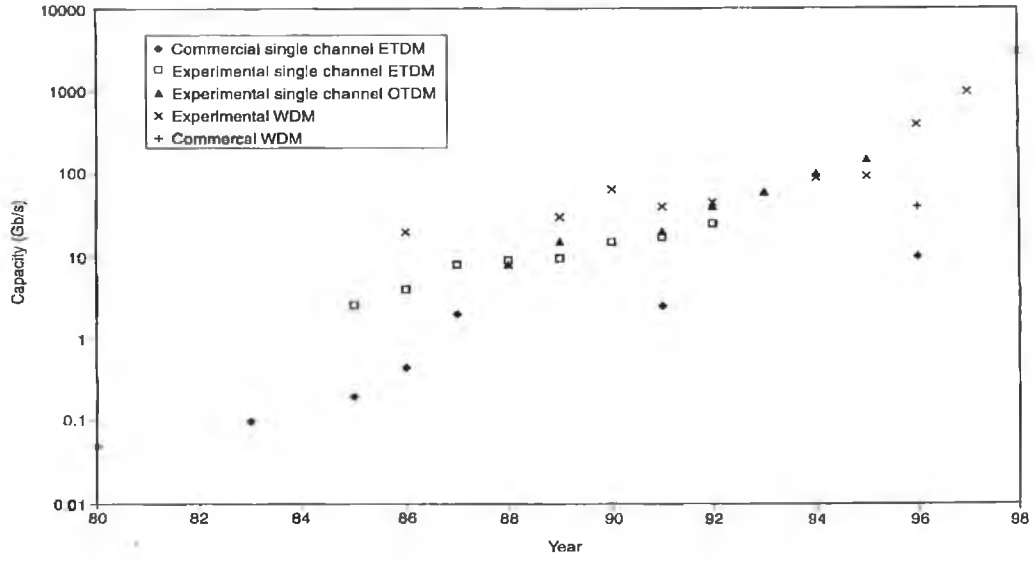

Figure 1-7: Evolution of optical fibre systems in terms of transmission capacity [25]

The continual increase in optical line speeds has played a crucial role in the changing telecommunications structure via the evolution of Synchronous Digital Hierarchy (SDH) in Europe and Synchronous Optical Network (SONET) in North America. SDH and SONET are the physical layer protocols that form the standard frame for almost all the transmission over optical fibre today [26]. In the case of SDH, the aggregate rates[8] are based on multiples of the Synchronous Transport Module 1 {(STM-1) = 155 Mb/s}. In the case of SONET, the aggregate rates are based on multiples of 51.8 Mb/s or STS-1 (Synchronous Transport Signal-1).

1.4 System expectations

The richness of the information industry over past 20-30 years was built around the modest copper twisted pair. However the possibilities seem limitless when one considers the introduction of optical networking. It brings about the potential of ten orders of magnitude improvements in bandwidth and many other advantages, as described above. The injection of optical networking into the midst of the existing communication infrastructure is and will take place in stages. As the solutions to the problems mentioned in the previous section become cheaper its domains of applicability will spread. Furthermore as the cost of optical components goes down, Fibre To The Home (FTTH) could start competing with high speed Digital Subscriber Lines (XDSL).

Responding to needs of new services, future speeds of several Tb/s could be achieved. Experimentally Tb/s rates have already been reported, using the multiplexing techniques mentioned earlier. Hence we will look at these techniques, their requirements and their limitations in much more detail in the next chapter. Another aspect that is appealing is the merging of the two multiplexing techniques. The merits of both techniques could be taken advantage in such an amalgamation.

A vital component required in constructing such high-speed networks is a source of short optical pulses. The generation of such pulses and their characteristics would also be analyzed later on in this work. Their performance within the hybrid WDM/OTDM

[8] Shown in Appendix A

networks is another crucial area that has been devoted with a lot of experimentation. Any experimental work done is best acknowledged and verified when simulations characterizing the same effects are carried out (either before or after experimental work as the case may be). Hence this report is finished off by performing simulations on most of the areas where experimental work was carried out.

References

[1] G. Khoe, "Presidents Column," *IEEE LEOS Newsletter*, Vol. 17, pp. 1, April 2003.

[2] S. V. Kartalopoulos, "Elastic Bandwidth" *IEEE LEOS Newsletter*, Vol. 16, pp. 15-19, April 2002.

[3] P. E. Green, Jr., "Optical Networking Update," *IEEE J. on selected areas in communications*, vol. 14, pp. 764-779, 1996.

[4] M. Riezenman, "Future of Optics," *IEEE Spectrum*, pp 32-33, January 2003.

[5] S. Akiba, "The Future of Optical Communications," *IEEE LEOS Newsletter*, Vol. 17, pp. 20-23, February 2003.

[6] M. Schwartz, "*Telecommunications Networks – Protocols, Modelling and Analysis*," Addision-Wesley,1988.

[7] J. Hecht, "*Understanding Fibre Optics (4th Ed.)*," Prentice Hall, 2002.

[8] G. Stix, "The Triumph of Light, "*Scientific American*, pp 81-86, 2001.

[9] M. Stellpflug, "40 Gb/s technology - Frequency Response Indicates Optical Receiver Performance," *WDM solutions*, pp 77-79, July 2001.

[10] J. M. Gill, "Lasers: A 40 Year Perspective," *IEEE J. on Selected topics in Quantum Electronics*, vol. 6, pp. 1111-1115, Nov/Dec 2000.

[11] H. Kogelnik, "High Capacity Optical Communications: Personal Recollections" *IEEE J. on Selected topics in Quantum Electronics*, vol. 6, pp. 1279-1286, Nov/Dec 2000.

[12] J. M. Senior, "*Optical fibre communications*," Prentice hall, UK, 1985.

[13] G. P. Agrawal, "*Nonlinear Fiber Optics (2nd Ed)*," Academic Press, 1989.

[14] J. Ash, "Going Beyond 10 Gbps," *International telecommunications,* Vol. 36, pp 33-36, July 2002.

[15] H. Sunnerud, M. Karlsson, C. Xie and P. Andrekson, "Polarization-Mode Dispersion in High-Speed Fibre-Optic Communication Systems," *IEEE J. of Lightwave Technol.*, vol. 20, pp. 2204-2219, 2002.

[16] J. Gowar, "Optical Communications Systems," 2nd Ed., *Prentice Hall*, 1993.

[17] H. D. Young, "*University Physics (8th Ed)*," Addison Wesley, 1992.

[18] B. Mukherjee, "*Optical Communications Networks*," McGraw Hill, 1997.

[19] S. A. Hamilton, B. S. Robinson, T. E. Murphy, S. J. Savage and E. P. Ippen, "100 Gb/s Optical Time-Division Multiplexed Networks," *IEEE J. of Lightwave Technol.*, vol. 20, pp. 2086-2100, 2002.

[20] T. Wolcott and H. Thelander, "Subcarrier Multiplexing: More Than Just Capacity", *Lightwave,* July 2001.

[21] T. E. Dracie and G. E. Bodeep, "Lightwave Subcarrier CATV Transmission Systems", *IEEE Transaction on Microwave Theory and Tech.s*, Vol. 38, pp 524-533, 1990.

[22] W. Krzysztof, "*Mobile Communication Systems*," John Wiley, 2002.

[23] J. Harris, "The Future of Radio Access in 3G," *BT Technol. Journal*, Vol. 19, pp 106-113, 2001.

[24] A. Stok and H. Sargent, "Lighting the Local Area: OCDMA and QoS Provisioning," *IEEE Network magazine*, Vol. 14, pp. 42-46, Nov./Dec. 2000.

[25] R. Sabella and P. Lugli, "*High Speed Optical Communications*," Kluwer Academic publishers, 1999.

[26] J. Ash, "Going Beyond 10 Gbps," *International telecommunications,* Vol. 36, pp 33-36, July 2002.

Chapter 2 - High Speed Optical Networks

2.1 Demand for higher capacity services and networks

The growth in demand for existing narrowband services and broadband interactive, multi media entertainment and educational services has led to a need for high capacity networks. Optical fibre networks would be the clear choice with the prospects of "limitless" bandwidth offered by the fibre transmission medium as already explained in the previous chapter. The rapid increase in the demand for more optical transmission bandwidth and the speed limitation of electronic components has led to the introduction of various multiplexing techniques[9]. Although optical technology offers advantages such as simple multiplexing / de-multiplexing and may finally remove the need to process signals electronically (bottleneck), currently it has to work alongside, to enhance, the ever improving and vast electronic technology.

2.2 Electrical Time Division Multiplexing (ETDM) for optical systems

The basic principle of Time Division Multiplexing (TDM) has long been the traditional method for electrically combining information channels and involves the allocation of a series of data slots for each of the baseband data streams on the multiplexed channel [1, 2, 3]. With the progressive roll out of standards, a number of different data rates have been specified as standard transmission rates. Synchronous Digital Hierarchy (SDH) being one of such standards has significantly enhanced network flexibility [4]. If we take the most fundamental data rate to be that of a simple voice call, 64 Kb/s, then the transmission of data at higher bit rates is achieved by electrically multiplexing a large number of 64 Kb/s channels in the time domain. SDH has a basic data rate of 155.52 Mb/s, which is known as Synchronous Transport Module – Level 1 (STM-1). This particular data rate is essentially obtained by electrically multiplexing over 2000 voice calls in the time domain (with some of the capacity required for overhead information). By subsequently multiplexing a number of STM-1 channels together we can obtain transmission at the higher standard data rates of STM-4 (622 Mb/s), STM-16

[9] More economical to transmit at higher rates via less fibre than vice versa.

(2.48 Gb/s) and STM-64 (9.88 Gb/s) etc. (as outlined in Appendix A). Figure 2-1 highlights the operation of ETDM in a simple optical communication system.

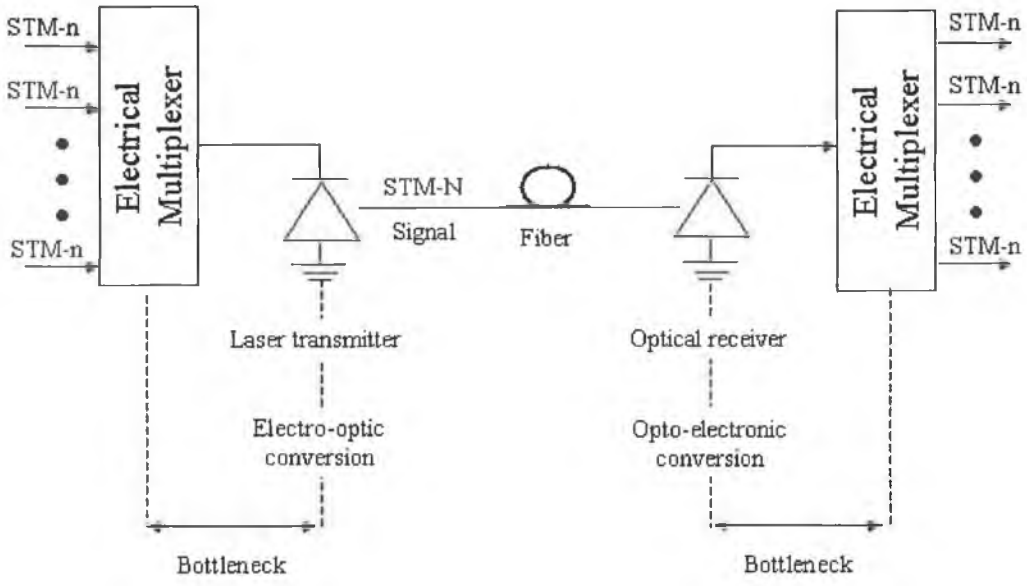

Figure 2-1: ETDM in a basic optical communication system

However, the maximum data capacity of optical systems will be dependent on the capability of the electronics within the switching and processing equipment. The potential bottlenecks are faced in the multiplexer, the Electro-Optic (E/O) converter (laser), the de-multiplexer and the Opto-Electric (O/E) converter (photodetector). The bottleneck occurs at these points where the electronics must operate at the full multiplexed rate and arise due to varied reasons such as the speed limitations of digital integrated circuits, speed limitations of amplifiers used to drive lasers or modulators in the E/O and O/E converters, limited modulation bandwidths of lasers and modulators and the fact that receiver sensitivity offered by an avalanche photodiode degrades by more than 3 dB for every octave increase in receiver bandwidth [5].

Currently, commercial Si and GaAs circuits have been able to meet bit rates of about 10 Gb/s. Although 40 Gb/s data rates have been achieved [6, 7] with research chips, at higher rates (especially at Tb/s rates) digital electronic circuits struggle [8]. In order to overcome the limitation imposed by the electronics on the network, it would be necessary to extend the well-known approach of ETDM into the optical domain [9, 10]. The two

main optical multiplexing techniques are Optical Time Division Multiplexing (OTDM) [11, 12, 13, 14] and Wavelength Division Multiplexing (WDM) [15-17]. The use of such innovations not only enables us to overcome limitations set by the restricted bandwidth of electronics but also capitalizes on the available bandwidth in the fibre transmission medium.

2.3 OTDM transmission systems

One of the optical multiplexing techniques mentioned above is OTDM. The basic principle of OTDM is to increase the system capacity (achieving faster single channel rates) by multiplexing optical data channels in the temporal domain. The concept of OTDM was proposed around 1988 [11]. Initial experiments involved bit rates in the Gb/s range (32 Gb/s transmission [18]). Since then OTDM transmission rates have increased significantly such that terabits/s transmission rates have been demonstrated [19-21]. A process known as bit interleaving achieves OTDM and is basically an extension and expansion of the well-known technology of time division multiplexing [22]. Generally OTDM involves a process where short pulses are generated, modulated and then optically multiplexed into a higher speed signal. At the receiver, a timing clock is extracted from the signal and the clock drives a time domain demultiplexer to recover the original sub-channels [23]. Hence a vital part of this system is a source of picosecond (ps) optical pulses. The power and the wavelength of the optical signal should be optimized to suit the transmission characteristics of the fibre system. Hence OTDM systems have primarily operated in the 1.55 μm transmission window especially due to the availability of the Erbium Doped Fibre Amplifiers (EDFA) and as such favour Dispersion Shifted Fibre (DSF) since low chromatic dispersion is normally required to maximize system lengths. The use of standard fibre would mean that dispersion compensation techniques have to be employed to permit transmission in the 1.55 μm window.

2.3.1 Generalized system

The process of multiplexing in the optical temporal domain could be best explained by considering the schematic of a generalized OTDM system shown in Figure 2-2. The first component, associated with the process of multiplexing, that is considered is a source of ultra narrow Return to Zero (RZ) optical pulses. The optical pulse train at a certain

repetition rate (n GHz), which corresponds to the individual data rate of the electrical signals, is split into N ways using a passive fibre coupler. Subsequently N different modulators are used to modulate the electrical data onto each of these optical channels. The resulting output from each modulator is essentially an optical data channel where the data is represented by ultra short optical pulses (RZ data format). Each channel is then passed through a fixed fibre delay line, which delays each channel by a time equal to 1/nN relative to its adjacent channel. The N modulated and delayed optical data channels are then recombined in another passive fibre coupler to form the OTDM data signal. The multiplexed data signal is then transmitted over optical fibre. Finally at the receiver end, demultiplexing of the OTDM signal into its discrete channels is carried out.

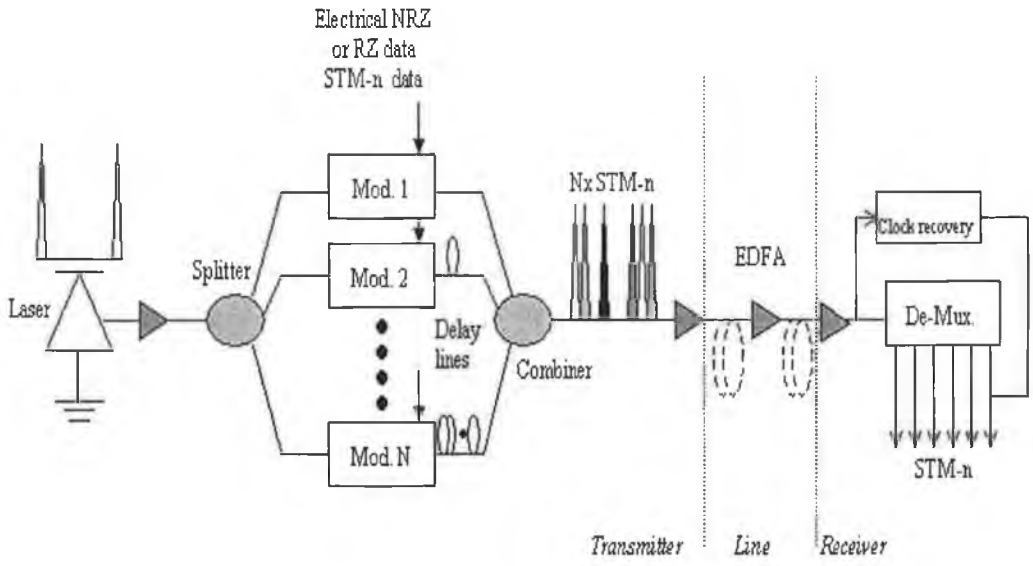

Figure 2-2: Schematic illustration of a generalized OTDM communication system

The scheme of multiplexing could be divided into three sub-functions: sampling, timing and combining [11]. An all optical multiplexer could be achieved by the serial or the parallel type. The latter, being easier to construct, is more common [24]. Sampling identifies the value of each incoming bit. As illustrated in Figure 2-3 electrical input data is sampled by ultra short optical pulses incident on an optical modulator. Each individual pulse train is modulated by an electrical data signal (STM-n). This results in N optical RZ format data channels. The presence (absence) of an optical pulse in a bit slot represents a one (zero). The electrical data could be in either RZ or Non-Return to Zero (NRZ)

format, although NRZ is preferable in certain aspects especially due to the fact that it minimizes the bandwidth requirements of the baseband digital electronics, the modulator and its drive amplifiers.

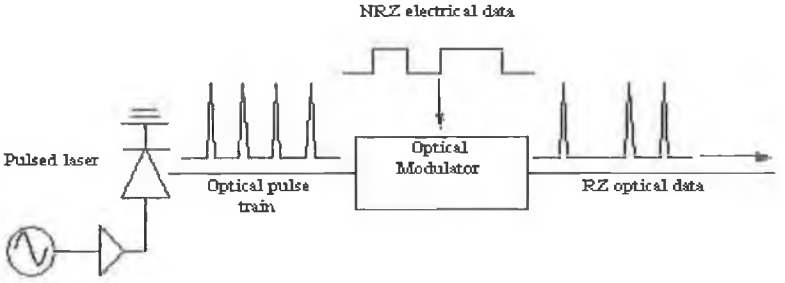

Figure 2-3: Schematic of an E/O converter sampling the input data

The timing ensures the assigning of each data channel to a specific bit slot in the overall time multiplexed signal. Subsequently the modulated pulse train is then delayed relative to its neighbour by a time equal to 1/N x STM-n of the original pulse train period. The combining function puts together the faster aggregate data rate. Therefore optical signals representing data streams from multiple sources are interleaved in time to produce a single, high-speed data stream. Interleaving applied to the case above results in a RZ signal that has an aggregate data rate of N x STM-n. The interleaving could be done on a bit-by-bit basis (bit interleaving) or on packet-by-packet basis (packet interleaving) as already discussed in the previous chapter. The process of bit interleaving is shown in Figure 2-4 below.

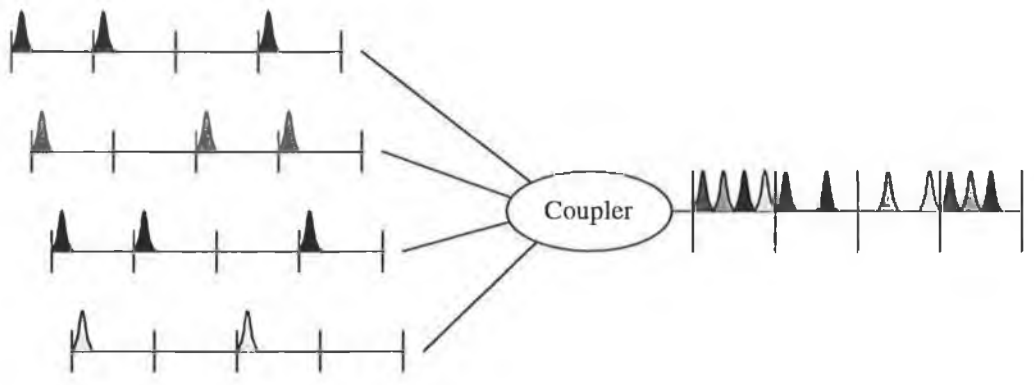

Figure 2-4: Combining operation using bit interleaving in OTDM

2.3.2 Key elements of an OTDM transmission system

2.3.2.1 Optical pulses

In order to enable demultiplexing, OTDM transmission systems have to operate with optical pulses that are considerably less than the duration of the allowed timeslot. In addition, the duration of the optical pulse is also extremely important due to the fact that temporal multiplexing is prone to inter-channel cross talk. Therefore in order to avoid possible overlap problems (Inter Symbol Interference - ISI) it is necessary to ensure that the pulses are significantly smaller than the temporal separation between channels. Furthermore the shorter the pulsewidth, the higher the overall data rate that can be achieved. For very high capacity or long distance transmission, the pulsewidth should be less than 30% of the channel spacing (bit slot). However shorter pulses occupy a wider optical spectrum thereby being prone to pulse spreading via dispersion during the transmission of the high-speed signal over standard fibre. Thus, the optimum pulsewidth may entail a compromise between system cross talk and pulse spreading caused by dispersion.

For example a system operating at 40 Gb/s, means that the source has to produce very short optical pulses typically around 8 ps duration (width). In addition the pulses have to be as spectrally pure as possible so that the pulse broadening problems due to the interaction of the source chirp with fibre chromatic dispersion are minimized. In summary we could say that some of the most important characteristics of pulses that will affect its usefulness in an OTDM system are its pulsewidth, spectral width and temporal jitter. A standard figure of merit for theses pulses is known as the time bandwidth product ($\delta\nu\delta t$) where $\delta\nu$ is the width of the optical spectrum (linewidth) and δt is the temporal width (pulsewidth). Depending on the pulse shape, the transform limited[10] value of the time-bandwidth product ranges between 0.32 – 0.45 (see Appendix B).

[10] Transform limited in effect means that the spectral width is as small as possible for the associated pulsewidth

2.3.2.2 *Optical pulse sources*

There are a large number of techniques employed in the generation of ultra short optical pulses suitable for use in OTDM systems (discussed in detail in the next chapter). The three main types of laser pulse sources used in OTDM systems to date are listed below.

1) The Gain Switched semiconductor Laser Diode (GSLD): Gain switching of semiconductor laser diodes is probably the simplest and most reliable technique to generate optical pulses. The technique involves the use of a high power electrical pulse, (or electrical sinusoidal signal) to modulate a laser in conjunction with a certain bias current [25, 26]. By ensuring that the electrical pulse signal and the bias signal have the correct level, the relaxation oscillation phenomenon of the laser results in the production of optical pulses with typical durations of a few picoseconds to some tens of picoseconds, at the repetition rate of the applied electrical signal. The frequency of the electrical signal applied to the laser is essentially arbitrary (provided it is not larger than the modulation bandwidth of the diode), thus making it straightforward to synchronize the optical pulse train to a SDH line-rate[11]. The main problem with this technique is the spectral width (frequency chirp) of the pulses. Frequency chirp results in a broadening of the optical spectrum from the laser due to a large variation in the carrier density of the laser (which leads to a variation in the refractive index). Therefore the generated pulses are far from transform limited ($\delta\mu\delta t>1$), which would affect their subsequent propagation in fiber. Another disadvantage of the gain-switching technique is the large temporal jitter exhibited by the pulses.

2) The Semiconductor Mode Locked Laser (SMLL): This pulse generation technique involves mode locking (active or passive) of a laser cavity. In this case the amplitude or frequency of the optical field inside the laser cavity is modulated at a frequency f_m, which is equal to, or a multiple of, the longitudinal mode spacing of the laser. The modulation signal generates side bands, and phase synchronization of each longitudinal mode occurs due to overlap of the modulation side bands with each of the longitudinal modes resulting in the generation of pulses at a repetition frequency (f_m)

[11] SDH line rates listed in Appendix A

equal to the applied signal [27]. Pulses generated using this technique possess excellent spectral and temporal jitter characteristics. Major drawbacks of mode locking are that it requires cavity complexity and is limited to locking at a harmonic of the cavity frequency. Hence accurate synchronization of the mode locked frequency to multiples of SDH line rates is difficult.

3) Pulse shaping using external modulators: External modulation of a CW light by an external modulator has a pulse compression effect due to nonlinear transfer characteristic of the driving voltage applied to the modulator [28]. Hence transform-limited (TL) optical pulses are generated by sinusoidally modulating the external modulator. Pulses can be generated at twice the applied electrical signal frequency by biasing the modulator at its null point and driving it with a signal that has peak-to-peak value of twice the switching voltage. This method also exhibits pulses with very low temporal jitter. A shortcoming of the external modulation technique is the need for an extra component (costly). In addition the insertion loss (~ 6 dB) of the modulator is also a disadvantage but is minor in comparison to the cost of an additional component.

2.3.2.3 Channel line multiplexer

The multiplexing technique can be achieved either actively (using fast electro-optic directional couplers) or passively. A passive combiner would incorporate devices such as fibre directional couplers. The required number of identical optical pulses, for an OTDM system, can be achieved using passive directional couplers. Hence due to their cost efficiency and simplicity, focus is placed on passive multiplexing techniques in this work. Insertion loss of directional couplers is the major problem in passive multiplexing.

Active multiplexing involves the use of optical switches such as electro-optic directional couplers. This technique has the advantage of reducing cross talk by cutting off the leading and trailing edges of pulses due to their time dependent switching function (finite on/off ratio) [29].

2.3.2.4 Line systems

The transmission performance of an OTDM data signal is vital in determining the distance over which the data can be sent successfully. The fiber parameters, which

hamper signal transmission, are attenuation, dispersion, and nonlinearity. The exact choice of transmission wavelength and power will be dictated by the length and loss of the transmission fibre within the link. As mentioned previously the operation in the 1.5 μm (minimum loss wavelength), transmission window is highly favourable especially due to the availability of the Erbium Doped Fibre Amplifiers (EDFA) [30], which could be used to overcome the losses experienced. To maintain a suitable optical power budget for the system, optical amplifiers are normally employed. OTDM systems generally have transmitter power amplifiers and pre-amplified receivers as well as in-line repeater amplifiers for every 40-50 km of transmission fibre. Assuming that the fibre attenuation problem is solved with the use of optical amplifiers, dispersion then becomes a major issue for high-speed OTDM systems. A wide variety of techniques have been established to reduce the effects.

In a very basic OTDM system operating at 1550 nm, with transmitter and receiver linked using standard fiber, (dispersion parameter of about 16-17 ps / (km.nm)), the maximum transmission distance will be limited by the overall data rate, and also by the pulse and spectral widths of the optical pulse source. For example, let us consider a 40 Gbit/s OTDM data signal. Such a system would have a bit slot of 25 ps. Hence we need to use optical pulses that are about 8 ps wide (1/3 of bit slot) with an associated spectral width of about 40 GHz (0.32 nm – sech pulses). From the spectral width we can calculate the signal broadening due to dispersion to be around 5 ps / km, and as the pulses broaden and spread into adjacent channels of the OTDM signal then this interference will make it increasingly difficult to correctly detect the signal at the receiver. In this case after propagation through 5 km of fiber, the signal pulses will have already dispersed to around 25 ps duration, the same value as the temporal bit slot into which each channel is placed, this will clearly result in serious loss of signal integrity due to ISI. A straightforward possibility to increase the transmission distance of OTDM systems is to employ dispersion shifted fiber, where the dispersion parameter is around 1 – 2 ps / km.nm at an operating wavelength of 1550 nm. This reduction in dispersion will obviously increase the allowed transmission distance by about an order of magnitude for the example described above, however, to develop ultra-high speed, long-haul OTDM

communications we require more complex transmission schemes. Two possibilities for this include dispersion compensation, and soliton transmission techniques [31, 32].

Dispersion compensation basically involves compensating for the dispersion that has been encountered during transmission by using some fiber with a total dispersion of opposite sign. The magnitude could vary from about 6-10 times that of the transmission fibre. Dispersion compensation may also be achieved using a suitably designed fiber grating. For a long-haul OTDM system, a dispersion compensator may be used every 50 or 60 km, in conjunction with the optical amplifier, thus allowing one to compensate both fiber loss and attenuation periodically along the link. Another technique that may be employed to greatly extend the transmission distance of high-speed OTDM communication systems is the use of soliton transmission. The basic principle of soliton transmission is to use optical data pulses with a particular shape, pulsewidth, and peak power, such that as the pulse propagates, the effects of fiber dispersion and nonlinearity counterbalance to allow the signal to propagate undistorted. By using optical amplifiers to ensure that the optical pulse peak power does not vary too much along the transmission link, OTDM transmission at data rates greater than 100 Gb/s, over distances approaching 200 km have been demonstrated [33].

2.3.2.5 Channel line demultiplexers

The availability of a stable and compact ultrafast switch for demultiplexing ultrahigh bit rate signals is essential for the future development of high capacity optical-time-division-multiplexed (OTDM) networks. The ability to drop a single channel from a high speed OTDM data stream is significant at a network node since optical demultiplexing is performed while still transmitting the other channels in an optically transparent manner for further processing. There are two approaches available for channel demultiplexing viz. electro-optic and all optical gating approaches.

1) Electro-optic demultiplexing: In OTDM demultiplexing applications the transmission window has to be very small in order to ensure that only the required channel is selected. Electro-Absorption (EA) and Mach Zehnder (MZ) modulators are suited for this reason as their non-linear transfer function permits narrow optical

switching windows. Furthermore the electrical extinction ratio[12] has to be high enough to prevent absorption of the un-dropped channels that may interfere with the dropped channels. If a new channel is to be inserted in the available slot after a channel is dropped, it is also important to have a large extinction ratio to prevent interference between the dropped channel and the channel to be inserted. Changing the amplitude of the applied sinusoidal voltage and the bias voltage to the modulator can control the gate width. Meanwhile different channels may be selected by changing the phase (delay) of the electrical drive signal to the modulator.

The demultiplexing of a single channel from a four-channel OTDM signal is schematically illustrated in Figure 2-5 (below).

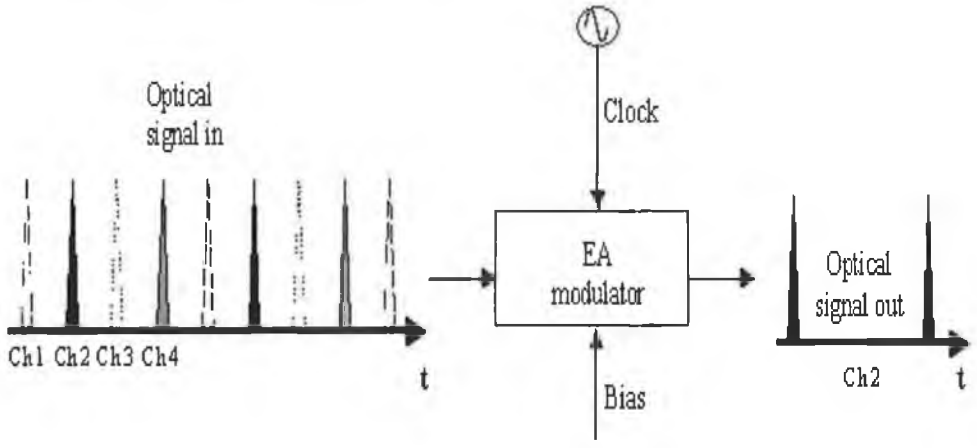

Figure 2-5: Basic configuration of a simple EA modulator used as a demultiplexer

In electrically controlled demultiplexing, the electronics only have to operate at the data rate of the base channel. A 10 Gb/s channel can be selected from a 40 Gb/s data stream, by sinusoidally driving an EA modulator at the channel clock frequency of 10 GHz to create the desired time window (20 ps). However in order to fully demultiplex (select out each channel) a 40–10 Gb/s system we would require 4 separate modulators.

2) All optical demultiplexing: For OTDM communication systems with data rates above 40 Gbit/s, it is not feasible to use electrical switching. Indeed for ultra-high speed systems operating at 100 Gbit/s and beyond, the only solution for demultiplexing is to use

[12] Ratio between the responsivity at high reverse bias and zero bias.

all-optical switching in which optical control signals are used to switch the OTDM data signal. All-optical switching devices are based on instantaneous optical nonlinearities either in optical fiber or semiconductors [34, 35]. A typical scenario involves the injection of both the OTDM data signal and an optical control signal into the nonlinear device. The control signal consists of a high power ultra-short pulse train at the repetition rate of the individual channels within the temporally multiplexed signal, and by synchronizing it with one of the OTDM channels it is possible to demultiplex this channel from the high-speed OTDM signal.

Two high-speed all-optical demultiplexers that have been previously reported, are the Non-linear Optical Loop Mirror (NOLM) [36], based on the Kerr effect in optical fibres, and the Terahertz Optical Asymmetric Demultiplexer (TOAD) [37], based on nonlinearities associated with the Non-Linear Element (NLE)[13]. Both devices rely on producing a difference in phase between two identical data signals propagating in different directions in a loop. Amongst them the most popular all-optical demultiplexer is the TOAD. Figure 2-6 schematically illustrates the operation of a TOAD switch.

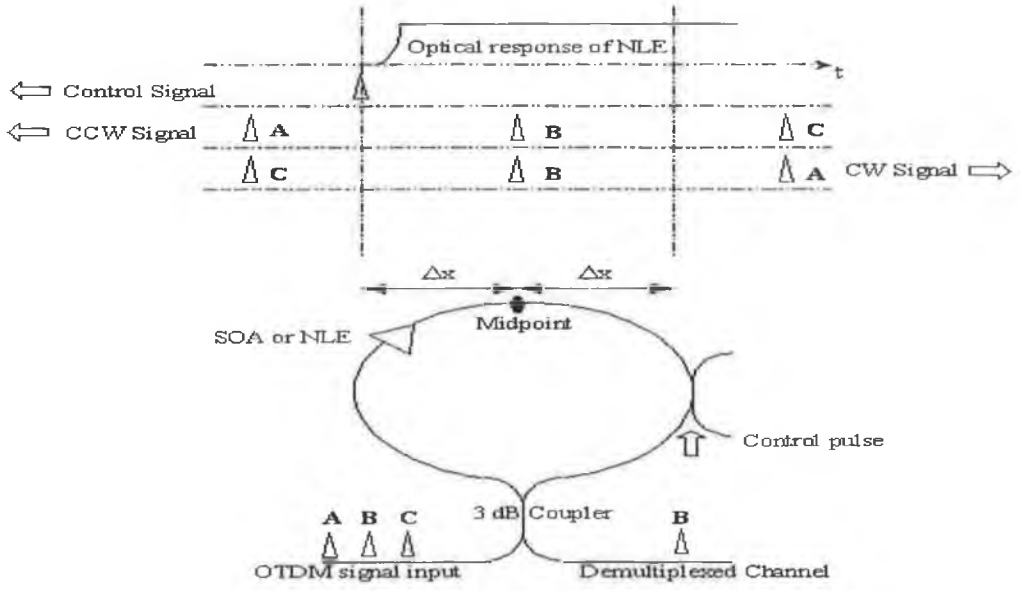

Figure 2-6: Schematic illustration of a TOAD

[13] [E.g.: carrier depletion in Semiconductor Optical Amplifiers (SOA's)]

The OTDM data signal is injected into the TOAD using one input of the coupler, such that it splits into two counter-propagating signals, while the control signal propagates unidirectionally in the loop containing the SOA. The SOA is placed asymmetrically within the loop in such a way that it is offset from the centre by a small but controlled amount [37]. Operation at high speeds (timescales of 1 ps) can be achieved in spite of the slow SOA nonlinearity since the switching time is determined by the offset of the SOA from the midpoint. Synchronizing or aligning the control signal with one channel in the OTDM signal switches a particular channel out [37, 38]. Considering the case shown in Figure 2-6, the transition occurs when both pulses are less than Δx from the loop's midpoint. The clockwise (CW) pulse passes through the NLE during the pre-transition property period while the Counter Clockwise (CCW) pulse passes during the post-transition property period. As a result the destructive interference between the two pulses at the TOAD's output is incomplete, and a pulse emerges. The TOAD based switch has a major advantage in that it can be developed into a very compact demultiplexer, suitable for deployment in OTDM based communication systems however gain depletion in the SOA has been shown to limit the minimum control pulsewidth and thus the maximum switching speed [39].

The second technique mentioned above is the NOLM. It essentially consists of 2x2 fibre coupler with its two outputs joined together using a certain length of fibre [40, 41]. As in the TOAD, the OTDM data signal is injected into one input of the coupler, such that it splits into two counter-propagating signals in the fibre loop. These signals when combined interfere and the overall signal is output through its initial input port. Here again a control signal is injected into the loop such that it propagates unidirectionally in the loop. When this control signal is synchronized with one of the multiplexed data channels, a phase shift is induced by the control signal on the co-propagating signal channel (due to the nonlinear refractive index of the fibre). This in effect switches out the chosen data channel, which is then output through the second input port of the coupler. The remaining data channels of the OTDM signal are then output through the same coupler port as they entered. The configuration of a NOLM demultiplexer is schematically shown in Figure 2-7.

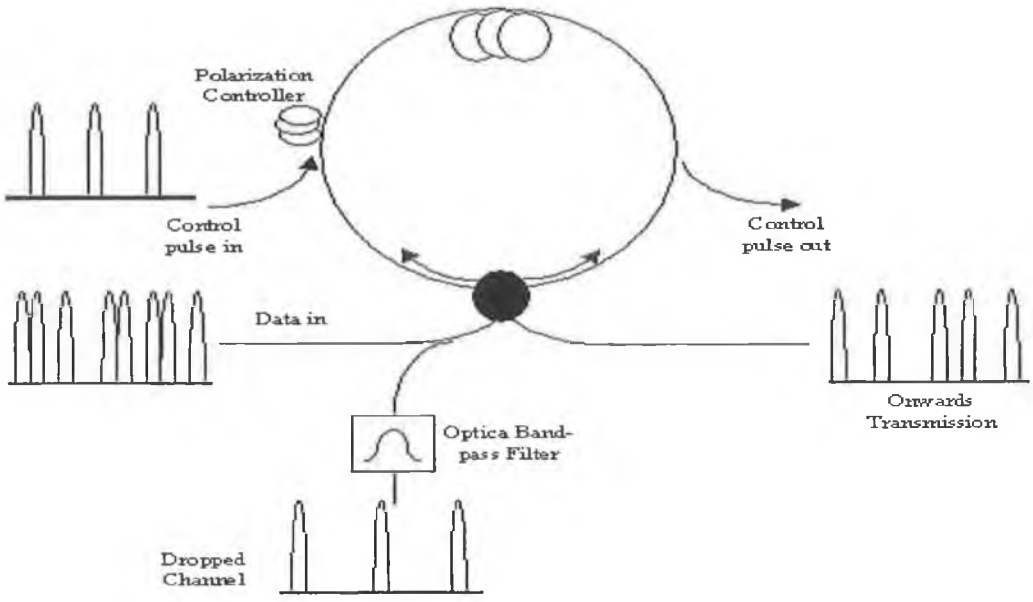

Figure 2-7: Schematic illustration of a NOLM

Although NOLM demultiplexers have sub-picosecond response times and have recently demonstrated all-optical demultiplexing in systems operating at up to 640 Gbit/s [42], a number of factors limit the performance of these devices. For example, high speed switching in the NOLM requires specialty fibre with high nonlinear index levels and precise wavelength control of signal and control pulses about the fibre zero dispersion wavelength [43].

2.3.2.6 Clock recovery

Regardless of the all-optical demultiplexing method used the generation or extraction of a control (clock) signal is vital. The extraction of a clock signal from the high speed OTDM signal is usually done at the base rate of the individual data channels. Depending on the base rate (2.5 Gb/s – 40 Gb/s) many different techniques could be employed in the recovery of a clock signal. Electronic and optical phase locked loops are two of the common methods which have been demonstrated at 40 and 50 Gb/s respectively [13]. Other clock recovery schemes involve more advanced schemes based on self-pulsating laser diodes and fibre modelocked Erbium ring lasers [44-46].

2.4 WDM transmission systems

Another multiplexing technique is Wavelength Division Multiplexing (WDM), which uses the wavelength of light as a degree of freedom for the simultaneous transmission of one or more wavelength signals through one fibre [47,48]. Therefore by using WDM, one can exploit the huge bandwidth available by carving up the optical transmission spectrum (available bandwidth of about 30 THz ~ 200 nm – 80 nm in the 1310 window and 120 nm in the 1550 nm window), into a number of non-overlapping wavelength bands with each wavelength supporting a single channel operating at an arbitrary rate. Obviously this brings about corresponding challenges such as the design and development of appropriate network architectures, protocols and algorithms.

Similar to any other multiplexing technique WDM multiplies the throughput or the transmission capacity of a single fibre. A provision of such efficiency avoids the need to install new fibres in existing systems thereby reducing the total fibre count. More importantly its major attraction is that it provides room for expansion with increasing bandwidth requirements. Hence its use is most widespread in backbone systems where there is a need for enormous capacity. WDM is also employed in Metro systems that typically span over a few kilometres. In comparison to OTDM which is still at its infancy, WDM is a much more mature technology. Furthermore it also has an edge over OTDM in that protocol non-transparency and timing synchronization problems are avoided.

2.4.1 Generalized system

A simple schematic of typical WDM optical communication system is shown in Figure 2-8. At the transmitting end there are several[14] independently modulated light sources, each emitting at a unique wavelength. Each optical channel is modulated separately by direct or external modulation. The modulated wavelength signals are then combined in a multiplexer. This could be a passive multi-input coupler although wavelength selective optics is preferred to isolate the input signals from each other. At the receiver end a

[14] In general the light sources are separate, but a single broadband source could be used with proper optics to supply all the wavelengths.

demultiplexer (optical filter) is then used to select out or direct particular wavelength channels before the signal is passed on to be detected.

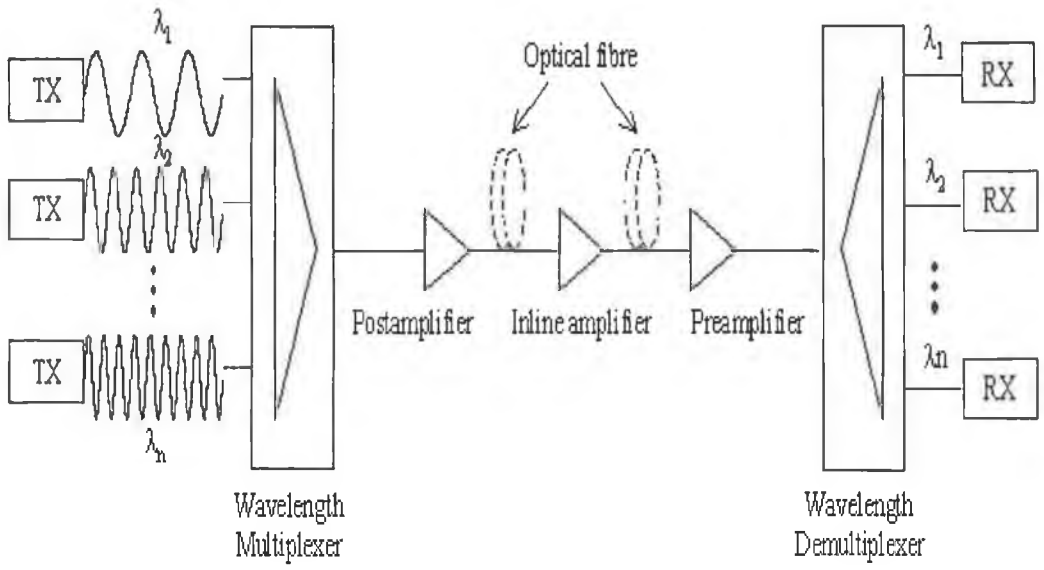

Figure 2-8: Schematic illustration of a generalized WDM system

2.4.2 Enabling technologies

Having looked at the basic operating principles of WDM, the next aspect described is the components needed for its realization. These components vary in complexity from simple passive optical couplers to sophisticated tunable sources and filters. Optical amplifiers are discussed first since they are the main components to have facilitated the designing of WDM technology

2.4.2.1 Optical amplifiers

Setting up an optical link involves the formulation of a power budget. Repeaters are then added when the path loss exceeds the available power margin. All signals require regeneration or amplification in long haul systems. Traditionally, the amplification of an optical signal was done by using conventional repeaters, which entails opto-electric conversion, electrical amplification, retiming, pulse shaping and then electro-optic conversion. Although electro-optic regenerators work well for moderate speed single wavelength operation, they are impractical for multiwavelength (WDM) systems since each wavelength needs a separate regenerator thereby increasing cost and complexity of the system. Currently WDM systems solely use all optical amplifiers to amplify all

wavelengths within particular operating ranges. These devices are used to amplify lightwave signals for the two long wavelength transmission windows of optical fibres [49, 50].

A stimulated emission process is used to boost the power levels of the incident light. The mechanism to create population inversion for stimulated emission is the same as in lasers diodes. Optical amplifiers can boost incoming signals but cannot generate a coherent output by itself due to the fact that it lacks an optical feedback mechanism. The basic operation involves the device absorbing energy from an external source (pump) to produce population inversion. An incoming signal then triggers these excited electrons to drop to lower levels through a stimulated emission process, thereby producing an amplified signal. Optical amplifiers can be classified under two categories as Semiconductor Optical Amplifiers (SOA) [51, 52] and active fibre or Doped Fibre Amplifiers (DFA) [53]. The most popular material for long haul communications applications is a silica fibre doped with Erbium (Er), and is known as an Erbium Doped Fibre Amplifier (EDFA) [54,55]. They are commonly used in the industry to operate mainly in the standard C – band (1530 nm – 1560 nm).

Pumped by a 980 or 1480nm laser, the energy level of the Erbium atoms jump. The optical pumping process requires the use of three energy levels. The pumped photons raise electrons into the excited state. From the top energy level the electron releases some of its energy and drops to the desired lasing level. Some atoms return to the ground state via spontaneous emission. However most of them are knocked back by signal photons (1510 nm and 1600 nm) and return to the ground state. This makes the Erbium ions emit a photon with a wavelength identical to the signal, thus providing gain. Since the pump photon must have a higher energy than the signal photon, the pump wavelength must be shorter than the signal wavelength.

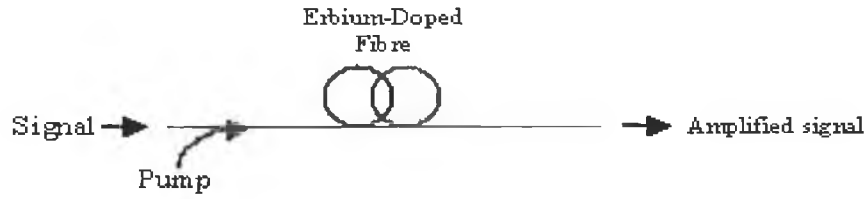

Figure 2-9: EDFA - stripped down

Generally the operation of an EDFA is limited to the 1530 nm – 1560 nm region due to the fact that Erbium atoms absorb light at shorter wavelengths damping possible amplification and at longer wavelengths the gain drops drastically to very low levels. Furthermore Erbium has a low saturation threshold at longer wavelengths. This means that after a certain point, Erbium will not respond to more pump photons. One of the important characteristics of an EDFA is that its gain is wavelength dependant in its normal operating window of 1530 nm – 1560 nm [56]. Therefore on a stricter basis Erbium's gain curve is less smooth outside the small window of about 10nm (1545-1555 nm). When it comes to the operation of an EDFA in a multi-channel environment the latter effect gives rise to a gain variation problem. The variations on per channel gain are cumulative thereby causing a gain ripple between the wavelengths in a cascaded amplifier set-up, which would lead to large signal to noise ratio differential among the channels. If there were a single dB of gain ripple in an EDFA, then it would add up span after span. Numerous techniques are available for the equalization of per-channel gain variation. One of such techniques involves the use of filters or compensating Bragg gratings that reduce the power at the strongest lines [57-59]. Another technique involves the use of Raman amplifiers, which have a stronger gain at wavelengths where EDFA's have a weaker gain. Most of these techniques equalize the gain reasonably well but do not achieve a totally flat gain but a gain flat to within 3 dB.

Multiwavelength operation of the EDFA does pose a few other problems as well. As channel counts increases, the amplification factor is reduced since all channels draw their power from a single source. Furthermore the saturation effect also limits the degree of amplification possible at all wavelengths. Thus as more channels are added, the output signal at each wavelength decreases slightly as the output power saturates. A way around this is to increase the level of pumping but this affects the gain profile: more power

equals less bandwidth and vice versa. Therefore it pays to increase the gain medium rather than the power. The latter could be achieved by lengthening the fibre component or by increasing the concentration of the Erbium dopant. An increase of 4-5 times more than the standard is required to get gain comparable to the C-band. Pouring in Erbium would not work because at high concentrations Erbium ions tend to cluster together. A way of overcoming this limitation is to use Aluminium, which tends to distribute the Erbium atoms more evenly and efficiently through the length of the fibre [30]. Another detrimental effect of an EDFA that needs to be considered is the noise. The dominant noise generated in an EDFA is amplified spontaneous emission (ASE). ASE originates from the spontaneous recombination of electrons and holes in the amplifier medium. Such a recombination gives rise to a broad spectral background of photons that get amplified along with the optical signal. This effect is shown in Figure 2-10.

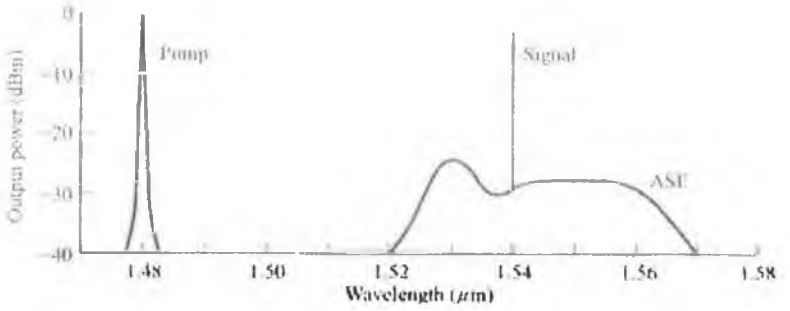

Figure 2-10: Operational characteristics of an EDFA

With the current advances in laser and associated technologies many new channels outside the C-band have come into existence. L-band amplifiers are relatively a new technology. By combining the EDFA with a Raman amplifier or by increasing the length of the doped fibre it has been shown that the gain could be boosted at higher wavelengths [60, 61].

Amplifiers occupy three typical locations in a long haul network. First comes the post or power amplifier. This has a simple design since its only job is to provide an initial boost for the transmitted signal. Next comes a series of line amplifiers. This fits in between a span of around 80 km of fibre. Finally we have the preamplifier to enhance the incoming signal strength before the receiver end. Such an arrangement is called a multistage set-up.

Since the mid 90's the workhorse has been the EDFA. It continues to pace the network evolution with the aid of higher pump sources and integrated functions such as gain flattening. EDFA's not only have enabled Dense Wavelength Division Multiplexing (DWDM) but also have defined it. The complexity of amplifiers increases as issues such as fibre non-linearities, receiver power, network topology, and a host of other factors are taken into account. Such issues impose severe demands on amplifiers, which in turn have to be extremely adaptable in design.

2.4.2.2 Passive components

Many important fibre optic components are passive devices in the sense that they do not require input power to operate on optical signals [62]. Passive components can be fabricated either by using optical fibres or by means of planar waveguides. Optical couplers are the most common of such passive devices and can be used to combine or split light [63]. The splitting ratio is the amount of power that goes to each output and the most common one is the 50:50 coupler better known as a 3 dB coupler. Typical fused bionical tapered couplers experience a return loss of 40-50 dB and an insertion loss of about 1-2 dB. Such passive couplers could be used as multiplexers in WDM systems. Another type of a passive device is the optical isolator that transmits light in only one direction. It plays an important role by preventing back reflections and scattered light from reaching sensitive components, particularly lasers. This blocking of light in one direction is based on polarization. The optical circulator is closely related to the optical isolator in both its function and design. Most attenuators are also passive devices. They block a specified fraction of light at certain wavelengths and can be used to equalize powers on all the WDM channels. Other passive devices such as Optical Add/Drop Multiplexers (OADM) direct or switch wavelengths to different destinations and are an important requirement in current WDM optical networks. OADMs split one or more wavelengths from a WDM signal and compensate by adding one or more others in their place. The borderlines of passive optical technology are so hazy that many components can be categorized under this class. Currently the label passive optical networks (PON) have come into wide use to describe certain systems that distribute signals to many terminals and are basically used to reduce the cost by avoiding the use of active components between terminals.

2.4.2.3 Fixed and tunable filters

Optical filters are frequently used in optical communication systems to separate different wavelengths [64-66]. In WDM systems, the optical filter performs functions from simple filtering in multiplexers and demultiplexers to more complex functions such as gain equalization, channel monitoring and dynamic provisioning in OADMs [67, 68]. Another key area of usage is in tunable lasers.

Commercially there are many types of filters available today. One of the first filters used in telecommunications was based on the fused coupler, in which the wave in one waveguide couples into an adjacent waveguide. This coupling is wavelength dependent, and by controlling the length of the coupling region it is possible to make a device that takes two wavelengths from a single waveguide and demultiplexes them at two output ports. A more useful of such types is the thin-film filter that uses many thin layers of dielectric material, with alternating high and low index of refraction [69-71]. This gives the filter its desired wavelength-dependent reflection and transmission characteristics.

Transmitted wavelengths are given by the formula

$$N\lambda = 2nD\cos\theta \qquad \textbf{Equation 2-1}$$

Where N = integer

n = refractive index of the layer

D = layer thickness

θ = angle of incidence

Tilting or more appropriately moving the filter thereby changing the angle of incidence (as in equation 2-1) can achieve tunability in such filters.

Another common type is the grating, which is a dispersive filter. A typical reflective grating consists of a mirrored surface with tiny grooves. When illuminated, the light reflected from one groove interferes with the light reflected from other grooves, and at certain wavelengths (or places in space) these multiple reflections interfere constructively (they add in phase), while in other regions they interfere destructively (they add out of

phase). The Fabry-Perot (FP) interferometer [72] is another type of filter. This filter consists of two highly reflective mirrors, separated by a small distance. Depending on the spacing and index of refraction between the mirrors, at some wavelengths the multiple reflections are cancelled, while the transmitted wavelengths are reinforced [66, 73]. At these wavelengths the overall transmission is high and the cavity is said to "resonate" at these wavelengths so that light passes through in seeming violation of the fact that both mirrors are individually highly reflective.

$$2L = \frac{N\lambda}{n} \qquad \textbf{Equation 2-2}$$

Where N = integer

n = refractive index

L = length of the cavity

For other wavelengths the transmitted waves add out of phase. At these wavelengths the interferometers overall transmission is low while its reflectivity is high. Tunability of these filters could be achieved by changing the length of the cavity. Closely related to the FP interferometer is the Fiber Bragg Grating (FBG) [74-76]. FBGs consist of a region in which the index of the fiber varies periodically between high and low, and they are formed in optical fibers by exposing the fiber to interferometric patterns from a UV laser. The FBG's central wavelength is governed by the following equation

$$\lambda_c = 2n_{eff} D_c \qquad \textbf{Equation 2-3}$$

Where n_{eff} =effective index of the fibre containing the grating

D_c = Period size of the index of perturbation

As in the FP interferometer, multiple reflected and transmitted waves result. For a specific wavelength the reflected waves all add in phase, and at this wavelength the grating appears to be highly reflective, while transmitting all the others. The tunable grating is an extension of this mature technology. The centre wavelength (λ_c) can be changed by stretching the fibre that linearly lengthens the period of the index of perturbation.

One of the most useful filters in WDM optical telecommunication systems is the arrayed waveguide grating (AWG) [77]. As its name implies, the AWG uses an array of optical waveguides in which the lengths of adjacent waveguides differ by a fixed amount. The input light from a single fiber illuminates all these waveguides, and because the waveguides are of different lengths, the phase of the light (at the output end of the array of waveguides) varies by a fixed amount, from one waveguide to the next. This variation results in a wavelength-dependent diffraction pattern that is similar to the one from a plane grating (thus the name "arrayed waveguide grating"). This diffraction pattern is then arranged so that different wavelengths illuminate different output fibers. So the AWG serves as a wavelength demultiplexer by taking multicolored light from a single fiber and sending different colors to different output fibers (it can also work in reverse as a wavelength multiplexer).

The Mach-Zehnder interferometer [78] consists of a pair of couplers connected by two paths of unequal length. The unequal length results in some wavelengths being output to the top port, and other wavelengths being output to the bottom port. This filter finds applications in interleaving the signals from two fibers, each of which carries information that has already been less finely multiplexed in the wavelength domain.

One of the most important performance characteristics, as per its contribution to system performance, is the filter's transmission loss at the center of its passband. This loss affects the overall system attenuation for that channel, and so it enters into considerations about the number of required amplifiers, the optical signal-to-noise ratio, and the bit-error rate (BER). However, it is not enough to simply have high transmission at a single wavelength, because there is always variability in the filter's center wavelength and the center wavelength of the laser transmitter. When used in tunable lasers this variability means the laser transmitter might actually be operating at a wavelength that is slightly off center relative to the peak transmission point of the filter.

Designing optical filters with square response curves[15] would make the system more robust. The ideal response is one with a flat top, infinitely steep sides, and complete rejection of light outside the passband. Of particular importance is the amount of attenuation that the filter presents to out-of-band wavelengths. If the filter allows even small amounts of optical power from adjacent channels to leak through, it will result in added crosstalk, which will increase the BER.

2.4.2.4 Fixed and tunable sources (lasers)

Physical characteristics of lasers, fixed or tunable, such as linewidth, frequency stability, and frequency chirp etc. can affect the performance of WDM systems. The laser spectral width not only affects the spacing of the channels but also acts as one of the main contributors to dispersion. Common frequency instabilities seen in lasers are mode hopping and mode shifting. Stable injection current sources and temperature controllers could be used to overcome these instabilities.

As the number of wavelengths in WDM (DWDM) systems escalates toward the 100-plus range, tunable lasers become increasingly important, in containing design and manufacturing complexity, by reducing the number of different lasers that must be produced and deployed [79, 80]. Unlike lasers manufactured for just a single wavelength, a tunable laser can be rapidly retuned to support several different wavelengths in the International Telecommunication Union (ITU) grid for WDM.

Maintaining an inventory of dozens of different laser transmitters, one for each optical channel in a WDM system would create logistical nightmares for telecommunications carriers making broadly tunable lasers a boon to both developers and users of WDM fiberoptic systems. The flexibility afforded by tunable lasers could also support, for the first time, wavelength-routing capabilities in the optical domain - a key element in the development of all-optical networks. With tunable lasers, network operators will be able to route traffic over fixed paths to different points in the network by changing the laser emission wavelength. Other potential applications might include network protection and the use of a single wavelength per large business customer to create future virtual private

[15] Determined by the order of the filter

networks [81]. The huge potential demand has created a quest for the ideal tunable laser, able to generate constant output power across a broad range of wavelengths so it could serve as a near-universal replacement. Its wavelengths should be adjustable on-site and ideally from remote operations centers. Considerable progress has been made both with several approaches under development and several commercially available types. The major characteristics of interest with tunable lasers are the tuning range, tuning time, continuous or discrete tunability and reasonable cost.

Tunable lasers, regardless of their specific architecture, contain three basic elements, namely a source diode with an active gain section and a resonant cavity, a tuning mechanism for varying and selecting wavelength and a means of stabilizing the output wavelength. Source diodes are generally a variation of the Fabry Perot (FP) device with an exception in the case of Vertical Cavity Surface Emitting Lasers (VCSELs) [82]. Each variety of different laser structure has its own advantages and disadvantages.

Two of the basic structures are distributed Bragg reflector (DBR) and distributed feedback (DFB) lasers, and are achieved by introducing a diffraction grating [83]. This diffraction grating (referred to as a Bragg grating or Bragg reflector) provides feedback to the optical signal oscillation and thereby acts to select out a single mode of oscillation (wavelength). Because the wavelength is selected by the spacing and refractive index of the DFB or DBR grating, adjusting either could tune the laser. In practice it is easier to change the refractive index, which depends on both temperature and current density, allowing development of temperature- and current-tuned lasers. In a DBR laser, the active region, which provides gain, and the grating, which provides wavelength selectivity, are separated. In a DFB laser, the two functions are combined, by having a reflector embedded in the cavity gain region [84] (Figure 2-11). They are commonly tuned to different wavelengths by changing the temperature, either through drive-current changes or a controlled heat sink. The temperature can be precisely controlled to within a tenth of a degree, which in turn produces a well-defined output wavelength. The DFB lasers are well characterized and extensive studies have verified their reliability. While DFB lasers offer manufacturing, performance, and operational advantages, their effective

tuning range tends to be limited because the efficiency and output power of the device goes down as the tuning temperature goes up.

DBR lasers have a reflector at each end of the laser cavity and use current tuning in the passive reflector region [85]. The typical continuous tuning range is about 10-20 nm, and it is limited by current injection. The DBR structure is electrically isolated from the active stripe, and changes in its operating temperature and/or in the current passing through it alter its refractive index, changing the wavelength it selectively reflects. The main drawback in using DBR lasers as tunable lasers is the difficulty of controlling the length of the optical path between the reflectors at the ends of the cavity.

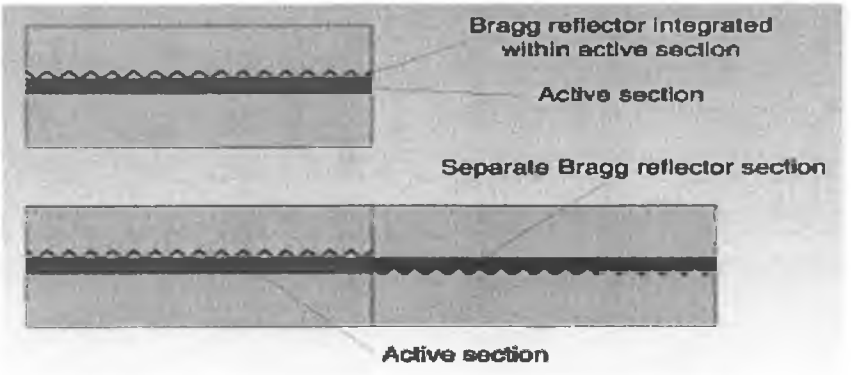

Figure 2-11: Schematic diagram of a DFB and a DBR lasers

Other laser structures exist that offer a wider tuning range, although they are more complex to manufacture and control. The Sampled-Grating Distributed Bragg Reflector (SG-DBR) [86] is one of such tunable lasers. A related approach to the SG-DBR tunable laser is the Grating assisted Co-directional coupler with Sampled Reflector (GCSR) [87]. External-Cavity Lasers (ECL's) [88, 89] are another configuration in which the wavelength selection and tuning functions are external to the semiconductor material. Tunable lasers continue to evolve and with the advances in design, current challenges in performance such as the tuning time, output power etc. may soon be a hitch of the past.

2.5 Limitations of performance in WDM systems

Optical fibre transmission technology has found widespread use in current networks of diversified speeds and sizes. However the use of optical technology in such networks

involves important challenges that have to be met in order to overcome various signal impairment effects [90-92]. Most of these limitations are brought about by the characteristics of silica fibre and can seriously degrade network performances. Such limitations could be broadly classified as linear and nonlinear effects. The inhibition of the performance of WDM optical communication systems is brought about by three major factors, of which attenuation and dispersion are linear fibre effects while SPM, XPM, Four Wave Mixing (FWM), Stimulated Raman Scattering (SRS) and Stimulated Brillouin Scattering (SBS) fall under the nonlinear category.

2.5.1 Attenuation

In long-range fibre optic communication systems, amplification or electro-optic regeneration of signals becomes a must. The latter proved to be impractical for WDM systems since each wavelength would require a separate regenerator. Optical amplifiers, which work far better by amplifying all wavelengths in their operating range, are used to overcome the limitation brought about by attenuation. An added impediment with fibre attenuation is that it varies significantly with wavelength. Loss in the 1310 nm region is about 0.35 dB/km while the 1550 region exhibits about 0.2 dB/km. This variation brings about unequal channel powers especially in Coarse Wavelength Division Multiplexed (CWDM) systems. However, at a price of complexity and cost, the variation can be accounted for by attenuating the other channels. Another solution would be to the use the low water absorption peak all wave fibre (Lucent), which has a more gradual variation across the wavelengths (Figure 2-12). A variation of 0.008 dB is faced when going from 1530 nm to 1610 nm. The techniques used to equalize amplifier gain could be used to compensate for this small variation as well.

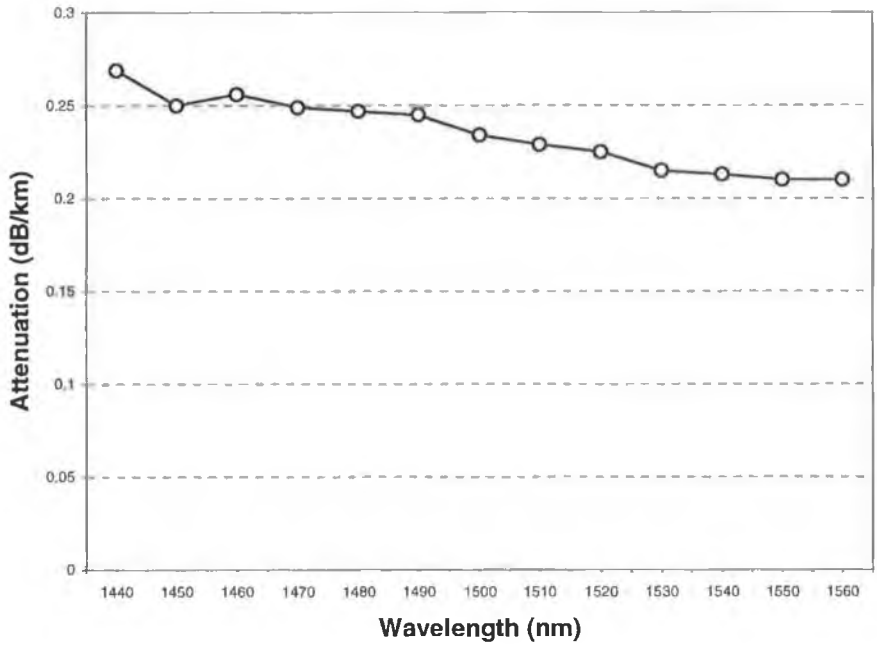

Figure 2-12: Attenuation profile of all-wave fibre

2.5.2 Dispersion

A WDM system finds material or chromatic dispersion to be the most detrimental of all types of dispersion. In a dispersive medium, the index of refraction is a function of the wavelength. Since WDM systems consist of many wavelengths, each of these wavelengths sees a different dispersion factor. This makes it necessary to consider the rate of dispersion change as a function of wavelength (dispersion slope) when designing WDM systems. As previously mentioned broadening of the pulses leads to ISI. The limit of the transmission distance due to fibre chromatic dispersion is given as follows [93]:

$$B^2 L = \gamma \frac{c}{\lambda^2 |D(\lambda)|}$$ **Equation 2-4**

Where B = transmission speed

γ = Chromatic dispersion coefficient (depending on the modulation/demodulation format – Appendix C)

c = Speed of light in a vacuum

$D(\lambda)$ = Chromatic dispersion at the signal wavelength

Among the modulation / demodulation formats listed in Appendix B, The Intensity Modulation – Direct Detection (IM-DD) scheme is the strongest against chromatic dispersion while the Continuous Phase Frequency Shift Keying (CPFSK) is the most sensitive.

Various compensation schemes are available to overcome this limitation. At present an overwhelming amount of deployed fibre has positive dispersion meaning that longer wavelength photons travel slower than those of shorter wavelengths. Therefore one simple solution to overcome dispersion would be to periodically place an optical device that produces negative dispersion (shorter wavelength photons travel slower than those of longer wavelengths). Even though a number of solutions have been proposed only two such non-tunable negative dispersion elements have been potential candidates for deployment [94, 95]. They are Dispersion Compensating Fibre (DCF) and chirped Fibre Bragg Gratings (FBG). DCF exhibits high levels of negative dispersion that is usually much larger than the conventional Single Mode Fibre (SMF).

Although most systems make use of DCF, the spectral dependence of SMF and DCF is not exactly balanced. Since the cumulative dispersion is zero at only one-wavelength exact compensation can be made for only one wavelength as shown in Figure 2-13 below.

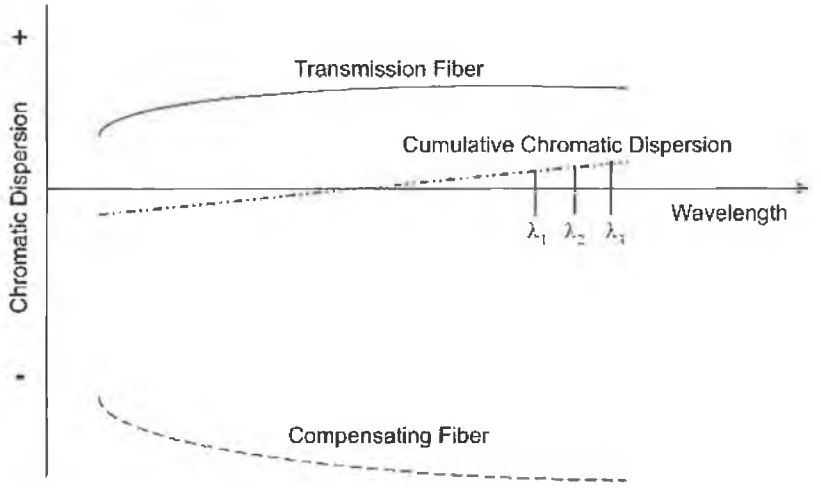

Figure 2-13: Cumulative dispersion in WDM systems

As previously mentioned each wavelength faces a different dispersion and in this case a different compensation as well resulting in residual dispersion, which tends to accumulate with distance (Figure 2-14).

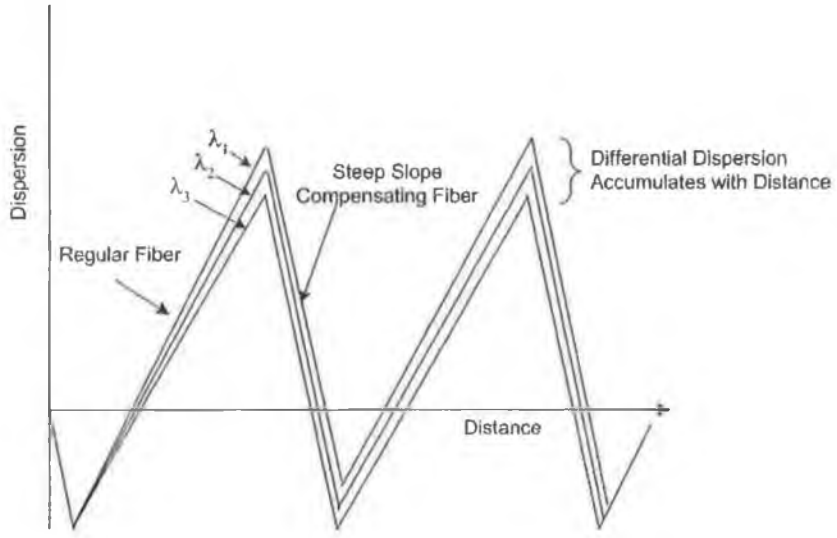

Figure 2-14: Residual dispersion in WDM systems

Fibre that induces zero chromatic dispersion where all frequencies travel at the same speed is incompatible with WDM systems. If all channels travel at the same speed down the fibre, then deleterious effects such as cross phase modulation and four-wave mixing are produced. Hence a certain amount of dispersion for minimizing the effect of non-linearities is required in the deployment of WDM systems.

Even though PMD can affect data transmission rates it has little dependence on wavelength, hence it is not a peculiar problem to WDM systems. One may also use soliton transmission technologies on each wavelength channel in order to compensate for dispersion.

2.5.3 Non-linearities

The response of any dielectric to lightwaves is non-linear. As long as the signal power in a fibre is at a low level, fibre can be considered as a linear system. However, when the optical power in a fibre increases, the non-linear effects become non negligible. These non-linear effects in fibre may have a significant impact on the performance of WDM optical communication systems [96, 97]. The processes SBS, SRS and FWM provide

gain to some wavelength channels while depleting power from the others thereby producing crosstalk between the wavelength channels. Both SPM and XPM only affect the phase of the signals, which causes chirping, which in turn can worsen pulse broadening due to dispersion. All non-linear effects can be classified broadly by considering the energy exchange between the optical field and the non-linear medium.

2.5.3.1 Elastic non-linear effects

Here no energy is exchanged between the lightwave electromagnetic field and the dielectric medium. The optical Kerr effect is a major elastic non-linear effect that has to be faced in optical fibre system design. This type of non-linearity arises from intensity dependant variations in the refractive index in a silica fibre and produces effects such as SPM, XPM and FWM.

1) Non-linear refraction – In optical fibres the index of refraction is dependent on the optical intensity of the signal propagating through the fibre. This weak dependence is given by

$$n = n_0 + n_2 I = n_0 + n_2 \frac{P}{A_{eff}} \qquad \textbf{Equation 2-5}$$

Where n_0 is the ordinary refractive index of the material and n_2 is the non-linear index coefficient. This non-linearity in the refractive index is known as the Kerr non-linearity, which produces a carrier induced phase modulation of the propagating signal. This effect in single wavelength links gives rise to SPM, which converts optical power fluctuations in a propagating light wave to spurious phase fluctuations in the same wave [98,99]. Figure 2-15 illustrates the phenomenological description of SPM and its effect on a pulse as it propagates in a fibre.

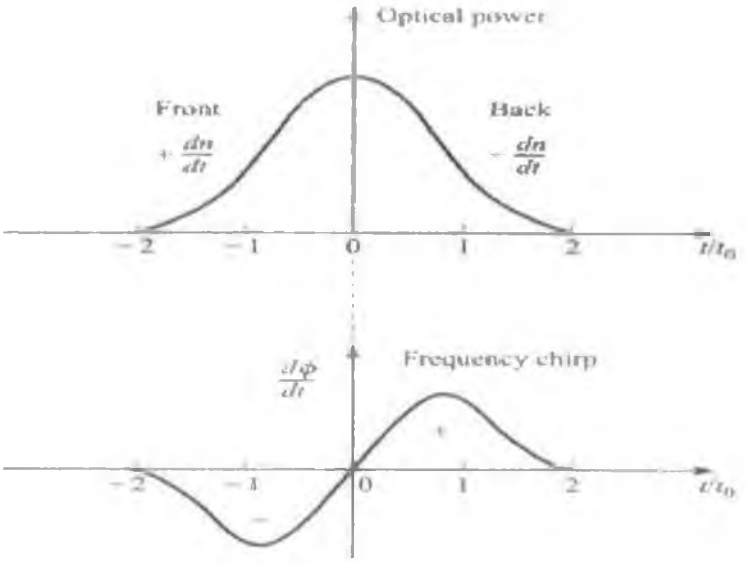

Figure 2-15: Spectral broadening of a pulse due to SPM

In a medium that has an intensity dependant refractive index, a time varying signal intensity will produce a time varying refractive index. Thus the index at the peak of the pulse would be different to that at the edges. The leading edge sees a positive dn/dt whereas the trailing edge sees as negative dn/dt. The temporally varying index change results in a temporally varying phase change as shown in the figure above. Therefore as previously mentioned since the phase fluctuations are intensity dependant, different parts of the pulse undergo different phase shifts. The consequence is that the instantaneous optical frequency differs from its initial value across the pulse leading to what is known as frequency chirping.

This effect of chirping may result in GVD induced spectral broadening of the pulse as it travels along the fibre. By using different types of fibre this effect could also be used advantageously to compress the pulse and compensate for dispersion.

In WDM systems, the Kerr non-linearity converts power fluctuations in one channel to phase fluctuations in other co propagating channels. This effect is known as XPM [98-100].

Four Wave Mixing (FWM) – In many non-linear phenomena the fibre plays a passive role except for mediating the interaction among several optical waves through a non-linear response of bound electrons. Such processes are referred to as parametric processes, as they originate from light induced modulation of a medium parameter such as the refractive index [101]. FWM is a third order non-linearity in silica fibres, which is analogous to intermodulation distortion in electrical systems [102], so that in multi-channel systems three optical frequencies mix to generate the fourth of frequency:

$$f_g = f_i + f_j - f_k \qquad \textbf{Equation 2-6}$$

In all high capacity long haul communication systems, the effects of chromatic dispersion and non-linearities accumulate during propagation, imposing limits on the achievable performance. Chromatic dispersion at 1.5μm can be effectively reduced by using Dispersion Shifted Fibre (DSF). The use of low dispersion fibre reduces the phase mismatch naturally provided by fibre dispersion, thereby enhancing the generation of four wave mixing. FWM can cause severe cross talk in multi-channel systems, since energy is transferred from the pump pulses into the bit slots of spaces (generating ghost pulses) and into the bit slots of the marks (inducing jitter in the energy of the marks). For N channels launched, the number of mixing products (M) generated is:

$$M = \frac{1}{2}(N^3 - N^2) \qquad \textbf{Equation 2-7}$$

Unequal channel spacing ameliorates the effects of mixing products on the performance of a WDM system [103]. An easier alternative to prevent the generation of those products in the first place can be achieved by avoiding phase matching [104]. The latter could be achieved by retaining low chromatic dispersion in the link.

2.5.3.2 Inelastic non-linear effects

The inelastic non-linearity is another class of non-linearity where the optical field transfers part of its energy to the dielectric medium. This category encompasses two inelastic non-linear scattering processes.

1) Stimulated Raman Scattering (SRS) – is caused by the interaction between light waves and molecular vibrations of silica [100, 105]. This effect transfers a small fraction of power from one optical channel to another with a frequency downshift that is determined by the vibration modes of the medium. The light generated at the lower frequencies is called the Stokes wave. The shorter wavelength channel acts as a pump for longer wavelength channels and this leads to cross talk amongst the channels. Under very high input power, SRS causes almost all the power in the input signal to be transferred to the Stokes wave.

If another signal is present at a longer wavelength, the SRS light will amplify it, and the pump wavelength signal will decrease in power since SRS process generates scattered light at a longer wavelength than that of the incident light. Consequently, SRS can severely limit the performance of a multi-channel optical communication system by transferring energy from short wavelength channels to neighbouring higher wavelength channels. Powers in WDM channels separated by up to 16 THz (125 nm) could be coupled through the SRS effect [105]. The limitation in power brought about by SRS is shown in Figure 2-16. The plot shows the maximum power per channel as a function of the number of wavelengths for three different channel spacings [106].

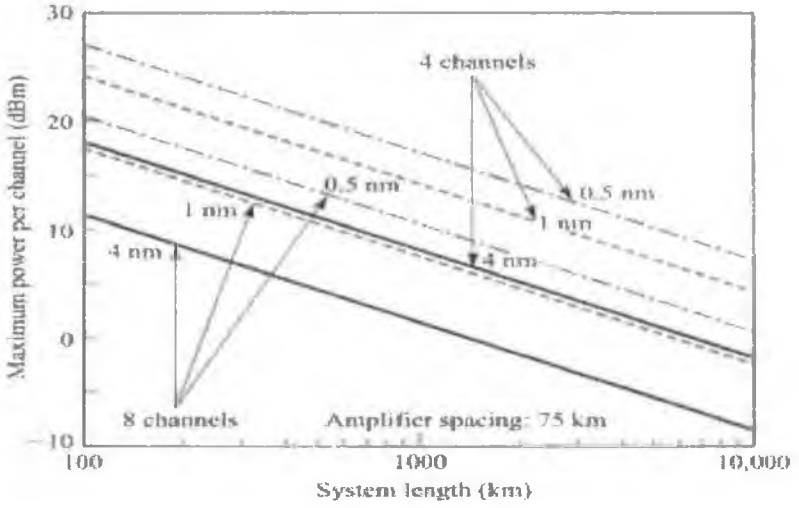

Figure 2-16: Maximum allowable power per channel vs transmission length for 3 different channel spacings [106]

2) Stimulated Brillouin Scattering (SBS) – is similar to SRS except that sound waves rather than molecular vibrations cause the frequency shift [107]. The resultant scattered wave propagates principally in the backward direction in single mode fibres. This backscattered light experiences gain from the forward propagating signals, which leads to a depletion of the signal power. In silica this interaction occurs over a very narrow Brillouin linewidth of $\Delta\nu_B$ = 20 MHz at 1550 nm. Meanwhile the frequency of the backscattered light experiences a Doppler shift given by:

$$\nu_B = \frac{2nV_s}{\lambda}$$ **Equation 2-8**

System impairment starts when the amplitude of the scattered power is comparable to the signal power. Measures such as keeping the power down below the SBS thresholds and increasing the linewidth of the source could be used to reduce the power penalty effects of SBS.

All these non-linearities may limit the number of channels, the spacing between the channels, the maximum bit rate and the optical power on each channel. When any of these non-linear effects contribute to signal impairment, an additional amount of power will be needed at the receiver to maintain the same Bit Error Rate (BER) as in their absence. This additional power (dB's) is known as the power penalty for that effect.

2.5.4 Non-uniform gain of EDFA's

It was shown earlier that the gain of the EDFA varies with wavelength. This leads to a gain ripple across the desired wavelength range. A range of techniques described earlier could equalize this.

2.5.5 Impact of source chirping

The direct modulation of single longitudinal mode semiconductor lasers causes a dynamic variation of the peak emission wavelength, especially at high bit rates. The intermingling of chirping with fibre dispersion can lead to signal distortion and eventually lead to ISI with consequent transmission penalties. This shortcoming could be overcome by operating the laser in Continuous Wave (CW) mode and by applying the modulating signal as a driving voltage on an external modulator. Even though chirp

would still be present, it would be much smaller in comparison to an intensity modulated laser. As a result, external modulation allows the transmission performance to be improved thereby improving the bit rate-span product. Figure 2-17 illustrates this effect by comparing the eye penalty as a function of the fibre length.

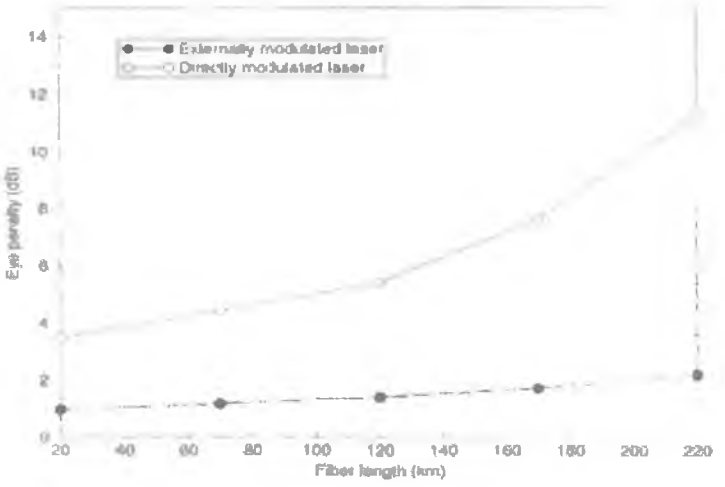

Figure 2-17: Eye penalty vs fibre length for direct and external modulation

2.6 Multiplexing density

The number of wavelength channels that can be transmitted in WDM networks depend on many issues, but can be broadly classified into three key categories. Figure 2-18 (below) schematically illustrates all these three factors.

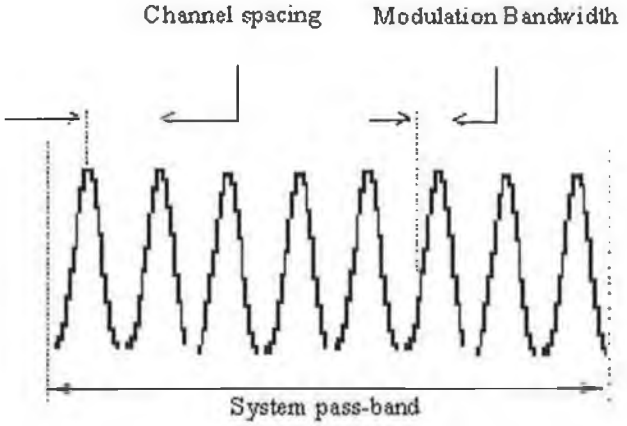

Figure 2-18: Multiplexing density as a factor of channel spacing, system bandwidth and modulation bandwidth per channel

Channel spacing is the first of such factors. Early WDM systems operated with very broad spacing to the extent that some had the channels in different transmission windows. The reduction in spacing has even brought about a change in the name of the technology. Dense Wavelength Division Multiplexing (DWDM) has no specific definition apart from the fact that it has channels packed much closer together in comparison to older WDM systems. Currently the spacings are governed by International Telecommunication Union (ITU) standards. The standards are set around a base frequency of 193.1 THz and a frequency grid with standard increments of 400, 200, 100, 50 or 25 GHz (3.2, 1.6, 0.8, 0.4 or 0.2 μm @1.5 μm). Of course the spacing of the channels are in turn related to many other factors such as XPM, FWM etc.

The total optical bandwidth of the entire system (system passband) is another factor that affects the number of wavelength channels that could be multiplexed. This of course depends on the type of system. In long haul systems the Erbium Doped Fibre Amplifiers (EDFA) bring about this limitation due to their passband. In unamplified systems fibre attenuation and/or dispersion set less severe constraints. Standard EDFA's have their strongest gain in the conventional (C) band that ranges from about 1530 - 1560 nm. However most practical amplifiers cover the center of this band, which then brings the passband down to about 30 nm limiting the number of channels to about 40 assuming that there is 100 GHz spacing. Other alternatives such as EDFA's in the L – band (1570 -1605 nm), Thulium doped fibres and Raman amplifiers are being investigated in order to accommodate more channels in other bands [108,109,110].

Modulated source bandwidth is the third of the factors that falls under the broad classification. This poses the ultimate limit in how closely wavelength channels can be squeezed together. A high quality (low linewidth) source would have an approximate spectral bandwidth of a few (10-50) MHz, especially when operated in continuous wave (CW) mode. However modulating the signal (even with an external modulator) adds on other frequency components to the original signal thereby spreading it over a broader range. The higher the modulation rate, the more frequency components found, hence the broader the resulting bandwidth as shown in Figure 2-19.

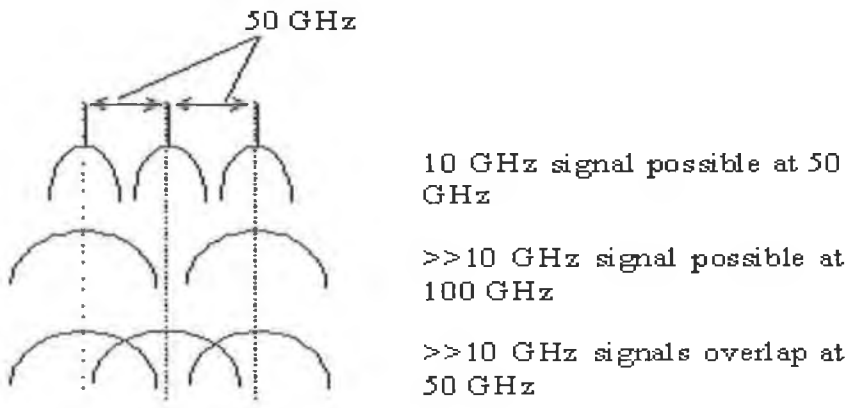

Figure 2-19: Broader modulation bandwidth limits channel spacing

As illustrated in the figure above, the signal modulated at 10 Gb/s remain adequately separated if channels are 50 GHz apart, but the signal modulated at much higher bit rates (>>10 Gb/s) signal tends to overlap with the same 50 GHz separation. In the latter case 100 GHz of separation may be required to avoid crosstalk.

A lot of effort is being put into the scalability of WDM networks with special focus on issues such as fibre nonlinearities involving SPM, XPM, SRS and FWM, the spectral dependence of amplifier gain and the limits they impose on the number of channels and the transmission distance.

2.7 Hybrid WDM/OTDM transmission systems

Ultra high bit rate optical communication systems are essential to construct the high speed / high capacity optical networks needed in the multimedia era. Furthermore the desire to fully exploit the enormous bandwidth of at least 25-30 THz (in the 1.3μm & 1.5μm transmission windows) has been a major incentive and challenge in devising these new optical communication systems. The key hurdle in the commercial development of these networks is the availability of cost effective photonic technologies that will enable the generation, transmission and processing of these vast amounts of data. Many carriers have choice between OTDM and WDM techniques thereby bringing telecommunication networks to another crossroad: faster or denser? Sometime in the future, it is possible that a solution incorporating both technologies will give service providers the flexibility and

strength their networks need. An alternative to having a large number of low data rate wavelength channels is to have a smaller number of wavelengths with very high data rates. Recently, hybrid approaches have been proposed that exploit the parallelism of WDM architectures and the speed of OTDM [111, 112].

The key philosophy behind using a hybrid approach is that state of the art system performance can be achieved without the necessity of operating at the limits of either a pure WDM or OTDM technology platform. Merging of these two multiplexing techniques brings about the merits of both of them.

The mitigation of the various signal impairments have brought about huge advances in very dense WDM technology [113-115] and also in ultra fast optical TDM [116] thereby allowing transfer rates in excess of 1 Tb/s to be achieved on a single fibre. However these corrective measures lead to very expensive and complicated components and networks. Hybrid approaches on the other hand may result in realizing a cost effective, high performance, state of the art optical communication system without pushing the performance limits of a pure WDM or OTDM approach. Different types of networks (access, national or international) might be implemented with the incorporation of different levels of WDM and OTDM.

One of the first WDM/OTDM transmission experiments with a total capacity of 400 Gb/s (4 x 100 Gb/s) was demonstrated in 1996 using a single supercontinuum pulse source [117]. More recently 1.4 Tb/s (7 x 200 Gb/s) transmission [118] and even 3 Tb/s (19 x 160 Gb/s) transmission [119] have been demonstrated. A key requirement for such high capacity hybrid networks, are optical pulse sources that are able to generate wavelength tunable picosecond pulses. In the 1 Tb/s and 3 Tb/s experiments mentioned above multiwavelength lasers were used. The set up used in the 1 Tb/s transmission experiment is shown in Figure 2-20 below.

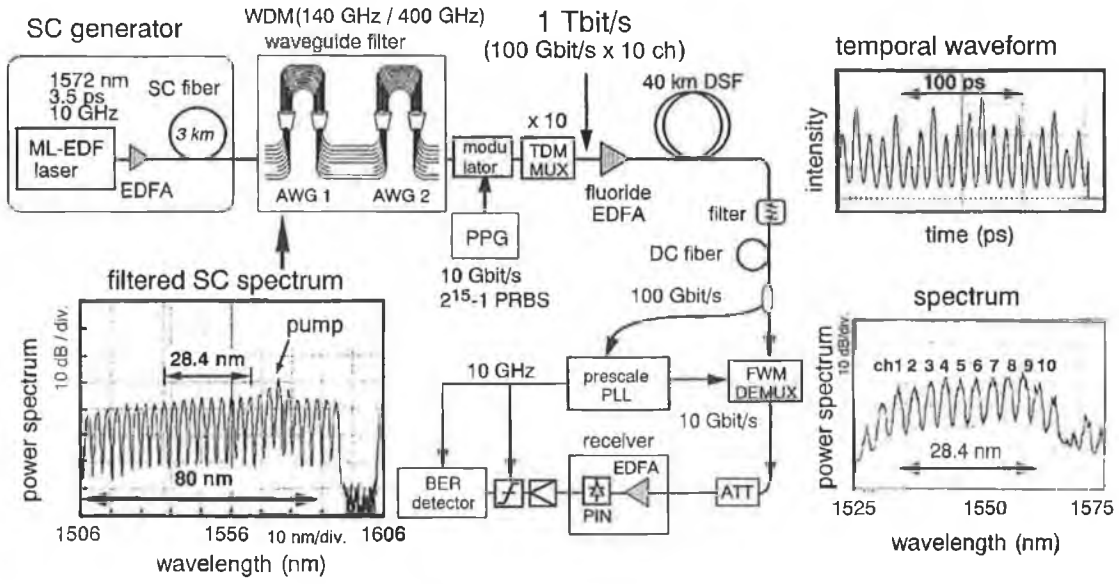

Figure 2-20: 1 Tb/s WDM-OTDM transmission experiment [118].

Here an actively Mode Locked-Erbium Doped Fibre (ML-EDF) laser is used to generate pulses at a repetition rate of 10 GHz. This is then amplified and passed through 3 km of single mode dispersion shifted fibre. When an intense optical pulse transits a low dispersion silica fibre, a Super Continuum (SC) pulse, spectrum of which is spread over a wide spectral range, is induced by the combining effects of various optical non linear processes [120]. By filtering a super broadened SC spectrum with AWG WDM demultiplexers, a multi-wavelength picosecond pulse source is constructed [121] consisting of 10 WDM channels. The 10 WDM channels were then modulated at 10 Gb/s after which they were time division multiplexed to produce 100 Gb/s x 10 channels. White *et al* show another novel method, which involves the use of a Multi-wavelength Grating Cavity (MGC) laser [122] as a multi wavelength picosecond pulse source. Another similar experiment performed by Delfyett [123] involves the use of a mode locked laser as the source of multi-wavelength picosecond pulses. The setup used in this experiment is shown below in Figure 2-21.

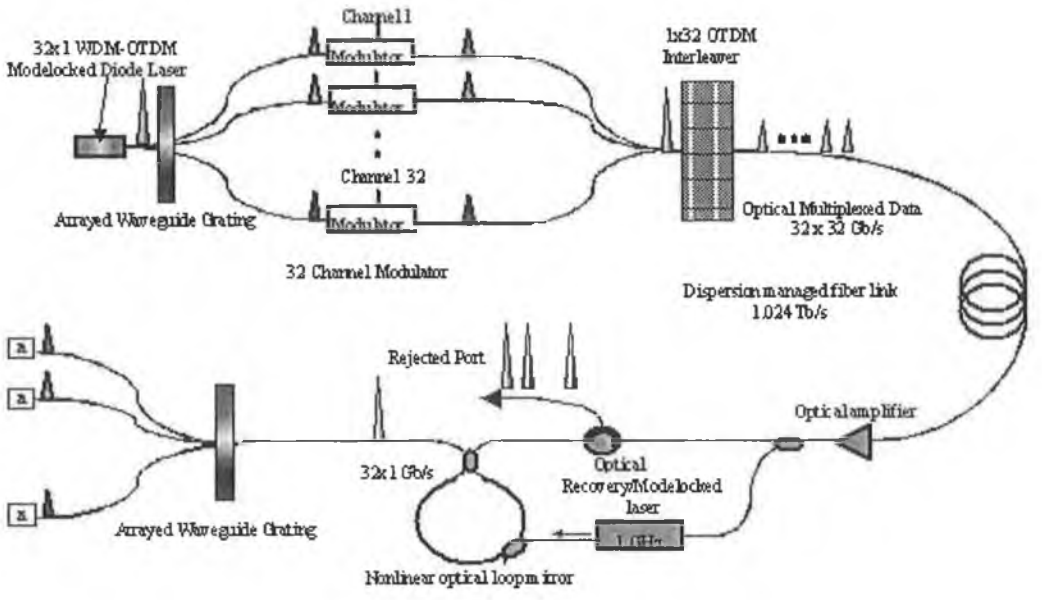

Figure 2-21: Schematic of a Hybrid WDM-OTDM optical link [123]

Wavelength tunable picosecond optical pulses, that are a vital requirement in such hybrid systems, could be obtained by using other techniques as well. Gain switching and pulse shaping using an external modulator are two of such techniques, which are available.

Attention should be given to the limitations that inhibit the performance of such hybrid systems. This is due to the fact that hybrid WDM / OTDM systems combine not only to provide both their merits but also their demerits. One of the major problems is the dispersion slope of the fibre. The gravity of this problem depends on the level of incorporation of WDM and OTDM. It is heightened if there are more wavelength channels in such a way that we occupy the C and L bands. Furthermore temporal spreading of the pulse could bring about ISI especially since the time slot of very high bit rate OTDM signal is very small. For instance in a 1 Tb/s OTDM signal the time slot is only about 1 ps. Temporal jitter is another factor which needs to be given attention essentially due to the same reason of the time slot being very small. Because of the turn on and turn off fluctuations of optical pulses, different portions of the received waveform are sampled from bit to bit. Resulting signal fluctuations lead to the degradation of the signal-to-noise ratio. Not only does it result in power penalties and degraded BER's but also limits the number of OTDM channels thereby limiting the overall hybrid rate.

Another limitation being PMD becomes a force to be reckoned with at very high bit rates. The PMD value for Dispersion Shifted Fibre (DSF) is about $0.1 ps/\sqrt{km}$ although this value is being improved through fibre fabrication technology. The major limitation brought about by the WDM part would be the non-uniform gain of the amplifiers. A very large power penalty could be incurred if the signals cover a very wide spectrum due to the gain variation of EDFA's.

By combining ultrafast OTDM and ultra high bit rate WDM technology, optical transmission systems and networks in the Tb/s region will become feasible. Although the technologies in this area are still premature to be applied to real systems, they are expected to play important roles in the development and construction future high capacity all optical networks.

References

[1] S. Haykin, "*Communication Systems (3rd Ed.)*," Wiley, 1994.

[2] R. Sabella and P. Lugli, "*High Speed Optical Communications (1st Ed.)*," Kluwer Academic Publishers, 1999.

[3] P. A. Lynn and W. Fuerst, "*Introductory Digital Signal Processing with Computer Applications (3rd Ed.)*," Wiley, 1998.

[4] L. P. Barry, "Introduction of Optical Multiplexing Technologies into Access Networks", *Telecom New Zealand Research Report*, 1997.

[5] B. L. Kasper and J. C. Campbell, "Multigigabit-per-second Avalanche Photodiode Lightwave Receivers," *IEEE J. of Lightwave Technol.*, vol. 5, pp. 1351-1364, 1987.

[6] W. Bogner, E. Gottwald, A. Schopflin, A. Richter and C. –J. Wieske, "40 Gbit/s Unrepeated Optical Transmission Over 148 km by Electrical Eime Division Multiplexing and Demultiplexing", *Electron. Lett.*, Vol. 33, pp. 2136–2137, 1997.

[7] P. M. Krummrich, E. Gottwald, C. –J. Weiske, A. Schopflin, K. Kotten and B. Lanki, "40 Gbit/s ETDM for Long Haul WDM Transmission," Annual meeting of LEOS, vol. 1, pp 71-72, Nov. 2002.

[8] S. K. Korotky, A. H. Gnauck, B. L. Kasper, J. C. Campbell, J. J. Veselka, J. R. Talman, and A. R. McCormick, "8 Gb/s Transmission Experiment Over 68 km of Optical Fibre," *IEEE J. of Lightwave Technol.*, vol. LT-5, pp. 1505-1509, 1987.

[9] Y. Zhu, W.S. Lee, C. Scahill, D. Watley, C. Fludger, P. Bontemps, M. Jones, G. Pettitt, B. Shaw and A. Hadjifotiou, "16 Channel 40 Gb/s Carrier Suppressed RZ ETDM/DWDM Transmission Over 720km of NDSF Without Polarization Channel Interleaving" *Optical Fiber Communication Conference and Exhibit*, vol. 4, pp. ThF4 -T1-4, March 2001.

[10] U. Feiste, R. Ludwig, C. Schubert, J. Berger, C. Schmidt and H. G. Weber, "160 Gbit/s Transmission Over 116 km Field Installed Fibre Using 160 Gbit/s OTDM and 40 Gbit/s ETDM," *Optical Fiber Communication Conference and Exhibit*, vol. 4, pp. ThF3 -T1-3, March 2001.

[11] R. S. Tucker, G. Eisenstein and S. K. Korotky, "Optical Time Division Multiplexing for Very High Bit Transmission," *IEEE J. of Lightwave Technol.*, vol. 6, pp. 1737-1749, 1988.

[12] X. Chen, "Optical Time Division Multiplexing (OTDM), "The optical networks group, http://www.ari.vt.edu/ece5516/opticalnetworks/otdm.htm

[13] D. M. Spirit, A. D. Ellis and P. E. Barnsley, "Optical Time Division Multiplexing," *IEEE Communications Magazine*, vol. 32, pp. 56-62, 1994.

[14] P. R. Prucnal, M. A. Santoro and S. K. Sehgal, "Ultrafast All-Optical Synchronous Multiple Access Fibre Networks," *IEEE J. of selected areas in Communications*, vol. 4, pp. 1484-1493, 1986.

[15] B. Mukherjee, "WDM Optical Communication Networks: Progress and Challenges," *IEEE J. of selected areas in Communications*, vol. 18, pp. 1810-1823, 2000.

[16] N. S. Bergano and C. R. Davidson, "Wavelength Division Multiplexing in Long-Haul Transmission Systems," *IEEE J. of Lightwave Technol.*, vol. 14, pp. 1299-1308, 1986.

[17] A. Shtainhart, R. Segal, A. Tsherniak, "WDM – Wavelength Division Multiplexing," http://www.rad.com/networks/1999/wdm/wdm.htm, 1999.

[18] P. A. Andrekson, N. A. Olsson, M. Haner, J. R. Simpson, T. Tanbun-Ek, R. A. Logan, D. Coblentz, H. M. Presby and K. W. Wecht, "32 Gb/s Optical Soliton Data Transmission Over 90 km," *IEEE Photonics Technol. Lett.*, Vol. 4, pp. 76–79, 1992.

[19] S. Kawanishi, H. Takara, K. Uchiyama, M. Saruwatari and T. Kitoh, "Fully Time-Division-Multiplexed 100 Gbit/s Optical Transmission Experiment," *Electron. Lett.*, vol. 29, pp. 2211 -2212,1993.

[20] S. Kawanishi, H. Takara, T. Morioka, O. Kamatani, K. Takiguchi, T. Kitoh and M. Saruwatori, "Single Channel 400 Gbit/s Time-Division-Multiplexed Transmission of 0.98 ps Pulses Over 40 km Employing Dispersion Slope Compensation," *Electron. Lett.*, vol. 32, pp. 916-918,1996.

[21] M. Nakazawa, T. Yamamoto, and K. R. Tamura, "1.28 Tbit/s-70 km OTDM Transmission Using Third- and Fourth-order Simultaneous Dispersion

Compensation with a Phase Modulator," *Electron. Lett.*, vol.36, pp. 2027-2029, 2000.

[22] R. Penty, "Fiberoptics: Optical TDM Makes Faster Networks Possible" *Laser Focus World*, http://lfw.pennnet.com/home.cfm, January 2000.

[23] H. Takara, "High-Speed Optical Time Division Multiplexed Signal Generation," *Optical and Quantum Electron.*, vol.32, pp. 795-810, 2001.

[24] S. Kawanishi, "Ultrahigh-speed Optical Time Division Multiplexed Transmission Technology Based on Optical Signal Processing," *IEEE J. Quantum Electron.*, vol. 34, pp 2064-2079, 1998.

[25] P. Gunning, R. Kashyap, A. S. Siddiqui and K. Smith, "Picosecond Pulse Generation of <5ps Gain Switched DFB Semiconductor Laser Diode Using Linearly Step-Chirped Fibre Grating," *Electron. Lett.*, Vol. 31, pp. 1066–1067, 1995.

[26] J. P. Van Der Ziel and R. Logan, "Generation of Short Optical Pulses in Semiconductor Lasers by Combined dc and Microwave Current Injection," *IEEE J. Quantum Electron.*, vol. 18, pp 1340-1350, 1982.

[27] J. E. Bowers, P. A. Morton, A. Mar, S. W. Corzine, "Actively Mode Locked Semiconductor Lasers," *IEEE J. of Quantum Electron.*, vol. 25, pp. 1426-1439, 1989.

[28] M.Suzuki, H. Tanaka, N. Edagawa, K. Utaka, Y. Matsushima, "Transform Limited Optical Pulse Generation up to 20GHz Repetition Rate by a Sinusoidally Driven InGaAsP Electroabsorption Modulator," *IEEE J. of Lightwave Technol.*, vol. 11, pp. 468-473, 1993.

[29] B. Mukherjee, "*Optical Communication Networks (1st Ed.)*," McGraw Hill, 1997.

[30] J. Hecht, "*Understanding Fibre Optics (4th Ed.)*," Prentice Hall, 2002.

[31] M. Nakazawa, et al., (2000), "Ultrahigh-speed Long Distance TDM and WDM Soliton Transmission Technologies," *IEEE J. Sel. Topics Quan. Electron.*, vol. 6, pp. 363- 396, 2000.

[32] G.P Agrawal, "*Fibre Optic Communications (2nd Ed.)*," Wiley, 1997.

[33] M. Saruwatori, "All-Optical Signal Processing on Ultrahigh-Speed Optical Transmission," *IEEE Communications Magazine*, vol. 32, pp. 98-105, 1994.

[34] M. Islam, "*Ultrafast Fiber Switching Devices*," Cambridge, Cambridge University Press, 1992.

[35] P. J. F. Maguire, M. Ruffini and L. P. Barry, "All Optical Switching Techniques to Enable High-Speed Next Generation Photonic Transport Systems," *First Joint IEI/IEE symposium on Telecomm. Systems Research*, Nov. 2001.

[36] N.J. Doran and D. Wood, "Nonlinear Optical Loop Mirror," *Opt. Lett.*, Vol. 13, pp. 56–58, 1988.

[37] J. P. Sokoloff, P.R. Prucnal, I. Glesk, and M. Kane, "A Terahertz Optical Asymmetric Demultiplexer (TOAD)," *IEEE Photonics Technol. Lett.*, Vol. 5, pp. 787–790, 1993.

[38] J. P. Sokoloff, I. Glesk and P.R. Prucnal, "Performance of a 50 Gb/s OTDM System using a Terahertz Optical Asymmetric Demultiplexer (TOAD)," *IEEE Photonics Technol. Lett.*, Vol. 6, pp. 98–100, 1994.

[39] J.M. Tang, P.S. Spencer and K.A. Shore, "Influence of Fast Gain Depletion on the Dynamic Response of TOADs," *IEEE J. Lightwave Technol.*, Vol. 16, pp. 86–91, 1998.

[40] L. P. Barry, P. Guignard, J. Debeau, R. Boittin and M. Bernard, "A High-Speed Optical Star Network Using TDMA and All-Optical Demultiplexing Techniques," *IEEE J. of selected areas in Communications*, vol. 14, pp. 1030-1038, 1996.

[41] K. Smith, N. J. Doran and P. G. J. Wigley, "Pulse Shaping, Compression and Pedestal Suppression Employing a Non-linear Optical Loop Mirror," *Opt. Lett.*, Vol. 15, pp. 1294–1296, 1990.

[42] T. Yamamoto, E. Yoshida, and M. Nakazawa, "Ultrafast Non-linear Optical Loop Mirror for Demultiplexing 640Gbit/s TDM Signals," *Electron. Lett.*, Vol. 34, pp. 1013–1014, 1998.

[43] D. Wang, E. A. Golovchenko, A. N. Pilipetskii, C. R. Menyuk and M. F. Arend, "Nonlinear Optical Loop Mirror Based on Standard Communication Fiber," *IEEE J. Lightwave Technol.*, Vol. 15, pp. 642–646, 1997.

[44] P. Rees, P. McEvoy, A. Valle, J. O'Gorman, S. Lynch, P.Landais, L. Pesquera, and J. Hegarty, "A Theoretical Analysis of Optical Clock Extraction using a Self Pulsating Laser Diode, " *IEEE J. Quantum Electron.*, vol. 35, pp 221-227, 1999.

[45] G. Li, Y. Li, W. Mao, "All Optical Clock Recovery using Self Pulsing Two-Section Gain Coupled DFB Lasers," *IEEE LEOS Newsletters*, vol. 16, pp. 9-10,2002.

[46] A. D. Ellis, K. Smith, and D. M. Patrick, "All Optical Clock Recovery at Bit Rates up to 40 Gbit/s," *Electron. lett.*, vol. 29, pp.1323-1324, 1993.

[47] C. A. Brackett, "Dense Wavelength Division Multiplexing Networks," *IEEE J. of selected areas in Communications*, vol. 8, pp. 948-964, 1990.

[48] S. S. Dixit, and A. Yla-Jaaski, "WDM Optical Networks: A Reality Check," *IEEE Communications magazine*, vol. 38, pp. 58-60, 2000.

[49] R. Giles, M. Newhouse, J. Wright, and K. Hagimoto, Special Issue on "System and Network Applications of Optical Amplifiers," *IEEE J. of Lightwave Technol.*, vol. 13, May 1986.

[50] M. Potenza, "Optical Fibre Amplifiers for Telecommunication Systems," *IEEE Communications magazine*, vol. 34, pp. 96-102, 1996.

[51] M. J. O'Mahoney, "Semiconductor Laser Optical Amplifiers for use in Future Fibre Systems," *IEEE J. of Lightwave Technol.*, vol. 6, pp. 531-544, 1988.

[52] T. Saitoh and T. Mukai, "Recent Progress in Semiconductor Laser Amplifiers," *IEEE J. of Lightwave Technol.*, vol. 6, pp. 1656-1664, 1988.

[53] S. Kinoshita, "Broadband Fibre Optic Amplifiers," *Optical Fiber Communication Conference and Exhibit*, vol. 2, pp. TuA1 -T1-4, March 2001.

[54] W. Miniscalco, "Erbium Doped Glasses for Fibre Amplifiers at 1500 nm," *IEEE J. of Lightwave Technol.*, vol. 9, pp. 234-250, 1991.

[55] B. Pedersen, K. Dybdal, C. D. Hansen, A. Bjarklev, J. H. Povlsen, H. Vendeltorp-Pommer and C. C. Larsen," Detailed Theoretical and Experimental Investigation of High Gain Erbium Doped Fibre Amplifier," *IEEE Photon. Technol. Lett.*, vol.2, pp. 863–865, 1990.

[56] A. E. Willner and S. M. Hwang, " Transmission of Many WDM Channels Through a Cascade of EDFA's in Long Distance Links and Ring Networks," *IEEE J. of Lightwave Technol.*, vol. 13, pp. 802-816, 1995.

[57] J. C. Dung, S. Chi, and S. Wen, "Gain Flattening of Erbium Doped Fibre Amplifier using Fibre Bragg Gratings," *Electron. lett.*, vol. 34, pp. 555-556, 1998.

[58] H. S. Kim, S. H. Yun, N. Park and B. Y. Kim, "Actively Gain Flattened Erbium Doped Fibre Amplifier over 35 nm using All Fibre Acousto-optic Tunable Filters," *IEEE Photon. Technol. Lett.*, vol.10, pp. 790–792, 1998.

[59] H. Ono, M. Yamada, T. Kanamori, S. Sudo and Y. Ohishi, "1.58 μm Band Gain Flattened Erbium Doped Fibre Amplifiers for WDM Transmission Systems," *IEEE J. of Lightwave Technol.*, vol. 17, pp. 490-496, 1999.

[60] H. Masuda, S. Kawai, K. I. Suzuki, and K. Aida, "Ultrawide 75 nm Gain-Band Optical Amplification with Erbium Doped Fluoride Fibre Amplifiers and Distributed Raman Amplifiers," *IEEE Photon. Technol. Lett.*, vol.10, pp. 516–518, 1998.

[61] J. Connolly, "Optical Amplifiers," *WDM solutions*, pp 57-62, June 2001.

[62] E. Pennings, G. D. Khoe, M. K. Smit, and T. Staring, "Integrated-optic versus Micro Optic Devices for Fibre Optic Telecommunication Systems: A Comparison," *IEEE J. Sel. Topics Quantum Electron.,* vol. 2, pp. 151-164, 1996.

[63] A. Ankiewicz, A. W. Snyder and X. H. Zheng, "Coupling Between Parallel Optical Fibre Cores – Critical Examination," *IEEE J. Lightwave Technol.*, vol. 4, pp. 1317–1323, 1986.

[64] Tom Hausken, "Tunable Lasers and Filters See a Delayed Market," *WDM solutions*, pp 13-16, May 2002.

[65] D. Sadot and E. Boimovich, "Tunable Optical Filters for Dense WDM Networks," *IEEE Commun. Mag.*, pp. 50–55, Dec. 1998.

[66] D. Anderson, "Mastering WDM," *WDM solutions*, pp 97-99, June 2001.

[67] B. Glance, "Wavelength Tunable Add / Drop Optical Filter," *IEEE Photonics Tech. Lett.*, vol. 8, pp. 245-247, 1996.

[68] M-C. Amann and J. Buus, "Tunable Laser Diodes," Norwood, *Artech House Publishers*, 1998.

[69] C. He, D. Ma and W-Z. Li, "Thin Film Filters are the Building Blocks of Multiplexing Devices," *WDM solutions*, pp 39-46, May 2001.

[70] M. Novak, M. Zecchino, E. Novak, "Accurate Metrology Improves Thin Film Filter Yield," *WDM solutions*, pp 49-54, May 2001.

[71] H. A. McLeod, "*Thin Film Optical Filters (2nd ed.)*," Hilger, 1985.

[72] C. M. Miller and J. W. Miller, "Tunable Fibre Filters Demultiplex WDM Systems," *Laser Focus World*, pp. 46-49, September 1996.

[73] A. Spisser, R. Ledantec, C. Seassal, J. L. Leclerq, T. Benyatu, D. Rondi, R. Blondeau, G. Guillot, and P. Victorovitch, "Highly Selective and Widely Tunable 1:55 μm InP/air-gap Micromachined Fabry–Pérot Filter for Optical Communications," *IEEE Photon. Technol. Lett.*, vol.10, pp. 1259–1261, 1998.

[74] C. Zhou, P. Chan, J. Yang and P. Kung, "Fibre Bragg Gratings Stretch Metro Applications," *WDM solutions*, pp 41-43, May 2002.

[75] S. Juma, "Bragg Gratings Boost Data Transmission Rates," *Laser Focus World*, pp 58-62, November 1996.

[76] A. M. Vengsarkar, P. J. Lemaire, J. B. Judkins, V. Bhatia, T. Erdogan and J. E. Sipe, "Long Period Fibre Gratings as Band Rejection Filters," *IEEE Journal of Lightwave Technol.*, vol. 14, pp. 58-65, 1996.

[77] K. A. McGreer, "Arrayed Waveguide Gratings For Wavelength Routing," *IEEE Communications Magazine*, vol. 36, pp. 62 -68, 1998.

[78] M. Abe, Y. Hibino, T. Tanaka, M. Itoh, A. Himeno and Y. Ohmori, "Mach-Zehnder Interferometer and Arrayed-Waveguide-Grating Integrated Multi / Demultiplexers with Photosensitive Wavelength Tuning," Electron Lett., vol. 37, pp. 376 –377, 2001.

[79] M. Zirngibl, "Multifrequency Lasers and Applications in WDM Networks," *IEEE Communications Magazine*, vol. 36, pp. 39-41, 1998.

[80] K. Kobayashi and I. Mito, "Single Frequency and Tunable Laser Diodes," *IEEE J. Lightwave Technol.*, vol. 6, pp. 1623–1633, Nov., 1988.

[81] E. Haroff, "The Beauty of Tunability," *Lightwave Europe*, Aug. 2002.

[82] C. J. Chang-Hasnain, "Tunable VCSEL" *IEEE Journal on Selected Topics in Quantum Electronics*, vol. 6, pp. 978 –987, Nov/Dec 2000.

[83] H. Kogelnik and C. V. Shank, "Coupled Wave Theory of Distributed Feedback Lasers," *J. Appl. Physics*, Vol. 453, No. 5, pp 2327-2335, 1972.

[84] K. C. Lee and V. O. K. Li, "Multiwavelength DFB Laser Array Transmitters for ONTC Reconfigurable Optical Network Testbed," *IEEE J. of Lightwave Technol.*, vol. 14, pp. 967-976, 1996.

[85] A. Nahata, C. J. DiCaprio, H. Yamada, A. I. Ryskin, A. S. Shcheulin and R. A. Linke, "Widely Tunable Distributed Bragg Reflector Laser using a Dynamic Holographic Grating Mirror," *IEEE Photon. technol. Lett.*, pp 1525-1527, 2000.

[86] Kevin Affolter, "Tunable Lasers," *WDM solutions*, pp 65-71, June 2001.

[87] O. A. Lavrova, and D. J. Blumenthal, "Accelerated Aging Studies of Multi-Section Tunable GCSR Lasers for Dense WDM Applications" *IEEE J. of Lightwave Technol.*, Volume: 18, pp. 2196 –2199, 2000.

[88] D. Chu and R. Potenza, "Optical Networks Promote Tunable Laser Development," *Laser Focus World*, Vol. 37, No. 8, pp 101-114, 2001.

[89] M. Telford, "Widely Tunable Lasers Power up for Narrow Spaced DWDM," *Lightwave Europe*, pp. 24-25, May 2002.

[90] J. P. Hamaide, P. Emplit, L. Prigent, O. Audouin and J. M. Gabriagues, "Effect of Chromatic Dispersion, Kerr Non-linearity and Amplifier Noise in Long PSK Optical Fibre Systems," *Electron. Lett.*, vol. 28, pp. 44-46, 1992.

[91] A. F. Elrefaie, R. E. Wagner, D. A. Atlas and D. G. Daut, "Chromatic Dispersion Limitations in Coherent Lightwave Transmission Systems," *IEEE J. of Lightwave Technol.*, vol. 6, pp. 704-709, 1988.

[92] X. Y. Zou, M. I. Hayee, S. M. Hwang and A. E. Willner, " Limitations in a 10 Gb/s WDM Optical Fibre Transmission When using a Variety of Fibre Types to Manage Dispersion and Non-linearities," *IEEE J. of Lightwave Technol.*, vol. 14, pp. 1144-1152, 1996.

[93] S. Saito, M. Aiki and T. Ito, "System Performance of Coherent Transmission Over Cascaded In-Line Fibre Amplifiers," *IEEE J. of Lightwave Technol.*, vol. 11, pp. 331-342, 1993.

[94] A. Willner, "Tunable Compensators Master Chromatic Dispersion Impairments," *WDM solutions*, pp 51-58, July 2001.

[95] J. F. Brennan, "Dispersion Compensation Gratings for the C-Band," *Photonics spectra*, pp 159-165, June 2001.

[96] A. R. Chraplyvy, "Limitations on Lightwave Communications Imposed by Optical Fibre Non-linearities," *IEEE J. of Lightwave Technol.*, vol. 8, pp. 1548-1557, 1990.

[97] A. R. Chraplyvy and R. W. Tkach, "What is the Actual Capacity of Single Mode Fibres in Amplified Lightwave Systems," *IEEE Photon. Technol. Lett.*, vol.5, pp. 666–668, 1993.

[98] N. Kikuchi and S. Sasaki, " Analytical Evaluation Technique of Self Phase Modulation Effect on the Performance of Cascaded Optical Amplifier Systems," *IEEE J. of Lightwave Technol.*, vol. 13, pp. 868-878, 1995.

[99] S. Yoshida and K. Iwashita, " Influence of Amplitude Modulation Induced by LD Direct Modulation on FM Signal Transmission," *IEEE Photon. Technol. Lett.*, vol.2, pp. 929–931, 1990.

[100] A. R. Chraplyvy, "Optical Power Limits in Multi Channel Wavelength-Division-Multiplexed System due to Stimulated Raman scattering," *Electron. Lett.*, vol. 20, pp. 58-59, 1984.

[101] J. Zweck and C. R. Menyuk, "Analysis of Four Wave Mixing between Pulses in High Data Rate Quasi-Linear Sub-Channel Multiplexed Systems," *Opt. Lett.*,vol. 27, pp. 1235-1237, 2002.

[102] K. Nosu, "*Optical FDM Network Technologies (1st Ed.)*," Artech house, 1997.

[103] F. Forghieri, R. W. Tkach and A. R. Chraplyvy, "WDM Systems with Unequally Spaced Channels," *IEEE J. of Lightwave Technol.*, vol. 13, pp. 889-897, 1995.

[104] R. W. Tkach, A. R. Chraplyvy, F. Forghieri, A. H. Gnauck and R. M. Derosier, "Four-Photon Mixing and High Speed WDM Systems," *IEEE J. of Lightwave Technol.*, vol. 13, pp. 841-849, 1995.

[105] A. Tomita, "Cross Talk Caused by Stimulated Raman Scattering in Single Mode Wavelength Division Multiplexed Systems," *Opt. Lett.*, vol. 8, pp. 412-414, 1983.

[106] M. J. O'Mahoney, D. Simeinidou, A. Yu and J. Zhou, "The Design of an European Optical Network," *IEEE J. of Lightwave Technol.*, vol. 13, pp. 868-88, 1995.

[107] D. A. Fishman and J. A. Nagel, "Degradations due to Stimulated Brillouin Scattering in Multi Gigabit Intensity Modulated Fibre Optic Systems," *IEEE J. of Lightwave Technol.*, vol. 11, pp. 1721-1728, 1993.

[108] K. Poturaj, J. Wojcik, B. Janoszczyk, P. Mergo, M. Makara, W. Spytek, W. A. Kowalski, K. M. Abramski, and E. M. Pawlik, "Erbium Doped Fibre For L-Band

EDFA," *2nd International Conference on Transparent Optical Networks*, vol.1, pp. 155 -158, 2000.

[109] J. Kani and M. Jinno, "Wideband and Flat-Gain Optical Amplification from 1460 to 1510 nm by Serial Combination of Thulium Doped Flouride Fibre Amplifier and Fibre Raman Amplifier" *Electron. Lett.*, vol. 35, pp. 1004-1006, 1999.

[110] M. N. Islam, "Raman Amplifiers for Telecommunications" *IEEE Journal on Selected Topics in Quantum Electronics*, vol. 8, pp. 548 –559, May/Jun 2002.

[111] P. J. Delfyett and B. Mathason, "Towards Terabit Networking, Instrumentation and Signal Processing Using Hybrid WDM-OTDM Technologies," *Terahertz and Gigahertz Electronics and Photonics II, Proceedings of SPIE*, vol. 411, 2000.

[112] S. Kawanishi, "High Bit Rate Transmission Over 1 Tbit/s," *IEICE Trans. Commun.*, vol. E84-B, pp. 11351141, May 2001.

[113] D. Cotter, J. K. Lucek and D. D. Marcenac, "Ultra-High-Bit-Rate Networking: from the Transcontinental Backbone to the Desktop," *IEEE Communications magazine*, vol. 35, pp. 90-95, 1997.

[114] A. R. Chraplyvy and R. W. Tkach, "Terabit/second Transmission Experiments," *IEEE J. Quantum Electron.*, vol. 34, pp 2103-2108, 1998.

[115] T. Ono and Y. Yano, "Key Technologies for Terabit/second WDM systems with high spectral efficiency of over 1 bit/Hz," *IEEE J. Quantum Electron.*, vol. 34, pp 2080-2088, 1998.

[116] S. Kawanishi, "Ultra-fast All-Optical TDM Transmission Technology," *2nd Opto-Electronics & Communications Conference (OECC '97)*, July 1997.

[117] T. Morioka, S. Kawanishi, H. Takara, O. Kamatani, M. Yamada, T. Kanamori, K. Uchiyama and M. Saruwatari, "100 Gbit/s x 4 ch, 100 km Repeaterless TDM-WDM Transmission using a Single Supercontinuum Source," *Electron. Lett.*, vol. 32, pp. 468-470, 1990.

[118] M. Saruwatari, "All Optical Signal Processing for Terabit/Second Optical Transmission," *IEEE Journal on Selected Topics in Quantum Electronics*, vol. 6, pp. 1363 –1374, Nov/Dec 2000.

[119] S. Kawanishi, H. Takara, K. Uchiyama, I. Shake and K. Mori, "3 Tbit/s (160 Gbit/s x 19 ch) OTDM/WDM Transmission Experiment," *Optical Fibre*

Communication Conference and the International Conference of Integrated Optics and Optical Fibre Communications (OFC/IOOC '99), 1999.

[120] M. Saruwatari, "Transform-Limited, Femtosecond WDM Pulse Generation by Spectral Filtering of Gigahertz Supercontinuum," *Electron. Lett.*, vol. 30, pp. 1166-1168, 1994.

[121] T. Morioka, K. Uchiyama, S. Kawanishi, S. Suzuki and M. Saruwatari, "Multi-wavelength Picosecond Pulse Source with Low Jitter and High Optical Frequency Stability Based on 200 nm Super Continuum Filtering," *Electron. Lett.*, vol. 31, pp. 1164-1166, 1995.

[122] I. H. White, M. Owen, M. F. C. Stephens, P. Vasil'ev, J. D. Bainbridge and R. V. Penty, "WDM and Hybrid WDM/OTDM Applications of the Multi-wavelength Grating Cavity (MGC) Laser," *5th Asia Pacific Conference on Communications (APCC '99) and 4th Opto-Electronics & Communications Conference (OECC '99)*, 1999.

[123] P. J. Delfyett, "Hybrid WDM – OTDM Technologies for Networking, Instrumentation & Signal Processing (NSF – PFF/PECASE)," *School of optics and centre for research and education in optics and Lasers (CREOL),* http://mrl.engr.uark.edu/EPDT/097delfyett.doc.

Chapter 3 - Ultra Short Optical Pulses

3.1 Introduction

Short optical pulse sources are key elements in ultrafast OTDM and hybrid WDM/OTDM networks since they support several of the important subsystems, including sources for optical modulation, demultiplexing, optical clocks and optical logic [1]. A prerequisite of a source for optical modulation is the duration of the pulse. The overall data rate is basically determined by the temporal separation between channels in the muliplex, which in order to avoid cross channel interference, must be significantly greater than the pulse duration. Thus to increase the overall data rate, one must use very short optical pulses. Furthermore to enable demultiplexing with low inter-channel crosstalk, OTDM transmission systems have to operate with optical pulses that are significantly less than the duration of the allowed timeslot. Many other applications (sampling, signal processing, microwave signal distribution etc.) also rely on the ability of laser diodes to generate short optical pulses at high repetition rates. The design of lasers for such applications depends on a number of system determined pulse characteristics. Control over the pulse profile, duration, peak power, repetition rate, wavelength shift (chirp) and stability are critical to sampling and communication applications.

Some of the most important characteristics of the pulse source, that will affect its usefulness in an OTDM system, are the pulsewidth, spectral width and temporal jitter. As explained earlier the pulse duration has to be clearly short enough to support the desired overall transmission rate. For very high capacity or long distance transmission the pulsewidth should normally be less than 1/3 of the channel spacing to avoid cross channel interference [2]. For a system operating at 40Gb/s, this means that the source has to produce very short optical pulses typically around 8 ps duration (Full Width Half Maximum - FWHM). The second characteristic is the spectral width of the optical pulse source. The width will have a major impact on how the pulse will evolve during propagation due to the influence of fibre dispersion. The impact of temporal jitter on the pulses is obvious in high speed OTDM communication system. In such systems the

channel spacing becomes smaller thereby making them more prone to the detrimental effects of temporal jitter. In addition other pulse properties such as, the repetition rate (high) and the oscillation wavelength (tunable) also determine their usefulness in high-speed optical communication systems.

A standard figure of merit for picosecond pulses is known as the Time Bandwidth Product (TBWP) and is denoted by $\delta\mu\delta t$ where $\delta\mu$ is the width of the optical spectrum (linewidth) and δt is the temporal width (pulsewidth). The transmission of high-speed (> 10GHz) bit streams over standard mono-mode fibres, utilizing the loss minimum around 1550 nm wavelength, is limited by fibre dispersion and laser chirping. Smaller bandwidth (smaller TBWP) of the signal would lead to less dispersion over standard fibre. A pulse, that is chirp free and has the minimal linewidth (FWHM) needed to support the associated pulsewidth (FWHM), depending on the temporal pulse shape, is known as a transform limited pulse. Hence one can deduce the degree to which a pulse is transform limited by assuming the functional form of the temporal pulse shape. A Gaussian pulse has to have a TBWP of 0.44 to be transform-limited while a hyperbolic secant pulse needs to have a TBWP of 0.31 in order to be transform limited. Other pulse shapes and their TBWP values are given in Appendix C.

Therefore the development of transform-limited optical pulse sources with broad wavelength tunability, short pulsewidths and high repetition rates are extremely important for use in future high speed communication systems, especially in applications such as Wavelength Division Multiplexing (WDM), Optical Time Division Multiplexing (OTDM), Hybrid WDM/OTDM and soliton systems [3].

3.2 Methods of short optical pulse generation

The generation of short optical pulses may be performed by several methods such as Q-switching [4], mode locking [5], gating of Continuous Wave (CW) light by an external modulator [6] and gain switching [7]. Other techniques such as non-linear compression of a beat signal [3] and harmonic mode locking of EDF lasers also exist but are not so common. A brief description of some of these common methods follows. Gain switching

is given the most attention since this was the pulse generation technique used in our experimental work.

3.2.1 Q-switching

This is a very useful technique employed to obtain relatively short optical pulses with a very high output power [8]. The process of Q-switching initially involves holding the losses in the laser cavity very high. Blocking or removing one of the end facets prevents laser oscillation inside the laser cavity. The above could be achieved by (rotating one of the end mirrors out of alignment or by introducing a high loss modulator into the cavity). The prevention of laser oscillation as the pumping process continues to lead the inversion to reach a very high level. In this situation, the cavity Q is said to be "spoilt". A step-by-step analysis of laser Q switching dynamics is shown schematically in Figure 3-1.

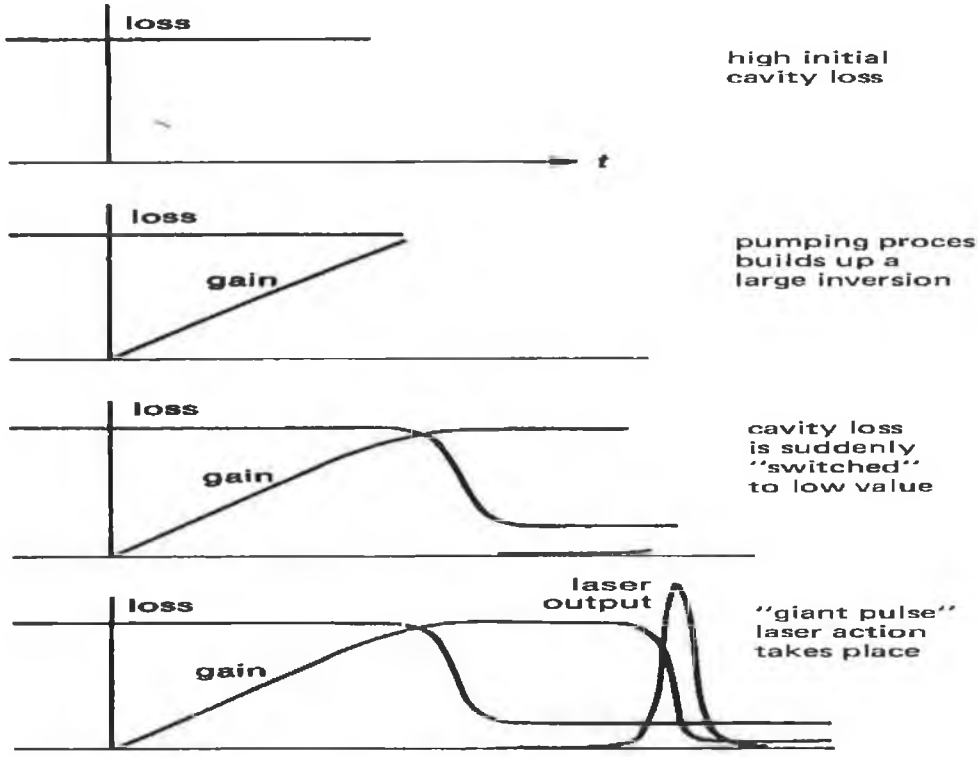

Figure 3-1: Process of laser Q switching

After the large inversion develops the cavity feedback / gain is restored (Q is suddenly switched back to its low loss value). The laser oscillation in the cavity then builds up very

rapidly. Hence the laser delivers nearly all its energy in a single instant resulting in a very short high intensity burst of optical power. The accumulated population inversion is dumped in a short laser pulse. There are many methods associated with the actual switching of the loss within the cavity some of which would be the rotating mirror, electro-optic, acousto-optic and passive Q switching. One of the major shortcomings of this technique, in comparison to the others, is that it requires specially fabricated devices.

3.2.2 Mode locking

It's another very useful technique in which many simultaneously oscillating axial modes in a laser cavity are locked or coupled together, using an intra cavity modulator. Such an arrangement is shown in Figure 3-2 (a). The modulator is then driven at a frequency (ω_m) that is equal to or a harmonic of the round trip frequency of the laser.

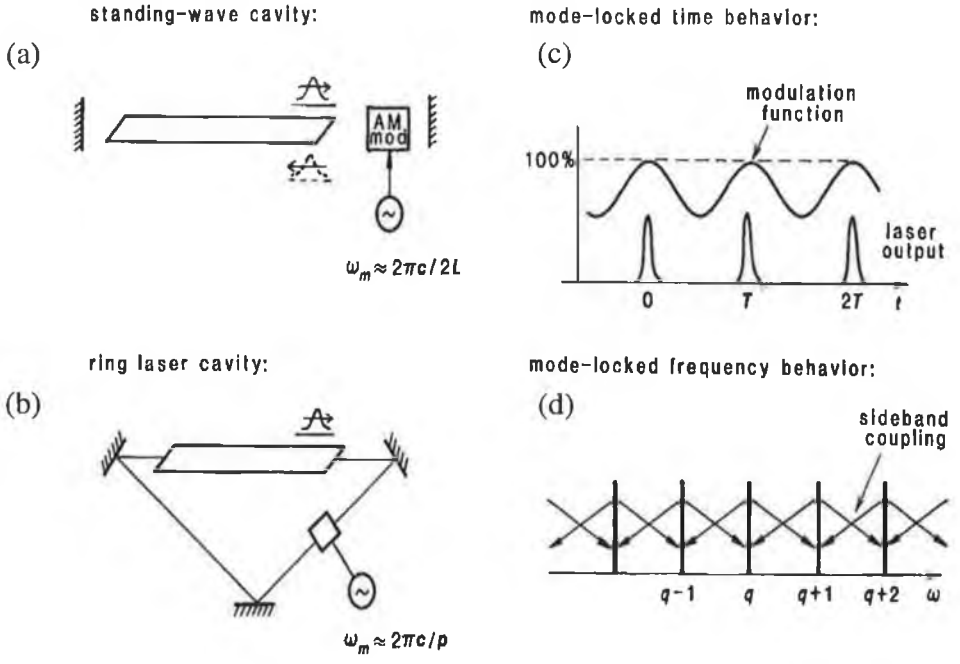

Figure 3-2: (a) Active mode locking (c) Description in the temporal domain (d) Description in the spectral domain

A time domain description (Figure 3-2 (b)) shows the laser oscillation in the form of a short pulse, which passes through the modulator only when the modulator transmission is at a maximum. The spectral domain on the other hand provides quite an interesting outlook to the process of mode locking as shown in Figure 3-2 (c). As a result of the

modulation, the oscillating axial modes of the laser cavity, will acquire side bands at frequencies $\omega_q \pm n \times \omega_m$. Since the modulation frequency is equal or close to the axial mode spacing or one of its integer multiples, the side bands of each axial mode would fall on top or very close to one of the axial modes of the cavity. Each of these side modes will tend to injection lock the axial mode with which it is in resonance. Hence the intra-cavity modulator will tend to couple together or mode lock each axial mode to one or more of its neighbouring modes.

This produces very rapid modulation of the laser output. Such an output takes the form of extremely short optical pulses, which circulate around inside the cavity and emerge through one end mirror at a repetition rate corresponding to the round trip transit time inside the laser cavity. Even though mode locking has been found to generate high power pulse trains with excellent quality (low jitter and chirp) it has a major disadvantage in that it is confined to narrow operating regimes.

3.2.3 Gain switching

Substantial attention is given to gain switching, as this is the pulse generation technique that has been extensively utilized in this thesis. Directly modulated pulse generation schemes have the advantages over the other methods in that they are simple, compact, robust, stable, operate at flexible data rates and do not require active stabilization techniques (such as regenerative mode locking) [9]. A direct modulation technique that has attracted attention involves the gain switching of semiconductor laser diodes. In general gain switching is one of the simplest techniques available for generating pulses with durations of tens of picoseconds.

3.2.3.1 Principle of operation

Short optical pulses with a pulsewidth of less than 50ps can be conveniently generated in a semiconductor laser by directly driving the laser with large amplitude, fast electrical pulses. The first indications that very short optical pulses could be generated by the gain switching technique came about with the observations of relaxation oscillations when turning on a laser diode from below threshold using electrical pulses with a fast leading edge [10]. It was also noticed that the optical pulse was considerably shorter than the

electrical pulse. The idea is to excite the first spike of relaxation oscillation and terminate the electrical pulse before the onset of the second spike. This translates down to the requirement that the electrical pulsewidth should be rather short and should lie in the 100 – 200 ps range.

The standard gain switching arrangement is to drive a laser, biased below threshold with an electrical comb generator, which is capable of delivering 50-100 ps pulses with current amplitudes that are up to 10 times the threshold current of the device (~15 V into 50 Ω). Alternatively the modulation of a laser biased below threshold with a large sinusoidal signal at sub-GHz or GHz frequency also results in gain switched optical pulses [11]. Figure 3-3 (below) illustrates the typical evolution of the photon and electron density, which takes place during the generation of ultra-short optical pulses by gain-switching a laser diode.

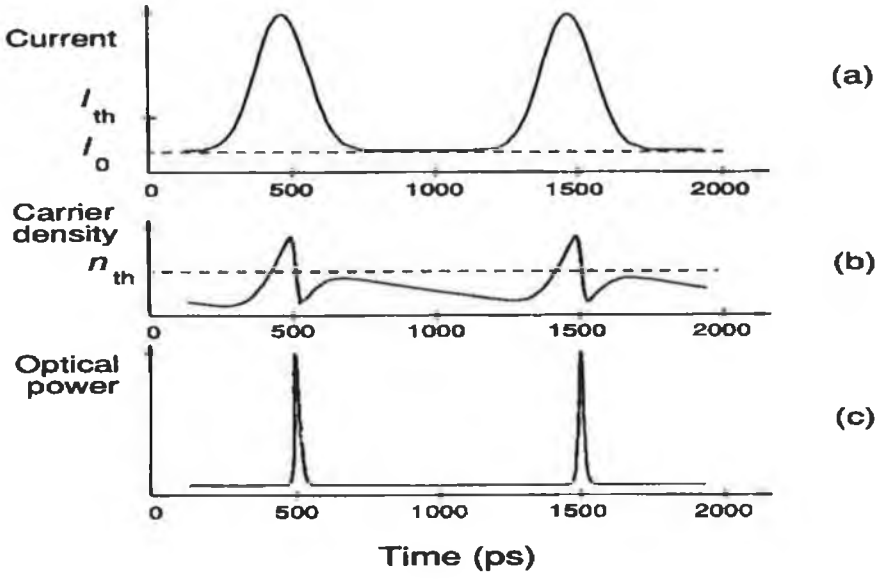

Figure 3-3: Gain switching of a laser diode (a) Applied current (b) Carrier density (c) Output optical pulses

The laser is biased with a DC current (I_0), which is below threshold (I_{th}) as shown in Figure 3-3 (a). A large amplitude pulsed current is then applied to the laser, which is also shown in the same Figure 3-3 (a). Since the laser is biased below threshold, the initial photon density is very low and since the stimulated emission rate is proportional to the

photon density, the photon density increases at a very slow rate. In the absence of a sizable amount of stimulated emission, the carrier concentration increases rapidly in the laser. When the electric pulse increases the injected carrier density above the carrier density threshold (n_{th}), lasing starts. The typical time development of the carrier density is shown in Figure 3-3 (b). At a certain point (peak inversion point [n_i]) the generated photon population rapidly depletes the electron concentration. If the current pulse is cut off at the appropriate time, as the photon and electron densities are decreasing after the initial peak, then the second oscillation will not be obtained. That is to say that above n_{th}, the carrier density reaches n_i, lasing occurs and represses the increase in carrier density and consequently n_i is pulled down to n_f. Therefore further lasing is prevented if the current is abruptly terminated after the charge carrier concentration is exceeded so that only a single resonance spike is generated (preventing further relaxation oscillations to occur). If the current pulse is not cut off the photon density will then oscillate at the resonant frequency before settling down to its steady state value.

One of the main reasons for not being able to further reduce the gain switched pulsewidth (10-40 ps) is due to the difficulty in sustaining a large inversion level before the emission of the optical pulse [12]. The maximum achievable inversion is limited by the fundamental parameters of the laser, such as the differential gain coefficient, spontaneous emission factor and the cavity loss. In gain switching initial inversion level is not controlled externally but is determined by how fast the photons can build up from spontaneous emission. A slow build up allows the carriers a longer time to build up to a higher inversion level. In a typical gain switched set-up the pump current pulse has an amplitude much higher than the threshold current of the laser. Therefore the charge required to fill the electron density in the laser to the threshold level is exceeded. Hence a large initial inversion could be achieved by having a long delay in the onset of stimulated emission. This could be achieved if the laser is left unbiased. However if the gain switched pulse contains a relatively limited amount of charge, it has been observed that the optical pulse is shortest when the laser is biased slightly below threshold [13]. The peak inversion not only determines the pulsewidth but also the peak power of the pulse.

The mechanisms involved in gain switching can be understood by studying the electron and photon equations (coupled differential equations), which describe the carrier-photon interaction in terms of the photon density, P, in the cavity and the carrier density, N, in the active region. A set of rate equations are given as:

$$\frac{dN}{dt} = \frac{j(t)}{Qd} - go(N - N_t)P - \frac{N}{\tau_s} \qquad \textbf{Equation 3-1}$$

$$\frac{dP}{dt} = \Gamma g_o(N - N_t)P - \frac{P}{\tau_{ph}} + \beta\frac{N}{\tau_s} \qquad \textbf{Equation 3-2}$$

N_t	=	Transparency density
g_o	=	Differential gain coefficient
β	=	Spontaneous coupling factor
Q	=	Electron charge
d	=	Active layer thickness
$j(t)$	=	Time varying current density
Γ	=	Optical confinement factor
τ_s	=	Carrier lifetime
τ_{ph}	=	Photon lifetime

The equations describe the evolution of the carrier and photon densities respectively. These equations are simple single mode equations. Therefore they do not take into account the distribution of P between the cavity modes. The first term on the R.H.S of equation 3-1 describes the injection of carriers by the current j(t) into the volume of interest. The stimulated emission or absorption that appear in the second and the first terms in both equations {3-1 & 3-2} respectively, introduce the non-linearity into these equations. g_0 and N_0 are constants, where N_0 determines the limit between optical absorption or optical gain. The third term takes into account the recombination of carriers by the spontaneous emission, characterized by τ_s. The second term in equation 3-2

describes the optical losses in the laser resonator, characterized by the photon lifetime τ_{ph}. The spontaneously emitted photon part, which contributes to the desired laser mode, is given by the last term in equation 3-2.

3.2.3.2 Characteristics of gain switched pulses

1. Pulsewidth and peak power

The strong depletion of carriers causes a short pulse to be generated, the width of which depends on the gain of the laser material and the carrier population at pulse turn on. As the carrier concentration is linked to the photon lifetime, devices with shorter lifetimes are preferred when it comes to short pulse generation. Therefore shorter devices also result in shorter gain switched pulses [12]. On the other hand a larger cavity allows higher total carrier injection to the active layer before pulse turn on resulting in higher optical pulse powers. However as mentioned earlier, longer pulse durations result from the increased, cavity length dependent, photon lifetime. Hence considering the peak power at the cost of the pulsewidth, there is no significant improvement in increasing the cavity length. The shape of the pulse also depends on the laser device structure and material [14].

The gain switched pulse can be described as a combination of two exponential curves with time constants τ_r (rising edge) and τ_f (falling edge). The risetime of the pulse (τ_r) is inversely proportional to the net charge (Q) transferred by the electrical pulse to the to the active region (as in equation 3-3) while the decay time depends on how far down below threshold the carrier density is pulsed during the optical pulse. If the carrier density is not brought down far enough below the lasing threshold then a pedestal is formed on the decaying edge. This problem could be overcome by transforming the electrical pulses being applied to the laser [15].

$$\tau_r \cong \frac{eV}{(Qg_0\Gamma)} \qquad \textbf{Equation 3-3}$$

For extremely short driving pulses {i.e. $j(t) = n_i\delta(t)$ where $\delta(t)$ is the Dirac δ-function and $n_i >> n_{th}$ } an approximate solution for the pulsewidth could be obtained as follows

$$\Delta\tau = \tau_{ph} + \frac{1}{g_0 n_i} \qquad \textbf{Equation 3-4}$$

Where

g_0 = Differential gain coefficient

n_i = Carrier concentration in transparent condition

τ_{ph} = Photon lifetime

The photon lifetime is given as

$$\tau_{ph} = \frac{1}{v_g(\alpha_m + \alpha_i)} \qquad \textbf{Equation 3-5}$$

Where

α_m = Mirror loss

α_i = Internal loss

v_g = Group velocity

Equation 3-3 backs up our earlier statement that a larger differential gain as well as higher excited carriers leads to shorter pulse generation. In essence increasing the differential gain and the photon density, while decreasing the photon lifetime, increases the resonance frequency. Clearly as the resonance frequency increases the pulsewidth will decrease. From equation 3-6 we can see that by increasing the differential gain, increasing the photon density and by decreasing the photon lifetime we increase the relaxation oscillation frequency, which in turn decreases the pulsewidth.

$$f_r = \frac{1}{2\pi}\left[\left(\frac{g_0 s_0}{\tau_p(1+\varepsilon s_0)}\right)\right]^{1/2} \qquad \textbf{Equation 3-6}$$

The bias current of the laser also governs the quality of pulses produced by gain switching. It has been shown [13] that n_i depends on the bias current I_0. For given electrical pulses (modulation amplitude) there exists an optimal dc bias level where the pulsewidth is at a minimum and the pulse amplitude is at a maximum. A laser must be

biased below threshold to achieve an optimum pulsewidth and power performance. When the laser is biased below the threshold level, the optical pulse amplitude decreases with decreasing dc bias and the pulse broadens. Furthermore the pulse is emitted with increasing delays. If left unbiased then the limited amount of charge delivered by the current pulse may not be able to make a positive inversion. On the other hand if biased above threshold a large amount of preexisting stimulated emission will clamp the maximum inversion at a level not much higher than threshold. Therefore the best performance is achieved if the laser is biased close to, and just below threshold. Hence we can conclude that the bias current is an effective parameter to be optimized, especially since electrical pulses cannot be varied easily in practical set-ups.

2. The optical spectra and frequency chirping

Another key parameter that plays a vital role in the application of gain switched pulses is the optical bandwidth of these picosecond pulses. An excessive emission bandwidth could result in a significant dispersion penalty in an optical communication system as mentioned in the previous chapter. Hence a single frequency laser such as a Distributed Feed-Back (DFB) [16] laser is commonly used in gain switching applications. However gain switching of a laser diode leads to broadening of the spectral bandwidth in comparison to when the laser is being run under CW operating conditions. It was shown earlier that the carrier concentration experienced large variations during the emission of a gain switched pulse. Hence the refractive index in the laser cavity should vary as well. Since the time dependence of the laser wavelength is related to the time dependence of the carrier concentration, due to the effect of free carriers on the refractive index of the semiconductor material, the wavelength changes as well [10].

Therefore the wavelength shift (chirping) is due to the fact that as the carrier density changes the refractive index of the active region varies and thus so does the wavelength. The frequency deviation could be expressed in terms of the deviation of the carrier density from equilibrium [17] as shown in equation 3-7:

$$\Delta f(t) = -\frac{1}{4\pi}\frac{\tau_s}{\tau_p}\alpha\Delta N(t) \qquad \textbf{Equation 3-7}$$

Where

τ_s = Spontaneous lifetime

τ_p = Cavity photon lifetime

α = Linewidth enhancement factor

An important property of semiconductor lasers is the degree to which variations in the carrier density (N) alter the index of refraction (n) of the active layer. This phenomenon is often characterized by the Linewidth Enhancement Factor (α). The coupling between the real (refractive index) and the imaginary (gain or loss) parts of the carrier dependant susceptibility is described by the ratio of their derivatives with respect to the carrier density [18]. This ratio commonly referred to as the α parameter is shown in equation 3-8. This dimensionless parameter affects other laser characteristics such as the chirp (as seen in equation 3-7), the modulation response and the effect of external feedback [19].

$$\alpha = \frac{\mathrm{Re}(\chi_p)}{\mathrm{Im}(\chi_p)} = -\frac{4\pi}{\lambda}\left(\frac{\partial n / \partial N}{\partial g / \partial N}\right) \qquad \textbf{Equation 3-8}$$

Where

χ_p = Complex susceptibility

N = Carrier density

n = Refractive index

g = Gain of the active layer

The chirping associated with gain switching of laser diodes means that optical pulses generated are far from the theoretical limit for bandwidth limited pulse. Hence the usefulness of such pulses in communication systems would be limited. It is important to note that the chirp across the pulse is non-linear. The centre of the pulse is linearly chirped while the wings of the pulse contain the non-linear chirp. To compensate for frequency chirping there are two methods that have been commonly employed:

a) Use a narrow band optical filter to extract a small fraction of the spectral components. In this way we could realize transform-limited pulses. Fabry Perot Resonators (FPR)

could be used as optical filters to select a small range of frequencies within a wide spectrum from the gain switched laser diode. By reducing the time-bandwidth product in this manner near transform limited pulses could be generated [20].

b) Use a Dispersion Compensating Fibre (DCF) to compress the pulse and thus reduce the time-bandwidth product. The use of a DCF compensates for linear frequency chirping. The spectrum from the gain switched laser shows red shift frequency chirping, that could be compensated for, by using a fibre with large normal dispersion at the output wavelength of the laser diode [21]. Dispersion Compensating Fibres (DCF) could serve to counteract the linear component of the red shifting frequency chirp across the pulse. Alternatively, the DCF could be replaced by a chirped Fibre Bragg Grating (FBG) to obtain pulse compression and thereby reduce the time bandwidth product (Figure 3-4).

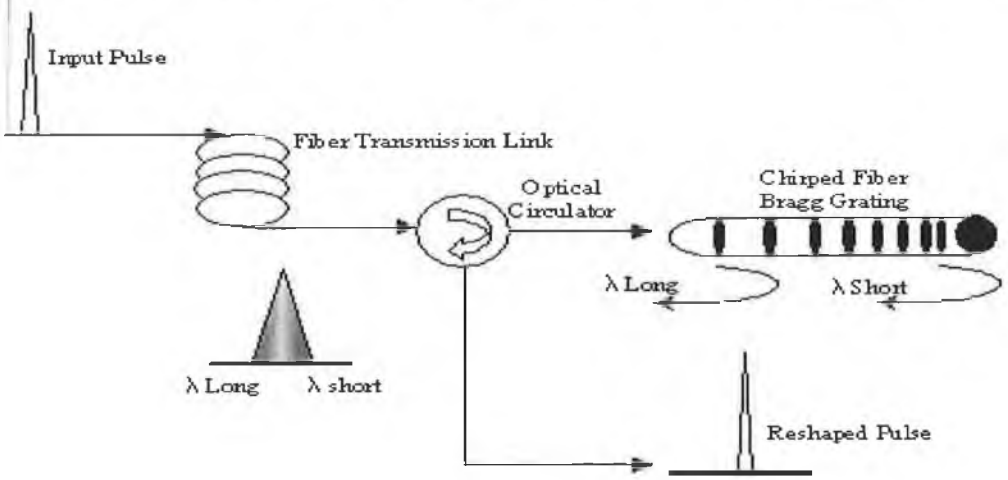

Figure 3-4: Pulse compression using a chirped FBG

As mentioned earlier the instantaneous frequency deviation of the gain switched pulse has a red shift in time, although initially there is a small blue shift (non-linear). In a normal dispersive medium the transit time for a pulse increases with wavelength. Therefore the rear part of the pulse will catch up with the leading part. Clearly an optimum total dispersion exists at which the pulsewidth has reached a minimum. However since the frequency chirping of most laser diodes under gain switching conditions have a non-linear part (initial blue shift) [22], even at an optimum compensation condition, transform limited pulses cannot be produced.

Various methods have been described in the literature to suppress the chirp and generate transform-limited pulses. Liu *et al* report using a monochromator (chooses the linearly chirped part) is used in conjunction with a DSF (-18 ps/km.nm) to reduce the time-bandwidth product from 5.6 to 0.26 [22]. Guy *et al* use an Electro-absorption (EA), which provides the spectral filtration, and then compensate for the linear chirp by passing it through a dispersive transmission filter [23]. Most of such techniques involve using additional filters, modulators and/or DSF's. This not only brings about an additional cost factor but also introduces higher losses in the system due to their insertion loss. A much simpler and cheaper technique to improve the spectral quality of a gain switched pulse involves the self-seeding [24] of a gain switched pulse source or injection of light from an external source into the gain switched pulse source [25]. We will deal with this technique in more detail later on in this chapter.

3. Timing jitter

In terms of their applications, timing jitter could be another key parameter of gain switched optical pulses, since it can dramatically affect the performance of a system where a gain switched laser is used. In high bit rate optical communication links, timing jitter could degrade the system performance. Performance could be limited in terms of the maximum data transmission by limiting the number of channels in an OTDM system and in terms of the Bit Error Rate (BER) by adding errors from the uncertainty in a pulse position over a significant fraction of the bit period. Timing jitter could be classified as correlated and uncorrelated. Correlated jitter is mainly caused by the drive circuits (phase noise) and is usually negligible (< 1 ps) [26]. Uncorrelated jitter contributes a major portion of the overall timing jitter and is related to spontaneous noise and pulse turn on dynamics [27]. The time interval between the onset of the electrical and the resulting optical pulse is called the turn on delay time. The Turn On delay time Jitter (TOJ) stems from the fluctuation in the photon density during the buildup of the optical pulse, caused by the random character of spontaneous emission. In a single mode laser the number of photons (when the carrier density reaches threshold) within modes that participate in the laser emission is lower by a factor approximately equal to the number of modes of a FP laser (~20). Due to the lower photon number in relevant modes a single mode DFB

suffers much stronger from spontaneous emission than an FP suffers (at the same bias current), thus exhibiting a larger timing jitter [28]. One of the traditional tools used in measuring jitter involved increasing the persistence of an oscilloscope. Another method mainly associated with eye diagrams entails the use of the colour grade function. In our work jitter measurements were carried out by using the histogram tool (a feature available in the oscilloscope used). In particular, it provides the standard deviation statistic at a chosen threshold that can then be used to "predict" the jitter performance.

There are several techniques available for addressing the ill effects of jitter. Jinno *et al* describe a gain switching experiment where the bias is optimized in conjunction with an external compression fibre in order to achieve low timing jitter of <0.5 ps [26]. Barry *et al* have reported another method, which involves a low level injection from a CW source [20]. Gunning *et al* also use this method and report an experiment where CW light injection is used to suppress the jitter [29]. They also show that CW light injection advances the turn on time of gain switched pulses by about 15-20 ps. A much simpler and cost effective method of (partially) overcoming TOJ involves the self-seeding of a gain switched laser [30]. Therefore self-seeding can be used for not only overcoming chirp (as mentioned in the previous section) but could also be used to overcome TOJ.

3.3 Experimental results

We decided to use gain switching as the major technique for the generation of short optical pulses and the results in this section will demonstrate different gain switched configurations used for the generation of pulses suitable for high speed optical communication systems. The pulses produced by gain switching could then be made closer to the transform limit by either self-seeding or by using external injection. The requirement of a wavelength tunable CW source for external injection makes self-seeding a preferred method of overcoming timing jitter as well as achieving single-mode operation. As mentioned earlier the generation of picosecond optical pulses by gain switching could be achieved by using two different gain switching techniques. One is by modulating the laser diode with using a large sinusoidal current [31]. The second technique involves using short electrical pulses of large amplitude [32]. The latter has

been reported to give narrower optical pulses in comparison to the first technique [33]. However it is difficult to generate electrical pulses at a high repetition rate, making the use of sinusoidal currents at high frequencies more attractive. Even though lasers at various wavelengths were used in experiments to generate optical pulses only the 1.5 μm pulse generation experiments are shown here. This is due to the fact that we were interested in the use of these pulses for optical communications. Our choice of wavelengths was further justified since in most experiments EDFA's were used.

3.3.1 Gain switching using a Step Recovery Diode (SRD)

3.3.1.1 Introduction to SRD's

The SRD is a two terminal P-I-N junction diode whose dc characteristics are similar to that of a usual P-N junction, but whose switching characteristics are different. It is also referred to as an Electrical Pulse Generator (EPG) or a comb generator. Like a normal P-N diode, the SRD conducts when forward biased but unlike a P-N diode, it also shows significant conduction when reverse biased. However, this only continues for a short time, after which the diode no longer conducts when reverse biased. The transition from the conducting to non-conducting states of the reverse biased diode occurs in a time of typically less than 100 ps [34]. Therefore when a forward biased SRD is suddenly reverse biased, it will initially appear as a low impedance until all the storage charge is depleted. Then its impedance will quickly rise to its normal, high reverse biased impedance. It is the extremely fast impedance transition, which enables SRD's to be used to generate fast pulses. The comb generator modules are driven by sinusoidal inputs at the required frequency, and they transform this to train of short electrical pulses at a repetition rate equal to that of the input frequency [35]. In the frequency domain the output is a comb of frequencies, which are multiples of the drive frequency. A comb generator driven at say 1 GHz will produce outputs at 2 GHz, 3 GHz etc. to some maximal value determined by the bandwidth of the device. The relative amplitude of these harmonics is related to the pulsewidth. In order to experimentally demonstrate this, a sine wave at a frequency of 500 MHz was amplified before being fed into a comb generator (GC 500 RC). The input sine wave is shown in Figure 3-5.

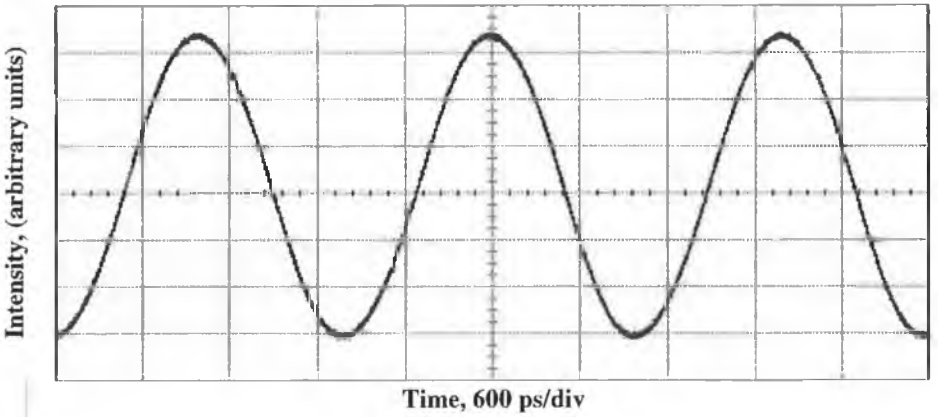

Figure 3-5: Electrical sinusoidal input to the SRD

The output of the comb generator was then fed into a 40 GHz electrical spectrum analyzer (Anritsu MS 2668 C – resolution bandwidth = 10 Hz) after being attenuated by 40 dB. The electrical spectrum obtained is shown in Figure 3-6 below.

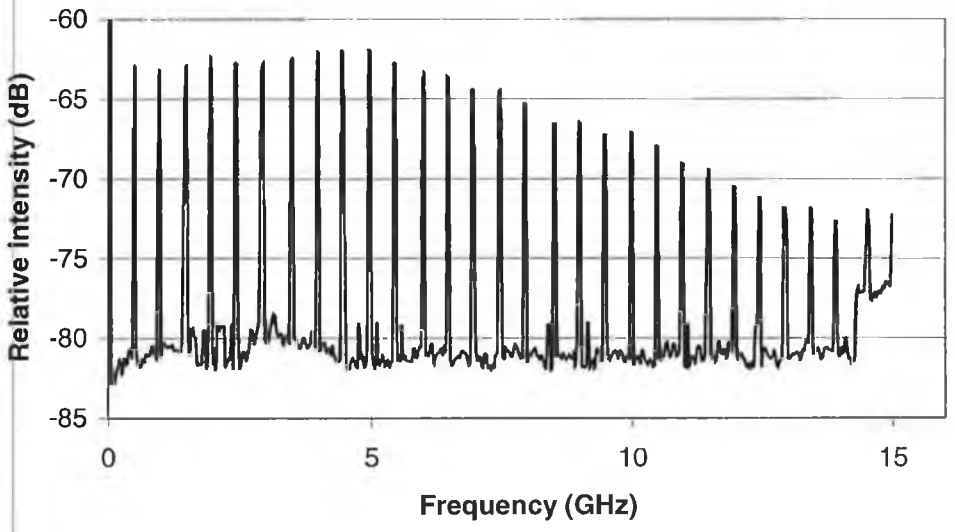

Figure 3-6: Spectral output of SRD

It can be noticed from this figure that the output is a comb of frequencies, which are multiples of the drive frequency, and the relative amplitudes of these harmonics are related to the pulsewidth (3 dB roll of point of spectrum).

Having examined the spectral output of the SRD we then looked at the characteristics of the generated electrical pulses from the same 500 MHz (GC 500 RC) comb generator. The experimental set-up used is shown in Figure 3-7.

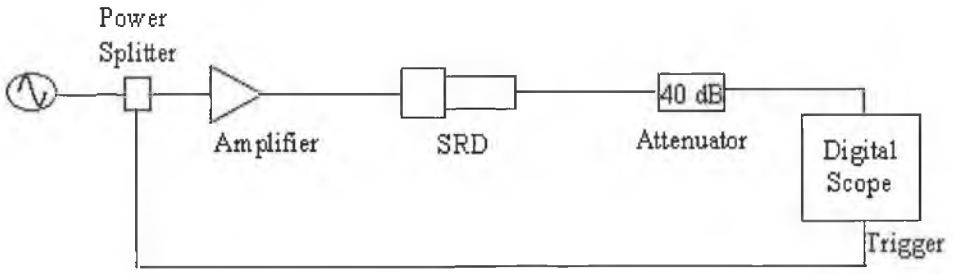

Figure 3-7: Experimental set-up

A sinusoidal signal with an output power of 1 dBm at 500 MHz was passed though an electrical amplifier. The amplified signal of 29 dBm was input into the SRD. The output of the SRD was monitored using a 50 GHz HP digitizing oscilloscope which had a 40 dB attenuator placed at the input of the scope. The output pulse was as expected (Figure 3-8), it had a width (Full Width Half Maximum - FWHM) of 60 ps and a pulse height of approximately 14.6 V (taking into account the 40 dB of attenuation).

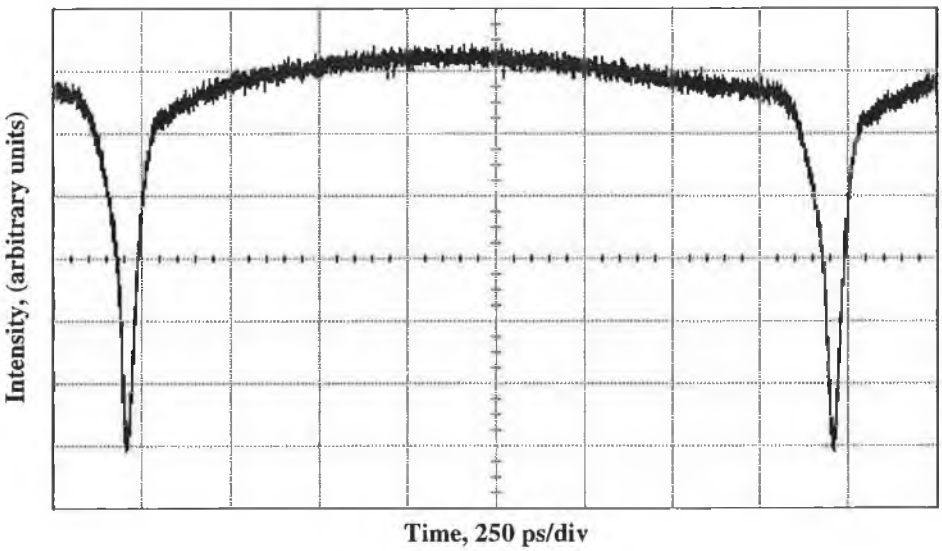

Figure 3-8: Electrical pulses output from SRD

Having examined the output electrical spectra and pulses from the comb generator, we then went ahead to use these short, large amplitude electrical pulses to gain switch various lasers.

3.3.1.2 Gain switching of a 1.55 μm DFB laser diode.

This section outlines the procedure followed and results obtained in gain switching a DFB laser with the aid of a SRD. The laser used was an NTT InGaAsP commercial

1.55 μm DFB (KELD 1551 CCC_1 -- Appendix D) laser diode. Firstly we set out by doing the dc characterization of the laser. The optical power versus the bias current (PI) characteristic was obtained and plotted. From this it was deduced that the laser had a threshold current of 19.3 mA. Then by using a network analyzer bandwidth measurements were carried out. The relaxation oscillation peak was found to be approximately 10 GHz at a bias current of 60 mA. This DFB laser had a central wavelength of 1552.4 nm at 25°C. The set-up that was used to gain switch this laser, using the 500 MHz SRD, is schematically shown in Figure 3-9.

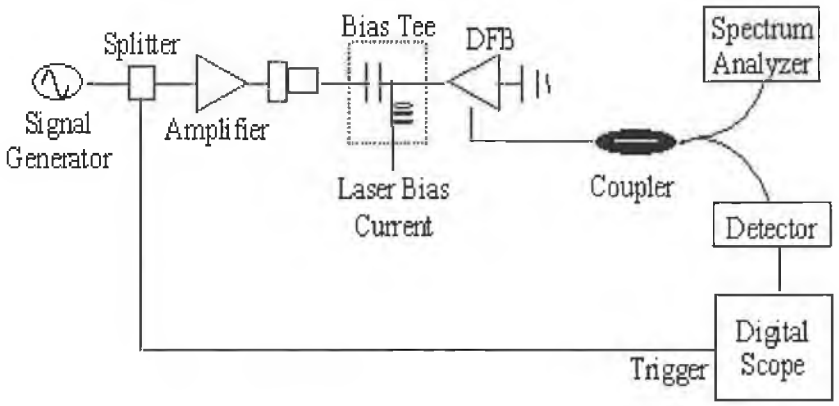

Figure 3-9: Simple set-up for gain switching using an SRD

In all the experiments described here the modulating signal was first passed through a (90:10) pick off tee. The 10% path was used to trigger the sampling oscilloscope while the 90% part was used to modulate the laser. The DFB laser used has its cathode grounded (P-side down). Hence, in order to gain switch this laser, the negative going pulse could be applied directly. A 500 MHz sinusoidal signal was amplified and converted into a stream of electrical pulses of amplitude of 14.6 V and 60 ps pulsewidth using a SRD (GC 500 RC). A bias tee was used to combine the electrical pulse stream with a variable dc bias to enable gain switching of the DFB chip laser. The dc bias was initially set to 15 mA to be changed later in order to optimize the output optical pulse. The output was composed of a train of optical pulses whose repetition rate was the same as the modulation frequency. The resulting gain switched optical pulses from the laser was passed through a 90:10 coupler. The 90% arm was taken into a detector before being passed into the 50 GHz digitizing oscilloscope while the other arm was taken into an

Anritsu Optical Spectrum Analyzer (OSA) which has a resolution of 0.07 nm. The dc bias (10 mA) and the modulation frequency (500 MHz) were optimized to obtain the shortest possible pulse duration. The optical pulses observed on the oscilloscope are shown below in Figure 3-10. The first pulse is non-averaged (Figure 3-10 (a)) while the second has an average of 16 (Figure 3-10 (b)) enabled.

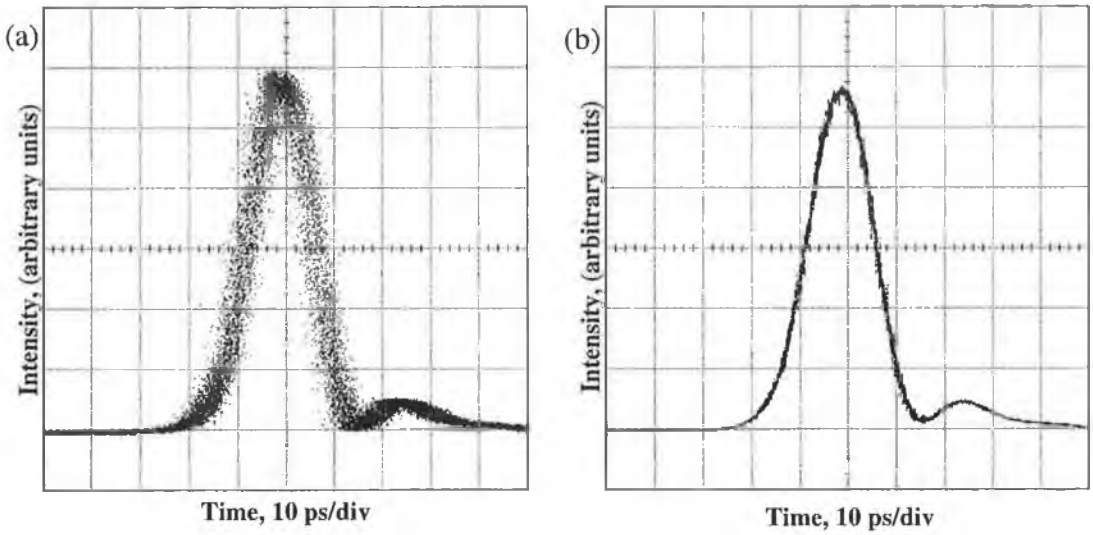

Figure 3-10: Gain switched pulses (a) Non-averaged (b) Averaged over 16

The width (FWHM) of the optical pulse was about 17 ps. The optical detector and the oscilloscope together have a temporal resolution of about 12 ps (mainly due to the resolution of the detector = 9 ps). Thus to find the actual pulsewidth it would be necessary to deconvolve using a simple sum of squares formula (equation 3-8).

$$T_A = \left(T_M{}^2 - T_R{}^2\right)^{1/2} \qquad \textbf{Equation 3-9}$$

Where

T_A = Actual pulsewidth

T_M = Measured pulsewidth

T_R = Temporal resolution of measurement system (12 ps)

Therefore the considering pulse obtained using the 500 MHz SRD above, the actual pulsewidth is calculated to be about 12 ps. The pulse peak powers can be calculated from the peak-to-peak (V_{pp}) voltage level on the oscilloscope (170 mV) by using the responsivity of the detector. The photodiode generates 0.55 amperes of electrical current

per watt of optical input power falling on it, at 1.5 μm. Thus taking the input resistance of the scope into account (50 Ω), the peak current from the detector is approximately (since the bandwidth of the detector might affect this) 3.4 mA. Hence the peak power of the optical pulse falling on the detector is calculated to be about 6.18 mW. Jitter is very noticeable in the case of the non-averaged optical output pulse and was measured to be around 4 ps. By looking at the electrical pulse shown in Figure 3-8 we can safely conclude that most of the jitter is introduced by the laser diode.

Having connected the second arm of the coupler to the spectrum analyser we then went on to examine optical spectrum of the DFB laser under two different conditions: firstly with the laser running CW and then with the laser under modulation. With the laser biased at 59.6 mA (CW) the spectral width (FWHM) was measured to be around 8.5 GHz. The actual width is much less than this because the resolution of the analyzer is 8.5 GHz. However when the laser is gain switched (modulated) to obtain optical pulses, the variation in carrier density introduced, will result in a frequency shift (chirp) and so the spectral width would increase. Figure 3-11 (a) shows the optical spectrum under CW conditions while Figure 3-11 (b) shows the optical spectrum when the laser is under modulation.

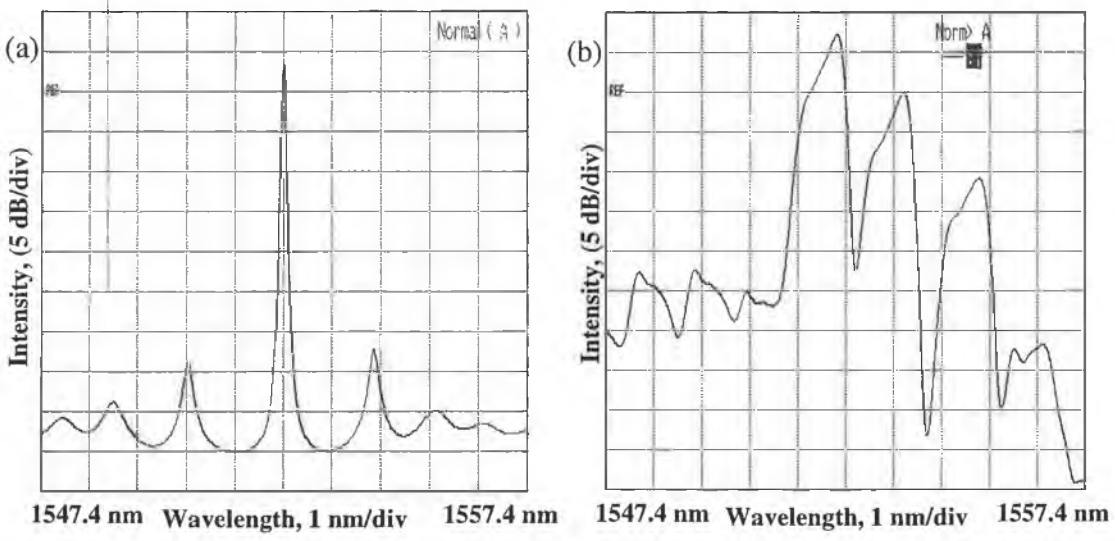

Figure 3-11 Optical spectra (a) CW (b) Gain switched

The effect of modulation on the optical spectrum from the laser can clearly be seen when comparing Figure 3-11 (a) {laser is not modulated} and (b) {resulting spectrum under

modulation}. The optical spectrum of the laser under modulation has its spectral width increase to about 130 GHz due to the effect of chirp. With a deconvolved pulsewidth of 12ps, the time bandwidth product ($\Delta\mu\Delta t$) goes up to 1.56, which is clearly far from the transform limit (0.44) for Gaussian pulses. Another problem associated with gain switching that could be noticed here is the degradation of the Side Mode Suppression Ratio (SMSR). The SMSR is a ratio between the output power emitted in the strongest mode and that emitted in the second strongest mode and is usually expressed in decibels. Under Continuous Wave (CW) operation this DFB laser has a SMSR of about 36 dB. However under gain switching conditions the very large fluctuations in the photon density (caused by the laser being pulled below threshold) result in the side modes of the laser being strongly excited [24] thereby pulling the SMSR down to less than 8 dB (Figure 3-11 (b)). If optical filtration of the gain switched optical pulses is necessary, then this degradation in the SMSR of the DFB will lead to an increase of the noise of the pulses due to the mode partition effect. This effect and its influence on the system performance will be discussed in detail in the next chapter.

We have seen that even DFB lasers exhibiting large SMSR when operated in CW mode, have a diminution in their SMSR when gain switched. A simple technique for addressing this problem involves self-seeding which entails reflecting back a portion of a pulse back into the laser cavity [24, 36, 37]. A wavelength selective element such as a Fibre Bragg Grating (FBG) could be used to seed only the required mode. Self-seeding not only overcomes the problem with the degrading SMSR but also overcomes the problem of jitter. Even the chirp caused by gain switching is reduced slightly, when a small portion of light is fed back in to the laser. The reduction in the chirp magnitude with increasing reinjection has been noted previously [38], [47], [58] and arises since the presence of the reinjected signal reduces the peak inversion reached during the pulse emission process.

3.3.1.3 Self-seeding of a gain switched DFB

A typical self-seeding set-up involves a small amount (0.2 – 6 %) of the optical output power of the DFB laser being fed back into the active layer of the laser diode. In order to achieve a large SMSR again the reflected pulse must arrive back at the laser diode during a narrow time window (around the time when the electrical pulse is initiated and before

the carrier density reaches threshold). The feedback causes an initial excitation well above the spontaneous emission noise level for the dominant mode which results in the laser emission being strongly single moded with a high SMSR. In order to demonstrate the improvement of the SMSR with self-seeding experimentally we used the following set-up shown schematically in Figure 3-12.

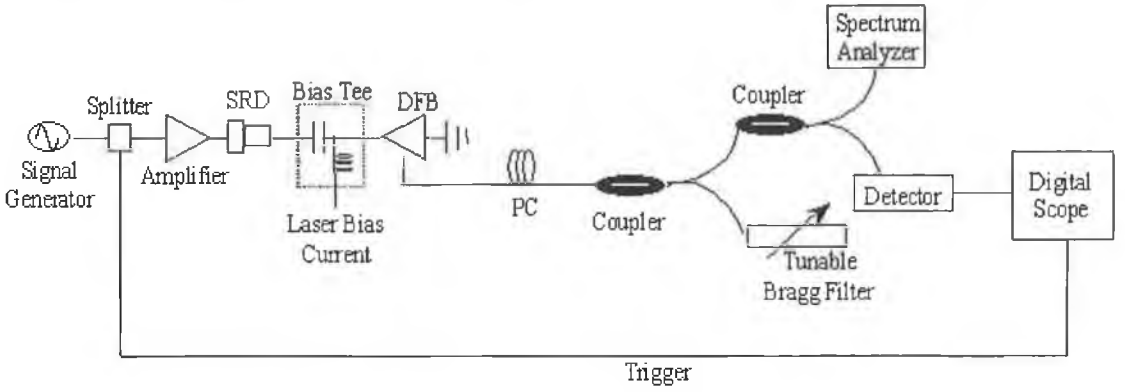

Figure 3-12: Experimental set-up for self-seeding of a gain switched (using an SRD) laser

The laser used here was the same as in the previous experiment. It was initially gain switched using the 500 MHz SRD (GC 500 RC). The dc bias was varied in order to optimize the output optical pulse (minimum pulsewidth) and was set to about 10 mA. The gain switched output optical signal was coupled into a fibre using a fibre pigtailed grin lens. A 50:50 coupler was used to split this output signal. Self-seeding of this laser diode was achieved by using an external cavity containing a polarization controller and a tunable FBG with a bandwidth of 0.4 nm.

In order to achieve optimum Self-Seeded-Gain-Switched (SSGS) pulse generation, the central wavelength of the fibre grating was initially tuned to the main longitudinal mode of the gain switched laser. The pulse repetition rate (sinusoidal modulation frequency) had to be adjusted (multiple of the inverse of the round trip time) to ensure that the signal, reinjected into the laser from the external cavity, arrived as an optical pulse was being built up in the laser. An operating frequency of 497.09 MHz was found to be suitable. In addition to tuning the fibre grating and the modulation frequency, we could also optimize the reinjection back into the laser cavity by adjusting the Polarization Controller (PC). The PC was adjusted until a maximum amplitude of the output pulse was obtained and/or

until a minimum time bandwidth product was obtained. The unused arm of the 50:50 coupler was passed into a 90:10 coupler where the 90% arm was used for the temporal characterization while the other was used for the spectral characterization.

The resulting gain switched spectra before (Figure 3-13 (a)) and after self-seeding (Figure 3-13 (b)) are shown below.

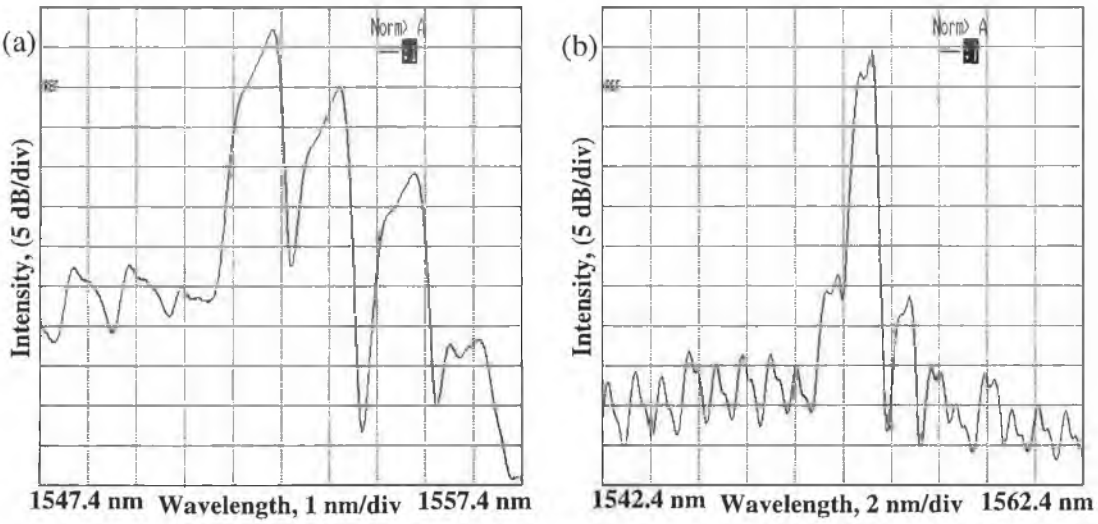

Figure 3-13: Optical spectra (a) Gain switched (b) Self-seeded and gain switched

The spectral broadening (~130 GHz) and the diminution of the SMSR (7 dB) in the gain switched spectrum can clearly be noticed in Figure 3-13 (a). However in Figure 3-13 (b) (with self-seeding) the SMSR of the SSGS spectrum is improved (30 dB) due to the feedback from self-seeding, which causes an initial excitation well above the spontaneous emission noise level for the principal mode. The linewidth is also brought down to 90 GHz (Figure 3-13(b)) thereby reducing the TBWP by a small margin. Even this minor reduction of the time bandwidth product of these pulses makes them more suitable for use in high-speed optical communication systems.

Figure 3-14 (a) shows the gain switched pulses, which characteristically exhibit a large timing jitter (~ 4 ps). The pulsewidth was measured to be 17 ps thereby yielding an actual pulsewidth of 12 ps. The V_{pp} level on the oscilloscope was observed to be 286 mV. Subsequently the pulse peak power falling on the detector was calculated to be 10.4 mW.

Figure 3-14 (b) illustrates the self-seeded gain switched pulses. Here the pulsewidth was measured to be about 19 ps (actual 14.7 ps) and the pulse peak power was calculated to be 4.5 mW. As can be clearly seen the timing jitter is greatly reduced (1.4 ps) in comparison to the gain switched pulse without self-seeding. Both traces shown in Figure 3-14 are non-averaged.

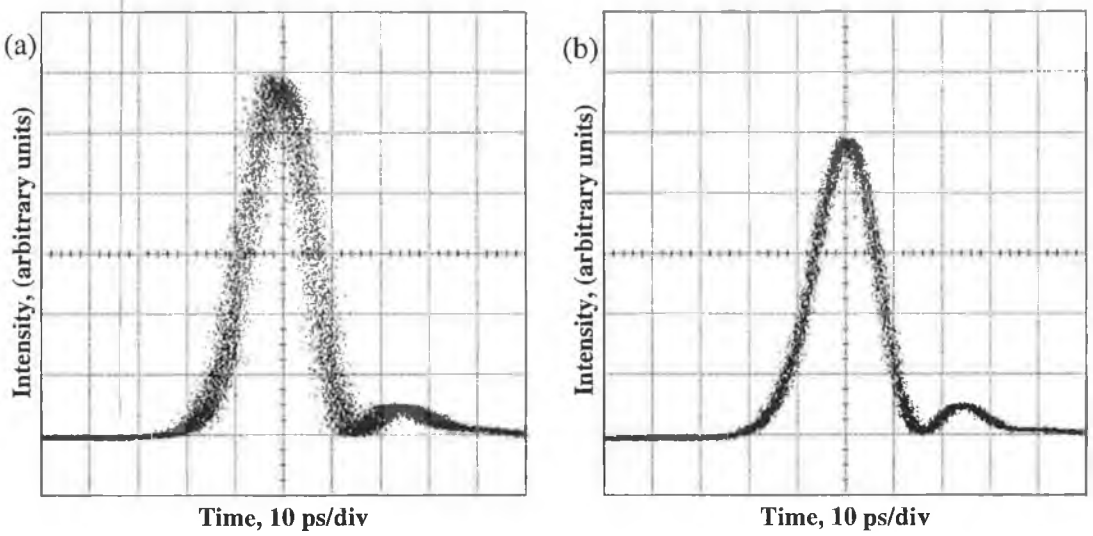

Figure 3-14: Non-averaged pulses (a) Gain switched pulse (b) Self-seeded gain switched pulse

Both effects, reduction of timing jitter and increasing of the SMSR, are due to the same fundamental physical mechanism. Regarding the timing jitter, the feedback increases the photon number in the relevant mode, which competes and suppresses the effect of spontaneous emission. This prevents the random fluctuations of the photon density thereby exhibiting a smaller timing jitter in the output pulses.

Hence SSGS pulse sources maybe suitable for use in high-speed optical communication systems. However one of the drawbacks in using DFB lasers is that being a single wavelength device one is restricted to a fixed emission wavelength (does not allow broad wavelength tuning). A solution to this problem is provided by the FP laser. Furthermore the timing jitter in gain switched DFB lasers is shown to be much larger in comparison to its FP counterpart under comparable driving conditions. The limitation of the repetition frequencies obtainable with comb generators induced another modification of our gain-switching set-up. Hence in most of our experiments, priority was given to gain switching

using large sinusoidal signals at GHz frequencies, the results of which are shown in the following section.

3.3.2 Gain switching by driving with a large amplitude sine wave

As mentioned previously gain switching could be carried out either by driving the laser with an electrical comb generator or by using a large sinusoidal signal at sub-GHz or GHz frequencies. The use of electrical pulses has been reported to give rise to narrower optical pulses [33] but it is very difficult to generate electrical pulses at a high repetition rate. Since the development of optical pulses at high repetition rates is of vital importance in high-speed OTDM systems, the technique of using sinusoidal currents at high frequencies (in comparison to using an SRD) to gain switch a laser becomes of great interest. The following section shows the results obtained using the above-mentioned configuration.

3.3.2.1 Gain switching of a 1.55 μm FP laser diode.

The results of gain-switching 1.55 μm lasers using sine waves is shown here. The frequency of modulation was initially maintained at 2.5 GHz. A schematic configuration of our experimental set-up used is shown in (Figure 3-15).

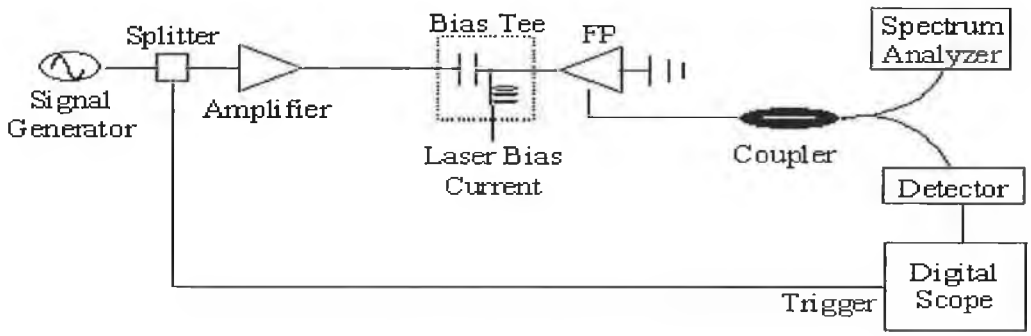

Figure 3-15: Experimental set-up used for gain switching using a large amplitude sine wave

The FP laser used here was a commercial 1.5 μm InGaAsP device (KELD 1501R-CCC_1 – Appendix E) from NTT electronics. From basic dc characterization (PI curve) it was found that this laser had a threshold current of 26 mA. Biasing the laser above threshold at about 60 mA (2.3 I_{th}) and running in CW mode the longitudinal mode spacing was found to be 1.12 nm. Furthermore the central wavelength at the same bias was found to be 1568 nm.

The laser was manufactured for use in 10 Gb/s systems and had a specified bandwidth of 8 GHz at an injection current of 50 mA. Gain switching of this laser was achieved by applying a dc bias current together with a sinusoidal modulation to the laser. Initial gain switching frequency was 2.5 GHz and the bias current was reduced to 16mA. The major portion (90%) of the split electrical sinusoidal signal was then amplified before being applied to the laser. The applied modulation signal power was about 28 dBm. The other part (10%) was used to trigger the sampling oscilloscope. The optical signal from the laser was then coupled into a fibre using a GRIN lens fibre pigtail, which was antireflection coated (to prevent reflections back into the laser). The optical pulses generated from this experimental arrangement were then characterized in the spectral and temporal domains by passing the optical signal through a 90:10 coupler. The 10% arm was used to scrutinize the optical spectra using an optical spectrum analyzer with a resolution of 0.07 nm while the 90% arm was used for the temporal measurements. This was conducted using a 50 GHz pin detector followed by an Agilent 50 GHz sampling oscilloscope. As mentioned previously, the time resolution of our measurement system is 12 ps.

The resulting pulses observed on the scope are shown in Figure 3-16 where figure (a) shows a non-averaged pulse and figure (b) shows a pulse averaged over 16.

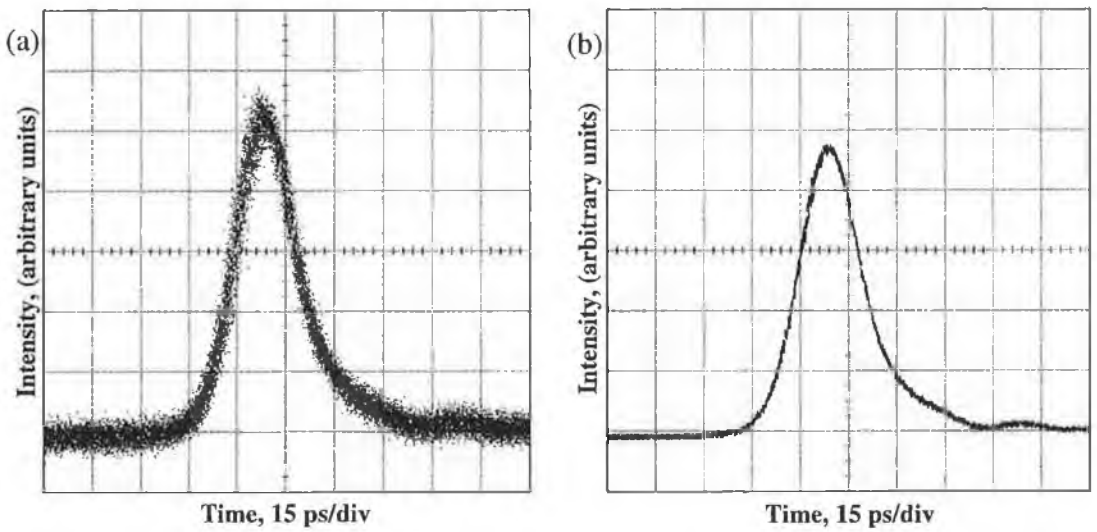

Figure 3-16: Gain switched pulses (a) Non-averaged (b) Averaged

Varying the bias current to about 16 mA optimized (minimized) the pulsewidth. The optimized pulsewidth was found to be 19 ps (14.7 ps after deconvolving). The timing jitter was measured to be about 1.4 ps using the non-averaged pulse shown in Figure 3-16 (a). By comparing the jitter of this multi-mode laser with that of the DFB case shown in Figure 3-10, we can clearly see that the timing jitter is smaller in the case of the multimode laser. This is in agreement with experiments performed by Weber *et al* where they report that the jitter of the single-mode lasers is always considerably higher than that of the multi-mode lasers at the same injection currents [28].

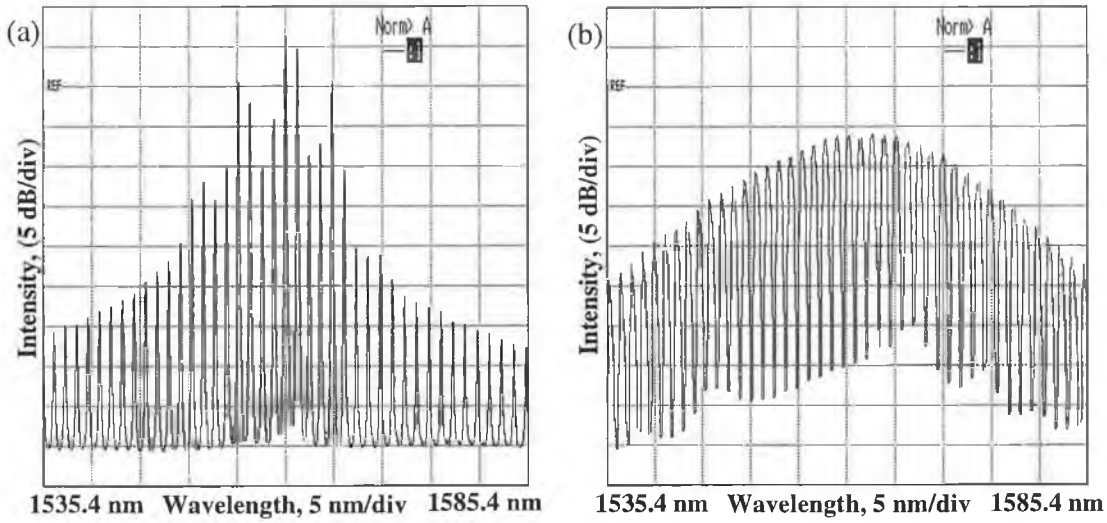

Figure 3-17: Optical spectra (a) CW (b) Gain switched – OSA resolution set to 0.1 nm

The associated gain switched spectra before and after gain switching are shown in Figure 3-17. By comparing the optical spectra before and after gain switching, we can clearly see that the longitudinal modes of the gain switched spectrum are broadened due to frequency chirp.

As we have seen, the gain switching of an FP laser resulted in the generation of 20 ps pulses (FWHM) with a multimode spectrum. Even though these pulses are more useful than those of a DFB laser in terms of temporal jitter, the multi-modal nature of the FP still causes a problem. The problem culminates from the fact that when an optical pulse with a multi-mode spectrum propagates in a dispersive fiber medium, the laser modes travel at different speeds and hence spread out in the temporal domain. Hence, as

explained earlier, single mode operation is imperative for high-speed links. It has been reported that a self-seeding set up could be sufficient to switch the laser from multi mode to single mode emission [39]. We have already seen in the case of DFB's, that the timing jitter and the degradation of SMSR could all be overcome by the use of self-seeding. In a small way self-seeding compensates for chirp as well.

Wavelength tunability is an aspect that has attracted a lot of interest in the short optical pulse generation schemes [40]. Hence, we proceeded to investigate and experiment on single wavelength operation of optical pulse sources that are also wavelength tunable over a wide range, the results of which are shown in the forthcoming section.

3.3.2.2 Self seeding of gain switched Fabry-Perot (FP) laser diodes

Owing to the increased demand in high bit rate WDM optical communications systems, a lot of attention has been expended in recent years to wavelength tunable picosecond pulse sources [41, 42]. One of the simplest and most cost-effective methods of generating such wavelength tunable single mode optical pulses involve the self-seeding of a gain switched FP laser diode and many experimental schemes using this technique have been reported [41-43]. In such a scheme, the laser diode is seeded with an optical feedback of an appropriate wavelength, and single mode pulse emission occurs, as long as the feedback arrives during the pulse buildup time. Generally self-seeding could be achieved by using a commercial laser diode and no antireflection coating is required on the diode facet. This and other advantages such as not requiring saturable absorbers and specific laser structure make it a very simple and cost effective method. As mentioned in the previous section, by self-seeding, we not only overcome the some of the disadvantages (timing jitter and degradation of SMSR) brought about by gain switching, but we also achieve single moded operation [30]. Therefore this technique could be capable of producing very low jitter pulses (< 2 ps) with a high side mode suppression ratio (> 30 dB). Recent experiments have also demonstrated that the generation of multiwavelength pulses suitable for use in WDM networks could be achieved by using the self-seeding technique [46].

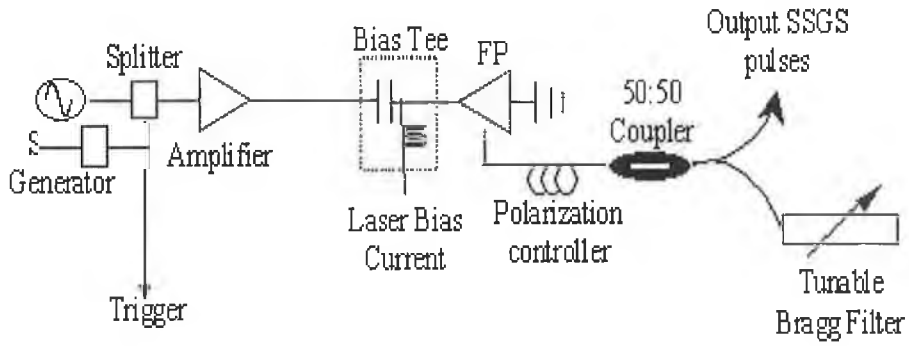

Figure 3-18: Experimental set-up used for SSGS pulse generation

Figure 3-18 shows our experimental set-up used to realize self-seeding of a gain switched pulse source. The FP laser employed in the gain switching experiment in the previous section was utilized here again. Gain switching of the laser was carried out by applying a DC bias current of 17 mA, and a sinusoidal modulation signal with a power of 29 dBm, to the laser diode. The sinusoidal modulation signal had a frequency around 2.6 GHz. Self-seeding of the gain-switched laser diode was achieved by using an external cavity containing a polarization controller (PC), a 3 dB coupler, and a tunable Fiber Bragg Grating (FBG -- HWT-BG-1) with a bandwidth of 0.4 nm.

To achieve optimum SSGS pulse generation, the central wavelength of the fiber grating was initially tuned to one of the longitudinal modes of the gain-switched laser. The frequency of the sinusoidal modulation was then varied to ensure that the signal reinjected into the laser, from the external cavity, arrives as an optical pulse is building up in the laser. An operating frequency of 2.654 GHz was found to be suitable. In addition to tuning the fiber grating and the modulation frequency, we could also vary the amount of light reinjected, and hence the SMSR of the output optical pulses, by adjusting the PC. The output pulses after the 50:50 fiber coupler were characterized in the temporal domain using a 50 GHz photodiode in conjunction with a 50 GHz HP digitizing oscilloscope. Pulse characterization in the spectral domain was carried out using an optical spectrum analyzer.

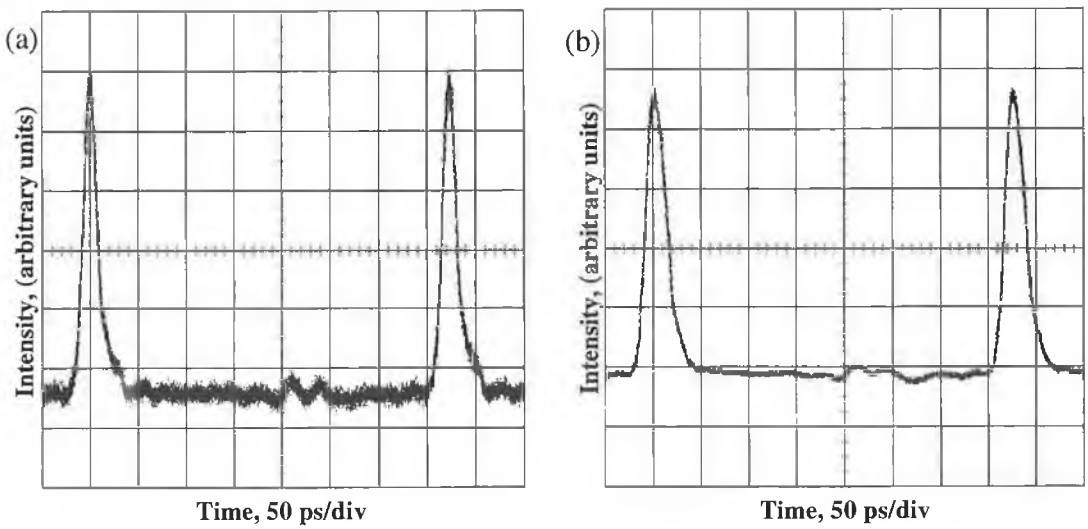

Figure 3-19: Non-averaged pulses (a) Gain switched (b) Self-seeded gain switched

Figure 3-19 (a) shows the gain switched pulses prior to self-seeding. The observed pulsewidth was about 19 ps. From the total response time of about 12 ps for the combination of the photodiode and the oscilloscope, we can deconvolve the output pulse duration to be around 14.7 ps.

With the PC adjusted to maximize the feedback into the FP device, the resulting output pulses from the SSGS set-up were as shown in Figure 3-19 (b). The output pulse duration was measured to be around 20.5 ps yielding an actual pulsewidth of about 16.6 ps. By comparing the different cases above we can clearly see that the jitter is reduced in the case of the self-seeded pulses in comparison to the unseeded gain switched pulses (~ 1ps). However the pulsewidth seems to increase by about 2 ps. The broadening of the self-seeded pulses is directly related to the modification of the laser gain dynamics in the presence of external optical feedback [36]. With self-seeding the laser medium is driven more rapidly into saturation. Therefore the laser switches sooner and the laser gain at the switching time is lower than that of the free running case. Hence the gain variation during pulse emission is reduced, which then leads to a larger pulsewidth.

From the spectral output, shown in Figure 3-20, we can determine that the FP mode selected using the Bragg grating was at a wavelength of 1555.4 nm. In addition, the SMSR of the signal was 30 dB, and the 3 dB spectral width was about 0.3 nm (36 GHz at

1.5 μm). This yields a time-bandwidth of about 0.59 that is quite close to the time-bandwidth product of transform limited Gaussian pulses (0.44). In order to account for the experimental errors a tolerance of about ± 10 % should be incorporated to the calculated TBWP values.

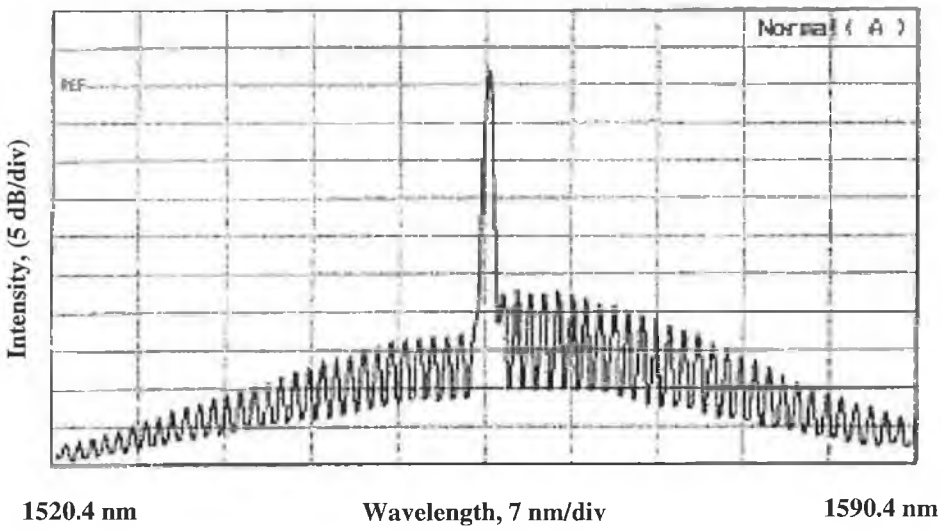

Figure 3-20: Optical spectrum of SSGS pulses

The self-seeding of a gain switched Fabry Perot laser as a pulse generation technique is validated by the experiments performed. As shown by the results obtained, self-seeding of a commercial gain switched FP laser is a simple way of generating short, wavelength tunable and low jitter pulses. It becomes the preferred method, when compared to the use of a DFB laser, when factors such as tunability and low timing jitter are taken into account.

3.3.2.3 Highly wavelength tunable SSGS pulse sources

In the self-seeding experiment carried out above, we could only achieve a tuning range of about 3-4 nm, due to the limited piezoelectric wavelength tunability of the fibre Bragg gratings that were used. To investigate on the expansion of this tuning range, we used a TB9 series optical grating filter from JDS Uniphase. This filter has a tuning range of 115 nm ranging from 1470 nm to 1585 nm and a 3 dB bandwidth of about 0.2 nm. The key parameters that were investigated, as the wavelength was tuned, were the SMSR and the pulsewidth.

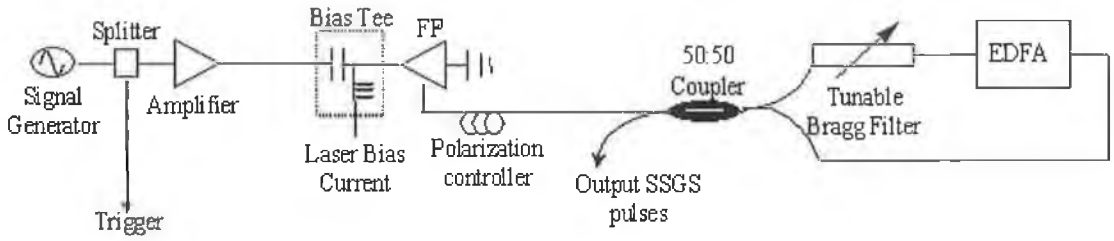

Figure 3-21: Experimental set-up for widely tunable SSGS pulse generation

Figure 3-21 illustrates our set up used for the wavelength tunable self-seeded pulse source experiment. The same semiconductor FP laser (KELD 1501R-CCC_1) employed in the gain switching arrangement is utilized here again. Gain switching was carried out by applying a sinusoidal modulation signal at a frequency of about 2.7 GHz and a power of 29 dBm in conjunction with a DC bias current of 17 mA, to the laser diode. The pulses generated (Figure 3-22 (a)), with the lowest possible pulsewidth of about 22 ps, were obtained by optimizing the bias current to about 17 mA. By deconvolving the actual pulsewidth was found to be 18.4 ps. The corresponding optical spectrum (Figure 3-22 (b)) comprised longitudinal modes with a FWHM of about 0.8 nm and a longitudinal mode spacing of 1.12 nm.

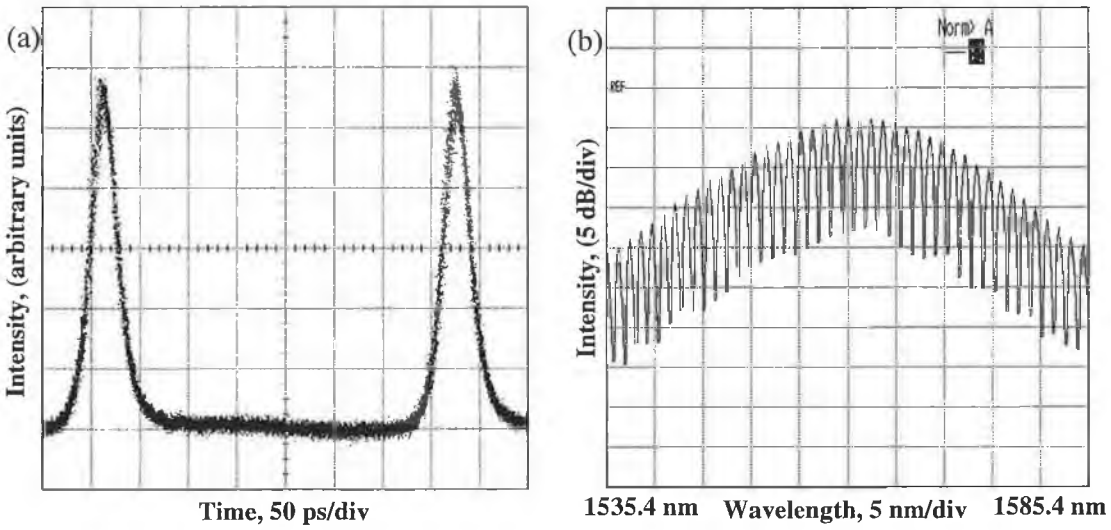

Figure 3-22: (a) Gain switched optical pulses (b) Corresponding gain switched spectrum

Self-seeding of the gain-switched laser diode was achieved by using an external cavity containing a polarization controller (PC), a 3 dB coupler, a tunable FBG (TB-9) and an EDFA. This set up differs slightly from the previous self-seeding schematic (Figure

3-18), in that the filter used here is a transmission filter rather than a reflection filter. Apart from the fact that the insertion loss of the filter was found to be high, the bandwidth of the filter being smaller than in the previous case resulted in the level of injection being smaller. The reduced level of injection tended to degrade the obtainable SMSR (<20 dB), which meant that the optical pulses produced, might have been unsuitable for optical communication applications (addressed in the next chapter). Hence, the wavelength element that was selected by the tunable filter was intensified by the use of an Erbium Doped Fibre Amplifier (EDFA), before being injected into the gain switched FP laser diode. Since the gain of the EDFA varies with the wavelength, the amplification had to be varied as the wavelength was tuned, to ensure that the re-injected power always remained constant. The re-injected power was monitored using an in-line optical power meter and was maintained at –13 dBm which was optimum in terms of the width and SMSR of the pulses.

Different longitudinal modes of the FP laser were selectively excited when the seeding wavelength was tuned near the centre of the desired mode and some of such results are shown in Figure 3-23 (a, b & c).

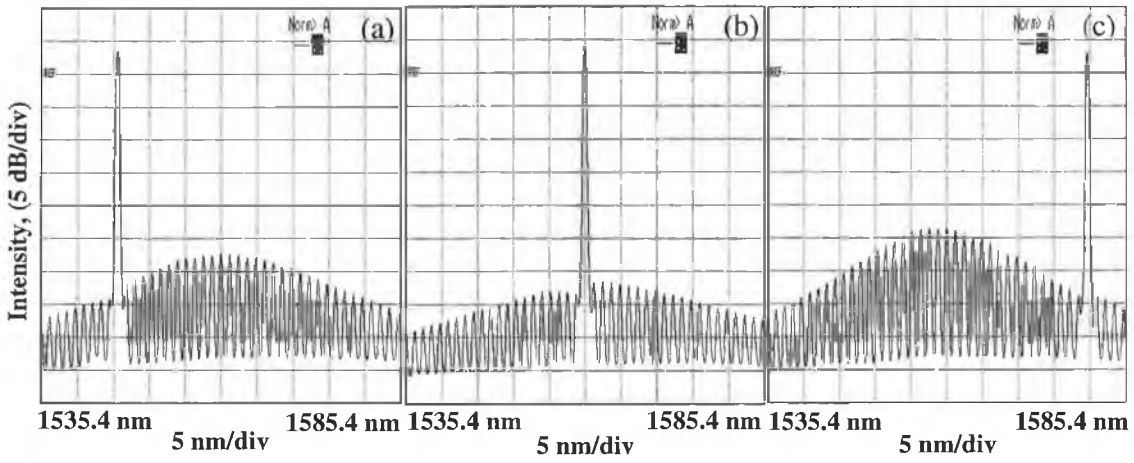

Figure 3-23: Optical spectra of wavelength tunable SSGS pulses (a) shortest wavelength with 30 dB SMSR, (b) Central wavelength with 35 dB SMSR and (c) Longest wavelength with 28 dB SMSR

It could be noticed from these figures that the SMSR decreases, as one tunes away from the gain peak (to longer or shorter wavelengths). This obviously relates to the fact that as one moves further away from the peak of the gain curve the power in the side modes

becomes smaller. Hence, as the seeded wavelength deviates away from the gain peak a reduction in the SMSR is expected. Figure 3-23 (a) shows the shortest wavelength that could be seeded and still obtain a SMSR of about 30 dB. Figure 3-23 (b) shows the selection of the central wavelength (gain peak) where the achieved SMSR was about 35 dB. The longest wavelength that could be seeded is shown in Figure 3-23 (c) and exhibits a SMSR of about 28 dB.

The pulse associated to the spectra above, is shown in Figure 3-24. The measured pulsewidth remained, almost constant at the central part of the tuning range, while it increased slightly at the extremes of tunability (as the seeding wavelength digressed away from the gain peak). The bias current was reduced to about 12 mA in order to obtain the minimum pulsewidth (29 ps). Actual pulsewidth by deconvolving was found to be about 26.4 ps.

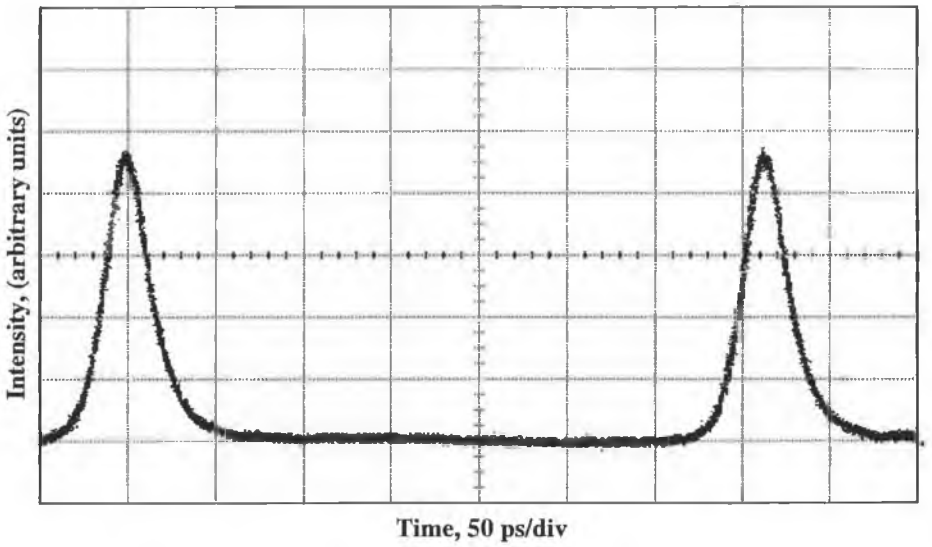

Figure 3-24: Widely tunable SSGS optical pulses under optimum operational conditions

The dependence of the SMSR on the seeding wavelength for a seeding power of –13 dBm was plotted and is shown in Figure 3-25. It can be clearly seen that we were able to obtain a SMSR of 25 dB and above within a range of 37 nm (1540 nm – 1577 nm). As the seeding power was increased, by increasing the pump power of the EDFA, the achievable SMSR increased and simultaneously the possible tuning range became

wider. However pulse deformation and instabilities [47] were observed beyond the above mentioned injection power.

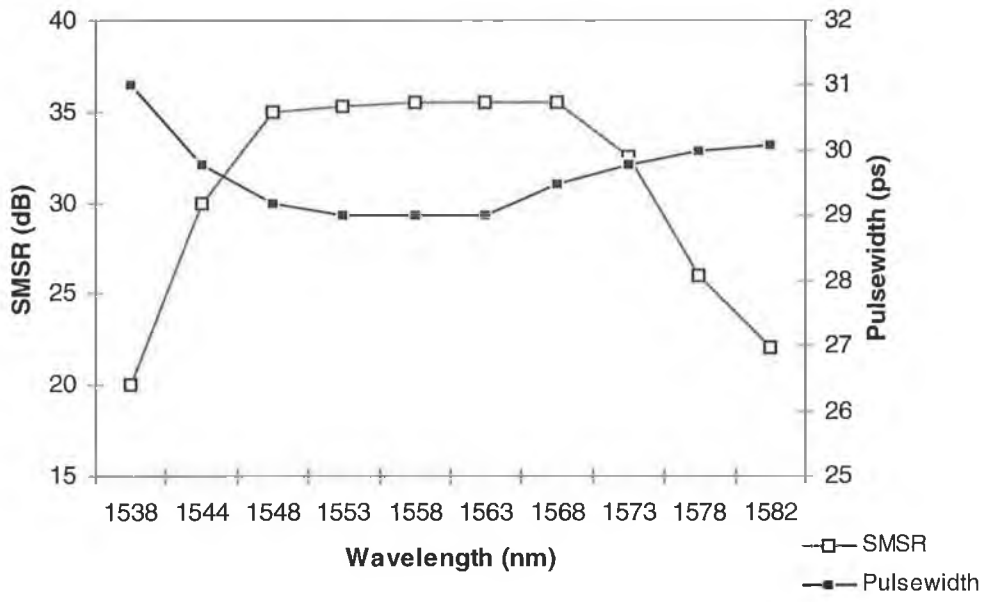

Figure 3-25: SMSR (left axis) and Pulsewidth (right axis) against tunable range in wavelength

So far, the generation of widely tunable (37 nm) self-seeded gain switched short optical pulses that exhibit low timing jitter and a high SMSR has been demonstrated. The results have also shown that self-seeding of a gain switched laser is one of the most simple and robust techniques available. However, in a self-seeding scheme, the repetition frequency or the length of the external cavity has to be adjusted to make the feedback pulses corresponding to the selected wavelength, arrive at the gain switched FP laser diode during the pulse build up time. Therefore the fact that the pulse repetition frequency has to be kept as an integer multiple of the round trip frequency actually reduces the flexibility of choosing the repetition rate, which is one of the distinct advantages (mentioned earlier) of a gain switched laser. External injection seeding [48, 49] is an alternative to self-seeding that overcomes the above-mentioned shortcoming. In an external injection-seeding system, the injected longitudinal wavelength mode, from an external CW source, is made to coincide with one of the longitudinal modes of the gain switched laser diode, leading to single mode pulse emission. It has also been reported that

an externally CW seeded laser shows a suppressed pulse timing jitter similar to that of a self-seeded laser [47].

The flexibility (independent of repetition rate) makes, the external-injection seeding of a gain switched FP laser, a very attractive technique in generating wavelength tunable short optical pulses. The flexibility comes about since no adjustment of the feedback loop or repetition frequency is required in an external-injection seeding system, and the output wavelengths can be selected and tuned easily by adjusting the wavelengths of the injection light beam. External injection seeding not only brings about the afore-mentioned advantages but also modifies many other characteristics of a semiconductor laser [50]. Reports in this area [51, 52], have revealed that the modulation bandwidth of an externally injection seeded laser could be substantially increased beyond the limit of the same laser under free running conditions.

The repetition rates of the gain switched pulses are usually limited to frequencies below 10 GHz. In most cases this limit is determined by the available bandwidth of the semiconductor laser diodes. Considering the rapid expansion in transmission rates in the field of high capacity WDM and OTDM optical communication systems, a further extension of the modulation frequency of gain switched lasers becomes vital. One of the methods available for improving the modulation response of semiconductor laser diodes involves external-injection seeding. However, a rather expensive continuous wave tunable laser is commonly required for external-injection seeding. The following section looks at some of the results obtained using the external-injection seeding technique. Initially we investigated the mechanism that improves the modulation bandwidth of semiconductor lasers. We then looked at ways in which this improvement in bandwidth could be used advantageously for our pulse generation schemes.

3.3.3 Improvement of the modulation bandwidth of laser diodes using external injection-seeding

The limited bandwidth of laser diodes means that we are normally unable to use these devices for high frequency (> 10 GHz) applications, like employing them to transmit very broadband data signals. One possible solution is to use active mode locking of a laser

diode cleaved to an appropriate length such that resonant enhancement of high frequency microwave signals may be achieved with direct modulation [53]. However this technique requires specially designed devices that only operate at specific frequencies. As mentioned earlier, another technique to overcome the limited bandwidth of laser diodes is to employ external optical injection into the laser, as this can greatly increase the intrinsic modulation bandwidth of the diode [54, 55]. In addition, at high injection levels the laser can start to self-pulsate. The frequency of self-pulsation has been reported to be suitable for RF transmission, thus making such devices useful for the generation of microwave optical signals in hybrid radio/fiber networks [56, 57]. Hence we went on to characterize the self-pulsation in the laser under external injection locking conditions after which we looked at how the injection-locked commercial laser maybe employed advantageously in various schemes such as hybrid radio fibre systems and high repetition rate pulse generation schemes.

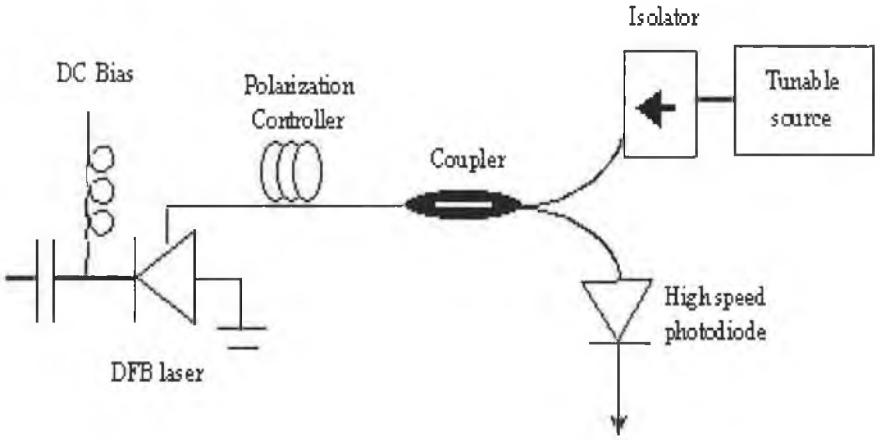

Figure 3-26: Experimental set-up for self-pulsation characterization

Figure 3-26 shows the experimental set-up used for the self-pulsation characterization. The laser diode used for the experiments was a standard multiple-quantum-well DFB device from NEL. The laser has a threshold current of 26 mA, a central lasing wavelength of around 1543 nm, and an intrinsic modulation bandwidth of around 8 GHz. By injecting light from a wavelength tunable External Cavity Laser (ECL), at the same wavelength as the DFB emission wavelength, we could significantly alter the modulation response of the device. It was also noticed that we could achieve excellent response at frequencies from 14 GHz to 25 GHz. The enhanced response at these frequencies is

caused by the external injection inducing instability in the laser diode. The instability in turn results in the output power from the laser undergoing strong oscillations due to beating between the optical field components in the laser cavity [56].

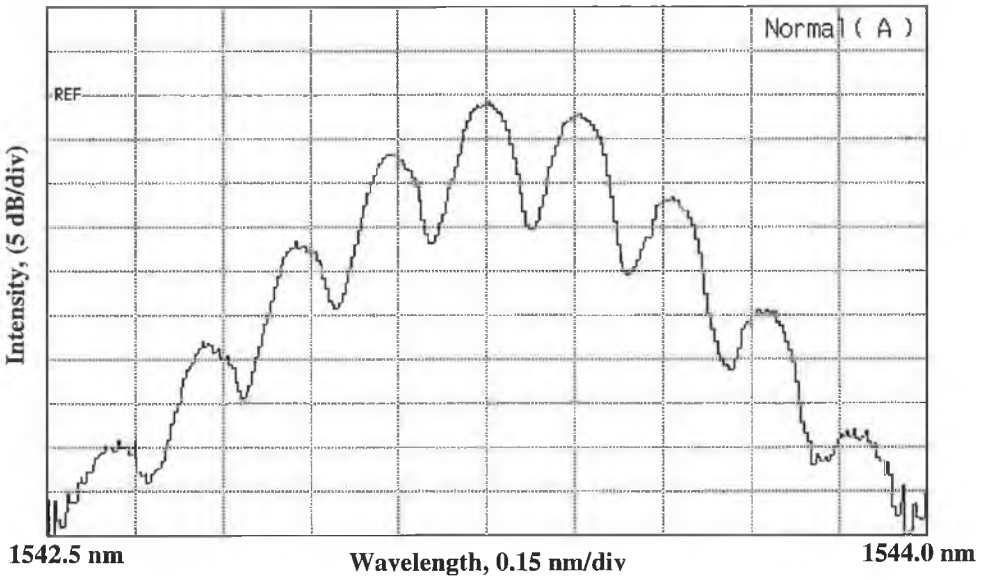

Figure 3-27: Optical spectrum of a self-pulsating laser

Figure 3-27 displays the optical spectrum from the laser when it is biased at 60 mA and the externally injected power from the external cavity laser is 5 mW. At this juncture, it is important to note that there was no electrical modulation signal being applied to the laser. However, we can clearly see the modulation on the spectrum at a frequency of around 20 GHz. To further investigate the oscillation from the laser, the optical output from the laser under external injection was detected with a 50 GHz photodiode and displayed on a 50 GHz oscilloscope. Triggering was achieved by splitting the electrical signal after the detector in two, and using one of these outputs as the trigger.

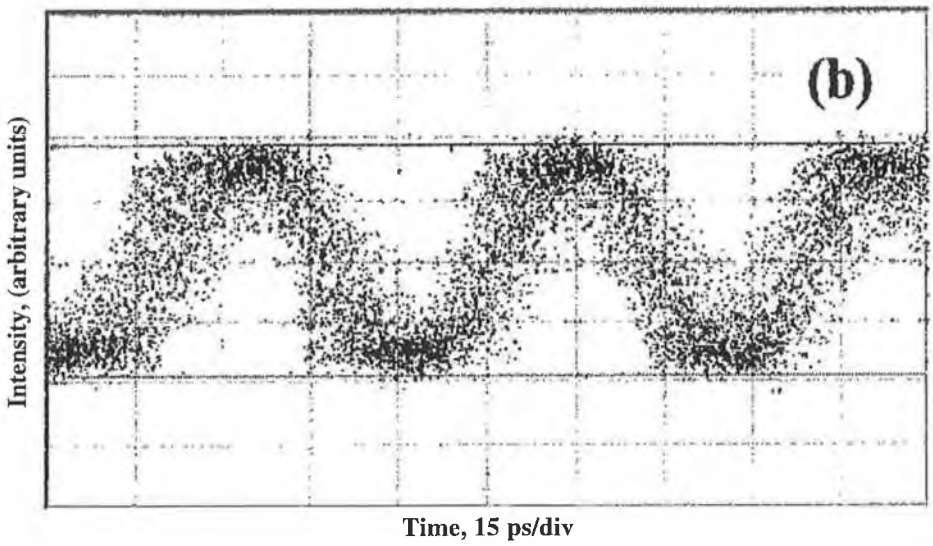

Figure 3-28: Detected output power oscillation

Figure 3-28 (above) displays the detected signal. We can clearly see the oscillation at a frequency of around 20 GHz and also the significant level of noise and jitter on the signal.

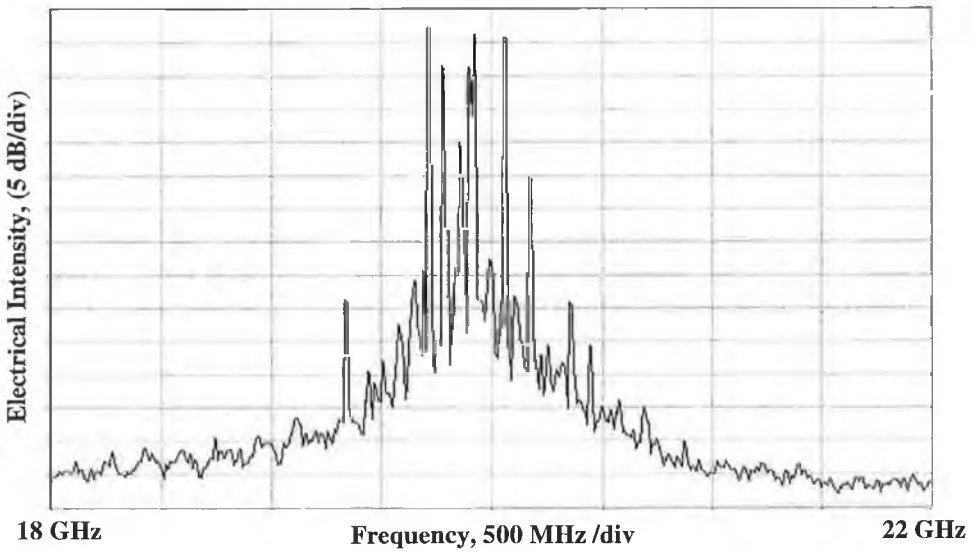

Figure 3-29: Electrical power spectrum of DFB laser biased at 60 mA with external injection level of 5 mW

This noise and jitter on the oscillation from the laser is also evident in the detected electrical spectrum (Figure 3-29), the broad linewidth is caused by the jitter between the DFB laser diode and the tunable cavity laser.

The frequency of the oscillation from the injection locked DFB laser depends on the strength of the injected optical signal [56], and Figure 3-30 displays how the oscillation frequency varies as a function of the injected power level. This graph shows that the laser could be successfully used for any application within this range of extended frequencies. In addition, by measuring the peak-to-peak voltage of the oscillation on the oscilloscope, we have been able to determine that the optical output from the laser is 100% modulated (using the average power level falling on the detector and the responsivity of the detector).

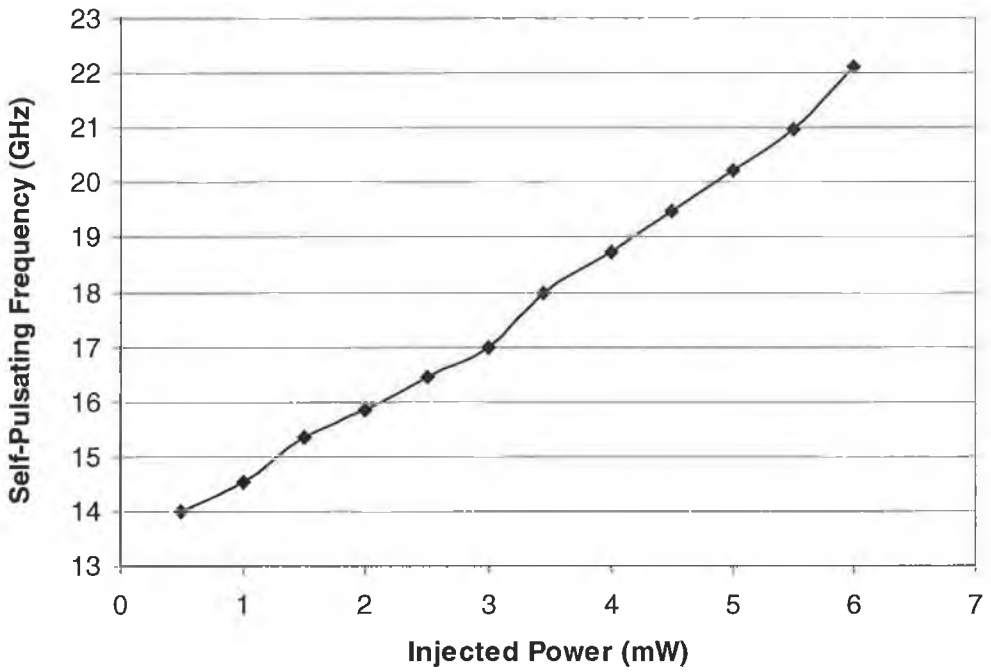

Figure 3-30: Self-pulsation frequency from externally injected DFB laser as a function of injected power level

3.3.3.1 Modulation response characterization with and without external injection

Having established the reason behind the improvement of the modulation bandwidth, we then characterised the modulation response of a free running, and the injection locked 1.5 μm FP laser, in order to examine the bandwidth enhancement achieved. In the previous case, the slave laser used was a DFB, while here an FP is being used as the slave laser. However, regardless of the type of laser used, it is vital to realise that the operational principle behind the bandwidth enhancement is the same.

The experimental setup used is shown in Figure 3-31. An external cavity tunable laser was used as the master light source to inject light into the FP laser (slave laser) through an optical isolator, a coupler and a polarisation controller. The response was then characterised with the aid of a 50 GHz network analyser (HP 8510C). The FP laser (same as before) used was a commercial 1.5 μm InGaAsP device (KELD 1501R-CCC_1) from NTT Electronics, with a threshold current of 26 mA, and a longitudinal mode spacing of 1.12 nm. The laser is manufactured for use in 10 Gbit/s systems, and has a specified bandwidth of around 8 GHz at an injection current level of 50 mA.

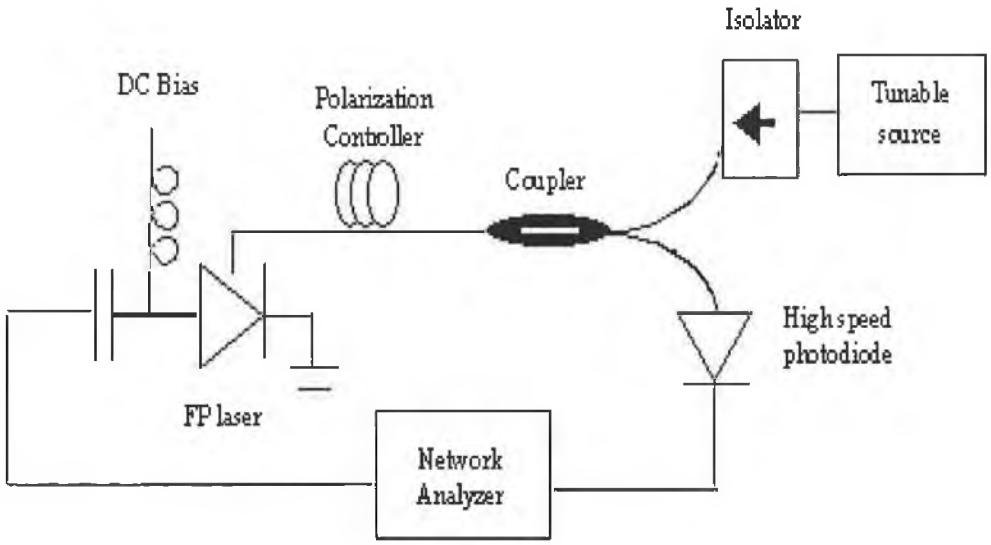

Figure 3-31: Experimental set-up for the characterization of laser response

Figure 3-32 shows the response of the laser diode under different injection conditions. The dotted line in Figure 3-32 shows the response when the free-running laser was biased at 40 mA. The relaxation frequency was 7.3 GHz, and the 3 dB bandwidth was around 8.4 GHz in this case. We then injected light from the ECL into the FP laser, using the same experimental setup shown in Figure 3-31, and tuned the wavelength of the injected light to one of the longitudinal modes of the FP laser. The polarisation controller was varied to maximise the SMSR of the output spectrum from the laser, in order to ensure maximum coupling of light from the ECL laser into the FP diode. The output power from the ECL was then set to 7 dBm (close to the maximum possible), and its wavelength was tuned slightly to obtain the maximum relaxation frequency.

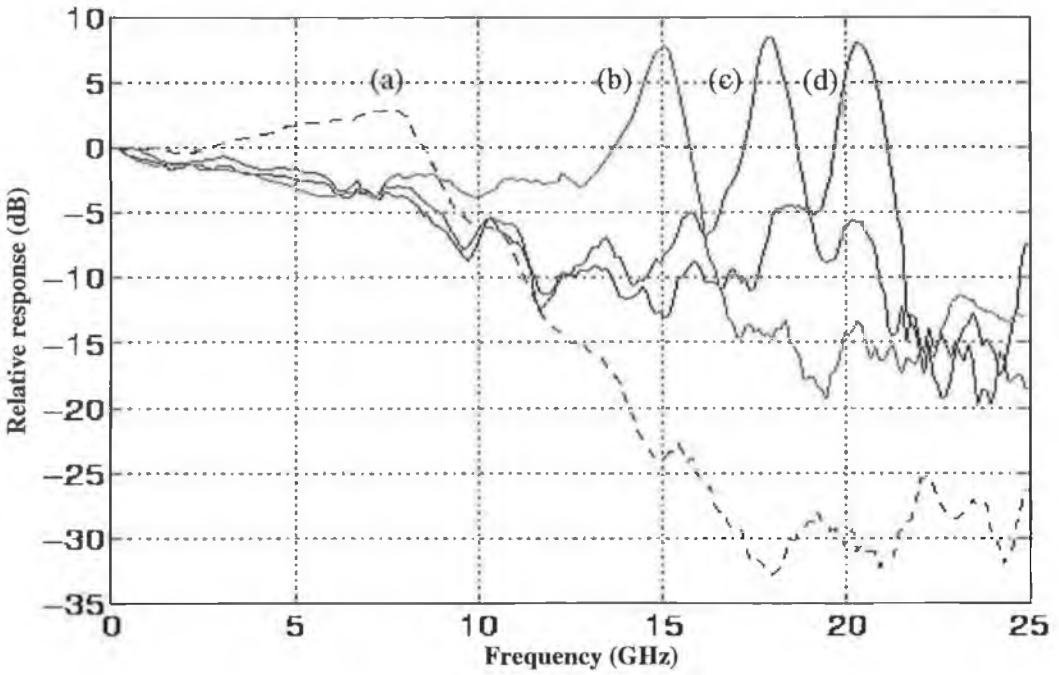

Figure 3-32: Modulation response (a) free running FP laser diode with applied bias current of 40 mA (b) with external injection levels of 1 dBm (c) with external injection levels of 4 dBm (d) with external injection levels of 7 dBm

The resulting response of the laser (biased at 40 mA) was as shown by case (d) in Figure 3-32, and we can see that the, relaxation frequency was greatly enhanced to about 21 GHz. By gradually reducing the output power from the external cavity laser, we were also able to reduce the relaxation frequency from 21 GHz to any frequency down to 10 GHz. The modulation response when the output power from the ECL was set to 1 dBm is also shown by case (b) in Figure 3-32.

Finally we looked at ways in which this phenomenon, could be used advantageously towards applications such as optical pulse generation

3.3.3.2 Optical pulse generation at high repetition rates using external-injection seeding of gain switched commercial Fabry-Perot (FP) laser diodes

The development of optical pulse sources at high repetition rates (> 10 GHz) is extremely important for use in future high speed optical communications systems [3]. However, as mentioned earlier, the repetition rate at which pulses can be generated using a gain-switched laser diode, is essentially limited by the inherent bandwidth of the device. In order to achieve gain-switched operation at frequencies in excess of 10 GHz, it is usually

necessary to have specially developed laser diodes with bandwidths greater than 10 GHz [58, 59]. However, as seen in the previous section, by using strong external-injection of light into a laser it has been shown that the laser bandwidth can be significantly enhanced [54, 55]. This bandwidth improvement should thus be useful for increasing the frequency at which pulses can be generated using the gain-switching technique with commercial lasers. In this section, we look into the experimental demonstration of how strong external-injection into a gain-switched FP diode increases the bandwidth of the laser such that pulses can be generated at frequencies up to 20 GHz, which is far beyond what would be possible with the lasers inherent bandwidth of 8 GHz. The optical pulses generated were near transform-limited (pulsewidths around 12 ps and spectral widths of 40 GHz) and hence suitable for use in high-speed optical communication systems.

3.3.3.3 Gain switching with and without external injection

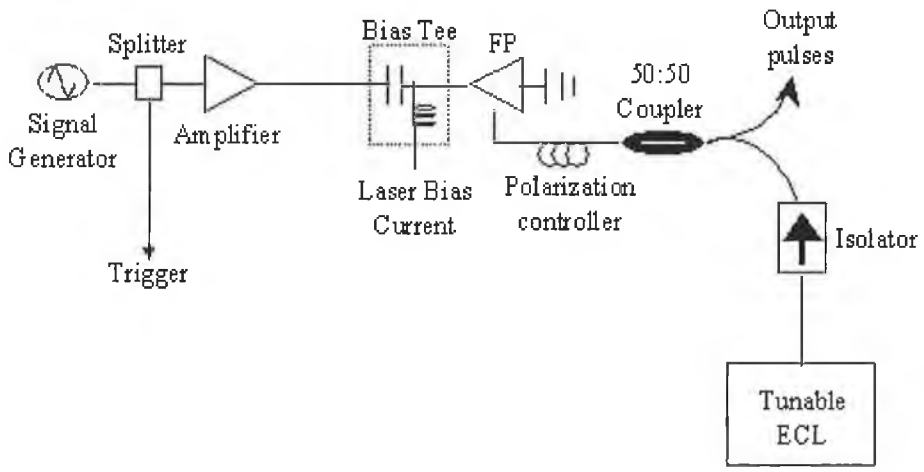

Figure 3-33: Experimental set-up for external-injection seeding of gain-switched FP laser

Gain-switching was carried out by applying a DC bias current in conjunction with a sinusoidal modulation to the laser, and the optical signal from the laser was then coupled into fibre using a GRIN lens fibre pigtail which is anti-reflection coated (to prevent reflections back into the laser). External-injection seeding of the gain-switched laser was carried out by injecting light from a tunable External Cavity Laser (ECL) into the gain switched laser diode via an isolator, a fibre coupler, and a polarisation controller. An isolator is used in the external injection-seeding branch in order to ensure that the

injection lightwave direction is maintained while the polarization controller is used to adjust the polarization state of the injected light in order to maximize the SMSR of the optical pulses. These optical pulses generated from the experimental arrangement were then characterised in the spectral and temporal domains. The optical spectra were examined using an optical spectrum analyser with a resolution of 0.07 nm, and the temporal measurements were conducted using a 50 GHz pin detector followed by an Agilent 50 GHz sampling oscilloscope. As mentioned previously the total time resolution of our measurement system is 12 ps.

The laser was then initially gain-switched at a frequency of 10 GHz without external injection, and optimum operation (minimum output pulsewidth) was achieved with a bias current of 42 mA and a sinusoidal modulation power of 28 dBm. Figure 3-34 displays the optical pulses generated from the FP laser, the pulsewidth (after deconvolving the time resolution of the measurement system) was around 18 ps and the pulse peak power was calculated to be 5.8 mW.

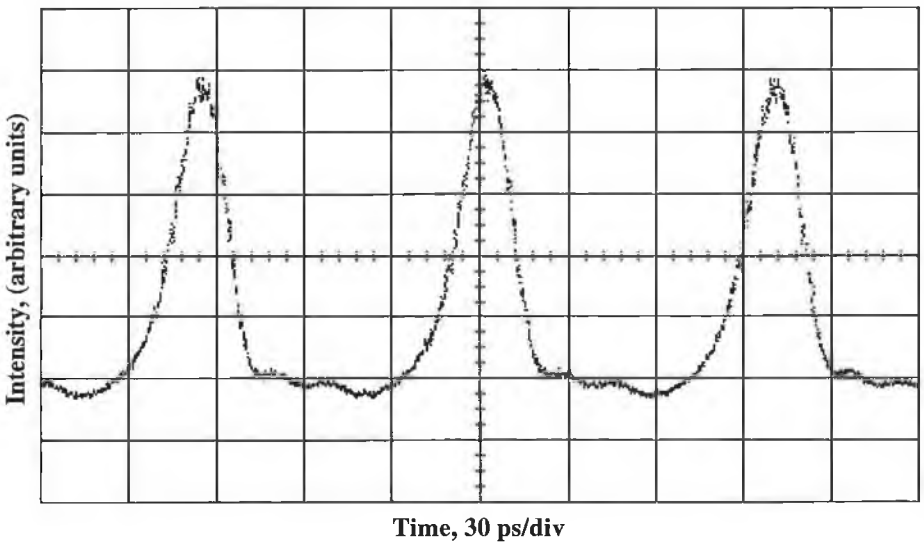

Figure 3-34: Optical pulse train from gain-switched FP laser without external-injection at repetition frequencies of 10 GHz

We then proceeded to increase the frequency of the modulation signal applied to the laser diode, and adjust the bias current to obtain optimum pulses from the set-up. At frequencies around 13 GHz it became increasingly difficult to gain switch the laser properly (as shown in Figure 3-35), due to the limited bandwidth displayed in the dotted

line of Figure 3-32, and at frequencies beyond 15 GHz, the modulated optical signal from the laser became negligible. This result is in agreement with the response characterisation done, and demonstrates how the limited bandwidth of the device determines the maximum frequency at which pulses can be successfully generated.

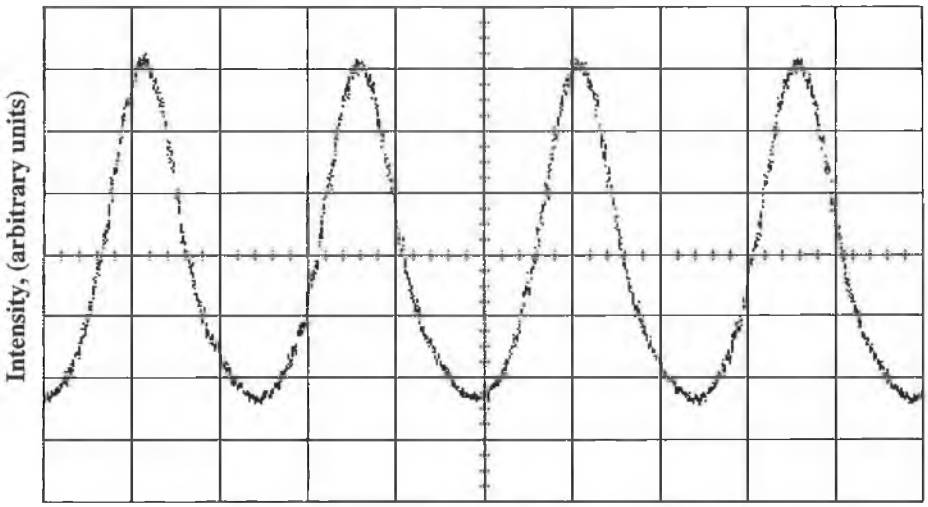

Figure 3-35: Optical pulse train from gain-switched FP laser without external-injection at repetition frequencies of 13 GHz

We then injected light from the CW external cavity laser into the gain-switched FP laser as shown in the set-up diagram (Figure 3-33), and tuned the wavelength of the injected light, and the polarisation controller as explained earlier. The output power from the CW laser was set to 4 dBm, and taking into account the attenuation of the isolator and the fibre coupler, and the coupling loss between the GRIN lens and the laser diode, we estimate the external injection level into the FP laser to be around -4 dBm. The laser was subsequently gain-switched at 10 GHz as before with a modulation power of 28 dBm, however this time the optimum bias current required was 29 mA. The frequency of the applied modulation signal was then increased, and the bias current adjusted to optimise the laser gain switching. Figure 3-36 displays the optical output pulses and Figure 3-37 displays the associated spectra (linear and log scales) when the laser was gain-switched using a bias current of 48 mA, and a modulation signal power of 26 dBm at 20 GHz. The pulse duration (after deconvolving the measured pulsewidth with the resolution of the measurement system), and spectral width were 12 ps and 40 GHz respectively, giving a time-bandwidth product of 0.48, which is close to the time bandwidth product of

transform-limit gaussian pulses (0.44). We can also see from Figure 3-37 that the SMSR of the pulse source was nearly 40 dB. By subsequently tuning the wavelength from the ECL to different modes of the FP laser diode we were also able to successfully tune the high frequency pulse train over a range of around 12 nm.

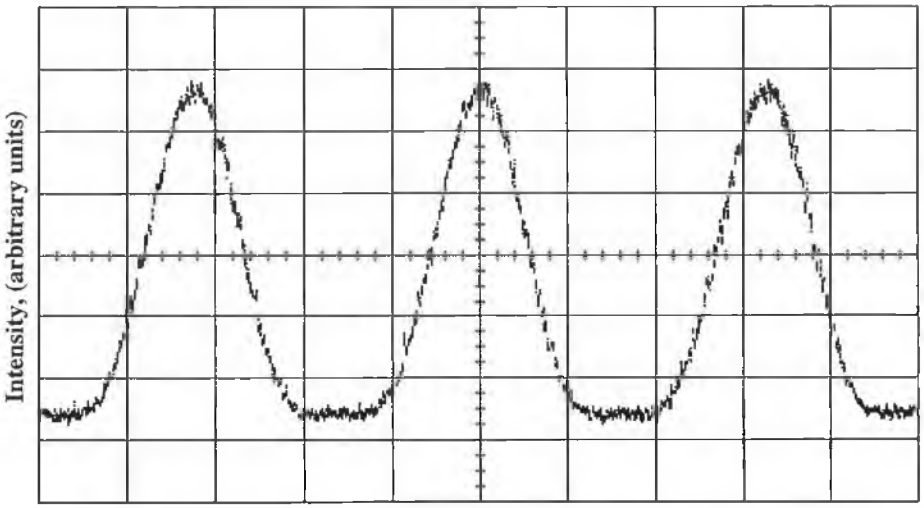

Figure 3-36: Optical pulse train from gain-switched FP laser with external-injection at repetition frequencies of 20 GHz

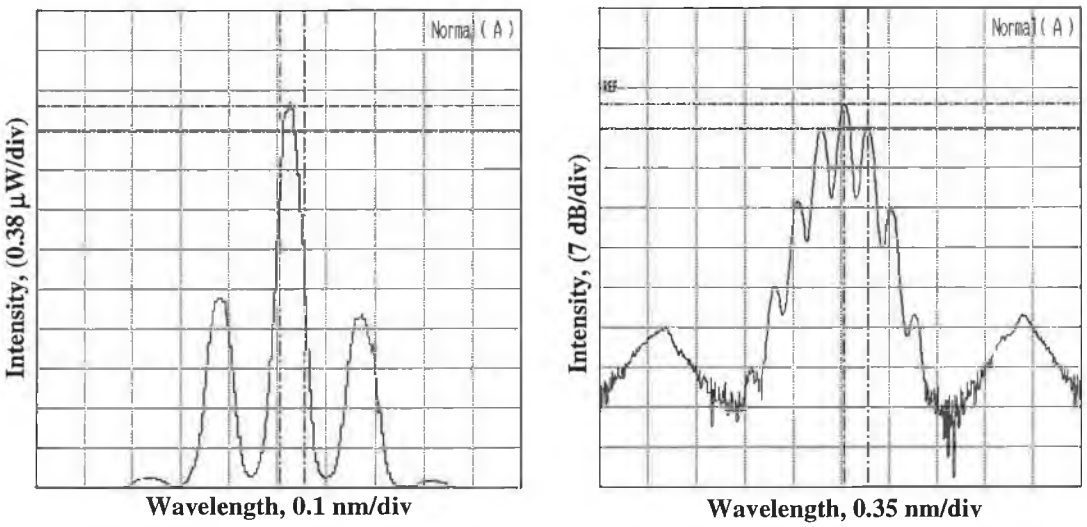

Figure 3-37: Associated optical spectra, from gain-switched laser with external-injection level of 7 dBm from ECL (a) linear scale (b) log scale

Figure 3-38 displays the temporal output from the laser under the same conditions as those used for Figure 3-36, except that the injected power from the ECL was set to

1 dBm. As we can see, the reduced injection level alters the response of the laser (see Figure 3-32) such that it cannot be gain-switched at 20 GHz.

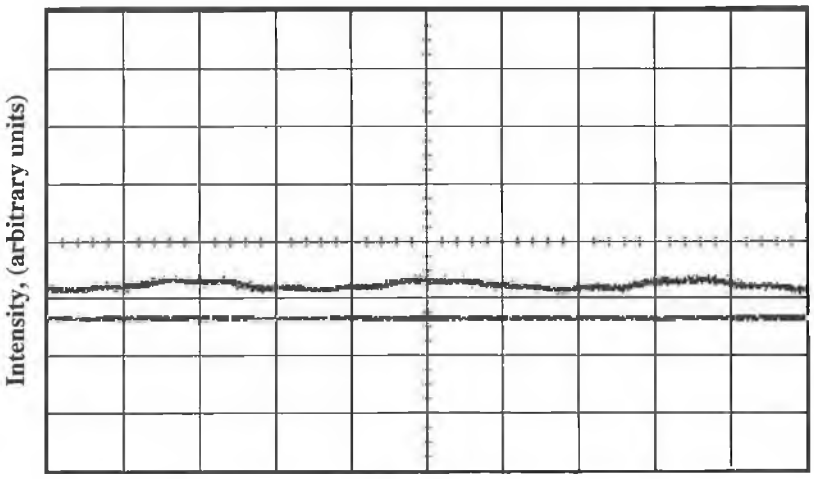

Figure 3-38: Output signal from laser diode when injection level from ECL was reduced to 1 dBm (with the zero optical power level also displayed) with 20 GHz modulation applied.

Previous studies on the bandwidth enhancement of lasers diodes under the influence of external-injection have shown that it is possible to increase the bandwidth by a factor of around three [54, 55]. In our experiment, we use a laser with a free running bandwidth of around 8 GHz, and we have managed to achieve a resonance frequency of beyond 20 GHz by using the strong external-injection. This bandwidth enhancement thus makes it possible for us to gain-switch the laser at far higher frequencies than what would be possible with the lasers inherent bandwidth. It should also be noted that the optical pulses generated from the set-up are nearly transform limited (time-bandwidth product of 0.48). This is because the external injection is not only responsible for the bandwidth enhancement, but also results in significant chirp reduction on the output signal [59, 54, 60].

The resulting optical pulsewidth due to injection seeding, as the wavelength of the injected light is varied, has been studied in [59]. It was found that for negative frequency detuning, the distortion in the pulse waveform can result in shorter optical pulses than would be obtained without injection seeding. In addition, from [54], the optimum improvement in relaxation frequency is obtained by external injection at frequencies, which are negatively detuned. Since our ECL is tuned to optimise the relaxation

frequency, this is therefore consistent with the slight reduction in pulsewidth obtained between the 10 GHz pulses without injection seeding, and the 20 GHz gain-switched pulses with external injection. In addition, the pulsewidth generated under gain-switching conditions will normally decrease as the frequency of the electrical modulation applied increases (laser will turn-off faster, resulting in a reduced fall time on the pulse).

We have demonstrated the generation of optical pulses at frequencies up to 20 GHz by using strong external-injection into a gain-switched laser. The commercial FP laser used has an inherent bandwidth of 8 GHz, but the external-injection increases the bandwidth sufficiently to generate near transform-limit pulses at repetition rates well in excess of the lasers free-running bandwidth. By employing this technique with higher speed lasers, it should thus be feasible to develop optical pulse sources suitable for use in optical systems with single channel bit rates of 40 Gbit/s.

3.3.4 Pulse shaping using an external modulator

As mentioned earlier, another suitable technique for generating short optical pulses involves the use of a continuous wave (CW) driven laser diode followed by a sinusoidally driven external modulator [61, 6].

3.3.4.1 Types of external modulators

There are various methods available for external modulation due to the presence of different sorts of modulators. The main types used in optical networks are electro-optic and Electro-Absorption modulators [62].

1. Electro-Optic Modulators

In electro-optic modulators, the refractive index of a material can be altered through an applied electric field. This change in refractive index can cause a change in the phase of a lightwave passing through it. If two light waves are in phase then their peaks occur at the same location and the waves add together to give a higher intensity of light. If two waves are out of phase by half a wavelength then when they combine they cancel each other out to give no light.

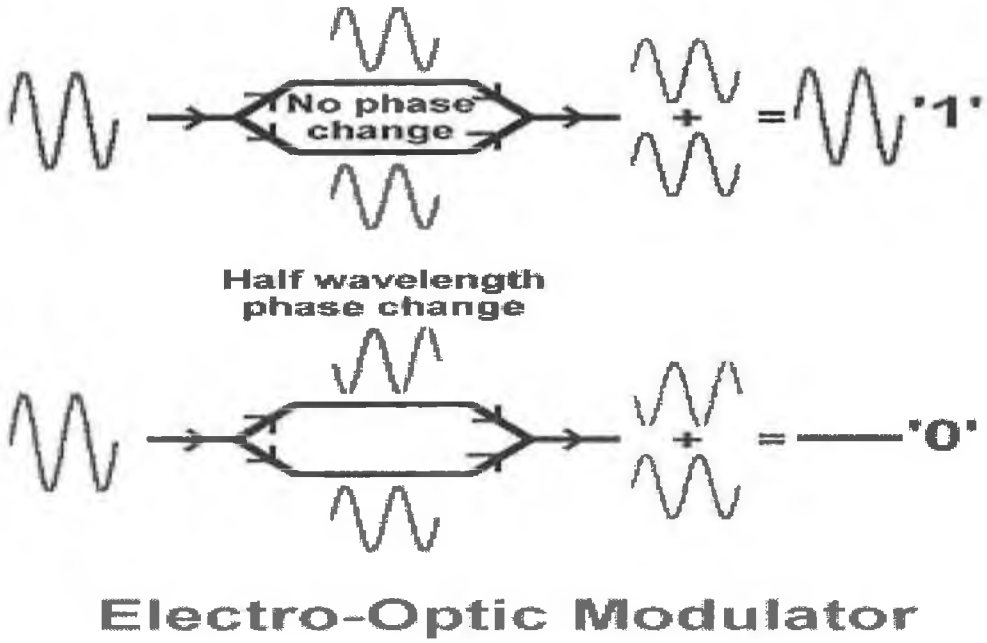

Figure 3-39: Operational principles of an electro-optic modulator

To make this usable as a modulator, the light from the laser arrives at the electro-optic modulator and is then split equally into two different paths. An electric field can be applied to each of these paths in order to shift the phase of the waves so that they arrive at the far end either in phase to give a pulse of light (a 1) or half a wavelength out of phase to give no light (a 0). These devices are commonly referred to as Mach-Zehnder Modulators (MZM) and Lithium Niobate ($LiNbO_3$) is the material most commonly used in such a device.

2. Electro-Absorption (EA) Modulators

Electro-absorption modulators like their counterparts (electro-optic modulators) can be integrated with the lasers they are to be used with. However EA modulators have an advantage over electro-optic modulators, since they are made of similar materials to semiconductor lasers. In the case of electro-optic modulators the material, which is incompatible with that of the laser, does not allow neat integration into small packages.

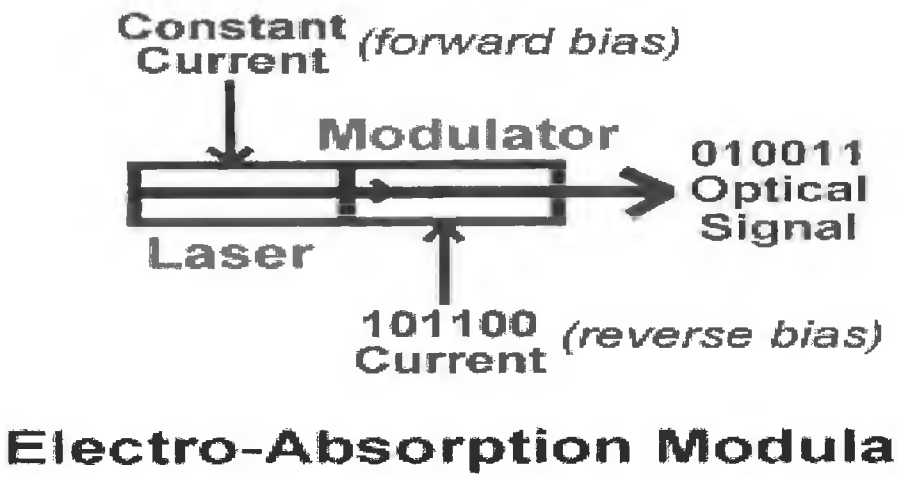

Figure 3-40: Schematic of an EA modulator

Figure 3-40 shows a basic schematic of an EA modulator. These modulators have an almost logarithmic attenuation of optical power that depends on a reverse voltage applied to them, as opposed to laser devices that require a forward bias. With no voltage, EA modulators are transparent and when a voltage is applied they absorb light at the laser wavelength they are designed for. Hence in order to represent a 1 it needs to allow light through, and so no current is applied thereby making it behave transparently to the laser light.

3.3.4.2 Pulse generation using external modulators

The transfer function is a fundamental property of the modulator, which provides repeatable device performance. The transfer function for an optical MZM is given in equation 9:

$$I(t) = \alpha I_0 \cos^2\left(\frac{V(t)\pi}{2V\pi}\right) \qquad \textbf{Equation 3-10}$$

Where

I(t) = Transmitted intensity

α = Device insertion loss

I_0 = Input intensity from the laser

V(t) = Applied voltage to the device

$V\pi$ = Voltage required to drive the device between adjacent maxima and minima

The static bias of the modulator can be set to any point on the transmission curve. This enables the user to adjust the static transmission point of the modulator to suit the application being employed. For instance by biasing at the quadrature (50 %) point, bipolar RF operation and the most sensitive section of the transfer function could be achieved. On the other hand, by biasing at the null point, attributes such as high extinction ratios and unipolar operation could be achieved.

3.3.4.3 Experimental results

The external modulator used was a Mach-Zehnder (MZ) Lithium Niobate ($LiNbO_3$) device with a bandwidth of 20 GHz and a switching voltage of about 5 volts. Using the set-up shown in Figure 3-41, we first set out to characterize the modulator by obtaining its transfer characteristic.

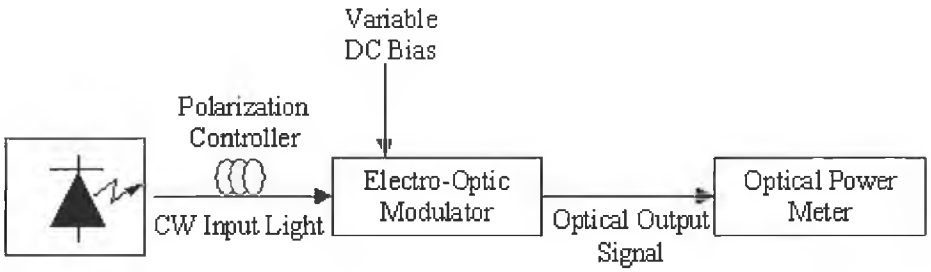

Figure 3-41: Experimental set-up used for the characterization of the modulator

CW light from a 1550 nm laser was coupled into a MZ modulator via a polarization controller as shown in the set-up diagram above. The DC bias was set to its transparency point and the polarization controller was then optimized to ensure that the output power was a maximum. The static DC bias of the modulator was then varied from –10 to +10 volts while the output power was monitored using an optical power meter at every discrete bias voltage. The results achieved were plotted and are shown in Figure 3-42.

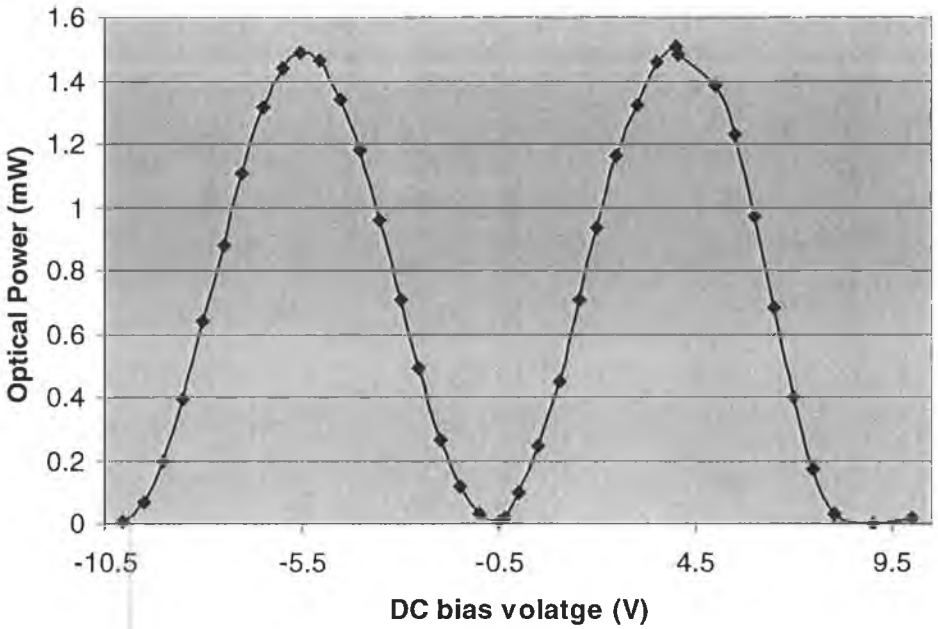

Figure 3-42: Transmission characteristic of a 20 GHz modulator

From the figure above, it can be seen that the switching voltage of the modulator is about 5 V with one of the maxima achieved at –5.5 V while one of the minima was achieved at –0.5 V. It has been reported, that by biasing the modulator at its null point and driving it with a RF data signal with a peak-to-peak voltage of twice the switching voltage of the modulator, optical pulses at twice the frequency of the applied RF signal could be generated [63]. Therefore, regarding pulse generation, the null point could be used advantageously to generate pulses at twice the repetition rate of the driving RF signal.

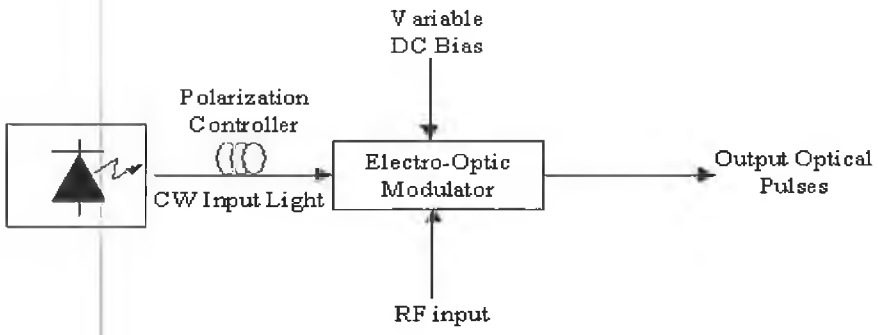

Figure 3-43: Pulse generation using an external modulator

Having characterized the modulator, we then set out to generate pulses using the set-up shown in Figure 3-43

CW light from the same 1550 nm laser used to characterize the modulator was coupled into a MZ modulator via a polarization controller as shown in the set-up diagram above. With the DC bias set to the null point (-0.5 V), a sine wave at varying frequencies (1.25, 5 and 10 GHz) with a peak-to-peak voltage of 12 V was then applied to the RF input of the modulator. The generated pulses were then observed using a 50 GHz photodiode in conjunction with a 50 GHz oscilloscope. An Anritsu spectrum analyzer was used to examine the corresponding optical spectrum of these pulses.

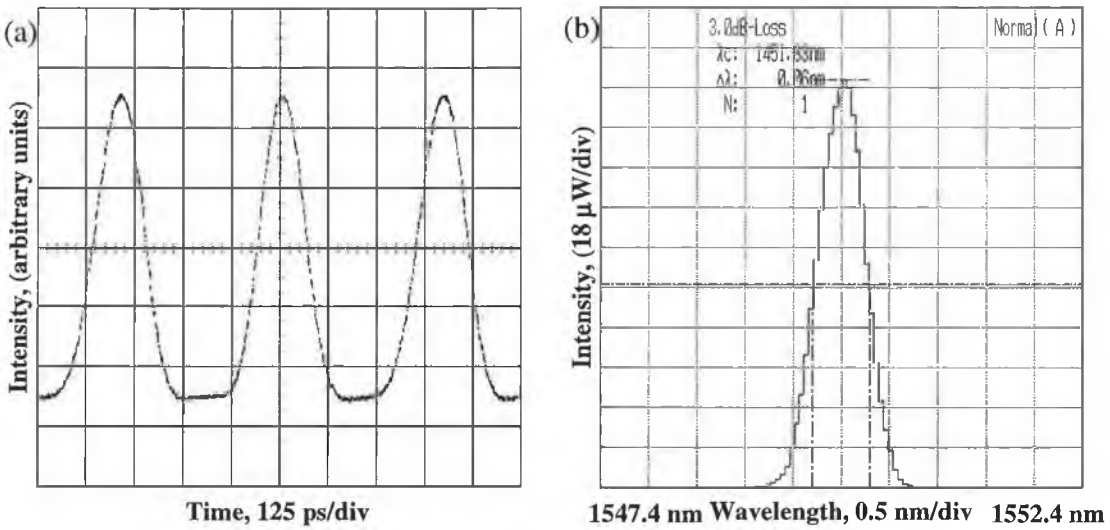

Figure 3-44: (a) 2.5 GHz pulse train (b) associated spectrum (linear scale)

With the conditions mentioned above and the RF frequency set to 1.25 GHz, the received pulses are shown in Figure 3-44 (a). The pulsewidth was measured to be about 110 ps. The associated spectrum in linear scale is shown in Figure 3-44 (b).

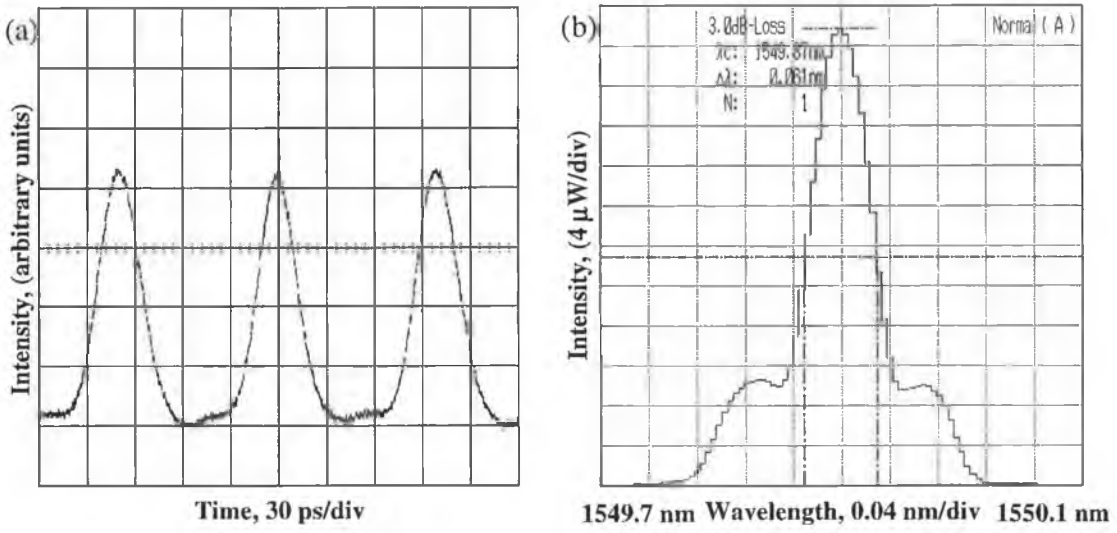

Figure 3-45: (a) 10 GHz pulse train (b) associated spectrum (linear scale)

The results achieved with the input RF frequency now being varied to 5 GHz are shown in Figure 3-45. The width of the pulses (Figure 3-45 (a)) this time around was measured to be about 37 ps. The associated spectrum in linear scale is shown in Figure 3-45 (b).

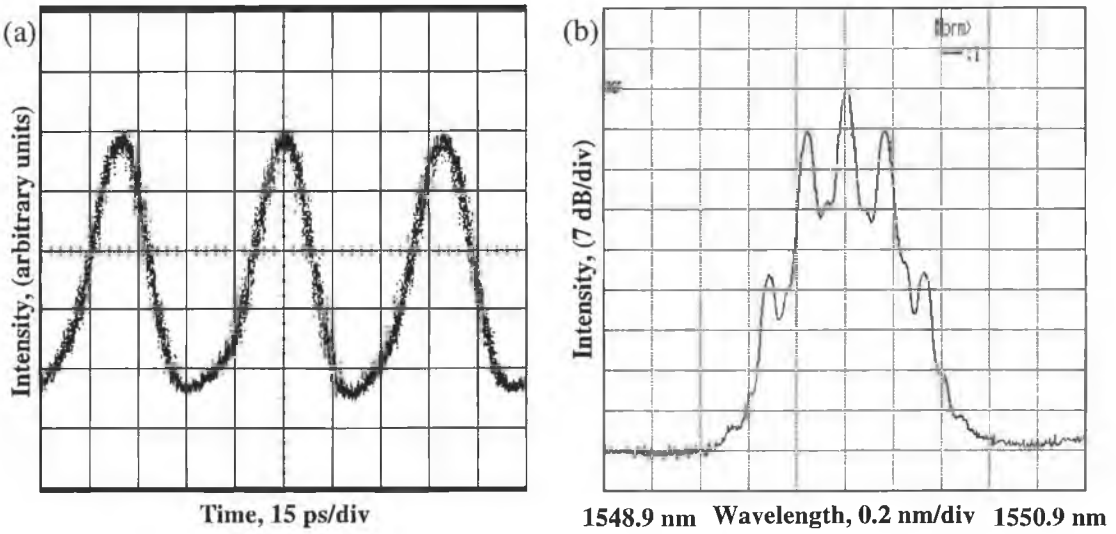

Figure 3-46: (a) 20 GHz pulse train (b) associated spectrum (log scale)

20 GHz pulses generated by varying the RF input frequency to 10 GHz (all other parameters unaltered) are shown in Figure 3-46 (a). The measured pulsewidth was about 20 ps. The associated spectrum in log scale is shown in Figure 3-46 (b).

Therefore by using the pulse compression effect due to nonlinear attenuation characteristics to the applied voltage, a near transform limited optical pulse could be generated just with sinusoidal modulation [64]. The advantages of this method over other conventional methods include high speed, low chirp, low jitter, and electrical tunability. However, The width of the pulses generated using modulators is comparatively wide. Since the pulsewidth of generated pulses depends on the modulator extinction efficiency, to reduce the pulsewidth, an extremely high reverse bias and a high modulation voltage are required [65]. The need for an additional component and the high insertion loss of modulators are other disadvantages associated with the use of this scheme for the generation of pulses.

In this chapter we have shown that the gain switching of commercially available laser diodes is one of the simplest and most cost effective methods of generating picosecond optical pulses. We then went on to show that by using self-seeding these gain switched pulse sources, interesting features such as broad wavelength tunability, reduction of the turn on timing jitter and achieving of single modal operation of the optical pulse could be obtained. Reduction (small) of chirp is an added advantage that is also achieved due to self-seeding. The limited repetition rates achievable due to the inherent bandwidth of the laser diode led us to investigate another technique, which involved the external injection seeding of a gain switched laser diode. Using this technique we showed that it would be possible to enhance the modulation bandwidth of a laser diode by a factor of 3. This would enable one to generate pulses at repetition rates of nearly three to four times the modulation bandwidth of the device. We rounded up by looking at another technique, being pulse shaping using an external modulator, which is also an effective method of generating transform limited pulses at high repetition rates.

References

[1] R. A. Barry, W. S. Chan, K. L. Hall, E. S. Kintzer, J. D. Moores, K. A. Rauschenbach, E. A. Swanson, L. E. Adams, C. R. Doerr, S. G. Finn, H. A. Haus, E. P. Ippen, W. S. Wong and M. Haner, "All-Optical Network Consortium-Ultrafast TDM Networks," *IEEE J. of selected areas in Communications*, vol. 14, pp. 999-1013, 1996.

[2] R. S. Tucker, G. Eisenstein and S. K. Korotky, "Optical time division multiplexing for very high bit transmission," *IEEE J. of Lightwave Technol.*, vol. 6, pp. 1737-1749, 1988.

[3] S. Kawanishi, "Ultrahigh-Speed Optical Time-Division-Multiplexed Transmission Technology Based on Optical Signal Processing," *IEEE J. Quantum Electron.*, vol. 34, pp. 2064-2079, 1998.

[4] A. Yariv, "*Optical Electronics (4th Ed.),*"Saunders college publishing, 1971.

[5] J.A. Leegwater, "Theory of Mode-Locked Semiconductor Lasers," *IEEE J. Quantum Electron.*, vol. 32, pp. 1782 –1790, 1996.

[6] M .Suzuki, H. Tanaka, N. Edagawa, K. Utaka and Y. Matsushima, "Transform-Limited Optical Pulse Generation up to 20 GHz Repetition Rate by a Sinusoidally Driven InGaAsP Electroabsorption Modulator," *IEEE J. of Lightwave Technol.*, vol. 11, pp. 468-473, 1993.

[7] P. Paulus, R. Langenhorst and D. Jáger, "Generation and Optimum Control of Picosecond Optical Pulses from Gain Switched Semiconductor Lasers," *IEEE J. Quantum Electron.*, vol. 24, pp. 1519-1523, 1988.

[8] A. E. Siegman, "*Lasers (1st Ed.),*" University science books, 1986.

[9] M. J. Guy, S. V. Chernikov, J. R. Taylor, D. G. Moodie and R. Kashyap, "Low Repetition Rate Master Source for Optical Processing in Ultrahigh-speed OTDM Networks," *Electron. Lett.*, Vol. 31, pp. 1767–1769, 1995.

[10] P. Vasil'ev, "*Ultrafast Diode Lasers: Fundamental and Applications (1st Ed.),*" Artech house, 1995.

[11] H. Ito, H. Yokoyama, S. Murata and H. Inaba, "Picosecond Optical Pulse Generation from an R.F. Modulated AlGaAs D.H. Diode Laser," *Electron. Lett.*, vol. 15, pp. 738-740, 1979.

[12] K. Y. Lau, "Gain switching of Semiconductor Injection Lasers," *Appl. Phys. Lett.*, vol. 52, pp 257-259, 1988.

[13] K. Y. Lau, "Short-Pulse and High-Frequency Signal Generation in Semiconductor Lasers," *IEEE J. of Lightwave Technol.*, vol. 7, pp. 400-419, 1989.

[14] I. H. White, "*Picosecond Optical Pulse Generation using Semiconductor Lasers / in Laser Sources and Applications,*" Institute of Physics Publishing, 1997.

[15] L. P. Barry, R. F. O'Dowd, J. Debeau and R. Boittin, "Tunable Transform Limited Pulse Generation using Self-Injection Locking of an FP Laser," *IEEE Photonics Technol. Lett.*, Vol. 5, pp. 1132–1134, 1993.

[16] D. R. Scifres, "Distributed Feedback Single Heterojunction GaAs Diode Lasers," *Appl. Phys. Lett.*, vol. 25, pp 203, 1974.

[17] T. L. Koch, "Nature of Wavelength Chirping in Directly Modulated Semiconductor Lasers," *Electron. Lett.*, vol. 20, pp. 1038-1039, 1984.

[18] M. Osinski and J. Buus, "Linewidth Broadening Factor in Semiconductor Lasers-An Overview," *IEEE J. Quantum Electron.*, vol. 23, pp. 9-29, 1987.

[19] G. P. Agrawal, "Intensity Dependence of the Linewidth Enhancement Factor and its Implications in Semiconductor Lasers," *IEEE Photonics Technol. Lett.*, Vol. 1, pp. 212–214, 1989.

[20] L. P. Barry, P. Guignard, J. Debeau, R. Boittin and M. Bernard, "A High-Speed Optical Star Network Using TDMA and All-Optical Demultiplexing Techniques," *IEEE J. of selected areas in Communications*, vol. 14, pp. 1030-1038, 1996.

[21] A. Takada, T. Sugie and M. Saruwatari, "High Speed Picosecond Optical Pulse Compression from a Gain Switched 1.3 μm Distributed Feedback Laser Diode (DFB-LD) Through Highly Dispersive Single Mode Fibre," *IEEE J. of Lightwave Technol.*, vol. 5, pp. 1525-1533, 1987.

[22] H. F. Liu, S. Oshiba, Y. Ogawa and Y. Kawai, "Method of Generating Nearly Transform Limited Pulses from Gain-Switched Distributed-Feedback Laser Diodes and its Application to Soliton Transmission," *Opt. Lett.*, Vol. 17, pp. 64–66, 1992.

[23] M. J. Guy, S. V. Chernikov, J. R. Taylor, D. G. Moodie and R. Kashyap, "Low Repetition Rate Master Source for Optical Processing in Ultrahigh-Speed OTDM Networks," *Electron. Lett.*, vol. 31, pp. 1767-1769, 1995.

[24] L. P. Barry, J. Debeau and R.Botittin, "Simple Technique to Improve the Spectral Quality of Gain Switched Pulses from a DFB Laser," *Electron. Lett.*, vol. 30, pp. 2143-2145, 1994.

[25] S. Nogiwa, Y. Kawaguchi, H. Ohta and Y. Endo, "Generation of Gain-Switched Optical Pulses with very Low Timing Jitter by using External CW-Light Injection Seeding," *Electron. Lett.*, vol. 36, pp. 235-236, 2000.

[26] M. Jinno, "Correlated and Uncorrelated Timing Jitter in Gain Switched Laser Diodes," *IEEE Photonics Technol. Lett.*, Vol. 5, pp. 1140–1143, 1993.

[27] A. Shen, S. Bouchoule, P. Crozat, D. Mathoorasing, J. –M. Lourtioz and C. Kazmierski, "Low Timing Jitter of Gain- and Q-Switched Laser Diodes for High Bit Rate OTDM Applications," *Electron. Lett.*, vol. 33, pp. 1875-1877, 1997.

[28] A. G. Weber, W. Ronghan, E. H. Bőttcher, M. Schell and D. Bimberg, "Measurement and Simulation of the Turn-On-Delay Time Jitter in Gain Switched Semiconductor Lasers," *IEEE J. Quantum Electron.*, vol. 28, pp. 441-446, 1992.

[29] P. Gunning, J. K. Lucek, D. G. Moodie, K. Smith, R. P. Davey, S. V. Chernikov, M. J. Guy, J. R. Taylor and J. S. Siddiqui, "Gain Switched DFB laser Diode Pulse Source using Continuous Wave Light Injection for Jitter Suppression and an Electro-absorption Modulator for Pedestal Suppression," *Electron. Lett.*, vol. 32, pp. 1010-1011, 1996.

[30] M. Schell, D. Huhse, W. Utz, J. Kaessner, D. Bimberg and I. S. Tarasov, "Jitter and Dynamics of Self-Seeded Fabry-Perot Laser Diodes," *IEEE J. Sel. Topics Quan. Electron.*, vol. 1, pp. 528- 534, 1995.

[31] H. Ito, H. Yokoyama, S. Murata and H. Inaba, "Generation of Picosecond Optical Pulses with Highly R.F. Modulated AlGaAs D.H. Laser," *IEEE J. Quantum Electron.*, vol. 17, pp. 663-670, 1981.

[32] P. Liu, C. Lin, I. P. Kaminow and J. J. Hsieh, "Picosecond Pulse Generation from InGaAsP Lasers at 1.25 and 1.3 μm by Electrical Pulse Pumping," *IEEE J. Quantum Electron.*, vol. 17, pp. 671-674, 1981.

[33] J. P. Van Der Ziel and R. A. Logan, "Generation of Short Optical Pulses in Semiconductor Lasers by Combined dc and Microwave Current Injection," *IEEE J. Quantum Electron.*, vol. 18, pp 1340-1350, 1982.

[34] D. R. Kirby, " A Picosecond Optoelectronic Cross Correlator using a Gain Modulated Avalanche Photodiode for Measuring the Impulse Response of Tissue," http://www.medphys.ucl.ac.uk/~davek/phd/chapter5.pdf, *PhD. Thesis*, 1999.

[35] Hewlett Packard Application Note 918, "Pulse and Waveform Generation with Step Recovery Diodes".

[36] S. P. Yam and C. Shu, "Fast Wavelength-Tunable Multichannel Switching Using a Self-Injection Seeding Scheme," *IEEE J. Quantum Electron.*, vol. 35, pp. 228-233, 1999.

[37] K. Chan and C. Shu, "Electrically Wavelength-Tunable Picosecond Pulses Generated from a Self-Seeded Laser Diode using a Compensated Dispersion-Tuning Approach, "*IEEE Photonics Technol. Lett.*, Vol. 11, pp. 1093–1095, 1999.

[38] L. P. Barry, B. C. Thomsen, J. M. Dudley and J. D. Harvey, "Characterization of 1.55 μm Pulses from a Self-Seeded Gain-Switched Fabry-Perot Laser Diode Using Frequency-Resolved Optical Gating," *IEEE Photonics Technol. Lett.*, Vol. 10, pp. 935–937, 1998.

[39] D. Huhse, M. Schell, W. Utz, J, Kaessner and D. Bimberg, "Dynamics of Single-Mode Formation in Self-Seeded Fabry-Perot Lasers," *IEEE Photonics Technol. Lett.*, Vol. 7, pp. 351–353, 1995.

[40] X. Fang and D. N. Wang, "Mutual Pulse Injection Seeding by the Use of Two Fabry-Perot Laser Diodes to Produce Wavelength-Tunable Optical Short Pulses," *IEEE Photonics Technol. Lett.*, Vol. 15, pp. 855–857, 2003.

[41] M. Cavelier, N. Stelmakh, J. M. Xie, L. Chusseau, J. –M. Lourtioz, C. Kazmierski and N. Bouadma, "Picosecond (<2.5 ps) Wavelength-Tunable (~20 nm)

Semiconductor Laser Pulses With Repetition Rates up to 20 GHz," *Electron. Lett.*, vol. 28, pp. 224-226, 1992.

[42] S. Li, K. S. Chiang, W. A. Gambling, Y. Liu, L. Zhang and I. Bennion, "Self-Seeding of Fabry-Perot Laser Diode for Generating Wavelength Tunable Chirp Compensated Single Mode Pulses with High Side Mode Suppression Ratio," *IEEE Photonics Technol. Lett.*, Vol. 12, pp. 1441–1443, 2000.

[43] J. Debeau, L. P. Barry and R. Boittin, "Wavelength Tunable Pulse Generation at 10 GHz by Strong Filtered Feedback using a Gain-Switched Fabry-Perot Laser," *Electron. Lett.*, vol. 30, pp. 74-75, 1994.

[44] Y. Zhao and C. Shu, "Single Mode Operation Characteristics of Self-Injection Seeded Fabry-Perot Laser Diode with Distributed Feedback from a Fibre Grating," *IEEE Photonics Technol. Lett.*, Vol. 9, pp. 1436–1438, 1997.

[45] J. W. Chen and D. N. Wang, "Self-Seeded, Gain Switched Optical Short Pulse Generation With High Side Mode Suppression Ratio and Extended Wavelength Tuning Range," *Electron. Lett.*, vol. 39, pp. 679-681, 2003.

[46] C. Shu and S. P. Yam, "Effective Generation of Tunable Single- and Multiwavelength Optical Pulses from a Fabry-Perot Laser Diode," *IEEE Photonics Technol. Lett.*, Vol. 9, pp. 1214–1216, 1997.

[47] D. S. Seo, H. F. Liu, D. Y. Kim and D. D. Sampson, " Injection Power and Wavelength Dependence of an External-Seeded Gain-Switched Fabry-Perot Laser," *Appl. Phys. Lett.*, vol. 67, pp 1503-1505, 1995.

[48] D. N. Wang and X. Fang, "Generation of Electrically Wavelength-Tunable Optical Short Pulses using a Fabry-Perot Laser Diode in an External-Injection Seeding Scheme with Improved Side Mode Suppression Ratio," *IEEE Photonics Technol. Lett.*, Vol. 15, pp. 123–125, 2003.

[49] M. Zhang, D. N. Wang, H. Li, W. Jin and S. Demokan, "Tunable Dual-Wavelength Picosecond Pulse Generation by the Use of Two Fabry-Perot Laser Diodes in an External Injection Seeding Scheme," *IEEE Photonics Technol. Lett.*, Vol. 14, pp. 92–94, 2002.

[50] F. Mogensen, H. Olesen and G. Jacobsen, "Locking Conditions and Stability Properties for a Semiconductor Laser with External Light Injection," *IEEE J. Quantum Electron.*, vol. 21, pp. 784-793, 1985.

[51] J. Wang, L .Li and F. V. C. Mendis, "Enhancement of Modulation Bandwidth of Laser Diodes by Injection Locking," *IEEE Photon. Technol. Lett.,* vol. 8, pp. 34-36, 1996.

[52] J. M. Liu, H. F. Chen, X. J. Meng and T. B. Simpson, "Modulation Bandwidth, Noise and Stability of a Semiconductor Laser Subject to Strong Injection Locking," *IEEE Photon. Technol. Lett.,* vol. 9, pp. 1325-1327, 1997.

[53] J.B. Georges, M.-H. Kiang, K. Heppell, M. Sayed, and K.Y. Lau, "Optical Transmission of Narrow-Band Millimeter-Wave Signals by Resonant Modulation of Monolithic Semiconductor Laser," *IEEE Photon. Technol. Lett.,* vol. 6, pp. 568-570, 1994.

[54] G. Yabre, "Effect of Relatively Strong Light Injection on the Chirp-to-Power Ratio and the 3 dB Bandwidth of Directly Modulated Semiconductor Lasers," *IEEE J. Lightwave Technol.*, vol. 14, pp. 2367-2373, 1996.

[55] X.J. Meng, T. Chau, and M.C. Wu, "Experimental Demonstration of Modulation Bandwidth Enhancement in Distributed Feedback Lasers with External Light Injection," Electron. Lett., vol. 34, pp. 2031-2032, 1998.

[56] T.B Simpson and F. Doft, "Double Locked Laser Diode for Microwave Photonic Applications," *IEEE Photonics Technol. Lett.,* vol. 11, pp. 1476-1478, 1999.

[57] O. Frazao, P. Tavares, J. Ferreira da Rocha, L.B. Ribeiro, "Tunable Optical Oscillator Based on a DFB-MQW Laser and a Fiber Loop Reflector," *IEEE Transactions on Ultrasonics, Ferroelectrics and Frequency Control,* vol. 46, pp. 1341-1342, 1999.

[58] Y. Matsui, S. Kutsuzawa, S. Arahira, and Y. Ogawa, "Generation of Wavelength Tunable Gain-Switched Pulses from FP MQW Lasers with External Injection Seeding," *IEEE Photonics Technol. Lett.*, vol. 9, pp. 1087-1089, 1997.

[59] Y. Matsui, S. Kutsuzawa, S. Arahira, Y. Ogawa, and A. Suzuki, "Bifurcation in 20 GHz Gain-Switched 1.55-μm MQW lasers and its Control by CW Injection Seeding," *IEEE J. Quantum Electron.*, vol. 34, pp. 1213-1223, 1998.

[60] S. Mohrdiek, H. Burkhard, and H. Walter, "Chirp Reduction of Directly Modulated Semiconductor Lasers at 10 Gbit/s by Strong CW Light Injection," *IEEE J. Lightwave Technol.*, vol. 12, pp. 418-424, 1994.

[61] H. –F. Chou, Y. –J. Chiu and J. E. Bowers, " Standing Wave Enhanced Electroabsorption Modulator for 40 GHz Optical Pulse Generation," *IEEE Photonics Technol. Lett.*, vol. 15, pp. 215-217, 2003.

[62] SDL Application Notes, "Introduction To Modulators," http://www.sdli.co.uk/products/appnotes.html

[63] L. P. Barry, S. Del Burgo, B. Thomsen, R. T. Watts, D. A. Reid and J. Harvey, "Optimization of Optical Data Transmitters for 40 Gb/s Lightwave Systems Using Frequency Resolved Optical Gating," *IEEE Photonics Technol. Lett.*, vol. 14, pp. 971-973, 2002.

[64] M. Suzuki, H. Tanaka, K. Utaka, N. Edagawa and Y. Matsushima, "Transform Limited 14ps Optical Pulse Generation with 15 GHz Repetition Rate by InGaAsP Electroabsorption Modulator," Electron. Lett., vol. 28, pp. 1007-1008, 1992.

[65] D. G. Moodie, A. D. Ellis, A. R. Thurlow, M. J. Harlow, I. F. Lealman, S. D. Perrin, L. J. Rivers and M. J. Robertson, "Multiquantum Well Electroabsorption Modulators for 80 Gbit/s OTDM Systems," Electron. Lett., vol. 31, pp. 1370-1371, 1995.

Chapter 4 - Performance Issues Associated with WDM optical Communication Systems employing SSGS Pulse Sources

4.1 Application of Self-Seeded Gain Switched (SSGS) pulse sources in lightwave communication systems

The development of a wavelength tunable source of short optical pulses is extremely important for an increasing number of photonic applications. In the telecommunication environment, the most relevant feature of these pulse sources is their use in future wavelength division multiplexed (WDM), optical time division multiplexed (OTDM), and hybrid WDM/OTDM optical communications systems [1]. One of the simplest, and most reliable, techniques[16] available to generate wavelength tunable, picosecond optical pulses involves the self-seeding of a gain-switched Fabry-Perot laser [2-5]. As we have already seen, the technique basically involves gain-switching a FP laser, and then feeding back one of the laser modes into the FP diode using a wavelength selective external cavity. Provided that the optical signal reinjected into the laser arrives during the build-up of an optical pulse in the FP laser, a single-moded output pulse is obtained. This technique has been shown to be capable of producing very low jitter optical pulses [6] with durations around 2-3 ps, and recent experiments have also demonstrated the generation of multiwavelength pulses suitable for use in WDM networks [7].

Some of the most important characteristics (pulsewidth, spectral width and temporal jitter) of such pulse sources that would affect its usefulness in a hybrid WDM/OTDM system were looked at in the previous chapter. Another vital parameter of Self-Seeded Gain Switched (SSGS) pulse sources that could affect their usefulness in high-speed optical communication systems is their Side Mode Suppression Ratio (SMSR). The SMSR[17] could be defined as the ratio of the output power emitted in the strongest mode and that emitted in the second strongest mode and is usually expressed in decibels [8].

An aspect that brings about novelty to this particular work is that although the generation of optical pulses using the self-seeding, gain-switching (SSGS) technique has been

[16] Discussed in the previous chapter.
[17] Lasers with a high SMSR are called dynamic single mode lasers.

widely investigated, the use of such pulses in optical communications systems has not yet been examined. The parameter that was used as a yardstick of these SSGS pulse sources, in our work here, was the side mode suppression ratio. Hence in this chapter, we started off by experimentally investigating the effect of the pulse Side Mode Suppression Ratio (SMSR) on the performance of SSGS pulses in optical communications systems. The next stage of experimentations that were carried out involved a two-channel wavelength multiplexed set-up using self-seeded gain switched pulse sources. This set-up was used to investigate the effects of cross channel interference that could be encountered if the SMSR of one of the sources became degraded. The two-channel WDM system was then extended to a three-channel WDM system, and the effect of the cross channel interference on the Bit Error Rate (BER)[18] on such a system was examined. A four-channel system, to further clarify the constraints on the minimum SMSR required as the number of channels increased, was the final stage of study in this area. Finally we went on to carry out some basic simulations to confirm the experimental findings.

4.2 Effect of Side Mode Suppression Ratio (SMSR) on the performance of Self-Seeded Gain Switched (SSGS) pulse sources

In this section, the SMSR of self-seeded, gain-switched optical pulses is shown to be an extremely important factor for the utilization of these pulses in optical communications systems. The effect of the pulse SMSR on the performance of SSGS pulses in optical communications systems is achieved by simply examining the propagation of these pulses through two key components of any optical network (i.e. optical fiber and an optical filter), as a function of SMSR.

4.2.1 Experimental set-up

Figure 4-1 shows our experimental set-up. The FP laser used was a commercial 1.5 μm InGaAsP device, with a threshold current of 26 mA, and a longitudinal mode spacing of 1.12 nm. Gain switching of the laser was carried out by applying a DC bias current of 17 mA, and a sinusoidal modulation signal with a power of 29 dBm, to the laser diode. The sinusoidal modulation signal had a frequency around 2.6 GHz. Self-seeding of the

[18] In telecommunication transmission, BER is the percentage of bits that have errors relative to the total number of bits received in a transmission, usually expressed as ten to a negative power.

gain-switched laser diode was achieved by using an external cavity containing a polarization controller (PC), a 3 dB coupler, and a tunable fiber Bragg grating with a bandwidth of 0.4 nm.

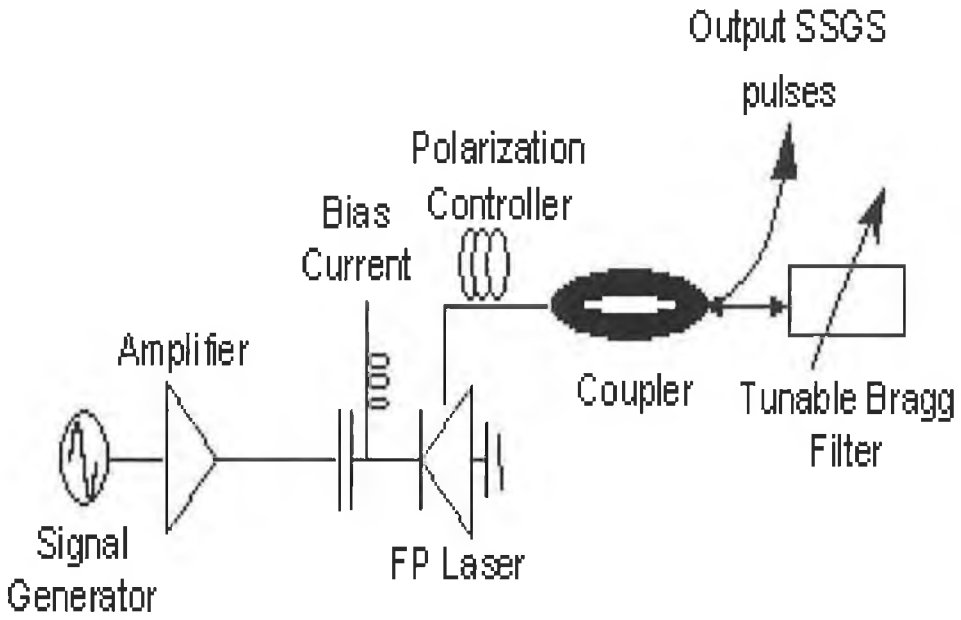

Figure 4-1: Experimental set-up for SSGS pulse generation

To achieve optimum SSGS pulse generation, the central wavelength of the fiber grating was initially tuned to one of the longitudinal modes of the gain-switched laser. The frequency of the sinusoidal modulation was then varied to ensure that the signal reinjected into the laser, from the external cavity, arrives as an optical pulse is building up in the laser[19]. An operating frequency of 2.654 GHz was found to be suitable. In addition to tuning the fiber grating and the modulation frequency, we could also optimize the polarization of the light reinjected, and hence the SMSR of the output optical pulses, by adjusting the polarization controller. The output pulses after the 50:50 fiber coupler were characterized in the temporal domain using a 50 GHz photodiode in conjunction with a 50 GHz HP digitizing oscilloscope. Pulse characterization in the spectral domain was carried out using an Anritsu optical spectrum analyser with a resolution of 0.07 nm.

[19] Reinjected pulse has to arrive within the sensitive time window

4.2.2 Experimental results and observations

With the PC adjusted to maximize the feedback into the FP device, the resulting output pulses from the SSGS set-up were as shown in Figure 4-2.

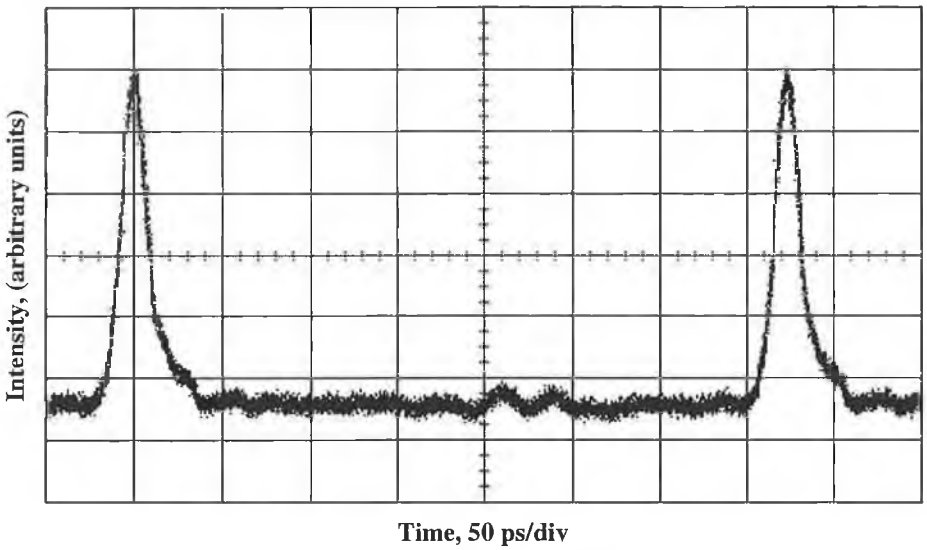

Figure 4-2: Optical pulses generated from SSGS set-up (non-averaged)

Assuming a total response time of about 12 ps for the combination of the photodiode and the oscilloscope, we can deconvolve the output pulse duration to be around 14.7 ps[20]. From the spectral output shown in Figure 4-3, we can determine that the FP mode selected using the Bragg grating was at a wavelength of 1555.4 nm. In addition, the SMSR of the signal was 30 dB, and the 3 dB spectral width was about 0.6 nm. To vary the SMSR of the generated optical pulses from 30 dB down to 10 dB, we simply had to adjust the polarization controller in order to reduce the amount of light fed back into the laser diode. The reduction in feedback and SMSR also resulted in a slight decrease in the pulse duration, and a slight increase in the spectral width, as expected from previous work [9, 10].

[20] Measured pulsewidth was 19 ps. Deconvolved by using $T_A = \sqrt{T_M^2 - T_R^2}$

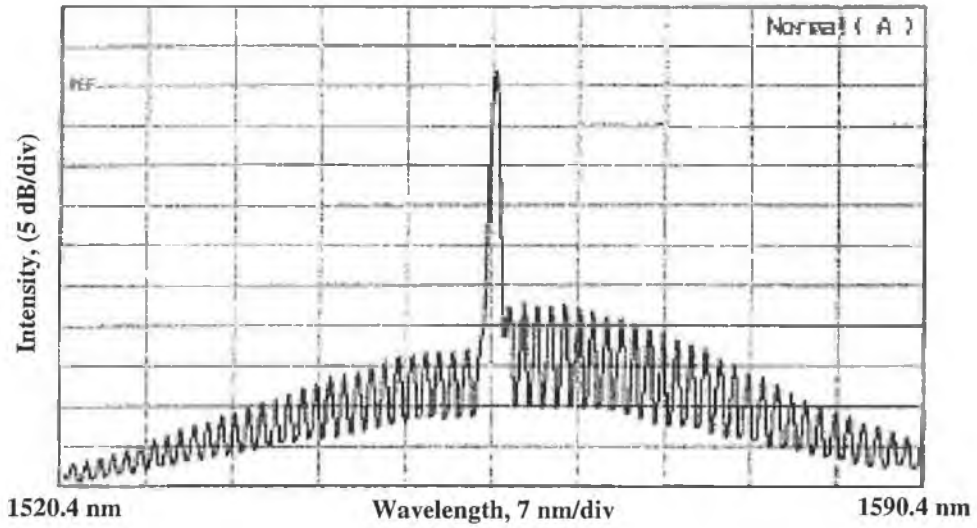

Figure 4-3: Optical spectrum of SSGS pulses

The optical pulses from the SSGS were initially propagated through 10 km of DSF and the effect of a varying SMSR on the pulse propagation was investigated. With the SMSR set to 30 dB the only effect of the fiber transmission was a slight broadening of the pulses due to the fiber dispersion[21]. However, as the SMSR was reduced, the noise level on the transmitted signal began to increase. Figure 4-4 (a)-(d) shows the output pulses (non-averaged) after fiber propagation corresponding to input SMSR's of 25, 20, 15, and 10 dB respectively.

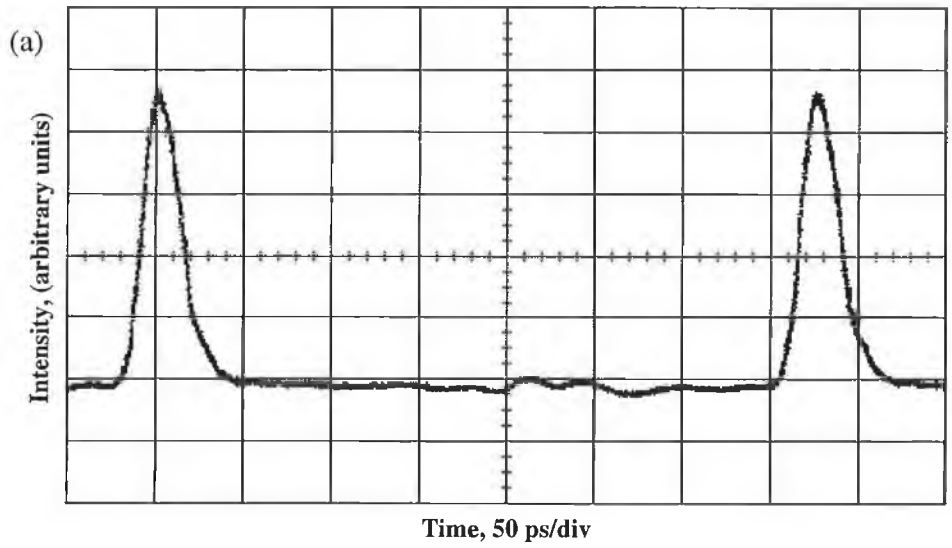

[21] (D = 1.8 ps/(km.nm) at 1555 nm)

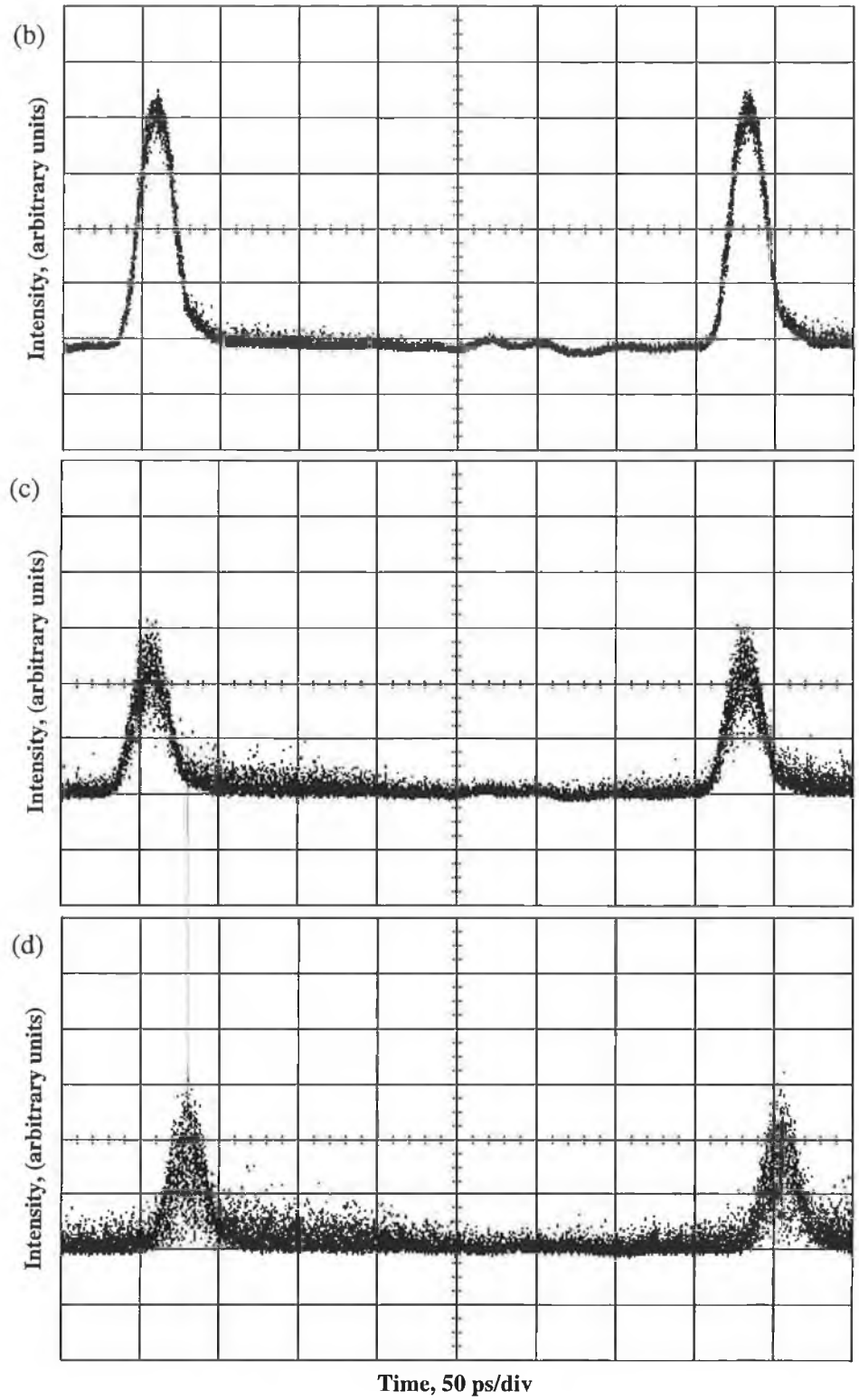

Figure 4-4: Output optical pulses after propagation through 10 km of DSF with the input SMSR of the pulses set to (a) 25 dB, (b) 20 dB, (c) 15 dB, and (d) 10 dB. Persistence of digitizing oscilloscope display set to 3 seconds

From this figure we can see the noise level on, and between, the transmitted pulses beginning to appear as the SMSR was reduced from 25 to 20 dB. When the SMSR was set to 15 and 10 dB, the noise on the optical pulses after transmission became even more obvious. This noise would clearly make the utilization of these pulses unfeasible in optical communication systems.

The increase in noise as the SMSR is reduced is associated with the mode partition effect of the FP laser [11]. Although Mode Partition Noise (MPN) in digital transmission systems has been known for long time, it still can severely affect the performance of an optical communication system, even when using DFB lasers. It is mainly caused by the laser turning on initially in a side mode, which has a different wavelength from the principal mode. An important magnitude to characterize the error due to MPN is the SMSR [12]. Even though DFB lasers could exhibit a SMSR larger than 30 dB at stationary conditions, spontaneous emission noise can trigger the laser to oscillate in a side mode under intensity modulation conditions [13].

Hence we can go on to say that mode partition effect is basically a fluctuation of the energy in each laser mode with time, due to a constant transfer of energy between the laser modes. After transmission over a dispersive medium (long length of fibre), the side modes arrive at the receiver at a different time from that of the principal mode[22]. The spectral fluctuation in the laser modes will thus manifest itself as an intensity fluctuation (noise) on the transmitted optical signal after fiber propagation. This results in either a degradation of the signal to noise ratio or an error in detecting the signal pulse.

In a SSGS scheme, setting the bias point of the laser above threshold could reduce the errors due to MPN. However raising the bias current reduces the achievable signal pulse powers in a gain switched scheme [14]. Consequently in order to eliminate this noise it is necessary to use a single-moded laser pulse in which the total power in the side-modes is negligible (in comparison to the main mode). From our experiment we have seen that

[22] When an optical pulse with a multi-moded spectrum propagates in a dispersive fiber medium, the laser modes travel at different speeds and hence spread out in the temporal domain.

with a SMSR of 25 dB or greater, the noise on the optical pulse after propagation is essentially negligible, because the total pulse power in the side-modes is negligible. However, as the SMSR is reduced, and the power in the side modes becomes non-negligible, the energy fluctuation of the modes[23] results in an increasing noise level on the transmitted pulses.

Having experimented the varying SMSR effect, on SSGS pulses, by transmitting through fibre, we then investigated the effect of a varying SMSR on the propagation of the optical pulses through a tunable FP filter with a 3 dB bandwidth of 0.7 nm. The filter was manually tuned to select out the main operating mode from the SSGS pulse spectrum. Optimization[24] of the self-seeding was done in order to ensure that the pulse input to the filter had its SMSR maintained at 30 dB. At this stage of the input pulse having 30 dB SMSR, the only effect of the filter on the optical pulse was a slight reduction in its duration [15]. However, as the SMSR was reduced, the pulse after the optical filter developed a large amount of amplitude noise. Figure 4-5 (a) & (b) displays the output pulses (non-averaged) when the SMSR of the input signal was 20 and 15 dB respectively. The amplitude noise on the pulses is once again due to the mode partition effect [16]. Since only the main mode is transmitted through the optical filter, any temporal fluctuations in the energy level of this mode will result in amplitude noise on the transmitted pulse. Clearly as the SMSR is reduced, the energy in the side modes increase and the fluctuation of the energy in the main mode increases, resulting in additional amplitude noise on the transmitted pulse.

[23] The lower the SMSR, the higher the power in the side modes and the higher the fluctuations in the selected mode.
[24] Tuning of the grating and also adjustment of the PC.

Figure 4-5: Optical pulses at output of FP filter with the SMSR of the input signal set to (a) 20 dB, and (b) 15 dB. Persistence of digitizing oscilloscope display set to 3 seconds

4.3 Cross-channel interference due to Mode Partition Noise (MPN) in a two-channel WDM optical system using self-seeded gain switched pulse sources

In this section, we experimentally investigate the effect of the pulse SMSR on the performance of 10 GHz self-seeded gain-switched (SSGS) pulse sources in a two-channel WDM-type system. We also examine the noise induced on one of the pulse sources due to a variation in SMSR of the other SSGS source. Our results show that although many of the previous reported wavelength tunable pulse sources, using the SSGS technique, had SMSR's which varied between 10 and 25 dB as the output pulse wavelength was tuned

[3, 6, 7], in practice, such pulses may be unsuitable for use in high speed WDM communication systems due to the mode partition effect.

4.3.1 Experimental set-up

Figure 4-6 shows our experimental set-up. The FP lasers used were commercial 1.5 μm InGaAsP devices, with threshold currents around 25 mA, and longitudinal mode spacings of 1.1 nm. The two lasers used had central frequencies of 1555 nm. Gain switching of the lasers was carried out by applying DC bias currents of 50 mA, and 10 GHz sinusoidal modulation signals with powers of 24 dBm, to each device. Self-seeding of the diode FP1 was achieved by using an external cavity containing a polarisation controller (PC), a 3 dB coupler, and a tunable Bragg grating with a bandwidth of 0.4 nm. The external cavity for self-seeding FP2 contained all the devices mentioned above plus a tunable optical delay line[25].

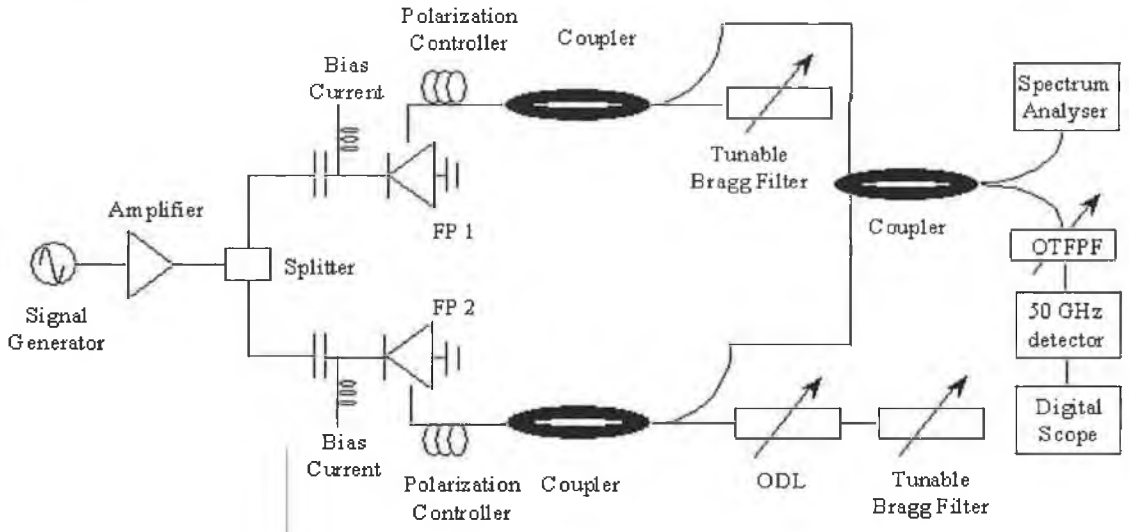

Figure 4-6: Experimental set-up for examining the effects of SMSR variation in a WDM-type system using two SSGS pulse sources

To achieve optimum SSGS pulse generation from FP1, the grating was tuned to reflect one of the laser modes (at 1556 nm), and the frequency of the sinusoidal modulation was then varied (~9.987 GHz) to ensure that the signal reinjected into the laser arrives at the correct time. For SSGS operation of FP2, the Bragg grating was tuned to reflect a laser

[25] Either the repetition rate or the length of the cavity has to be adjusted to ensure that the reflected pulse arrives back at the laser diode during the narrow time window.

mode at 1546 nm, and the optical delay line was varied to ensure that the signal fedback from the grating arrives at the correct time. It should also be noted that the wavelength of each source may be tuned using the fibre grating, but the tuning range was limited to about 5 nm by the tunability of the grating. As mentioned in the previously, in addition to tuning the grating, and adjusting the sinusoidal frequency, the feedback can be adjusted, (and thus the SMSR on the output pulses varied), by using the PC's.

4.3.2 Experimental results and observations

Figure 4-7 displays the optical spectrum of the two pulse sources after being combined together using a fibre coupler, (with the feedback from the gratings optimized using the polarisation controllers). The 3 dB bandwidths of the 10 GHz pulse sources were both around 0.25 nm, and the SMSR of the sources at 1546 nm and 1556 nm were 27 dB and 25 dB respectively.

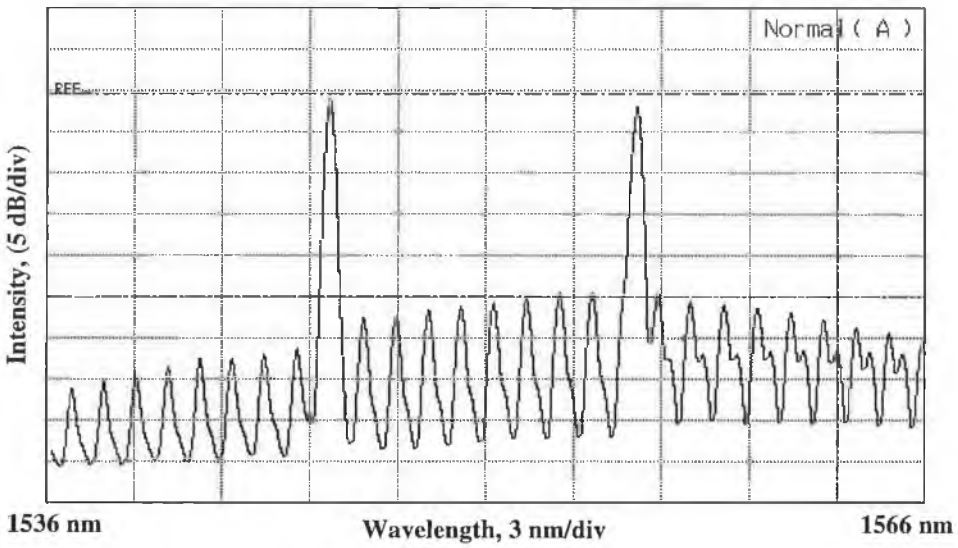

Figure 4-7: Optical spectrum of the two 10 GHz pulse sources after fibre coupler

Figure 4-8 & Figure 4-9 display the two pulse waveforms from the sources when they were subsequently filtered out from the composite signal using a tunable FP filter with a bandwidth of 0.7 nm. The pulses were detected and measured using a 50 GHz pin photodiode in conjunction with a 50 GHz digitizing oscilloscope. The output pulse duration (after deconvolving with the measurement system) was 18 ps for the 1546 nm source, and 19 ps for the 1556 nm source. The average optical power from both sources

after passing through the FP filter was around 0.25 mW, which corresponds to optical pulse peak powers[26] of about 1.4 mW.

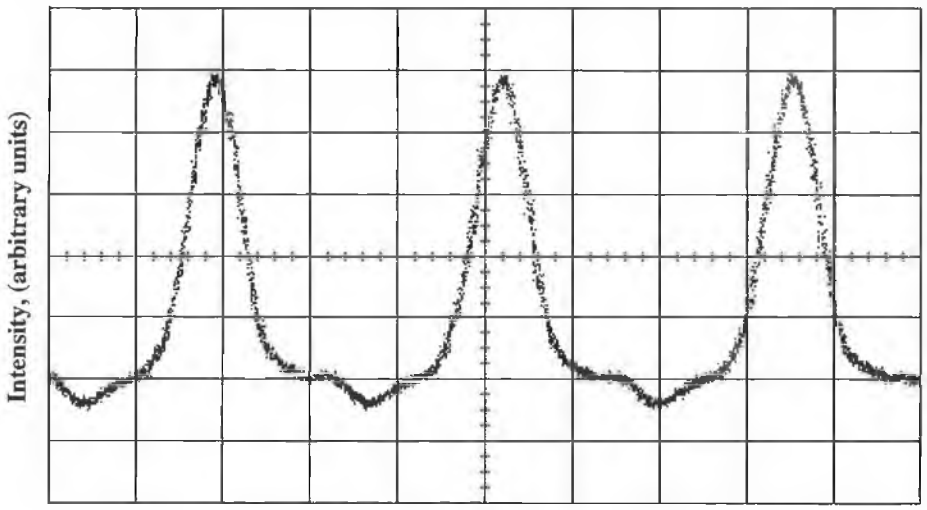

Figure 4-8: 10 GHz pulse trains of the 1546 nm source (non-averaged)

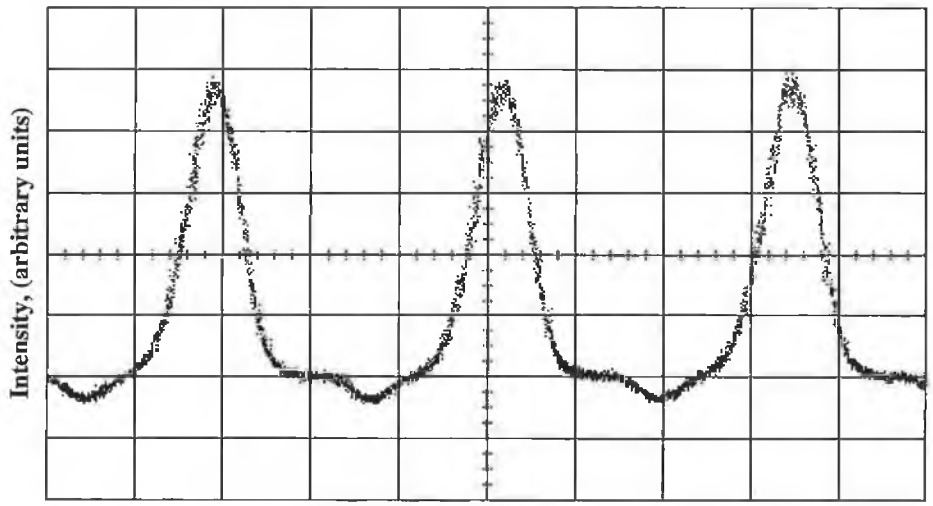

Figure 4-9: 10 GHz pulse trains of the 1556 nm source (non-averaged)

To determine the effect of SMSR on the filtered signals, we initially varied the SMSR of the 1556 nm pulses using the PC, and examined the noise added to the filtered signal at 1546 nm (which had its SMSR maintained at 27 dB).

[26] Pulse peak power $= \frac{P_{avg}.T}{\tau}$

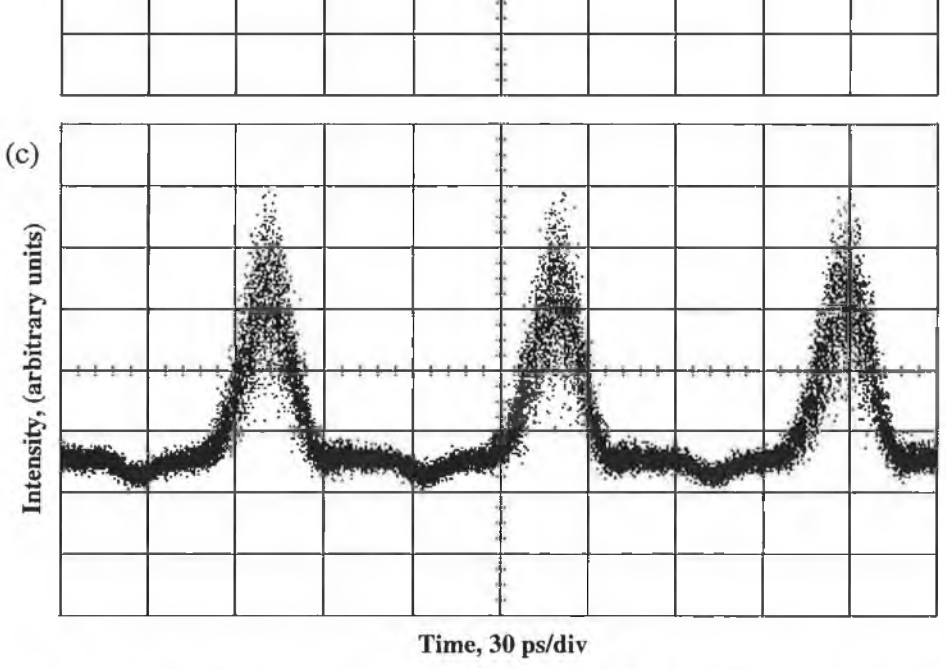

Figure 4-10: 1546 nm pulses after FP filter with the SMSR of the 1556 nm pulse source set to (a) 20 dB, (b) 15 dB, and (c) 10 dB

Intensity, (arbitrary units)
(b)
Intensity, (arbitrary units)
(a)

Figure 4-10 (a, b, & c) displays the non-averaged output waveforms with the SMSR of the 1556 nm pulse train set to 20, 15, and 10 dB respectively. We can clearly see that when the SMSR was reduced to 15 dB, the noise on the 1546 nm pulse train after the optical filter became noticeable, and as the SMSR was reduced further, the noise on the signal greatly increased.

The noise acquired on a filtered pulse source as the SMSR of the other SSGS pulse source is reduced, is due to the mode partition effect [11, 16]. As explained earlier, the mode partition effect is basically a fluctuation of the energy in each laser mode with time, due to a constant transfer of energy between the modes. For a single mode laser with a large SMSR, the power in the side modes is negligible, thus the power fluctuation of the main mode is negligible. However, as the SMSR decreases, the power fluctuation of the main mode, and the side modes, may become non-negligible. When the optical filter is tuned to select out either the 1546 nm or 1556 nm signal, the noise on the pulse train will be negligible provided the SMSR's of both sources is large (as shown in Figure 4-8 & Figure 4-9). If the SMSR of the filtered signal is reduced, then the noise level on that pulse source would clearly increase due to the mode partition effect, as already demonstrated and explained in the previous section. However, in this experiment we have demonstrated the increased noise induced on one filtered pulse source due to a reduction in SMSR of a second SSGS source. This noise is also due to the mode partition effect, because as the SMSR of one SSGS pulse source is reduced, the power (and the power fluctuation) in its side-mode, which is at the same wavelength as the second pulse source selected by the FP filter, increases. The temporal fluctuation in power of this side mode can thus manifest itself as noise on the filtered source.

We then examined the effect of varying the SMSR of the 1546 nm source using the PC, when the FP optical filter was tuned to select out the 1556 nm pulse train (which had its SMSR maintained at 25 dB). Figure 4-11 (a and b) displays the filtered 1556 nm pulse train when the SMSR of the 1546 nm signal was set to 20 and 15 dB. We can clearly see that noise level on the signal increases as the SMSR of the 1546 nm source was reduced. By comparing Figure 4-10 and Figure 4-11 we can also observe that the noise level on

the filtered signal, for the case when the SMSR of the adjacent wavelength source is set to 15 dB, is far greater when the 1556 nm pulse source is filtered out.

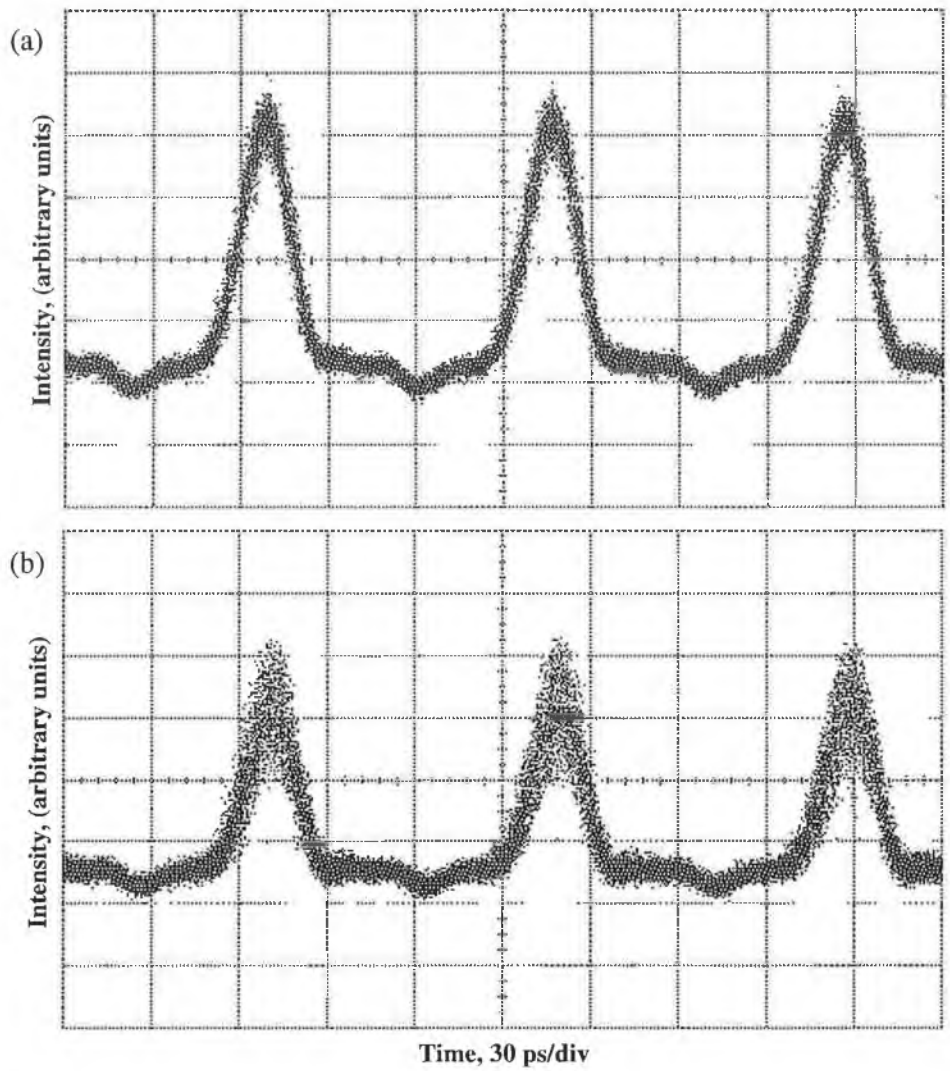

Figure 4-11: 1556 nm pulses after FP filter with the SMSR of the 1546 nm source set to (a) 20 dB, and (b) 15 dB

The difference in noise level on the two filtered wavelength signals, when the SMSR of the adjacent sources were both set to 15 dB, can be explained by the examination of the spectrum shown in Figure 4-7. Each of these lasers, used to generate the SSGS pulses, exhibits a unique gain curve of their own. In the case of this experiment, both lasers had their central wavelengths (principal modes) at 1555 nm. By comparing the two scenarios, we can say that in the first case (1556 nm channel filtered out), the variation in the SMSR of the 1546 nm source would affect the 1556 nm channel by introducing more noise than

in the second case (1546 nm channel filtered out) where the SMSR of the 1556 nm source varies and the 1546 nm channel is filtered out.

When the 1556 nm signal is filtered out, the side-mode of the 1546 nm signal with the maximum power (and also maximum power fluctuation) is around 1556 nm, which is the central wavelength of the FP laser. However, when the 1546 nm signal is filtered out, the side-mode of the 1556 nm source with the maximum power is around 1555 nm, and not 1546 nm. Thus, as a general case, the cross channel interference on the filtered signal is more accurately determined by the suppression ratio between the main mode and the side mode of the adjacent wavelength source at the same wavelength as the filtered out pulse source.

In WDM systems, the wavelength channels could be spaced from as close as 0.2 nm to as far as 30 nm. Hence it was important to investigate the dependence of cross channel interference on the spectral spacing of the two channels. However, we were limited to a tuning range of 5 nm due to the FBG available. We subsequently investigated how the mode-partition-noise was affected by varying the spectral spacing between the two sources. In this case, the amplitude noise on the detected pulse was characterized by measuring its RMS noise voltage using the digitizing oscilloscope. Figure 4-12 displays the results when the SSGS source using FP2 was tuned from 1543.8 to 1548.2 nm with its SMSR kept constant while the SMSR of the other SSGS pulse source using FP 1 was degraded. During the process of tuning, the SMSR of the SSGS pulse source (FP 2) was maintained at around 27 dB, by optimizing the polarization controller and adjusting the voltage applied across the piezo electric controller. The SMSR of the SSGS at 1556 nm (FP 1) was set to (degraded) 15 dB.

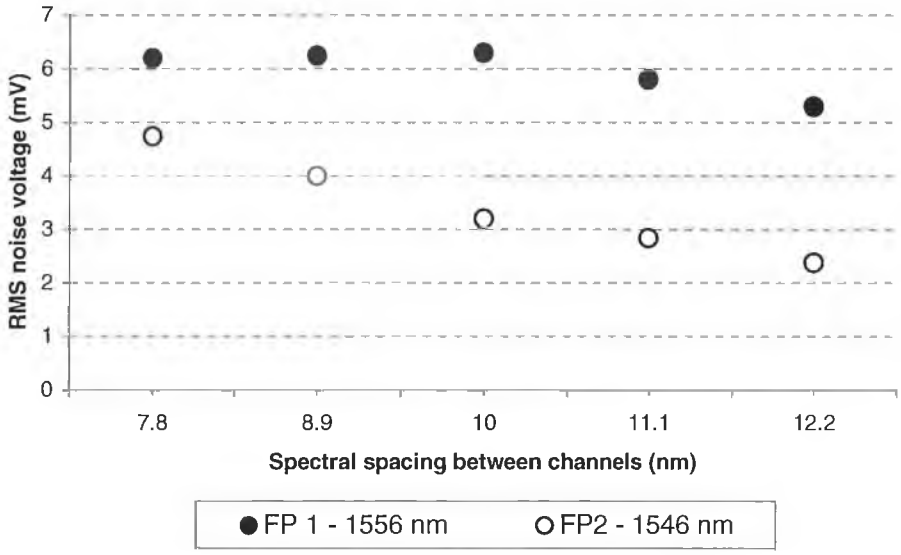

Figure 4-12: RMS noise voltage (due to cross-channel interference) on detected pulses from FP1 (solid circles) and FP2 (open circles), as their wavelengths are tuned over 5 FP modes, with the SMSR of the adjacent pulse source (fixed wavelength) set to 15 dB.

We can see that as the spectral spacing decreases, the noise level on the signal filtered out from FP2 increases. We then tuned the pulse source from FP1 between 1553.8 and 1558.2 nm (with its SMSR kept constant around 25 dB), and examined the interference due to the 1546 nm SSGS source from FP2 (with its SMSR set to 15 dB). These results are also shown in Figure 4-12, and demonstrate that in this case the noise level on the filtered out pulse is actually maximum when it is at 1556 nm (approx. 10 nm spacing between the SSGS sources), and decreases slightly as the source is tuned to higher or lower wavelengths.

The variation in amplitude noise as the spectral spacing between the sources is changed, is basically due to the same phenomenon explained in the previous section. It is necessary to understand that the cross-channel interference (caused by mode-partition-noise) on channel 1 due to channel 2, is determined by the power in the side mode of channel 2 which is at the same wavelength as channel 1. The power in the side mode of any SSGS pulse source (using an FP laser) is determined by the spacing between the side mode and the peak of the FP gain curve. Thus as the wavelength of channel 1 is varied, the cross channel interference due to channel 2 is determined by the position (wavelength) of

channel 1 relative to the gain curve of the FP laser used to generate the SSGS pulses for channel 2.

In conclusion we have shown that the SMSR of wavelength tunable SSGS pulse sources at 10 GHz is extremely important for determining their usefulness in WDM communication systems. If the SMSR of one source in a WDM system become degraded, then the interaction of the mode partition effect with spectral filtering can result in a large amount of noise on all the wavelength channels in the communications system. This noise could clearly lead to an unacceptable error rate in the communication system. It is thus vital that any WDM transmission system based on tunable SSGS pulse sources maintains a large SMSR (preferably greater than 30 dB) at all wavelengths.

4.3.3 Characterization of MPN due to cross channel interference

In order to characterize how the increased noise affected the system performance we then went on to modulate data onto one of the pulse sources. We then measured how the received bit error rate (BER) is affected by varying the SMSR of the adjacent source.

4.3.3.1 Experimental set-up

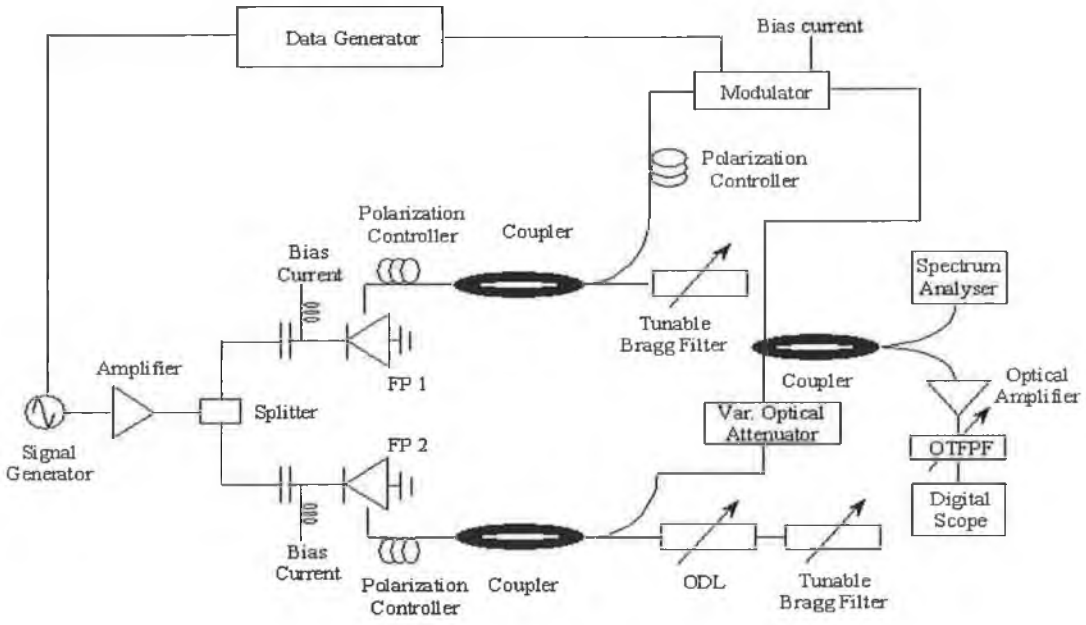

Figure 4-13: Experimental set-up to verify cross channel interference

Figure 4-13 shows our experimental set-up, which is essentially the same as the set-up shown in Figure 4-6. The only difference being that an Anritsu Digital Data Analyser (MP 1632 A - 3.2 Gb/s) was used to encode data onto one of the channels. The data analyser consisted of a Pulse Pattern Generator (PPG) and an Error Detector (ED) within one cabinet. Since we were limited to 3.2 Gb/s by the PPG, gain switching was carried out at a lower repetition rate (2.5 GHz) in comparison to the previous set-up involving a two-channel WDM system.

The FP lasers used were the same (as in the preceding experiment) commercial 1.5 μm InGaAsP devices, with threshold currents around 25 mA, and longitudinal mode spacings of 1.1 nm. Gain switching of the lasers was carried out, by applying DC bias currents of around 17 mA and 2.5 GHz sinusoidal modulation signals with powers of 24 dBm, to each device. Self-seeding of the diode FP1 was achieved by using an external cavity containing a polarisation controller (PC), a 3 dB coupler, and a tunable Bragg grating with a bandwidth of 0.4 nm. The external cavity for self-seeding FP2 contained an additional tunable optical delay line (ODL).

To achieve optimum SSGS pulse generation from FP1, the grating was tuned to reflect one of the laser modes (at 1556 nm), and the frequency of the sinusoidal modulation was then varied (~2.4836 GHz) to ensure that the signal re-injected into the laser arrives at the correct time. For SSGS operation of FP2, the Bragg grating was tuned to reflect a laser mode at 1546 nm, and the ODL was varied to ensure that the signal fed back from the grating arrives at the correct time. In addition to tuning the grating and the electrical frequency, the feedback can be adjusted, (and thus the SMSR on the output pulses varied), by using the polarisation controllers (PC).

A 2^{11}-1 pseudo random data signal from the pattern generator, at a bit rate of 2.5 Gbit/s, was then used to modulate the 1556 nm (SSGS using FP 1) pulse train. The resulting 2.5 Gbit/s RZ data signal from the modulator was then coupled together with the 1546 nm pulse train in a fibre coupler. The 1546 nm signal was attenuated before the coupler to ensure that the power level in both wavelength signals was the same after the

coupler. The composite signal was then amplified before the 1556 nm data signal was filtered out using a tunable filter with a bandwidth of 0.7 nm. The received data signal was then detected using a 50 GHz pin photodiode, before a 50 GHz oscilloscope was used to examine the eye diagrams, and an error analyser was used for BER measurements.

4.3.3.2 Experimental results and observations

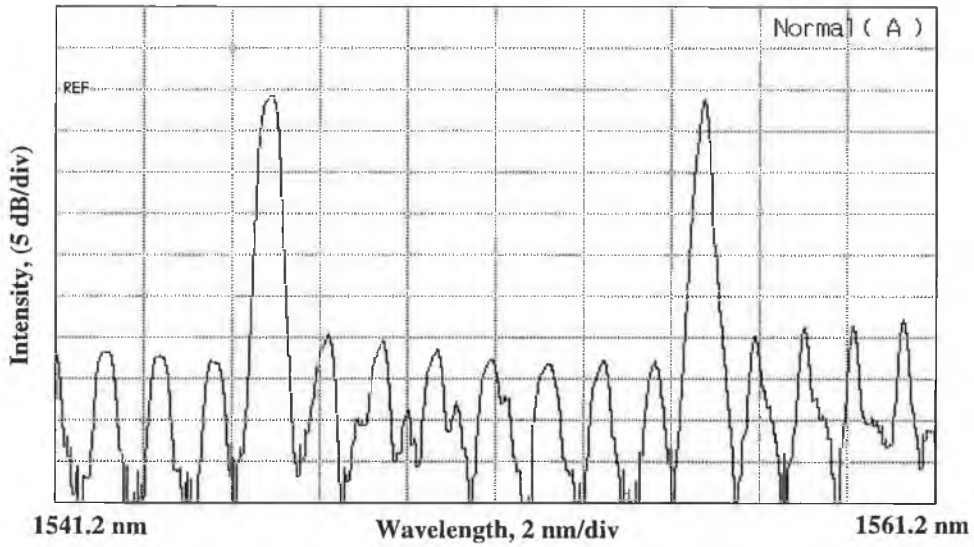

Figure 4-14: Optical spectrum of the dual wavelength signal after fibre coupler

Figure 4-14 displays the optical spectra of the composite channel (one is a data channel while the other is a pulse source) after being combined together using a fibre coupler, (with the feedback from the gratings optimized using the polarisation controllers). The 3 dB bandwidths of the 2.5 GHz pulse sources were both around 0.25 nm, and the SMSR of the sources at 1546 nm and 1556 nm were 30 dB and 27 dB respectively.

To determine, once again the effect of cross channel interference due to SMSR variations, we varied the SMSR of the 1546 nm source using the PC, while the optical filter was tuned to select out the 1556 nm data channel (which had its SMSR maintained at 27 dB). Figure 4-15 (a, b and c) displays the received eye diagrams of the1556 nm data signal when the SMSR of the 1546 nm signal was set to 30, 22, and 15 dB. The received optical power level after the FP filter was noted to be about -8 dBm.

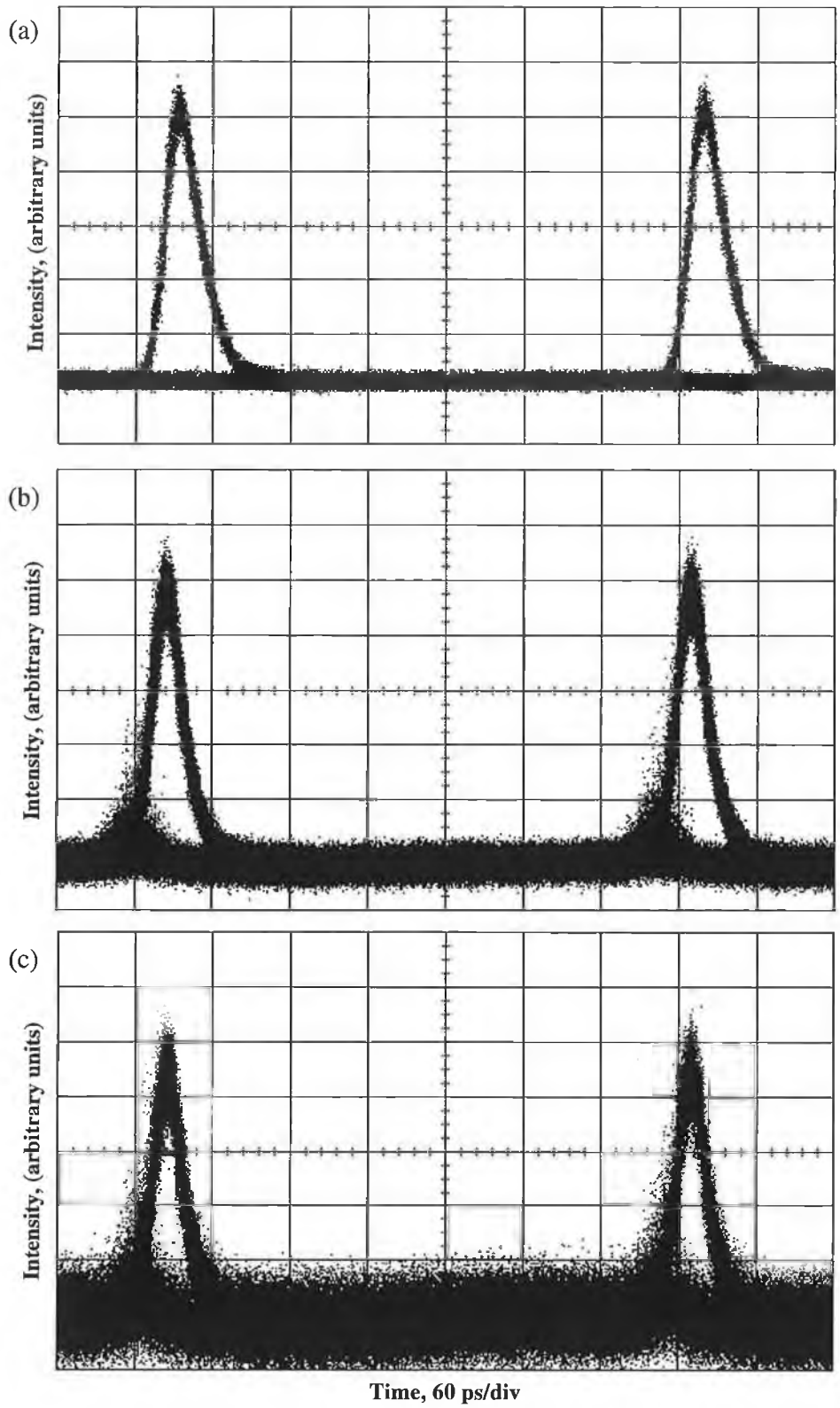

Figure 4-15: Received eye diagrams for 1556 nm data channel with varying SMSR of the 1546 nm source set to (a) 30 dB, (b) 22 dB & (c) 15 dB

The eye is wide and fully open in the case where the SMSR of the 1546 nm channel is maintained at the maximum value attained (30 dB) as can be seen in Figure 4-15 (a). We can also undoubtedly see (Figure 4-15 (b) & (c)) that when the SMSR was reduced to 22 and 15 dB, the noise on the 1556 nm data signal became significant.

To characterize the system performance with the increasing noise level as the SMSR was degraded, we then measured the BER of the received 1556 nm signal as a function of the SMSR of the pulse source at 1546 nm (shown in Figure 4-16). We can clearly see that a minimum SMSR exists in order to achieve an acceptable BER of 10^{-9}. However, it is important to note that the achievability of an acceptable BER depends on the received power level. Therefore when the SMSR is not optimum, the transmitted power must be increased to maintain the same BER. The extra power required to account for the degradations (in SMSR), is known as the power penalty.

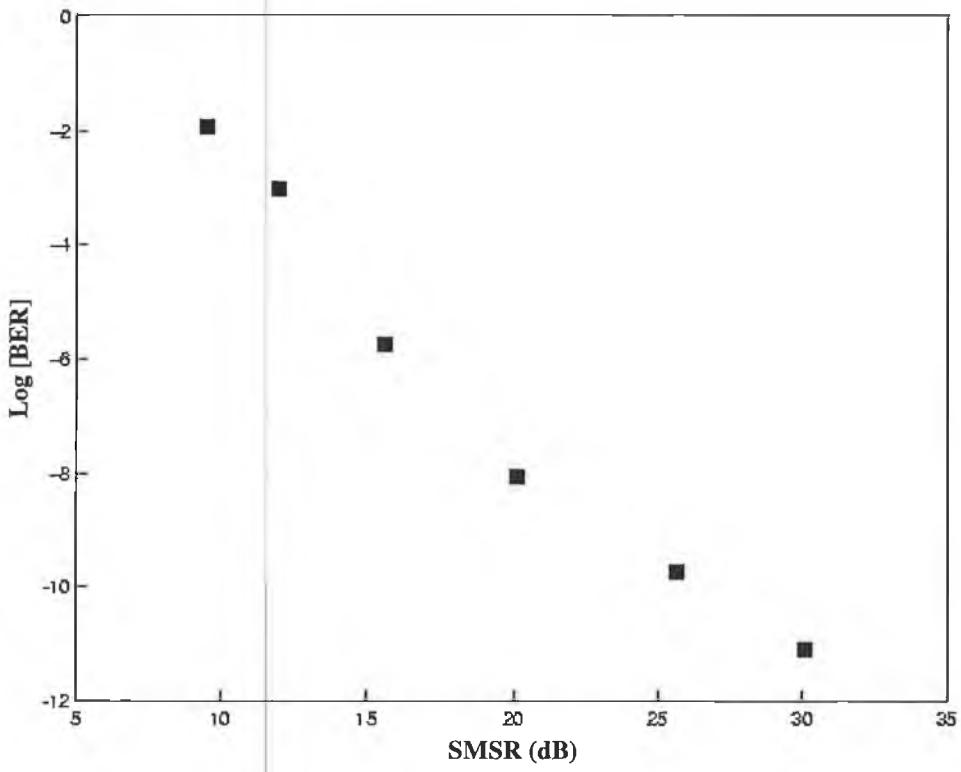

Figure 4-16: BER vs. SMSR

The noise acquired on the filtered 1556 nm data signal (and its degraded BER), as the SMSR of the 1546 nm pulse source is reduced, is once again due to the mode partition

effect. We already demonstrated, the cross channel interference on one received data signal to a reduction in SMSR of pulse source at a different wavelength, in the previous section. However, in this part we have gone on further to show that the temporal fluctuation in power of the 1546 nm side mode can thus manifest itself as noise on the filtered data channel (at 1556 nm), which will thereby degrade the BER of the received signal. Hence we could conclude that, a 2-channel WDM system employing SSGS pulse sources needs at least 26 to 28 dB of suppression of the side modes (as can be seen in Figure 4-16) to achieve satisfactory operation of the system[27].

It has been shown that the noise buildup leads to an unacceptable error rate in such a communication system. Yet, in this particular case, we have only looked at a two-channel system in which the SMSR of one of the channels gets degraded. In order to investigate whether a system with more channels will place even more stringent specifications on the allowed SMSR of the channels due to accumulative MPN, we went on to build a three-channel WDM system employing SSGS pulse sources.

4.4 Effect of cross-channel interference on the BER of a three-channel WDM optical system using self-seeded gain switched pulse sources

Here we experimentally investigated the effect of the pulse SMSR on the performance of self-seeded gain-switched (SSGS) pulse sources in a three-channel WDM-type system by examining how the received Bit-Error-Rate (BER) of one channel is affected by varying the SMSR of the two adjacent channels.

[27] At an optimum transmitted power

4.4.1 Experimental set-up

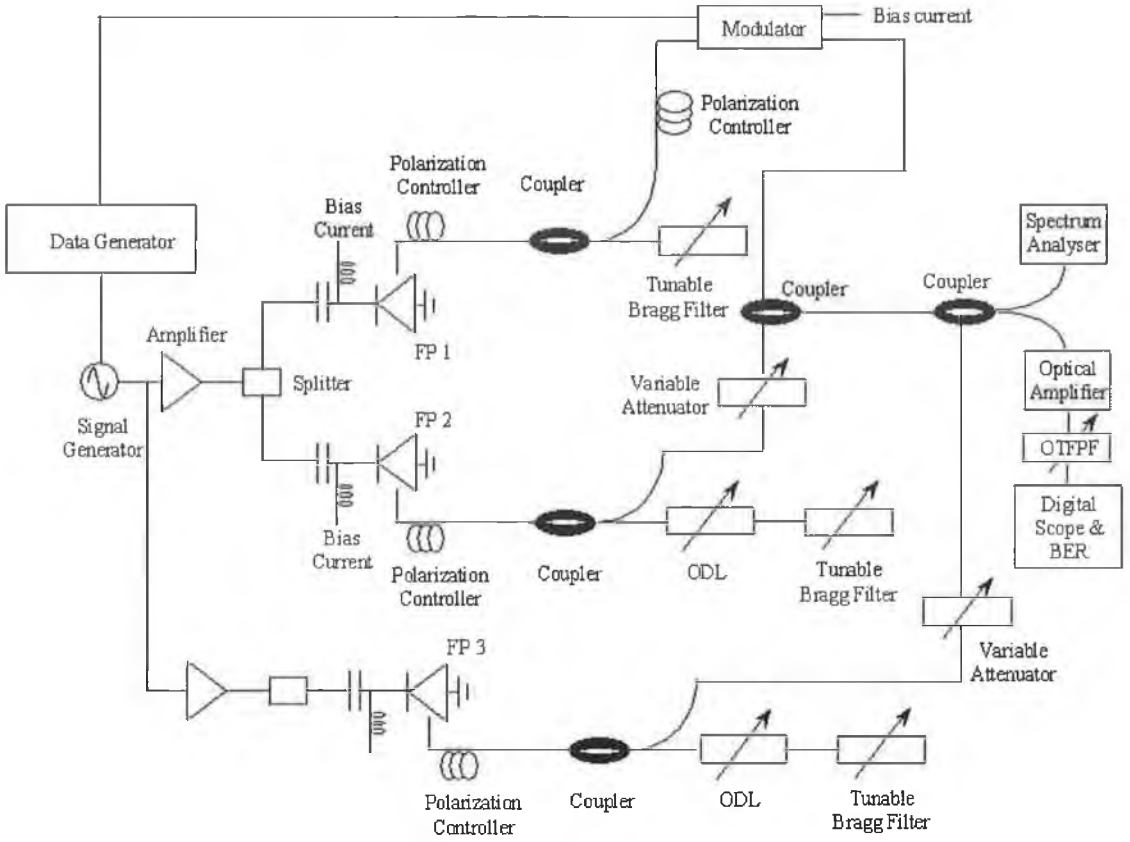

Figure 4-17: A basic schematic of the experimental set-up

Figure 4-17 shows a basic schematic of our experimental set-up. The three FP lasers used were commercial 1.5 μm InGaAsP devices, with threshold currents around 25 mA, longitudinal mode spacings of 1.1 nm, and central emission wavelengths of 1551 nm. Gain-switching of the lasers was carried out by applying DC bias currents of around 17 mA, and 2.5 GHz sinusoidal modulation signals with powers of 24 dBm, to each device. Self-seeding of the diode FP1 was achieved by using an external cavity containing a polarisation controller (PC), a 3 dB coupler, and a tunable Bragg grating with a bandwidth of 0.4 nm. The external cavities for self-seeding FP2 and FP3 contained additional tunable optical delay lines. The three Bragg grating used were tunable over about 5 nm, and their central transmission wavelengths were 1545 nm, 1554 nm, and 1561 nm.

4.4.2 Experimental results and observations

Figure 4-18 displays the optical spectrum of the three pulse sources after being combined together using a fibre coupler. The gratings have been tuned to generate SSGS pulses at 1545 nm, 1554 nm, and 1561 nm, and by optimizing the feedback from the gratings using the polarisation controllers, we have obtained a SMSR of between 30 and 35 dB for the three sources. The spectral and temporal widths of the three sources were around 0.25 nm and 18 ps respectively.

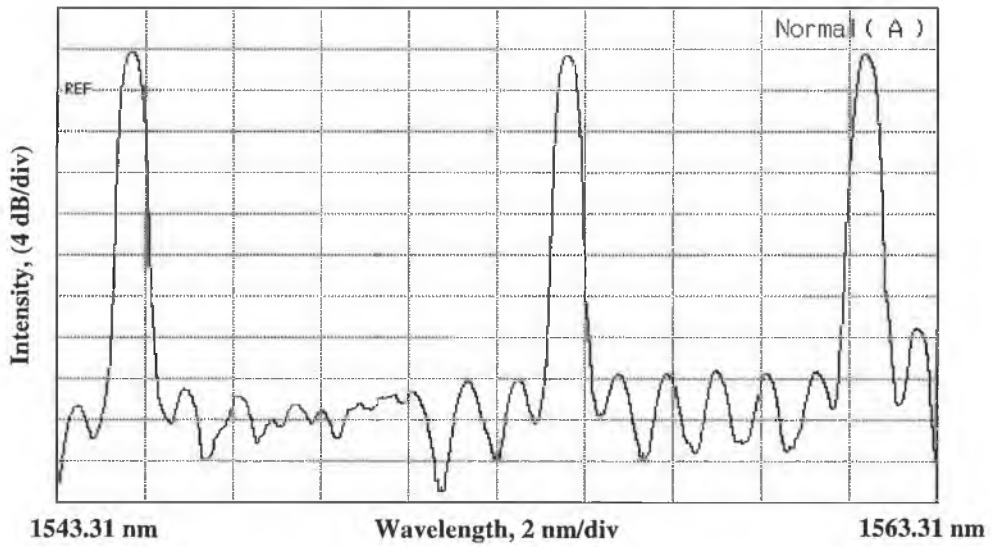

Figure 4-18: Optical spectrum of composite wavelength signal after fibre coupler

The 1554 nm pulse source was then passed through an external modulator to which 2.5 Gbit/s NRZ data (2^{11}-1 pattern) was applied from an Anritsu pattern generator. The resulting RZ optical data signal at 1554 nm was subsequently coupled together with the pulse sources at 1545 and 1561 nm (which had their power levels attenuated to equalize the power in the three wavelength signals). The overall WDM signal was then amplified before the 1554 nm data signal was filtered out using an Optical Fabry Perot Tunable Filter (OFPTF) with a bandwidth of 0.7 nm, and detected using a 50 GHz photodiode. The system performance was characterized by examining the eye diagram of the detected signal using a 50 GHz oscilloscope, and measuring the BER of the received signal using an Anritsu error analyser.

To determine the effect of SMSR on the filtered 1554 nm data channel, we initially varied the SMSR of the 1545 nm signal using the PC. The data signal had its SMSR maintained at 30 dB while the 1561 nm signal was plugged out. The received (RZ) eye diagrams of the 1554 nm data signal with the SMSR of the 1545 nm signal set to 30, 20 and 15 dB were basically similar to those shown in Figure 4-15. We then examined the effect of varying the SMSR of the 1561 nm signal. The SMSR of the data channel was still at 30 dB but with the 1545 nm signal was plugged out. We observed that the noise level on the filtered signal increased as the SMSR of the adjacent channel was degraded. We subsequently degraded the SMSR of both signals (1545 and 1561nm) and checked its effect on the filtered data channel, which had its SMSR still at 30 dB.

Finally to characterize how the increased noise affected the system performance we measured the received optical power required to maintain a BER of 10^{-9} as the SMSR of the adjacent channels were varied (in the manner mentioned above). The result obtained is shown in the form of plot in Figure 4-19.

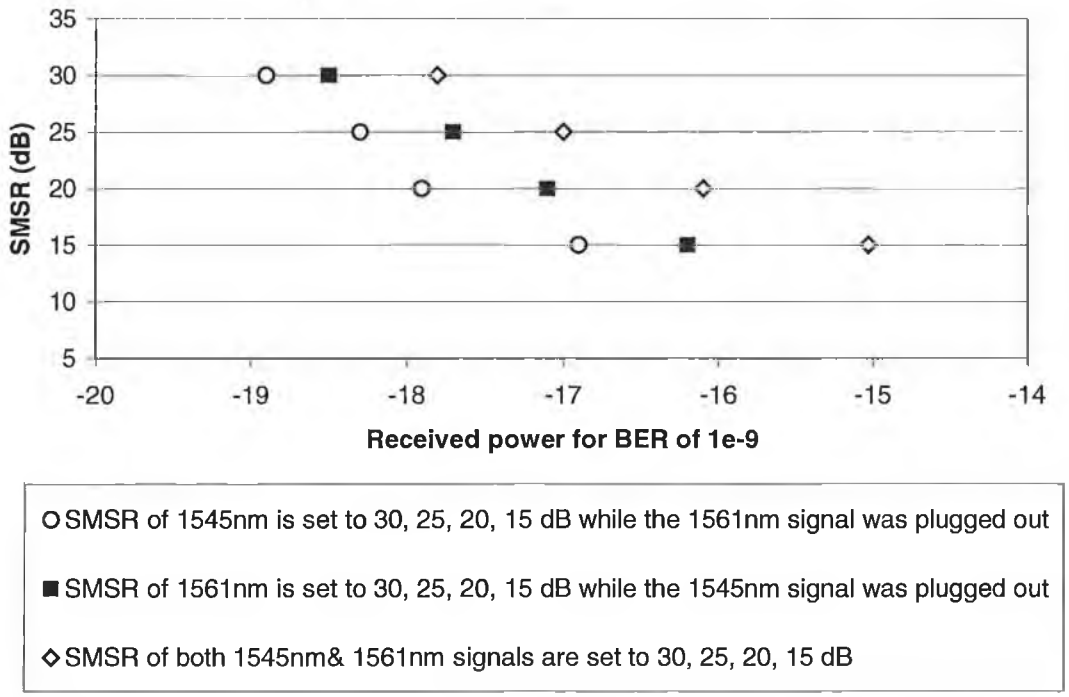

Figure 4-19: SMSR against received power required to maintain a BER of 10^{-9} for the 1554 nm data channel

The noise acquired on the received data signal as the SMSR of the adjacent SSGS pulse sources are degraded is due to the mode partition effect[28]. Our results clearly show how the pulse SSMR affects the performance of a WDM system using tunable SSGS sources. In addition, the extra power penalty incurred when we go from a 2-channel to a 3-channel system (with SMSR's maintained at 30 dB) suggests that for a WDM system based on SSGS pulse sources, the SMSR's must be kept in excess of 30 dB.

So far the particular issue we have addressed and experimentally demonstrated entails the effect of mode partition noise on the power penalty due to cross channel interference. At this juncture, in order to provide a quantitative analysis of how MPN degrades a WDM system that employs SSGS pulse sources, we realized that the number of WDM channels would need to be increased. The available facilities in a typical academic laboratory environment, limited us to a maximum of a four-channel WDM system. The following section looks at Bit Error Rate (BER) measurements that have been carried out on a four-channel wavelength division multiplexed set-up using tunable self-seeded gain-switched pulse sources.

4.5 Performance degradation of a four-channel WDM optical system using self-seeded gain switched pulse sources due to mode partition noise

We experimentally investigated the system performance, by using Bit-Error-Rate (BER) measurements, of a 4-channel WDM system employing SSGS pulse sources, as the SMSR of the sources was varied. The cross channel interference due to mode-partition-noise results in significant power penalties in the system as the SMSR of the pulse sources are degraded. Our results also demonstrate that as the number of channels in a WDM system using SSGS pulse sources increases, the specifications on the required SMSR become more stringent.

4.5.1 Experimental set-up

Figure 4-20 shows our experimental set-up. The FP lasers used were commercial 1.55 μm InGaAsP devices, with threshold currents around 20 mA, and longitudinal mode spacings

[28] Already determined and discussed in the previous sections.

of 1.1 nm. The four lasers were gain-switched by applying DC bias currents of around 25 mA in conjunction with 2.5 GHz electrical sinusoidal signals (with powers of 24 dBm), to each diode. Self-seeding of the diode FP1 was achieved by using an external cavity containing a polarisation controller (PC), a 3 dB coupler, and a tunable Bragg grating with a bandwidth of 0.4 nm. The external cavities for self-seeding FP2, FP3 and FP4 contained additional tunable optical delay lines (ODL).

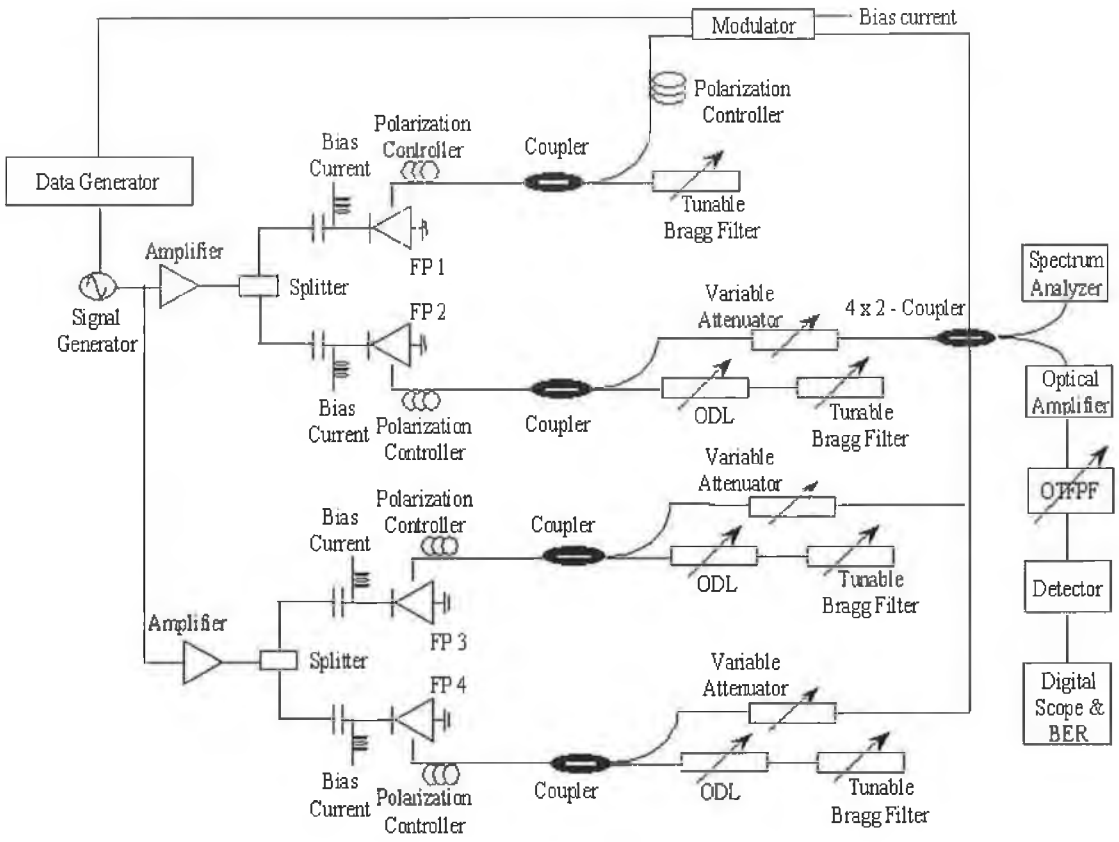

Figure 4-20: Experimental set-up for examining the effects of SMSR variation in a WDM system using self-seeded, gain-switched pulse sources

To achieve optimum SSGS pulse generation from FP1, the grating was tuned to reflect one of the laser modes (at 1552.6 nm), and the frequency of the sinusoidal modulation was then varied (~2.4836 GHz) to ensure that the signal re-injected into the laser arrives at the correct time. For SSGS operation of all the other FP's 2-4, each of the Bragg gratings were tuned to reflect laser modes at 1544.1, 1548.1, 1556.3 nm respectively. The ODL was varied to ensure that the signals fed back from the gratings arrive at the correct

time. In addition to tuning the grating, the feedback can be adjusted, (and thus the SMSR on the output pulses varied), by using the polarisation controllers (PC) at the laser output.

A 2^{11}-1 pseudo random data signal from a pattern generator, at a bit rate of 2.5 Gbit/s, was then used to modulate the 1552.6 nm pulse train. The resulting 2.5 Gbit/s RZ data signal from the modulator was then coupled together with the other 3 pulse trains with the aid of a 4x2 fibre coupler. The other three pulse train signals were attenuated before the coupler to ensure that the power level in each wavelength signal was the same after the coupler. The composite signal was then amplified before the 1552.6 nm data signal was filtered out using a tunable filter with a bandwidth of 0.7 nm. The received data signal was then detected using a 50 GHz pin photodiode, before a 50 GHz oscilloscope was used to examine the received eye diagrams, and an error analyser was used for BER measurements.

4.5.2 Experimental results and observations

Figure 4-21 displays the optical spectrum of the composite signal after being combined together using the fibre coupler, (with the feedback from the gratings optimized using the polarisation controllers).

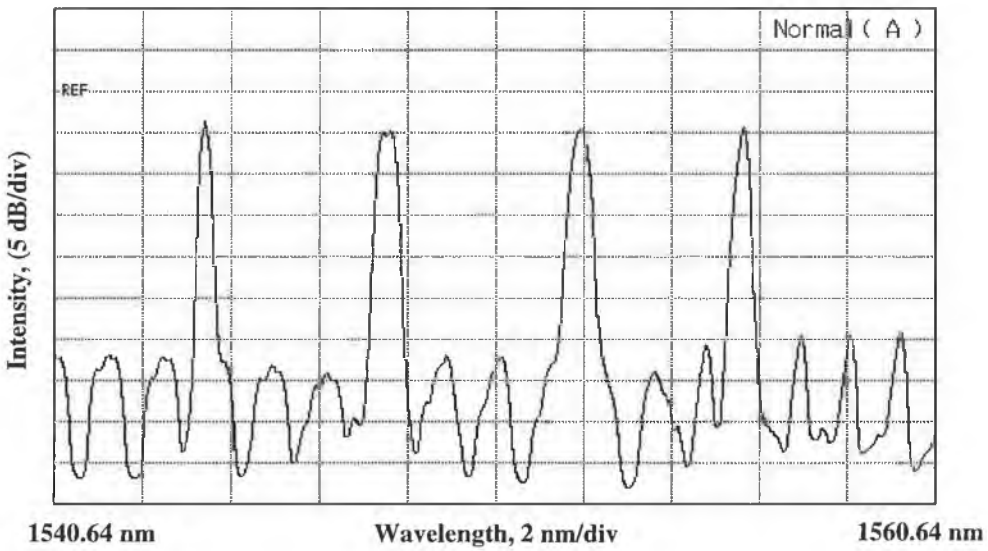

Figure 4-21: Optical spectrum of the composite wavelength signal after fibre coupler

The 3 dB bandwidth of the 2.5 GHz pulse sources varied from 0.2 to 0.3 nm, and the pulsewidth varied from about 18 to 26 ps (measured using oscilloscope and deconvolved

with response time of measurement set-up). The optimized SMSR of each source was about 30 dB.

Figure 4-22 displays back-to-back eye diagram of the 1552.6 nm data signal (when the three adjacent pulse sources were momentarily turned off). To determine the effect of SMSR variations on the four channels WDM system, we proceeded to vary the SMSR of the adjacent pulse sources using the PC's, while the optical filter was tuned to select out the 1552.6 nm data channel (which had maximum SMSR ~ 30 dB maintained throughout). Figure 4-23 displays one of the results, and is the received eye diagram (of 1552.6 nm data channel) when the SMSR of the three pulse sources were set to 20 dB. The increased noise can be clearly seen in the eye diagram that corresponds to the case when the SMSR of adjacent channels is degraded in comparison to the eye when all channels have maximum suppression maintained Figure 4-22.

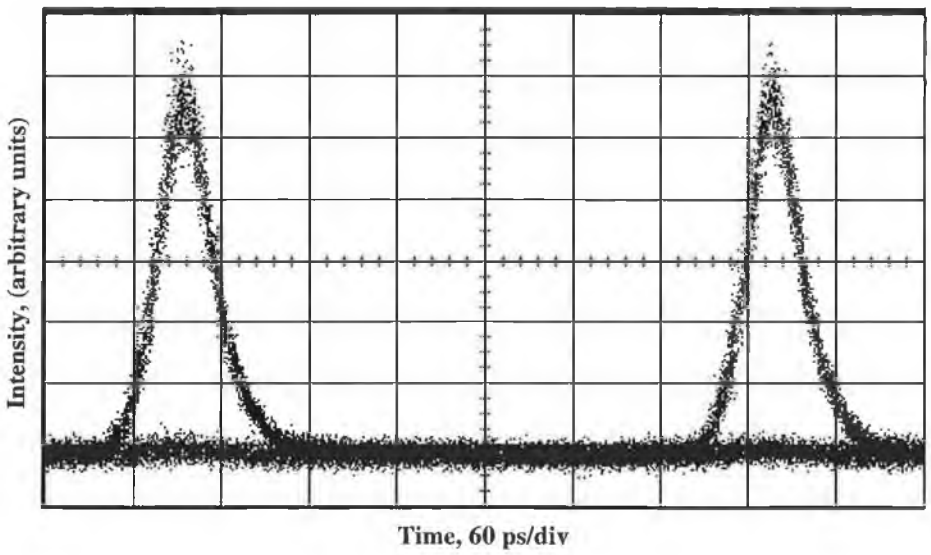

Figure 4-22: Back-to-back eye diagram for 1552.6 nm data channel

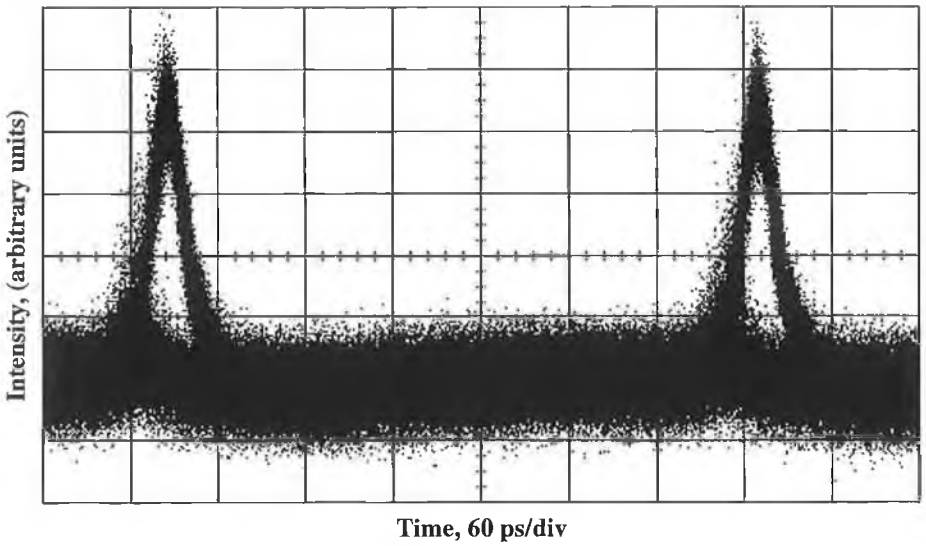

Figure 4-23: Received eye diagram of 1552.6 nm data channel with SMSR of other pulse sources in the WDM signal set to 20 dB

As the SMSR of the three pulse sources were varied in the experimental arrangement, measurements of the BER vs. received optical power, for the 1552.6 nm data channel were recorded. Figure 4-24 displays BER vs. received power curves for the back-to-back case, and when the SMSR of the three pulse sources in the WDM signal, were set to 30, 25, 20, and 15 dB. The power penalty introduced by each of these settings was 0.9, 1.3, 1.6, and 2 dB respectively.

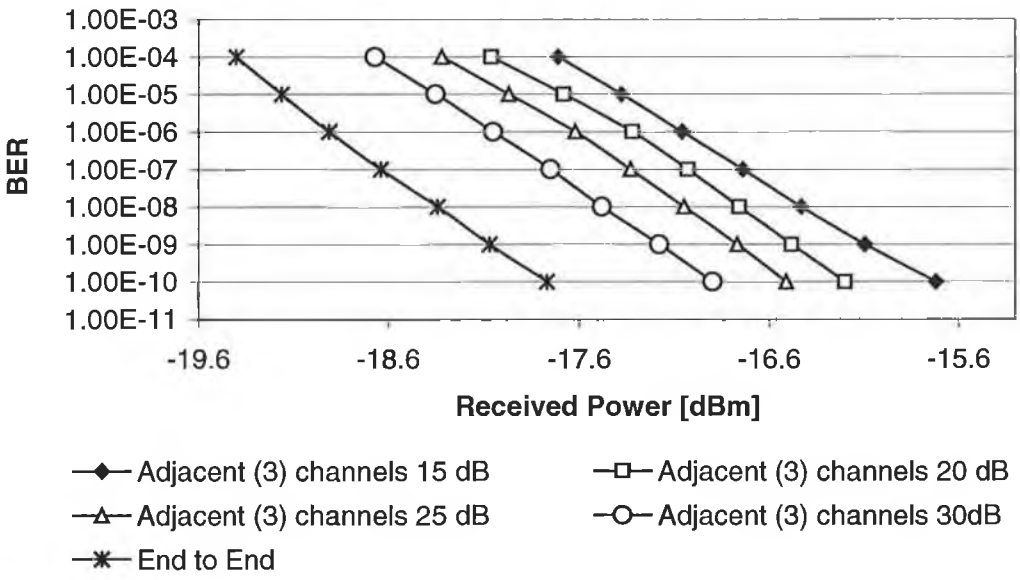

Figure 4-24: BER vs. Received power for back-to-back case, and when the SMSR of adjacent pulse sources were set to 30, 25, 20, and 15 dB

We then examined the effect of multiplexing the 1552.6 nm data channel with each one of the pulse sources individually, with the SMSR of the pulse source maintained at 30 dB. As we can see from Figure 4-25, the power penalty presented due to the introduction of one source, with a SMSR of 30 dB, can vary from 0.3 to 0.7 dB, for a BER of 10^{-9}.

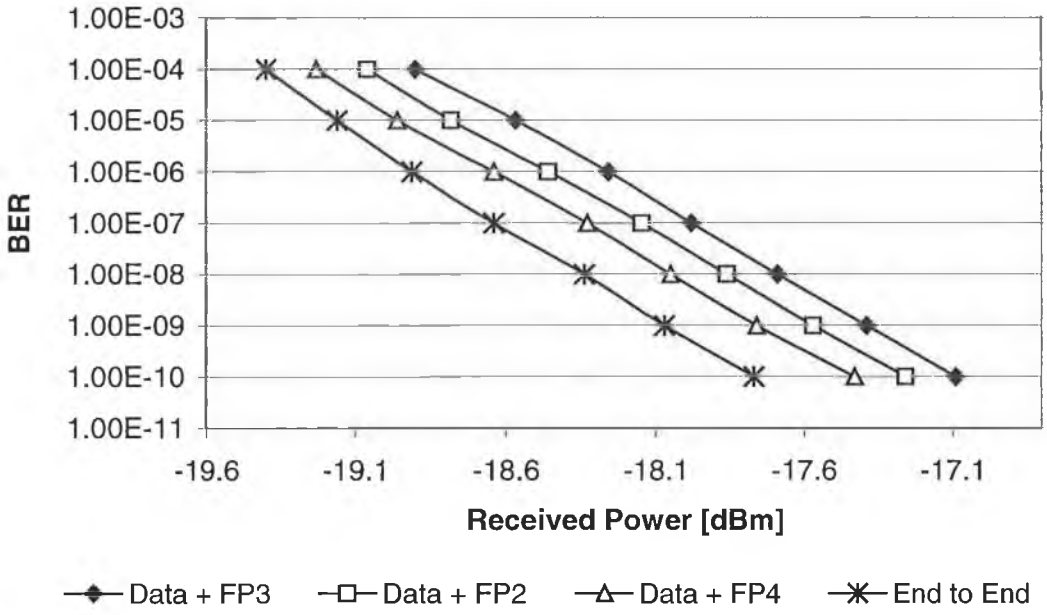

Figure 4-25: BER vs. Received power for back-to-back case, and when data signal was multiplexed individually with each pulse source (SMSR maintained at 30 dB)

The degradation in BER of the 1552.6 nm data signal as we introduce additional wavelength channels, and reduce the SMSR of these pulse sources, is due to the mode partition effect [11], [16]. The cause of this effect has already been discussed in the previous sections. However, the results shown here further validate the fact that as the SMSR decreases, the power fluctuation of the main mode, and the side modes may become non-negligible.

With the optical filter tuned to select out the 1552.6 nm data signal, if the SMSR of the adjacent pulse soures is so large that the fluctuation in power of their side modes (around 1552.6 nm) is negligible, then there will be no power penalty for the received data signal. However, as the SMSR of the adjacent channels is degraded, the system performance decreases, due to the increased fluctuation in power of the side modes (as presented in Figure 4-24). The overall power penalty experienced for the WDM system is due to the

cumulative effect of the power fluctuation in the side-modes, which are at the same wavelength as the filtered data signal. Table 4-1 displays the power penalties introduced (relative to back-to-back measurement) as the 1552.6 nm data channel is multiplexed with the various combinations of the three pulse sources (which have their SMSR maintained at 30 dB).

Data Signal Multiplexed with pulse source	Power Penalty Introduced (dB)
FP2	0.5
FP3	0.7
FP4	0.3
FP2 + FP3	0.8
FP3 + FP4	0.7
FP2 + FP4	0.6
FP2 + FP3 + FP4	1.0

Table 4-1: Power Penalties relative to back-to-back measurement, as 1552.6 nm data channel is multiplexed with all combinations of the three pulse sources (SMSR maintained at 30 dB)

Clearly as the number of channels increases, so does the power penalty, however the increase in power penalty is determined by which of the sources are multiplexed with the data channel. This is because the FP lasers used to generate the pulses have different gain curves. The result of this is that even though the SMSR of all the sources is maintained at 30 dB, the powers in the side mode, which lies at the same wavelength as the data signal (and cause the power penalty), are different for each pulse source. This effect is clearly seen by examining the system performance introduced when the data signal is multiplexed with just one source (Figure 4-25). The degradation in system perfomance in this case is dependent on which pulse source is multiplexed with the data (due to the different gain curves of the lasers) channel. By examining the spectra from the three different pulse sources, we can determine the difference in power levels between the side mode of each source at the wavelength of the data signal (1552.6 nm), and the power level in the data signal. The relative differences are 31.9 dB, 33.6 dB, and 35.3 dB for sources FP3, FP2, and FP4 respectively. We can thus see from these values, and from

Figure 4-25, that as the difference in power level between the data signal and the side mode of the multiplexed source at the data signal wavelength decreases, the power penalty in the system increases, as expected.

The experiments carried out thus far have depicted the effect of SMSR degradation on WDM systems that make use of self-seeded gain switched pulse sources. At this juncture simulations were performed, in order to verify the results obtained and validate the techniques used in all the experiments performed in this area. Three sets of simulations were carried out. The first set involved the verification of the effect of the pulse side mode suppression ratio on SSGS pulse sources used in lightwave communication systems. The next stage entailed modeling a two-channel WDM system using self seeded gain switched optical pulse sources. The effect of cross channel interference on one channel due to the degradation of the pulse SMSR on the other channel was simulated. Finally an eight-channel WDM type system also employing SSGS pulse sources was modelled. Using this model, tests were carried out on how the addition of channels affected system performance that led to new standards of requirements on the minimum pulse SMSR required. Another aspect that was investigated was the cross channel interference on one channel due to the degradation of SMSR of all other channels. The main question to be answered here was whether there was a cumulative cross channel interference effect.

4.6 Photonic Design Automation (PDA) tools

The design of photonic systems has reached a stage in which simulation is no longer a luxury, but a necessity [17]. Until the last decade, optical communications systems were chiefly limited by loss, dispersion, and transmitter and receiver performance [18]. The advent of optical amplifiers[29] and the exponential growth in the number of channels[30] operating with channel spacings that are reduced to a few times the channel bit rate bring about new problems. In order to solve these problems and achieve optimized operation of high-speed optical links, many design variables have to be assessed. This assessment

[29] Enabling high powers and long unregenerated distances have caused significant fiber nonlinearity that necessitated the use of numerical modeling.
[30] DWDM.

could be addressed with the help of automated software design tools [19]. Just as Electronic Design Automation (EDA) tools have become an essential part of the semiconductor and electronics industry, Photonic Design Automation (PDA) tools have brought in huge advances in the optical communications world.

One of such PDA tools (used in our work) is the Virtual Photonics Incorporated (VPI) Transmission Maker. With similar returns in using PDA tools being carried over from the industry to the laboratory environment, their use in the research environment has become quite common. Some of the advantages of using such automated design tools in the laboratory environment are listed below:

1. Reduces the need for initial physical experimentation.
2. Establishes and supports raw research ideas.
3. Stimulates innovation by being able to expand on design ideas and resources.

The VPI software package has an extensive library of photonic modules and sample demonstrations. The description of these photonic modules/components ranges over several levels of abstraction (ranging from detailed physical models to black box and data sheet models). Furthermore it also has a tailored Graphical User Interface (GUI) with drag and drop, easy to use modules. All modules (depending on the level of abstraction) have a set of parameters (variable), which define and control their functionality. Signals in VPI are modelled using sample (supports aperiodic signals) and block modes (supports periodic signals). Sample to block conversions had to be performed while working with multi-section lasers since most of such lasers were supported by sample mode signals.

4.7 Simulations

4.7.1 Effect of SMSR on the usefulness of SSGS pulse sources

4.7.1.1 Simulation model

A schematic of the initial simulation model that was used is shown in Figure 4-26. A bulk FP laser with a nominal wavelength of 1553 nm (at a bias current of 50 mA) and a threshold current of 18 mA[31] was used.

[31] Found by performing a DC characterization (PI curve)

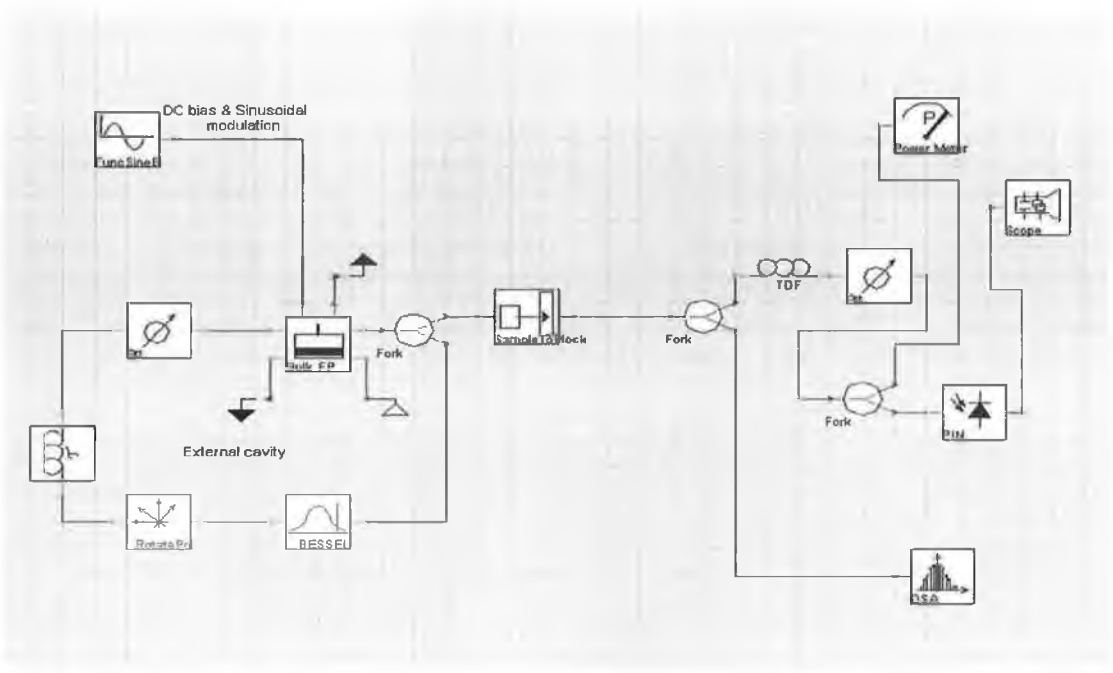

Figure 4-26: Experimental set-up for SSGS pulse generation

Applying a DC bias current of 14 mA and a sinusoidal modulation signal with a power of 12 dBm, enabled us to carry out gain switching of the laser. The sinusoidal modulation frequency was set to 2.5 GHz. Self seeding of the gain switched laser diode was achieved by using an external cavity consisting of a 50:50 coupler, a Bessel transmission filter, a polarization controller, an optical delay line and an optical attenuator. The best possible SSGS operation was achieved by using the filter to select one of the longitudinal modes and then to re-inject this selected mode into the gain switched laser. A sweep of the delay was performed in order to find an optimum delay to ensure that the signal fed back in to the laser arrives as a pulse is being built up[32]. Once optimum SSGS operation was achieved, the resulting SSGS output pulses were split in two. Part of the signal was received using a pin photodiode after which temporal characterization of the output pulses was done with the aid of an oscilloscope. The other arm of the splitter was passed into an optical spectrum analyser, which was used to analyse the associated pulse spectra.

[32] Within the sensitive time window.

4.7.1.2 Simulation results

With the feedback optimized into the FP laser, to achieve single mode operation, the resulting output pulses are shown in Figure 4-27.

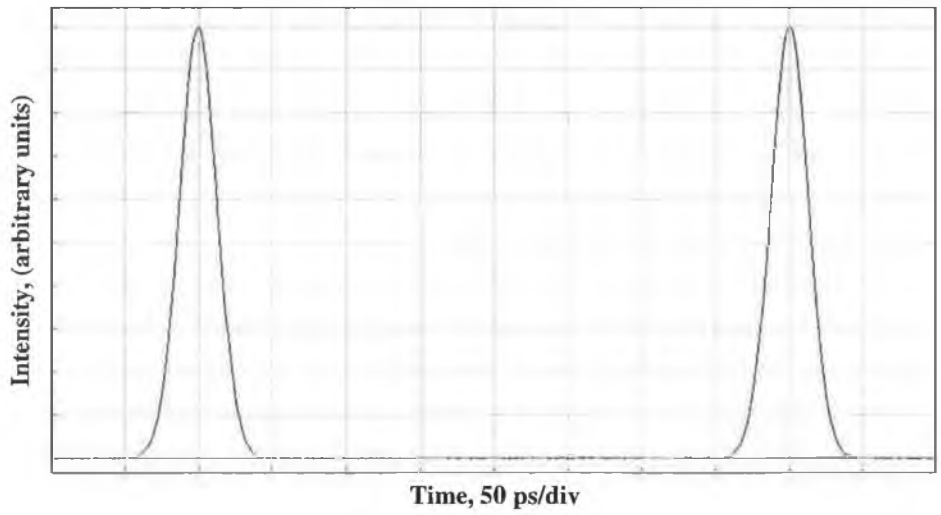

Figure 4-27: Self-seeded gain switched optical pulses

The pulse duration was found to be about 30 ps. The associated pulse spectrum is shown in Figure 4-28. By observing the spectrum we can see that the selected mode is about 60 GHz away from the reference frequency of 193.1 THz (1553.6 nm). Hence the chosen wavelength was calculated to be around 1553.1 nm. The achieved SMSR of the signal was noted to be about 32 dB. It could also be seen from the same figure that the longitudinal mode spacing was about 160 GHz (1.3 nm).

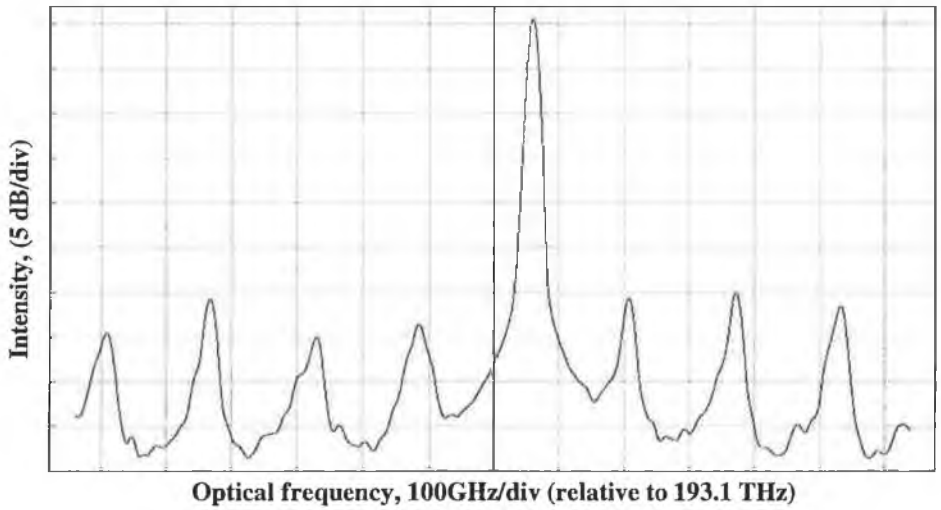

Figure 4-28: Optical spectrum of SSGS pulses (with SMSR of 32 dB)

The generated SSGS optical pulses were then propagated through a length (10 km) of Dispersion Shifted Fibre (DSF), which exhibited a dispersion parameter of 2 ps/km.nm at a wavelength of 1553 nm. In order to degrade the SMSR, the re-injected power was reduced by using an attenuator. With SMSR set to its maximum, there was no noticeable effect on the pulses apart from slight broadening[33]. However as the SMSR was degraded, by attenuating the re-injected signal, the level of noise started to increase. The resulting pulses with the SMSR degraded to 25, 20, 15 and 10 dB are shown in Figure 4-29 (a, c, e & g). Also shown in Figure 4-29 (b, d, f & h) are the spectra associated to these pulses.

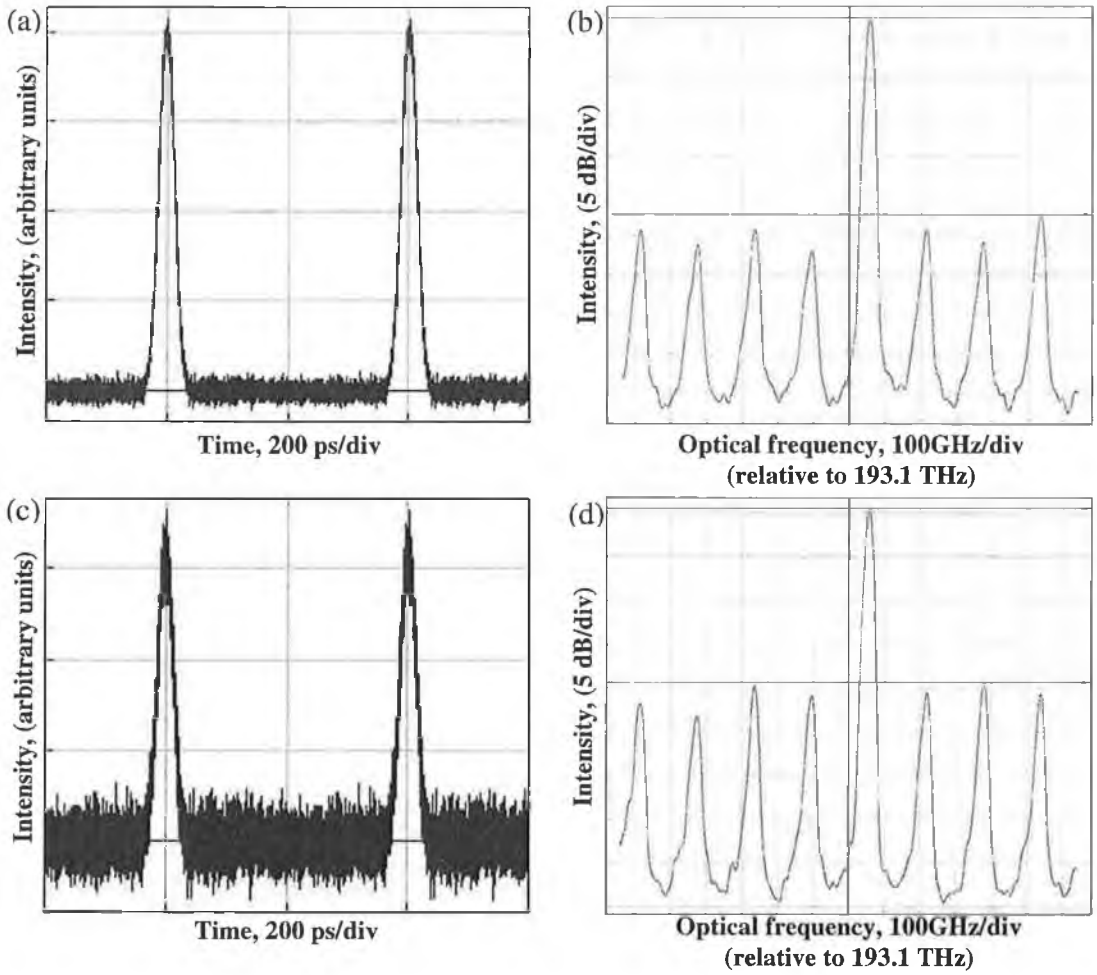

[33] Due to dispersion (D = 2 ps/km.nm)

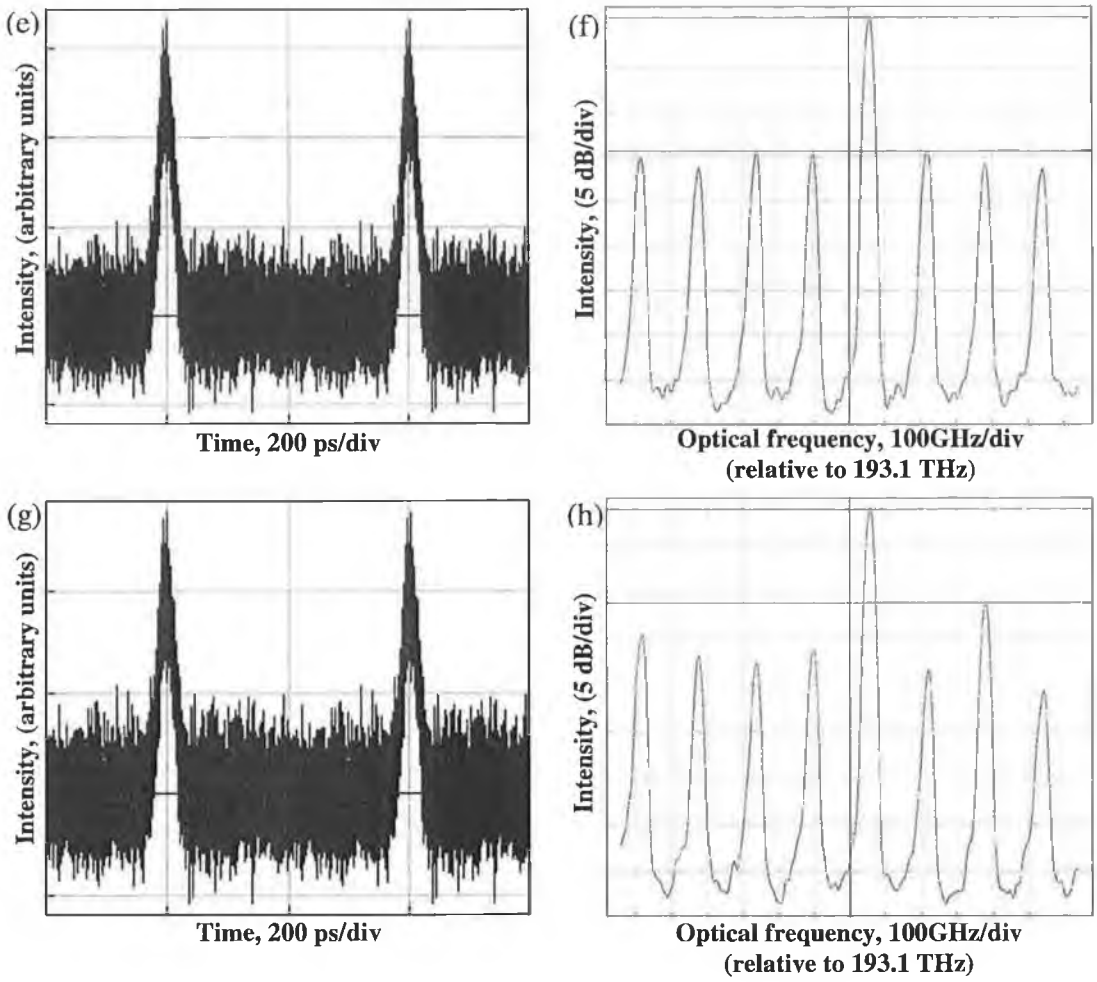

Figure 4-29: Output optical pulses after propagation through 10 km of DSF with the input SMSR of the pulses set to (a) 25 dB, (c) 20 dB, (e) 15 dB, and (g) 10 dB. Spectra corresponding to these pulses with SMSR set to (b) 25 dB (d) 20 dB (f) 15 dB and (h) 10 dB

We can clearly see the introduction of noise, on the pulses as the initial SMSR degradation takes place from 32 down through 25 and then to 20 dB. The noise, on and between the pulses is much more exaggerated when the SMSR is brought down to 15 and 10 dB. Furthermore on comparing with the experimental part, we can clearly see the similarity, not only in the introduction of noise as the SMSR is degraded slightly, but also in the increase in the level of noise as the SMSR of the pulse sources are degraded even further. As already established in the experimental section, the noise introduced as the SMSR is degraded is due to the mode partition effect of the FP laser.

In order to characterize this noise, we then went on to modulate data onto the pulse source. By doing so we were able to measure the BER to give us an insight into the performance of the system. The model shown in Figure 4-26 was modified slightly by incorporating a data source (PRBS generator and a NRZ coder) and an external (MZM) modulator and is shown in Figure 4-30.

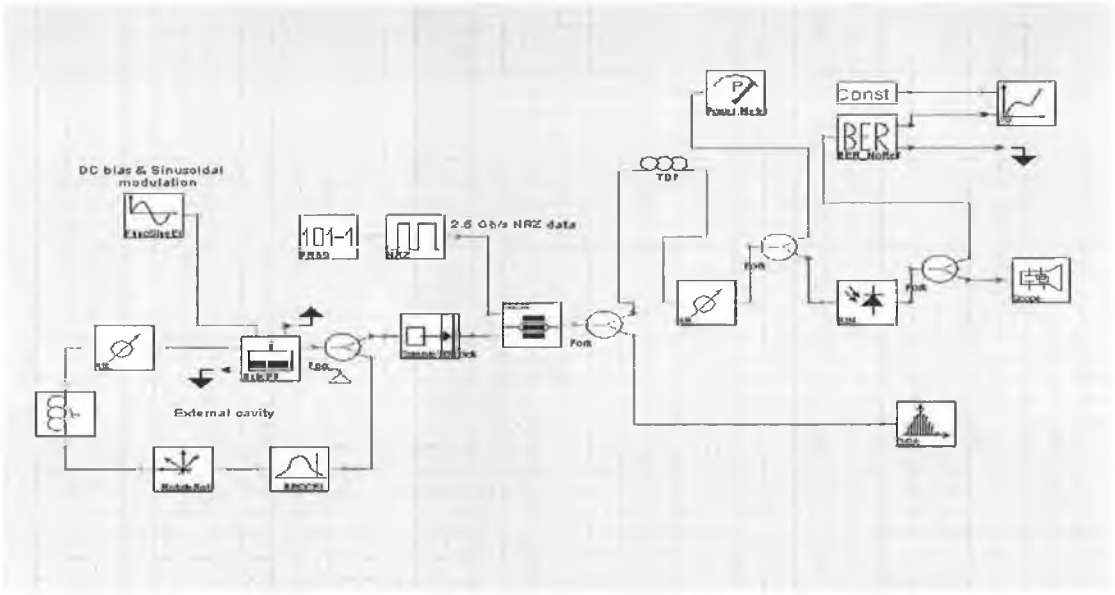

Figure 4-30: experimental set-up

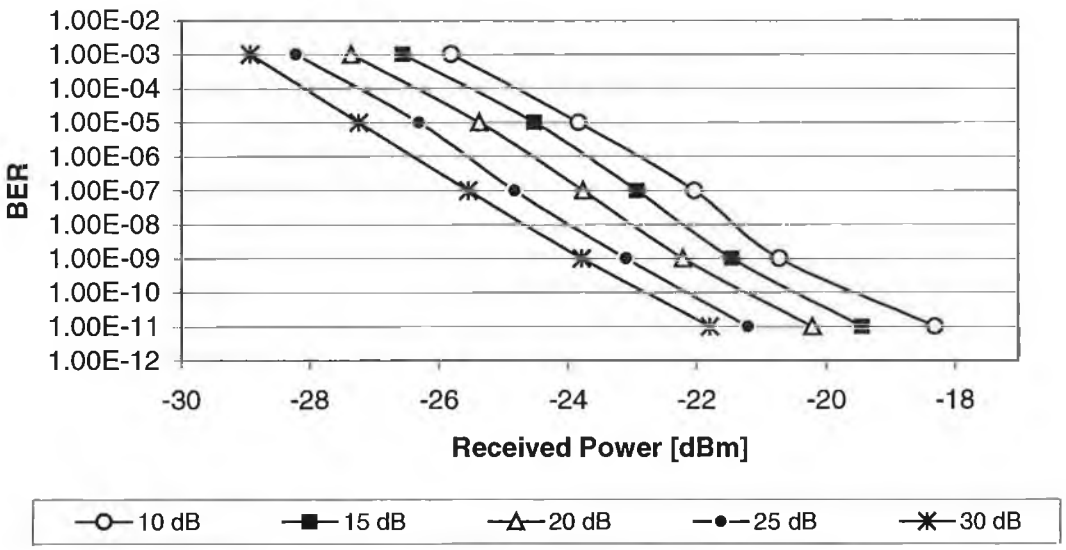

Figure 4-31: BER vs received power when the SMSR of pulse source is set to 30, 25, 20, 15 & 10 dB

The SSGS pulses were generated in the same manner as described in the previous set-up. A 2^7-1 pseudo random data signal at bit rate of 2.5 Gb/s was initially passed through an NRZ coder, and then used to modulate the generated pulse train. The data signal was then passed through 10 km of DSF with a dispersion parameter of 2 ps/km.nm at 1553 nm. The pulse SMSR was again varied from 30 dB down to 10 dB. The BER was measured as a function of the received optical power. This result is shown in the form of a plot in Figure 4-31. It can be clearly seen that as the SMSR is degraded, the BER gets worse (when the received powers are kept constant). Hence we can say that, trying to achieve an acceptable BER of 10^{-9} for the various levels of pulse SMSR, results in a power penalty. The power penalties, relative to the case where the SMSR is set to 30 dB, are tabulated and shown in Table 4-2

SMSR (dB)	Penalty (dB)
25	0.68
20	1.57
15	2.33
10	3.06

Table 4-2: Power penalties (to achieve BER 10^{-9}) due to SMSR degradation

The penalties involved here go on further to show that the degradation in the SMSR of SSGS pulse sources, bring about an enhancement of energy in the side modes and increases the fluctuations of energy in the main mode. This results in the increased amplitude noise seen on the optical pulses.

4.7.2 Cross channel interference effects in WDM systems employing SSGS optical pulse sources

4.7.2.1 Simulation model

Figure 4-32 illustrates a schematic of the simulation model used. The same bulk FP laser was used as in the previous model with identical physical characteristics.

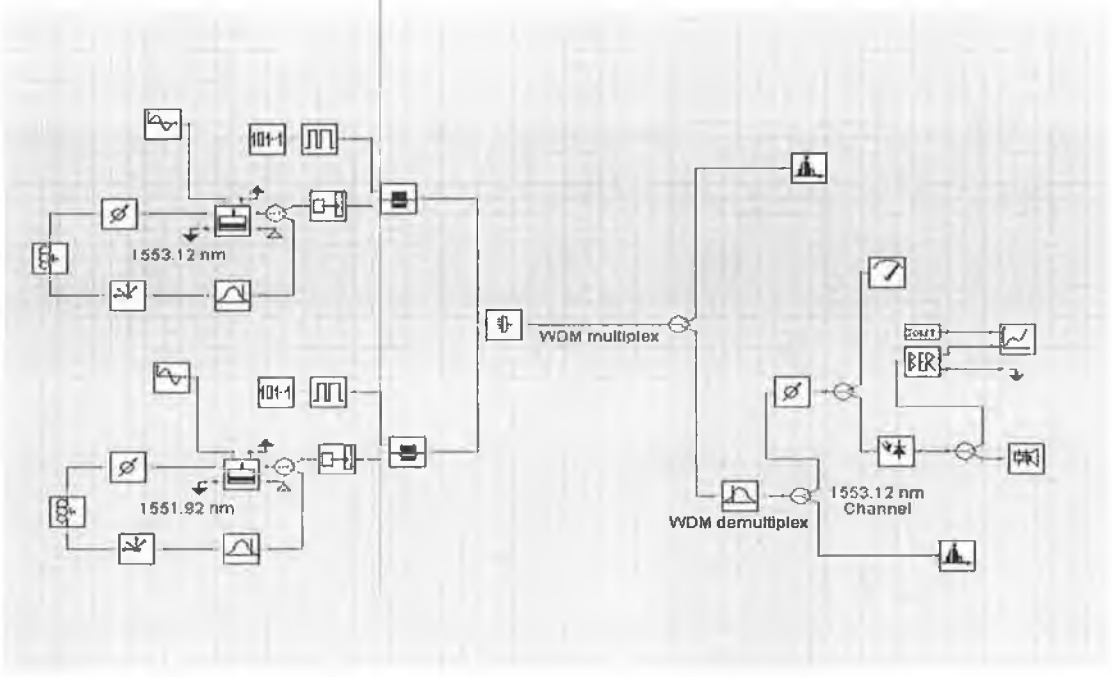

Figure 4-32: Experimental set-up used for the assessment of cross channel interference in a two-channel WDM system using SSGS pulse sources

Gain switching of the two lasers was achieved in the exact same manner as in the previous simulation model. The sinusoidal modulation frequency was also set to 2.5 GHz. Self-seeding of both lasers was achieved by having both external cavities consisting of a 3 dB coupler, a transmission filter, a polarization controller, an optical delay line and an optical attenuator.

SSGS operation of the lasers was optimized in order to achieve single moded operation at 1553.12 nm and 1551.92 nm. The SMSR of the sources at 1553.12 nm and 1551.92 nm were 30 dB and 32 dB respectively. A PRBS of length 2^7-1 at a bit rate of 2.5 Gb/s was then used to modulate both pulse trains with the aid of an external modulator. Figure 4-33 displays the optical spectrum of the two data channels, after being combined together using a coupler.

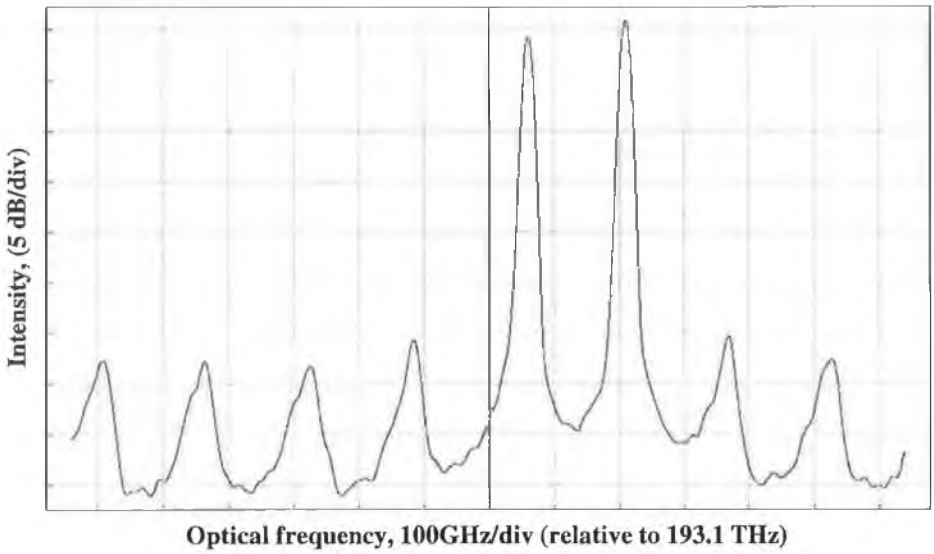

Figure 4-33: Optical spectrum (combined signal) of the two 2.5 Gb/s data channels

The 1553.12 nm channel was then filtered out before being received by a p-i-n photo detector. The received channel was then scrutinized with the aid of a scope and BER analyser. The received eye, with maximum suppression maintained on both channels, is shown in Figure 4-34.

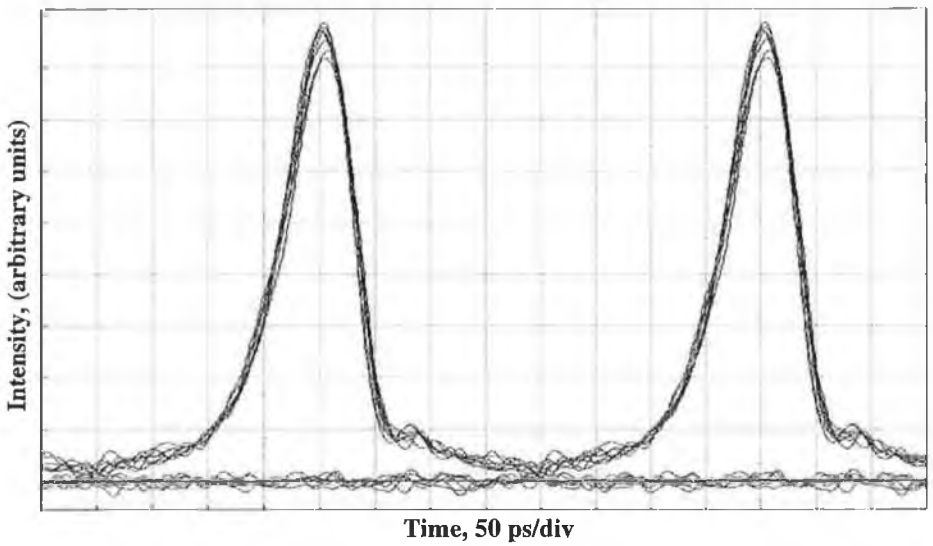

Figure 4-34: Received eye diagram of 1553.12 nm channel with both pulse sources having their SMSR set at maximum values

In order to verify the effect of the degrading SMSR of one channel on the second channel, we varied the SMSR of the 1551.92 nm channel in discrete steps, and examined the worsening eye (BER) of the filtered channel at 1553.12 nm (which had its SMSR

maintained at 30 dB). The received eye diagrams of the filtered channel, as the SMSR of the adjacent channel was degraded is shown in Figure 4-35.

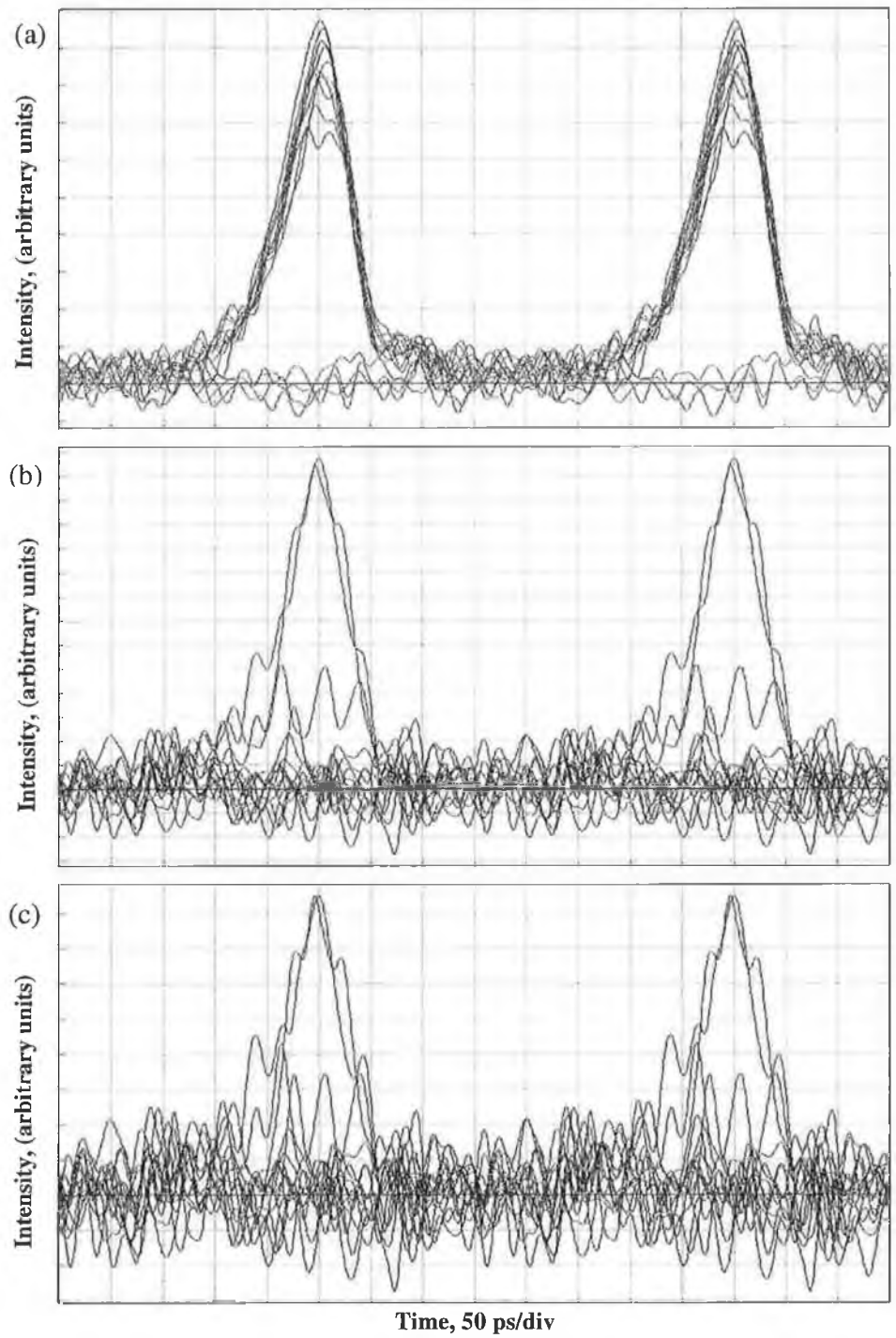

Figure 4-35: Received eye diagrams for the 1553.12 nm data channel with varying SMSR of the 1551.92 nm channel (a) eye at 25 dB, (b) eye at 17 dB, (c) eye at 10 dB

The effect (addition of noise) on the received channel, due to a reduction in SMSR of the adjacent channel, can be seen clearly from Figure 4-35. To further characterize this effect, we went on to measure the BER on the received channel as the SMSR was degraded. Once again we varied the SMSR of the 1551.92 channel, but this time from 30 dB down through 25 dB, 20 dB, 15 dB and 10 dB while the SMSR on the filtered 1553.12 nm channel was kept constant (30 dB). The BER on filtered channel was then measured as function of the received power (as the SMSR of the adjacent channel was varied). The results obtained are shown in the form of power penalty plot in Figure 4-36.

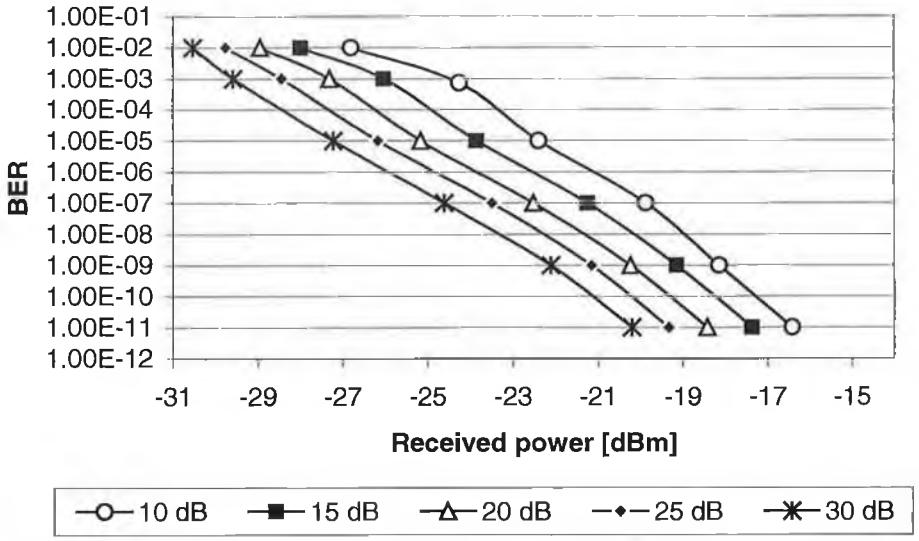

Figure 4-36: BER vs received power when the SMSR of adjacent pulse source is set to 30, 25, 20, 15 & 10 dB

The penalties in power (relative to the case where both channels have SMSR set to 30 dB), due to cross channel interference introduced by the degradation of SMSR in the adjacent channel, are tabulated in Table 4-3.

SMSR (dB)	Penalty (dB)
25	0.95
20	1.87
15	2.96
10	3.96

Table 4-3: Power penalties (to achieve BER 10^{-9}) due to cross channel interference

This tends to establish the fact that, as the SMSR of one channel is degraded in a two channel WDM type system, the noise added on to the received channel increases, thereby degrading the BER. The degradation of the BER results in an incurred power penalty. This dire effect (cross channel interference) is due to the mode partition effect, which has already been discussed in detail in the experimental part. The increasing noise within the eye diagrams and the worsening trend of the BER, as the SMSR of the adjacent channel is degraded, validates the results obtained in the experimental part of this chapter.

4.7.3 Cross channel interference effects in an eight-channel WDM systems employing SSGS optical pulse sources

Experimentally, we were limited to a four channels, in trying to provide a quantitative analysis of how MPN degrades the performance of a WDM system employing SSGS pulse sources. Hence we decided to simulate an eight-channel WDM system to verify if the results achieved would show the same trend (degradation of system performance as the SMSR was reduced).

4.7.3.1 Simulation model

The set-up used in modeling an eight-channel WDM system is shown in Figure 4-37.

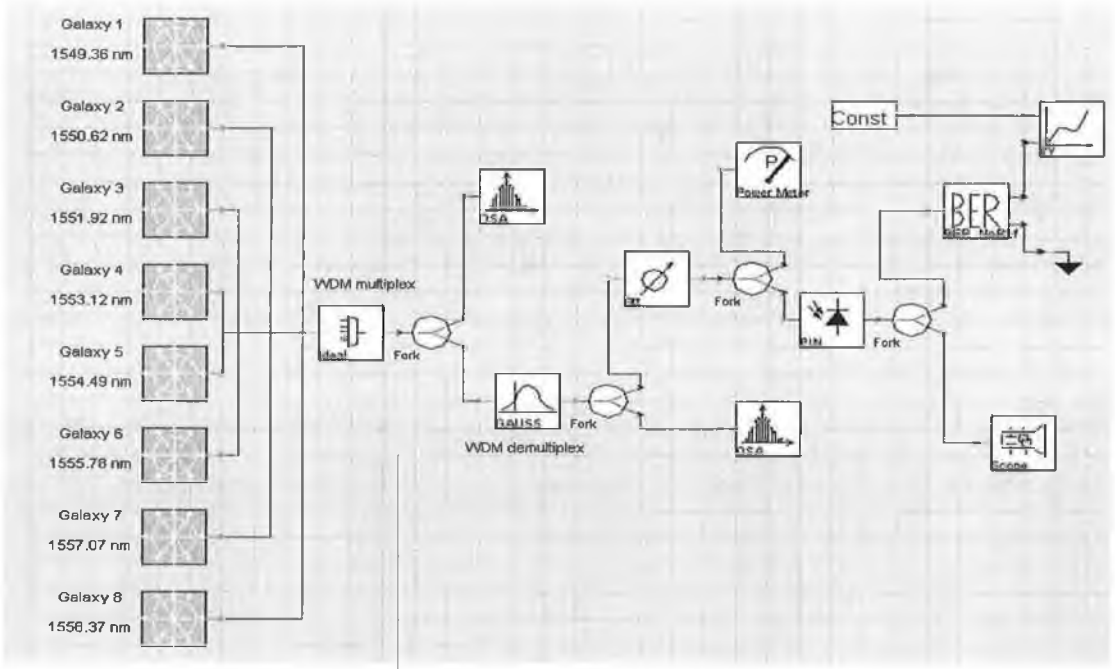

Figure 4-37: Experimental set-up

The eight different transmitters are modelled using individual galaxies[34]. An expansion of a single galaxy is shown below. As mentioned earlier, the main reason for carrying out this test was to determine whether the mode partition effect had a cumulative effect as the number of channels in a WDM system was increased.

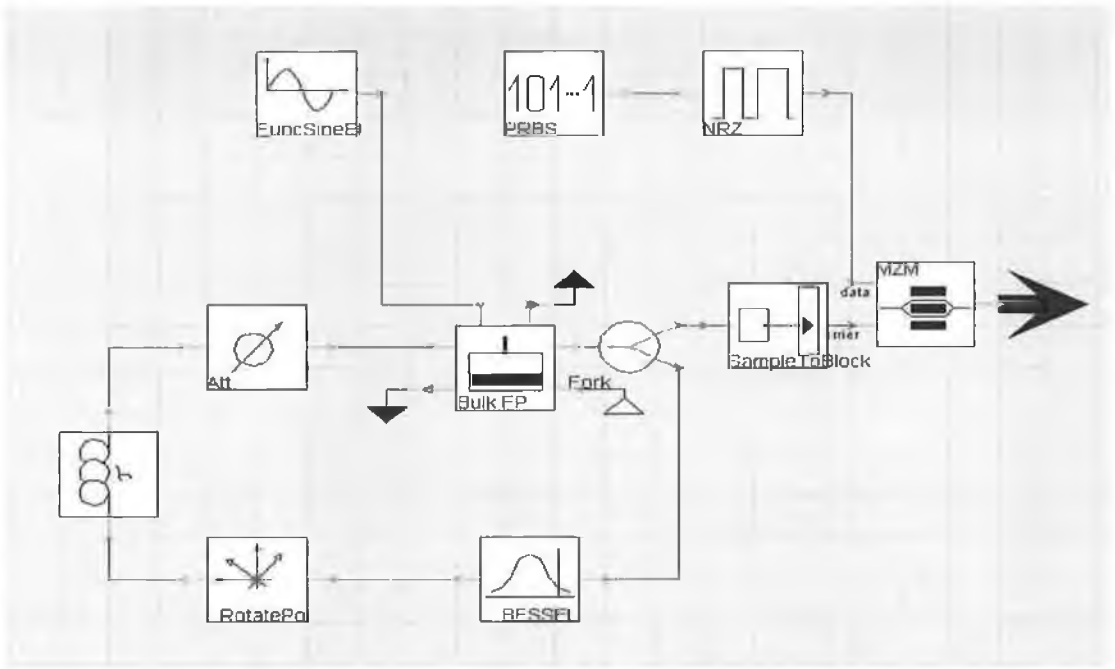

Figure 4-38: Make up components of a transmitter galaxy

As can be seen from Figure 4-38, the galaxy basically consists of a SSGS pulse source onto which a pseudo random NRZ data signal at 2.5 Gb/s is modulated. The gain switching was again carried out in the same manner as described in the single channel simulation.

Self-seeding gain switched operation of the eight lasers was optimized in such a way as to achieve single moded operation at 1549.36, 1550.62, 1551.92, 1553.12, 1554.49, 1555.78, 1557.07, 1558.37 nm. The SMSR of all the sources was at least 30 dB. All eight-pulse sources were externally modulated with a 2.5 Gb/s NRZ pseudo random bit sequence after which they combined together using a WDM multiplexer. The composite spectrum of the eight data channels is shown in Figure 4-39.

[34] Galaxies consist of a network of various interconnected modules.

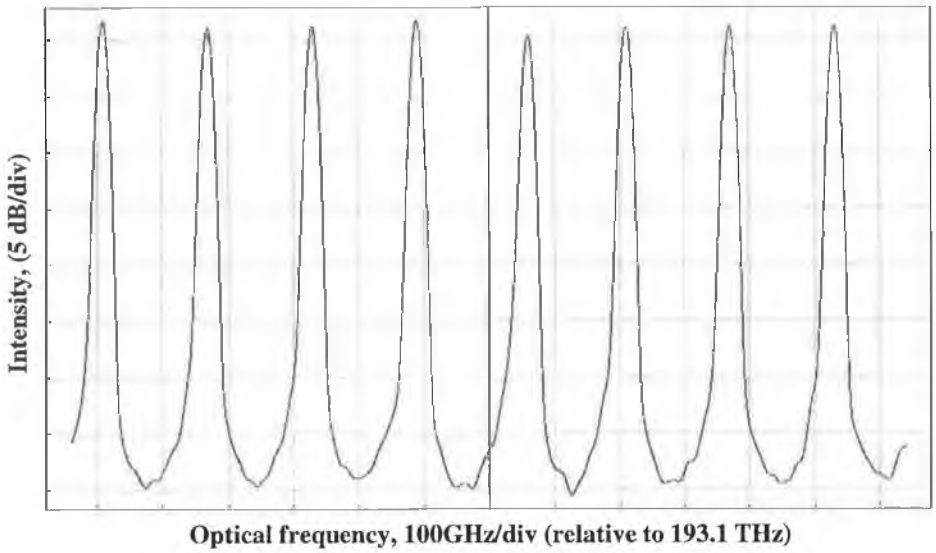

Figure 4-39: Optical spectrum of the eight 2.5 Gb/s data channels

Filtration of the 1553.12 nm channel from the composite signal was carried with the aid of a Gaussian band pass filter. The received signal was then inspected using a scope and a BER analyser. With maximum suppression maintained on all the channels, the received eye looked wide and clean and is shown in Figure 4-40.

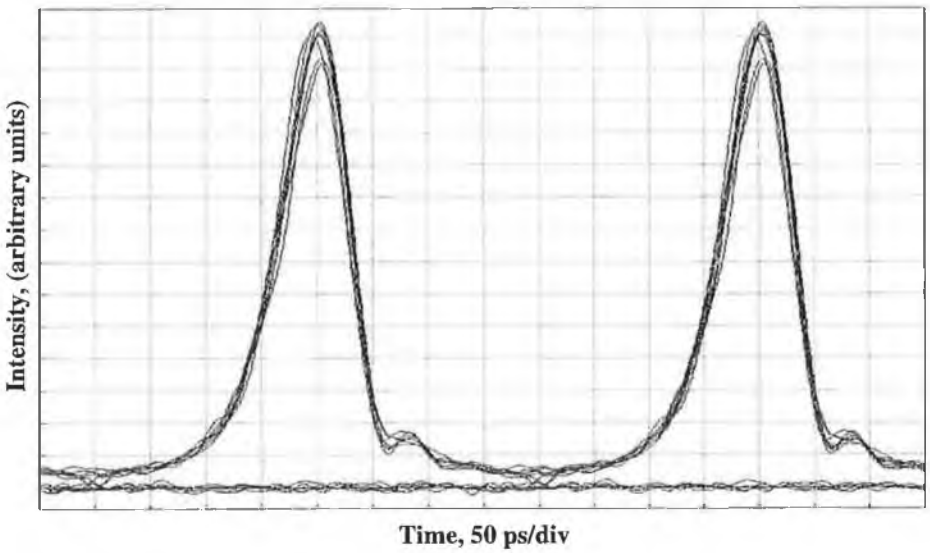

Figure 4-40: Received eye diagram of 1553.12 nm channel with all eight pulse sources having their SMSR set at 30 dB

The seven channels, apart from the channel filtered out (1553.12 nm which had its SMSR maintained at 30 dB) had their SMSR varied in steps of 5 dB from 30 down to 10 dB. During this process of SMSR degradation, the BER of the filtered channel was

monitored. Shown below is a plot (power penalty) of these results. Shown in the same figure is the back-to-back case where all the adjacent (7) channels were turned off.

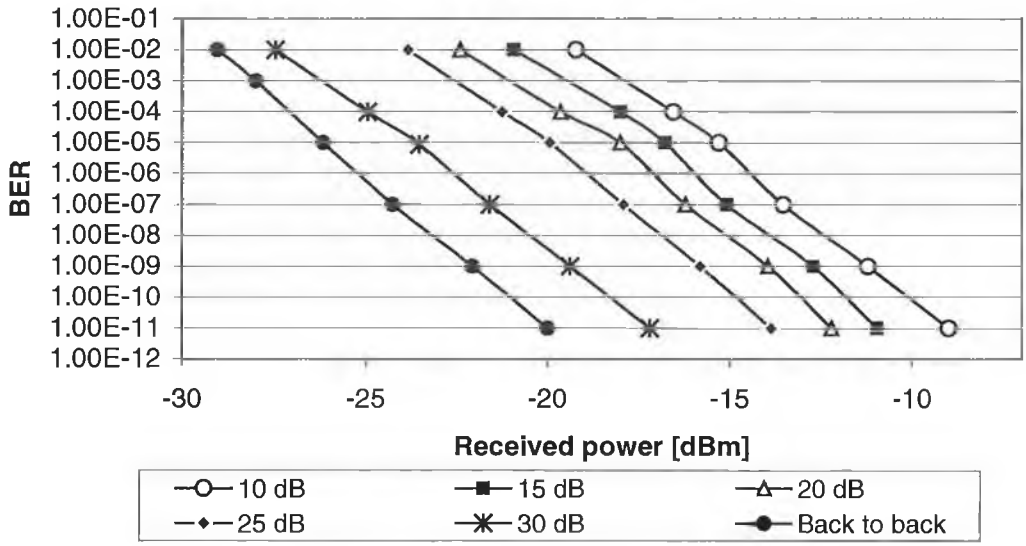

Figure 4-41: BER vs received power of the back-to-back case and when the SMSR of 7 adjacent pulse sources are set to 30, 25, 20, 15 & 10 dB

The penalties in power acquired in trying to achieve an acceptable BER of 10^{-9} relative to the back-to-back case, is summarized and shown in Table 4-4.

SMSR (dB)	Penalty (dB)
30	2.67
25	6.23
20	6.67
15	8.09
10	10.85

Table 4-4: Power penalties (to achieve BER 10^{-9}) relative to the back-to-back case, due to cross channel interference in an eight-channel WDM system

The penalties due to SMSR degradation of adjacent channels, which are incurred in the eight-channel system (Table 4-4) are much higher than that sustained in the two-channel system (Table 4-3). In the two-channel system, when the SMSR of the adjacent channel is degraded, the only one side mode that contributes to the addition of noise on the

filtered channel is that of the adjacent channel. However in the eight-channel system, when the SMSR of seven adjacent channels are degraded, the fluctuation of all these channels would affect the filtered channel. Hence we could go on to say that, due to the cumulative effect of the fluctuations in all the side modes of the adjacent channels (seven) that are at the same wavelength as that of the channel filtered out, the noise added would be much larger.

On the whole, the results from the three sets of simulations carried out follow same trend as the results obtained in the experimental part. There was only one effect that couldn't be verified, which was exhibited in the experimental results. This was the system performance dependency on the particular pulse source multiplexed. As mentioned before this dependency arose from the different gain curves exhibited by the different lasers. The distribution of power in the spectral modes, in the laser model used in the simulation, did not exhibit a perfect gain curve. Hence it was not possible to get a reasonable result.

4.8 Conclusion

In conclusion we have shown[35] how the SMSR of wavelength tunable SSGS pulse sources affects the performance of WDM communication systems, which employ such sources. As the SMSR of one or more sources in a WDM system becomes degraded, then the interaction of the mode partition effect with spectral filtering will result in increased noise on all the received wavelength channels in the system. This additional noise introduces a power penalty into the overall system performance. In addition, as the number of channels in a WDM system using SSGS sources increases, the minimum required SMSR of each source, such that it does not affect system performance, would increase. Simulations carried out helped verify all the experimental configurations and results. As mentioned in the simulation section, most of the simulation results were in good agreement with the experimental results.

[35] Using experiments and simulations.

This chapter has shown the performance of SSGS pulse sources in WDM type systems as one of its key physical characteristics is varied. Experiments and simulations carried out, give an insight into the corrective and stringent measures that need to be taken to avoid the fore-mentioned ill effects. Having established a clean source of pulses, the next step to be focused on involved their application in a hybrid system, and verifying system performance form a higher (systems) perspective. This aspect is scrutinized in the following chapter. It proved impossible to carry out experiments on hybrid WDM/OTDM systems based on the resources available and rigorous measures that needed to be effected within our laboratory. Hence simulations with the aid of the Virtual Photonics Incorporated (VPI) software were carried out.

References

[1] T. Morioka, H. Takara, S. Kawanishi, O. Kamatani, K. Takiguchi, K. Uchiyama, M. Saruwatari, H. Takahashi, M.Yamada, T. Kanamori, and H. Ono, "1Tbit/s (100Gbit/s times 10 channel) OTDM/WDM Transmission Using a Single Supercontinuum WDM Source," *Electron. Lett.*, vol. 32, pp. 906-907, 1996.

[2] M. Cavelier, N. Stelmakh, J.M. Xie, L. Chusseau, J.M. Lourtioz, C. Kasmierski and N. Bouadama, "Picosecond (<2.5 ps) Wavelength Tunable (~ 20 nm) Semiconductor Laser Pulses with Repetition Rates up to 12 GHz," *Electron. Lett.*, vol. 28, pp. 224-226, 1992.

[3] L.P. Barry, R.F. O' Dowd, J. Debeau, and R. Boittin, "Tunable Transform Limited Pulse Generation Using Self-Injection Locking of a FP Laser," *IEEE Photonics Technol. Lett.*, vol. 5, pp. 1132-1134, 1993.

[4] D. Huhse, M. Schell, W. Utz, J. Kassner, and D. Bimberg, "Dynamics of Single-Mode Formation in Self-Seeded Fabry-Perot Laser Diodes," *IEEE Photonics Technol. Lett.*, vol. 7, pp. 351-353, 1995.

[5] J. W. Chen and D. N. Wang, "Self Seeded, Gain Switched Optical Short Pulse Generation With High Side Mode Suppression Ratio and Extended Wavelength Tuning Range," *Electron. Lett.*, vol. 39, pp. 679-681, 2003.

[6] M. Schell, W. Utz, D. Huhse, J. Kassner, and D. Bimberg, "Low Jitter Single Mode Pulse Generation by a Self-Seeded, Gain-Switched Fabry-Perot Semiconductor Laser," *Appl. Phys. Lett.*, vol. 65, pp. 3045-3047, 1994.

[7] C. Shu and S.P Yam, "Effective Generation of Tunable Single- and Multiwavelength optical pulses from a Fabry Perot laser diode," *IEEE Photonics Technol. Lett.*, vol. 9, pp. 1214-1216, 1997.

[8] G. Morthier and P. Vankwikelberge, "*Handbook of Distributed Feedback Laser Diodes*," Artech house, 1997.

[9] L. P. Barry, B. C. Thomsen, J. M. Dudley, and J. D. Harvey, "Characterization of 1.55 μm Pulses from a Self-Seeded Gain-Switched Fabry-Perot Laser Diode Using Frequency-Resolved Optical Gating," *IEEE Photonics Technol. Lett.*, vol.10, pp. 935-937, 1998.

[10] S. Bouchoule, N. Stelmakh, M. Cavelier, and J.-M. Lourtioz, "Highly Attenuating External Cavity for Picosecond-Tunable Pulse Generation from Gain/Q-Switched Laser Diodes," *IEEE J. Quantum Electron.*, vol. 29, pp. 1693-1700, 1993.

[11] N. H. Jensen, H. Olesen, and K. E. Stubkjaer, "Partition Noise in Semiconductor Lasers under CW and Pulsed Operation," *IEEE J. Quantum Electron.*, vol. QE-23, pp. 71-79, 1987.

[12] A. Valle, C. R. Mirasso and L. Pesquera, "Mode Partition Noise of Nearly Single Mode Semiconductor Lasers Modulated at GHz Rates," *IEEE J. Quantum Electron.*, vol. 31, pp. 876-885, 1995.

[13] M. M. Choy, P. L. Liu and S. Sasaki, "Origin of Modulation Induced Mode Partition and Gb/s System Performance of Highly Single Mode 1.5 μm Distributed Feedback Lasers," *Appl. Phys. Lett.*, vol. 52, pp. 1762-1764, 1988.

[14] S. E. Miller, "On the Injection Laser Contribution to Mode Partition Noise in Fibre Telecommunication Systems, "*IEEE J. Quantum Electron.*, vol. 25, pp. 1771-1781, 1989.

[15] M. Nakazawa, K. Suzuki and Y. Kimura, "Transform Limited Pulse Generation in the Giga-Hertz Region From a Gain Switched Distributed Feedback Laser Diode Using Spectral Windowing, " *Opt. Lett.*, Vol. 15, pp. 715–717, 1990.

[16] D. Curter, P. Pepeljugoski, and K.Y. Lau, "Noise Properties of Electrically Gain-Switched 1.5 μm DFB Lasers After Spectral Filtering", *Electron. Lett.*, vol. 30, pp. 1418-1419, 1994.

[17] A. Lowery, O. Lenzmann, I. Koltchanov, R. Moosburger, R. Freund, A. Richter, S. Georgi, D. Breuer and H. Hamster, " Multiple Signal Representation Simulation of Photonic Devices, Systems and Networks," *IEEE J. Sel. Topics Quan. Electron.*, vol. 6, pp. 282-296, 2000.

[18] A. E. Willner, "Mining the Optical Bandwidth for a Terabit per Second," *IEEE Spectrum*, vol. 32, pp. 32-41, 1997.

[19] A. J. Lowery, "Computer-Aided Photonics Design," *IEEE Spectrum*, vol. 34, pp. 26-31, 1997.

Chapter 5 - Modeling of High-Speed Optical Networks

5.1 Introduction

The major aim of carrying out modeling here was to design a high-speed hybrid WDM/OTDM optical communication system with optimized system parameters (pulsewidth and channel spacing). In the process of constructing such a system we initially went through intermediary stages of building an OTDM and a WDM system. By doing so we were then able to choose the parameters and functionalities of the modules in such a way as to suit the building of the hybrid system (which basically consists of an OTDM and a WDM system). The results of the WDM model have been omitted[36], while the results obtained with the OTDM model are shown in the following section. The fore-mentioned system parameters of the initial hybrid model built were chosen so as to ensure that maximum performance was achieved at a cost of spectral efficiency. On building this initial hybrid model and exhibiting the results obtained, we then moved on to the next point of focus, which involved the verification of the various effects that spectral spacing and width of the pulse source would have on system performance. System performance was characterized by performing BER measurements over a wide range of the parameters mentioned above. The power penalties obtained in the characterization demonstrated the optimum values for these system parameters. Using these optimum parameter values one could obtain efficiency (spectral and temporal) as well as favourable performance as shown in the forthcoming section.

5.2 Simulation model of an OTDM communication system

5.2.1 OTDM systems

One of the strategies available for increasing the bit rate of digital optical fibre systems beyond the bandwidth capabilities of the drive electronics is known as Optical Time Division Multiplexing (OTDM)[37]. The development of very short optical pulse technology has allowed the possibility of realizing such high-speed networks. As previously mentioned, the underlying principle of this technique is to extend the well-

[36] Since WDM technology is well established.
[37] Discussed in detail in chapter 2.

known Electrical Time Division Multiplexing (ETDM) by optically combining a number of lower speed electronic baseband digital channels [1]. Obviously the data channels in this scheme are multiplexed together in the temporal domain. A basic description of the process involved in multiplexing is given below.

A laser source produces a regular stream of very narrow Return-to-Zero (RZ) optical pulses at a repetition rate B. This rate typically ranges from 2.5 to 10 Gb/s, which corresponds to the bit rate of the electronic data tributaries feeding the system. An optical splitter divides the pulse train into N separate streams. Each of these channels is then individually modulated by the electrical NRZ data to be transmitted also at a bit rate B. The modulated outputs are delayed individually by different fractions of the clock period, and are then interleaved through an optical combiner to produce an aggregate bit rate of NxB.

5.2.1.1 OTDM model

Initially a 10 Gb/s OTDM system model was created. The model consisted of 4 channels, each at a base rate of 2.5 Gb/s, optically multiplexed together to construct a 10 Gb/s aggregate rate. For the sake of simplicity and clarity, an end-to-end system was modelled. The modeling was carried out in two stages. Firstly the multiplexing part of the OTDM system was done after which we moved on to concentrate on the demultiplexing section.

A schematic of the four-channel OTDM optical communication model is shown in Figure 5-1. By connecting a Gaussian pulse module to a constant input, a Gaussian pulse train could be generated. The generated pulses had a FWHM of 20 ps and a repetition frequency of 2.5 GHz[38]. The relative emission frequency was set at 193.1 THz, which corresponds to a wavelength of 1553.6 nm.

[38] Period of 400 ps.

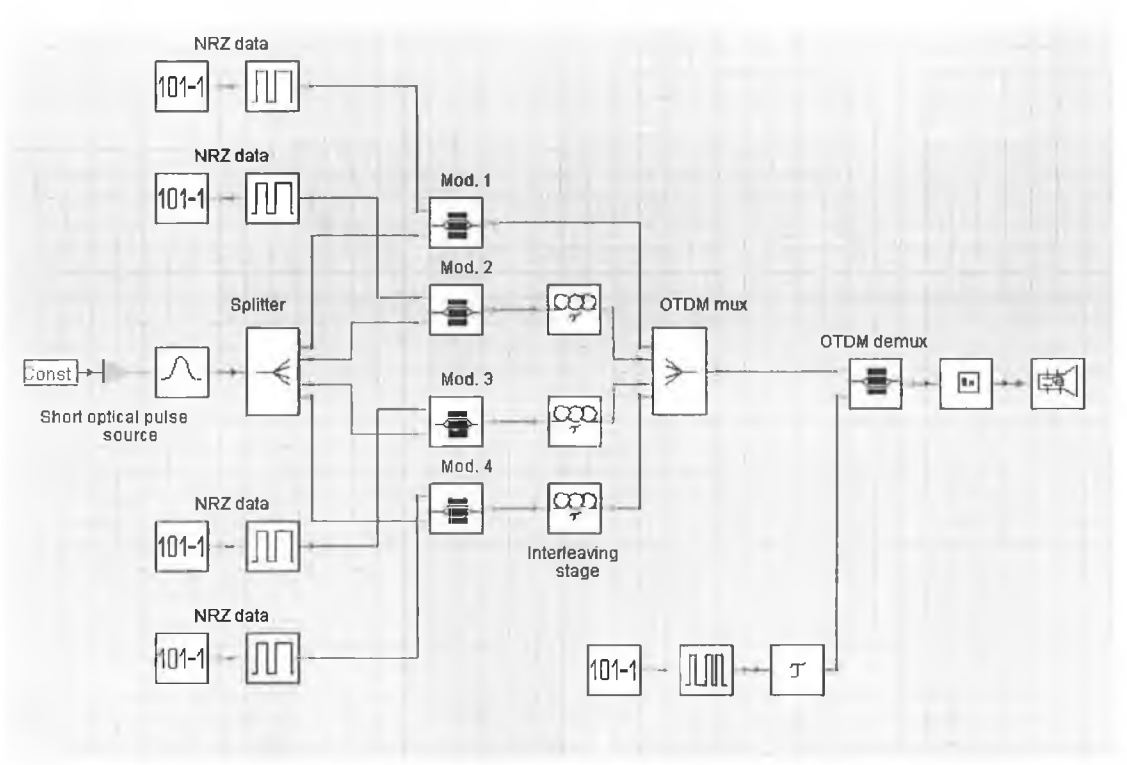

Figure 5-1: Simulation model of a 4-channel OTDM system

The 2.5 GHz pulse stream was then split into four streams, by passing it through a 1x4 optical splitter. Mach-Zehnder Modulators (MZM) were used to modulate the NRZ electrical data at 2.5 Gb/s, onto each of the four pulse streams. Before being merged with the aid of a 4x1 combiner, each data channel was assigned a bit slot with a width of 100ps. Thus, each channel was delayed by 100ps with respect to the previous channel, apart from the first channel as shown in Figure 5-1. After achieving the temporal multiplex at an aggregate rate of 10 Gb/s, we then moved on to look at the demultiplexing part. The demultiplexing stage consisted of a PRBS generator, RZ coder, a MZM and an electrical delay module. Demultiplexing could be achieved, by applying a generated clock signal[39] to the MZM and delaying the output according to the required channel. The Pulse Length Ratio (PLR) had to be optimized in order to ensure that the transmission window remained small enough to prevent interference from the other channels. Analysis of the output signal, at various stages of the set-up, was carried out by using an oscilloscope.

[39] A continuous stream of ones (RZ format) at the same rate as the base rate (2.5 Gb/s).

5.2.1.2 Simulation results

Initial pulses generated by the Gaussian pulse module are shown in Figure 5-2. As mentioned earlier the pulsewidth was set to 20 ps and the period was 400 ps.

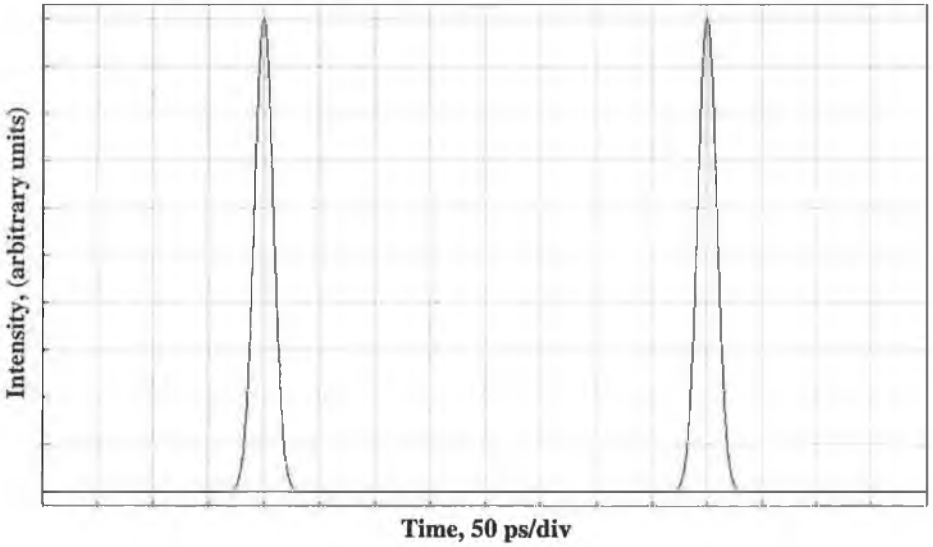

Figure 5-2: Optical pulse train

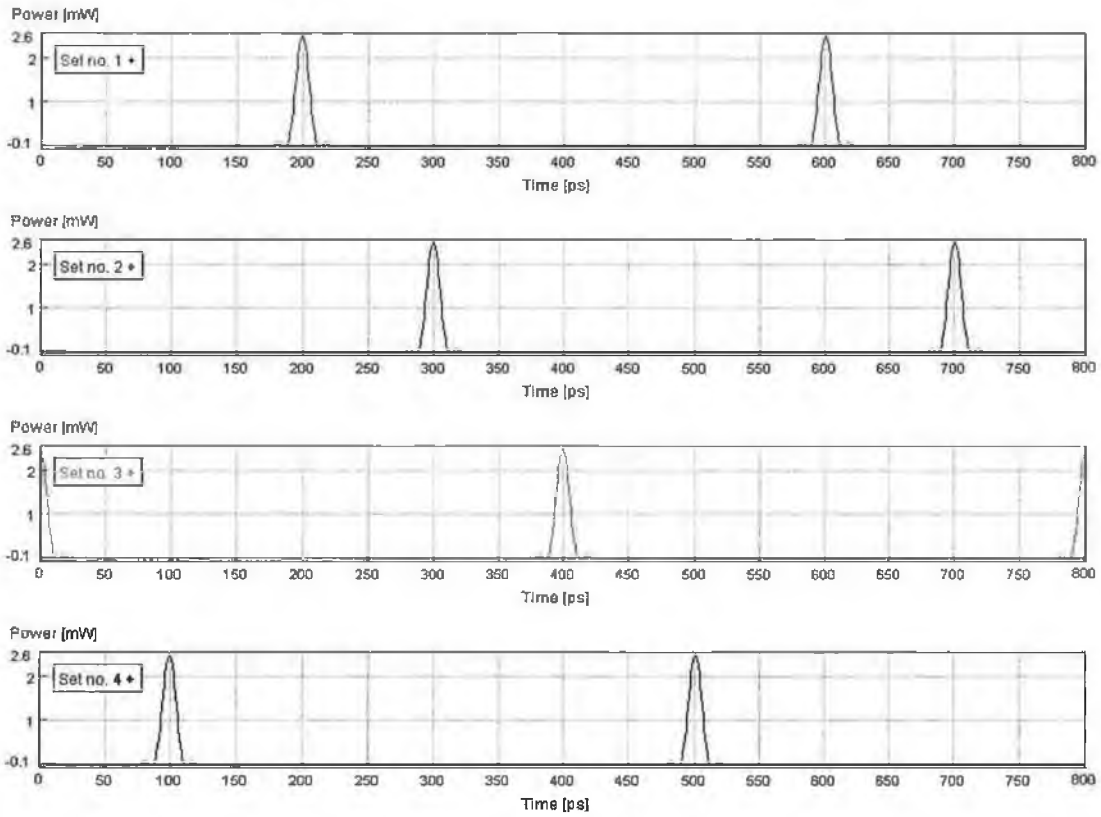

Figure 5-3: Four data channels with a continuous sequence multiplexed in temporal domain.

These pulses were then split in four ways and each stream was inserted into a MZM where data was then modulated on them. Initially a continuous stream of ones (data) was applied to verify that the pulsewidth and the delay lines were set at the optimum level for system operation. The temporally multiplexed signal was then input into an oscilloscope and the resulting trace is shown in Figure 5-3. It can be seen that the pulses belonging to the same channel are spaced 400 ps apart while each channel is separated by 100 ps.

A Pseudo Random Binary Sequence (PRBS) is commonly used to model an information source associated with digital communication systems. Hence a 2^7-1 PRBS was initially passed through an NRZ coder. The NRZ data was then externally modulated onto the pulses with the aid of a MZM. The 1st channel was passed straight into a 4x1 combiner. The 2nd, 3rd and the 4th were initially passed through delay lines and delayed by 100, 200 and 300 ps respectively, before being combined together using the remaining three inputs of the 4x1 combiner. The temporally combined (OTDM multiplex) signal is shown in Figure 5-4.

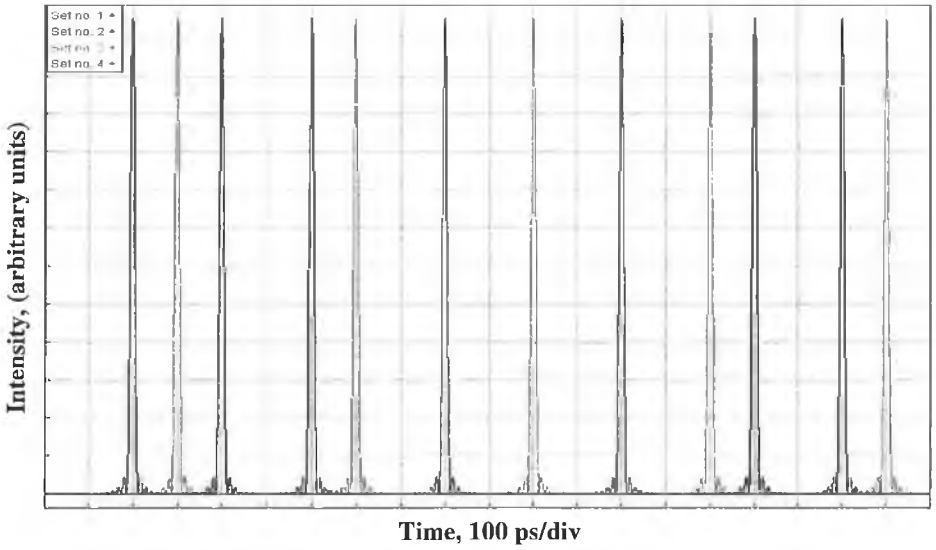

Figure 5-4: Four-channel OTDM signal

The eye diagram of the demultiplexed and received channel is shown in Figure 5-5. By varying the delay line, one could choose to switch the required channel. Since the

switching out of one channel would suffice for illustration purposes[40], we chose to switch out channel 2 by setting the delay to 100 ps. As mentioned earlier the PLR determines the size of the switching window. In this case the PLR was set to 0.08, which resulted in a switching window of 32 ps. The received eye is clear and wide open, as can be seen from Figure 5-5, indicating that satisfactory performance is achieved.

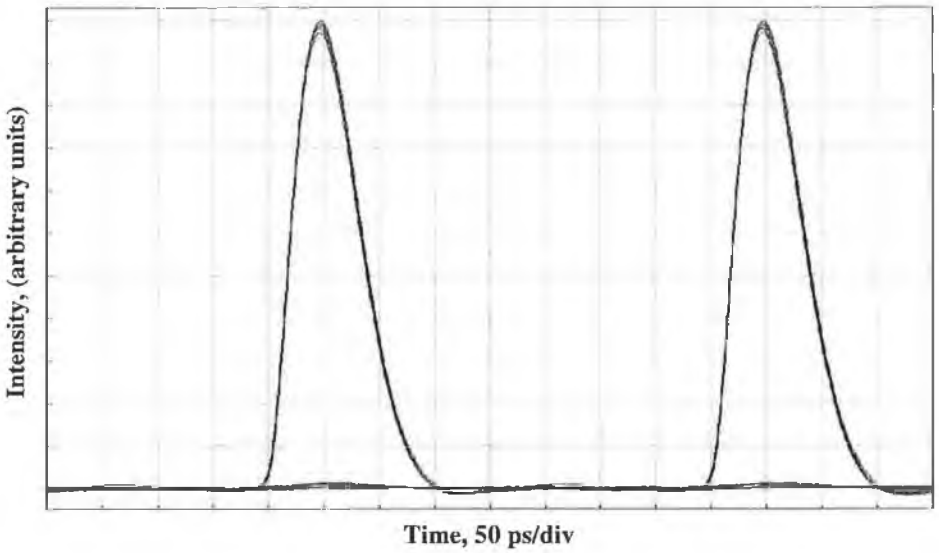

Figure 5-5: Eye, channel 2 demultiplexed

Having successfully modelled a basic 10Gb/s end-to-end OTDM system, we then went to use it as a block within the overall hybrid system. The model and results obtained with the hybrid system are shown in the following section.

5.3 Simulation model of a hybrid WDM/OTDM optical communication system

5.3.1 Hybrid WDM/OTDM systems

Ultra high bit rate optical transmission technology, offering Tb/s data rates, will soon be needed due to the rapid growth in the data traffic and also due to the continuous demand for new services in the communications sector. Many approaches have been reported to date using either OTDM or WDM technologies [2-4]. However, in order to increase the capacity in this manner, several problems need to be addressed.

[40] No dispersion since an end-to-end system was modelled. Even if fibre was involved, transmission is at one wavelength, hence no serious variation in the dispersion parameter would be expected.

Let us first consider increasing the transmission rate of an OTDM system to 1 Tb/s. The time slot of such a system would be 1 ps. Since the bit slot is so small, pulses in the femtosecond (fs) range are required. The bandwidth required to support such a pulse would be in the THz range (~12 nm)[41]. Maintaining the dispersion at low levels, in order to avoid ISI, becomes very challenging with such spectral widths. Another problem, which arises, is the scale of the timing accuracy of such a system (around a tenth of a ps) also due to the tiny bit slot. Hence issues such as timing jitter have to be precisely dealt with.

Let us now consider problems associated with very high capacity WDM networks. Broadband amplifiers are required to support such WDM networks since the span of frequencies that would be occupied is large. With the large range of frequency occupancy, design complexity and cost become issues due to the attenuation factor in fibre and gain of optical amplifiers both being dependent on the wavelength. Proper equalization techniques have to be used to address these problems. Dispersion is another hitch that is wavelength dependent. Hence proper dispersion maps have to be designed to overcome the slopes that are encountered.

The major advantage of using the hybrid approach is to ensure that none of the constituent platforms (OTDM and WDM) are pushed to their limit. This advantage of the hybrid network poses at least as a partial solution to the fore-mentioned problems encountered when individual techniques are used. Another benefit that is brought about by the fact that combining the two individual techniques provides about both their merits. Smaller number of pulse sources and better spectral efficiency are the immediate advantages that stand out.

5.3.1.1 Hybrid WDM/OTDM model

A schematic of the hybrid model is shown in Figure 5-6. Four channels on a single wavelength, at a base rate of 10 Gb/s are combined together in the optical temporal domain forming a 40 Gb/s OTDM channel. The hybrid system consists of four such wavelengths incorporating the same temporal multiplex as described above, thereby

[41] Assuming that they are transform limited Gaussian pulses.

bringing the aggregate bit rate to 160 Gb/s. A detailed description of the modeling process follows, where each individual platform was modelled separately.

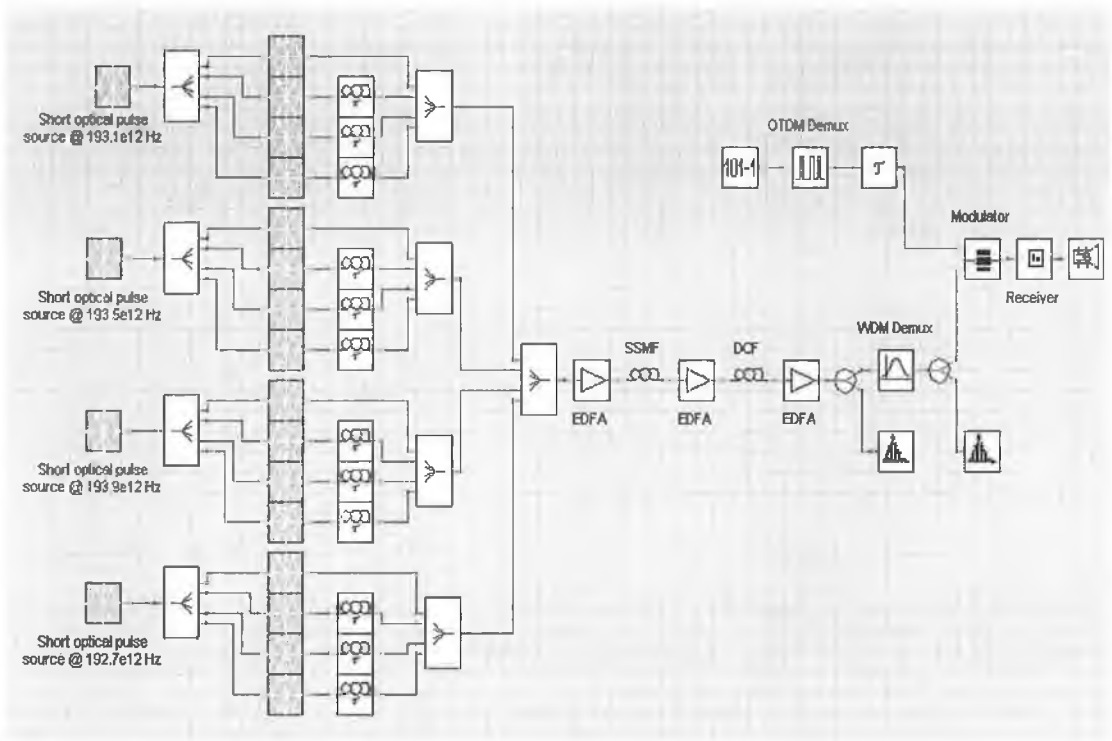

Figure 5-6: Simulation model of a 4x4 – 160 Gb/s hybrid system

As mentioned previously, for the sake of simplicity we initially built the OTDM system before going on to build the WDM system and finally combine the two together. The model of the OTDM system is similar to that shown in Figure 5-1.

5.3.1.2 Simulation results

The generation of pulses was performed by selecting one among the various VPI modules available. A Gaussian pulse source emitting at 193.1 THz was chosen. The repetition rate of the generated pulses was set to 10 GHz while the width (FWHM) of the pulses was set to 5 ps[42]. The temporal output of this pulse source is shown in Figure 5-7.

[42] Since the width has to about 1/3 of 25 ps which is the bit slot of the 40 Gb/s OTDM system .

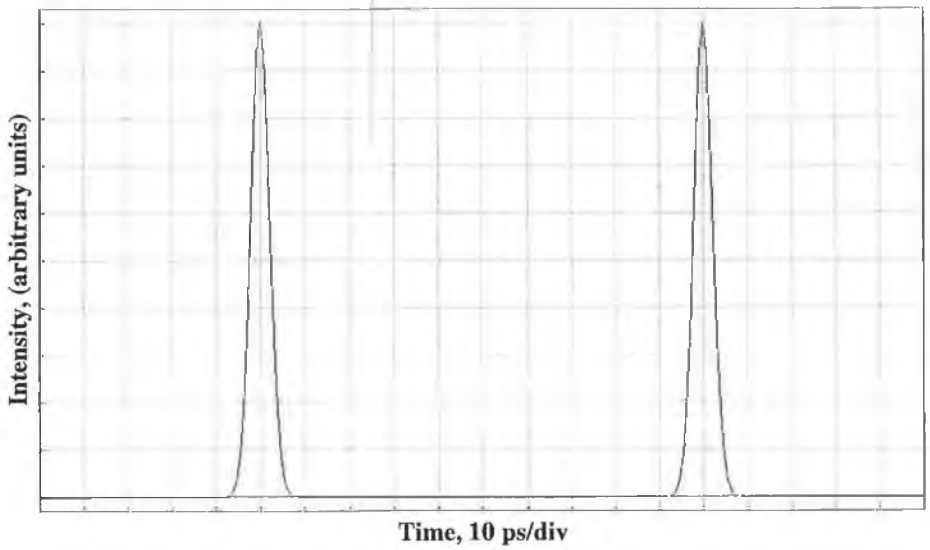

Figure 5-7: 10 GHz Gaussian pulse train

The associated spectral output of the fore-mentioned pulse source used is shown in Figure 5-8. The bandwidth required to support such a narrow (5 ps) transform limited Gaussian optical pulse would be 88 GHz as can be seen from the spectrum (Figure 5-8).

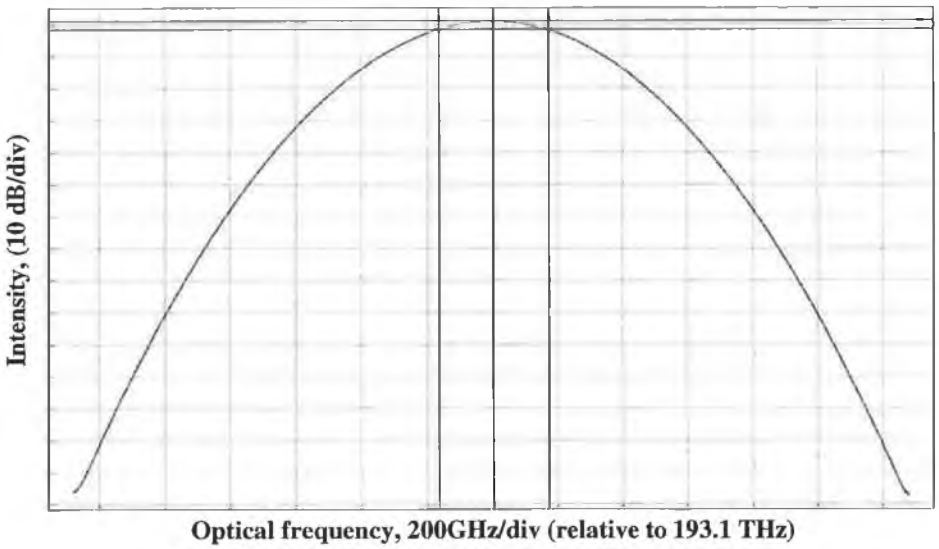

Figure 5-8: Spectrum associated to input pulse

The pulse train was split into four and each stream was individually modulated at rate of 10 Gb/s using an electrical NRZ pseudo random data stream with a length of 2^7-1. Using the first channel as a reference, the other three channels were delayed by 25 ps with respect to each other. All four channels were then combined together with the aid of 4x1 passive coupler, which resulted in a 40 Gb/s OTDM multiplex. The same procedure was

carried out on three other wavelength channels. The four wavelength channels were then multiplexed together with the spectral spacing set to 400 GHz. This meant that the four channels were centralized at frequencies of 192.7, 193.1, 193.5 and 193.9 THz.

The composite signal carrying 160 Gb/s data was then pre-amplified before being passed through 40 km of Standard Single Mode Fibre (SSMF). The amplifier had a gain of 21 dB, which brought the power level up to about 9 dBm. An inbuilt filter with an inverse transfer function compensated for the non-uniform gain of the amplifier. The attenuation coefficient of the SSMF was 0.2 dB/km while the dispersion parameter was 16 ps/km.nm. Dispersion compensation was carried out by passing the output of the SSMF through 4 km of DCF with a dispersion parameter of – 160 ps/km.nm. The signal was then pre-amplified before going into the demultiplexer stage. The spectrum of the hybrid signal is shown in Figure 5-9.

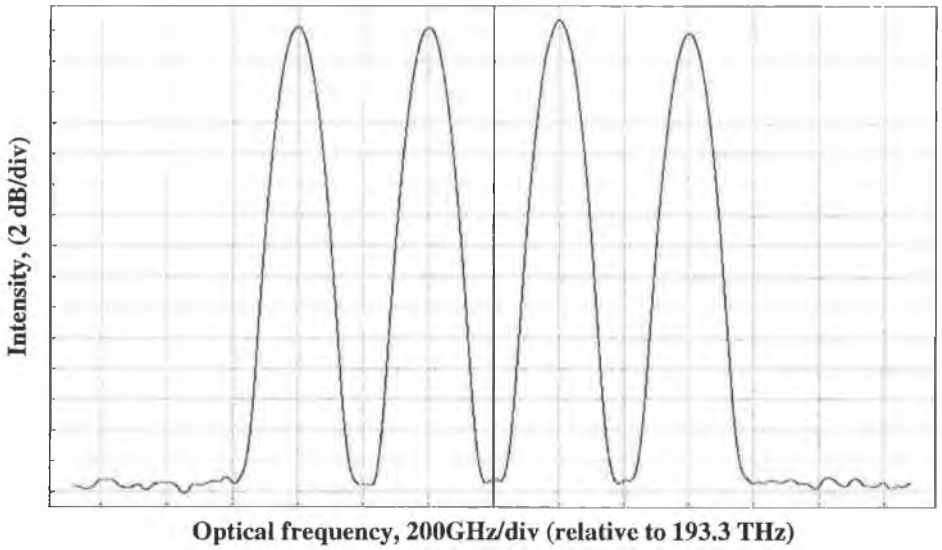

Figure 5-9: Spectrum of 4x4 hybrid signal

Having analyzed the transmitter stage and launching through fibre, the next phase that we looked at was the demultiplexing. A Bessel filter was used to initially demultiplex one of the wavelength channels. For the purpose of illustration we set out to filter the second wavelength channel (1553.6 nm), since the demultiplexing of all the channels involves the same procedure[43]. The filter bandwidth was set to about 100 GHz in order to

[43] The dispersion parameter would vary for the different channels.

accommodate for the 5 ps pulse. The spectrum of the demultiplexed WDM channel is shown in Figure 5-10.

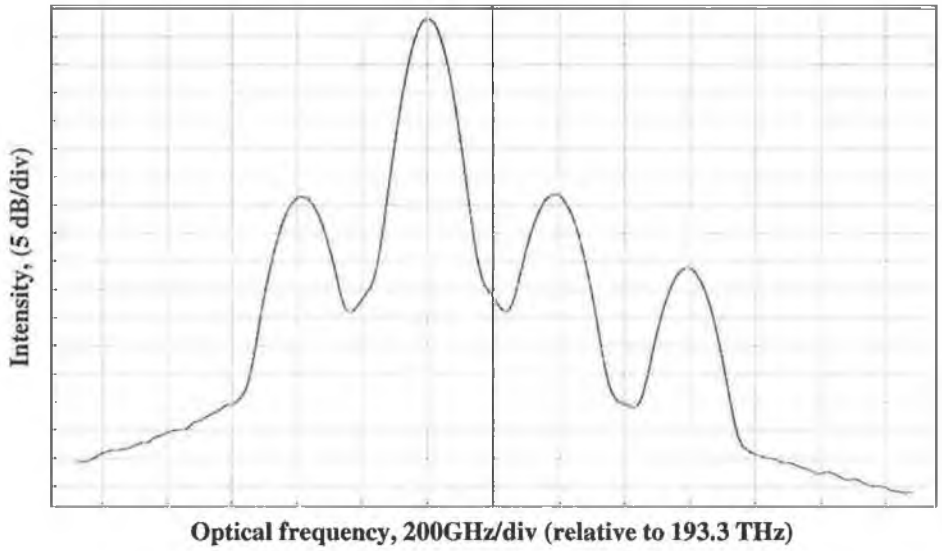

Figure 5-10: Spectrum of the filtered WDM channel

A 32 dB rejection of the closest channel was achieved as can be seen from the figure above. Having successfully carried out the WDM demultiplexing we then set out with the OTDM demultiplexing. The eye diagram of the demultiplexed channel (channel 2) is shown in Figure 5-11.

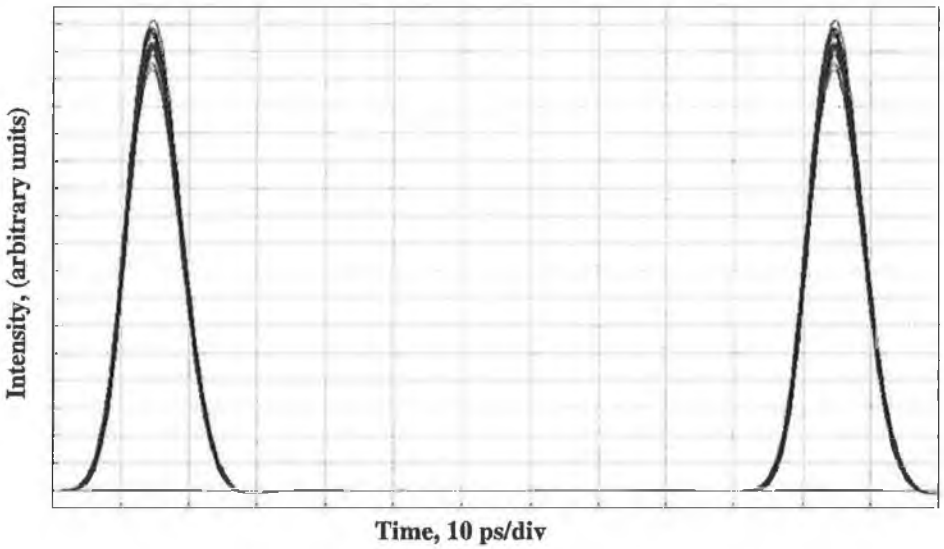

Figure 5-11: Eye of demultiplexed channel

Once again (as in the OTDM modeling section) the demultiplexing stage consisted of a PRBS generator, RZ coder, a MZM and an electrical delay module. By applying a continuous stream of ones[44] to the MZM and delaying the output according to the required channel, would achieve demultiplexing. This time around the PLR was set to about 0.2 (switching window of 20 ps) in order to account for any pulse broadening. The delay was set to 25+3 ps. The 3 ps added on compensated for the delay in traversing the length of fibre.

The 160 Gb/s hybrid system modelled above is based on system parameters chosen with a large degree of freedom, so as to ensure that no temporal or spectral interference would occur. However the tolerance added on to these parameters is so large that the spectral efficiency is lost. Hence in order to optimize the values of these parameters so as to strike a balance between the system performance and efficiency, a sweep through the values of each parameter was carried out.

5.3.2 Optimization of system performance and efficiency

The main contention with the previous hybrid model comes about due to the chosen spectral spacing (400 GHz) of the WDM platform. This results in a spectral efficiency[45] of 0.1 bps/Hz. Ideally the same system could operate with a spacing of 200 GHz at a cost of a very small (negligible) power penalty. Furthermore the narrower (broader) the pulsewidth, the broader (narrower) the spectral width that would be required to support it. Hence by increasing the pulsewidth[46] to a reasonable value we could obtain a narrower spectrum. This could enable channel spacings of 100 GHz to become feasible thereby offering efficiencies of 0.4 bps/Hz. Such efficiencies are more than acceptable for standard RZ coding schemes [5]. In conventional standard fibre transmission lines, RZ and NRZ are the two modulation formats that are commonly used [6]. When Bandwidth Efficient Modulation (BEM) schemes such as Carrier Suppressed Return to Zero (CSRZ) [7], Single Side Band Return to Zero (SSB-RZ) [8] and duo-binary modulation formats [9] are used, better spectral efficiencies could be obtained.

[44] RZ format and at the same rate as the base rate (10 Gb/s).
[45] The ratio of bit rate to available bandwidth is known as spectral efficiency.
[46] The chosen pulsewidth (5 ps) also had quite a large tolerance to avoid temporal interference.

The main aim in carrying out tests in this section was to choose optimum values for the spectral spacing and pulsewidths. This would thereby enhance the efficiency in comparison to the previous model.

The channel spacings to be tested were taken from the ITU grid standards. Logically a spacing of 25 GHz would not be viable for proposed speed of 160 Gb/s. Spectral spacings of 50 GHz are not feasible either for such a high-speed system and is portrayed by the simulation results obtained for two different pulsewidths (5 and 15 ps). Hence simulation sweeps were carried out in such a way that six different pulsewidths (7 ps; +2: 15 ps) at three different channel spacings (100, 200 and 400 GHz) were encompassed.

5.3.2.1 Simulation model

Shown below (Figure 5-12) is the schematic of the simulation model used. The model is basically the same as that shown in Figure 5-6 apart from the BER modules added on.

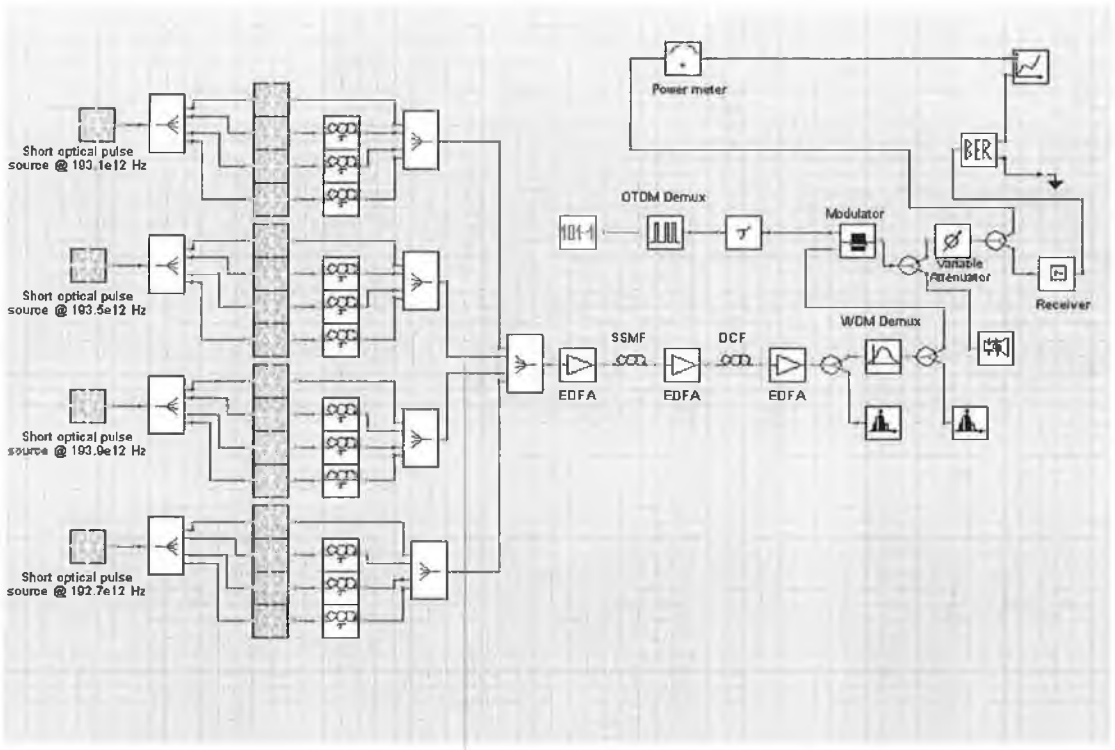

Figure 5-12: Schematic of simulation model used for system parameter optimization

The sweep of the system parameters was run as described earlier. Three different WDM channel spacings used were 400, 200 and 100 GHz. At each of these channel spacings the width of the optical pulses were changed from 5 ps in steps of 2 ps up to 15 ps and a power penalty plot was carried out. An additional WDM spectral spacing of 50 GHz was investigated at the extremes of the two pulsewidths. The demultiplexing filter bandwidth was reduced each time the channel spacing was reduced, in order to ensure that a reasonable rejection of the adjacent channels was maintained.

5.3.2.2 Simulation results with channel spacing set to 400 GHz

For the scenario of 400 GHz spectral spacing, the bandwidth of the WDM demultiplexing filter was set to 100 GHz. Furthermore the PLR in the OTDM demultiplexing stage was set to 0.2, which reflects a switching window of 20 ps, in order to accommodate for the largest pulse. The power penalty plot obtained with the fore-mentioned channel spacing and the pulsewidths varied from 5 to 15 ps in steps of 2 ps is shown below (Figure 5-13).

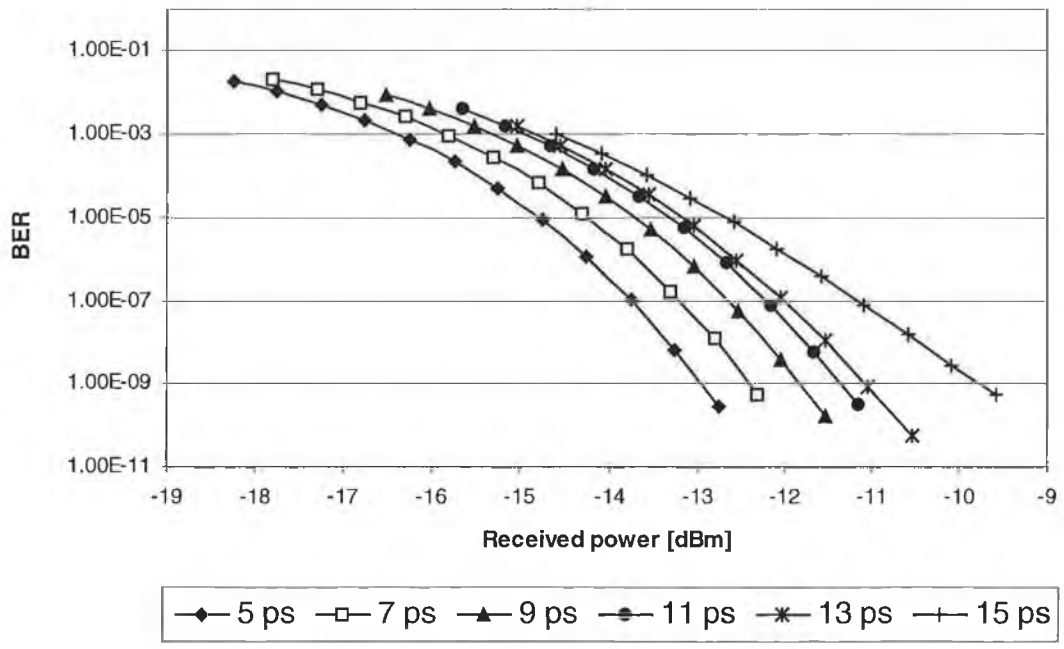

Figure 5-13: Power penalty with various pulsewidths for 400 GHz channel spacing

The results show that, in a hybrid system employing 400 GHz channel spacing, spectral interference is virtually negligible at all the pulsewidths used. Furthermore a pulsewidth of 5 ps ensures that no temporal interference takes place. Both of the inferences above could be justified by observing the demulitplexed spectrum (Figure 5-10) and the

received eye (Figure 5-11). As can be seen from Figure 5-13, the best performance is achieved, when the pulsewidth is set to 5 ps. A pulse with such a width would require a spectral width of 88 GHz as shown in Figure 5-8. Since there is no spectral interference with such a narrow pulse, there would not be any spectral interference for larger pulsewidths[47].

It could also be observed from the power penalty plot above that, the power penalty incurred gets progressively worse as the pulsewidth is increased. This could be attributed to temporal interference between the neighbouring bit slots leading to ISI. Therefore as expected the largest penalty is sustained, when the width of the pulses is set to 15 ps. At a BER of 10^{-9} the observed penalty in power was about 3.5 dB, when the width of the pulse is increased from 5 ps to 15 ps.

5.3.2.3 Simulation results with channel spacing set to 200 GHz

With the channel spacing set to 200 GHz, the passband filter bandwidth was reduced to 80 GHz, which proved to be an optimum value (adequate rejection as well as least amount of broadening effect on the pulses). The rest of the simulation settings were the same as previously used in the 400 GHz channel spacing. The power penalty plot, with the same variation in pulsewidths, is shown in Figure 5-14.

The results obtained show that 200 GHz spectral spacing could be applied to the 160 Gb/s hybrid WDM/OTDM system, in place of the 400 GHz spacing, at the cost of a minor power penalty. The penalty relative to the 400 GHz channel spacing is negligible in comparison to the spectral efficiency obtained, which is doubled (0.1 to 0.2 bps/Hz). Hence spacing the channels by 200 GHz could also accommodate[48] for 5 ps pulses (exhibits the widest spectral width within the range of pulsewidths used).

Here again the penalty in power gets progressively worse as the pulses get larger. Once again with the pulsewidth varied from 5 ps to 15 ps the power penalty incurred, relative to a BER of 10^{-9}, was observed to be about 3.5 dB. The power penalty being the same as

[47] As the pulsewidth gets larger, the required spectral width needed to support it gets smaller.
[48] No spectral interference.

in the previous case (400 GHz channel spacing) enables us to conclude that the penalty is entirely due to temporal interference and not due to spectral interference.

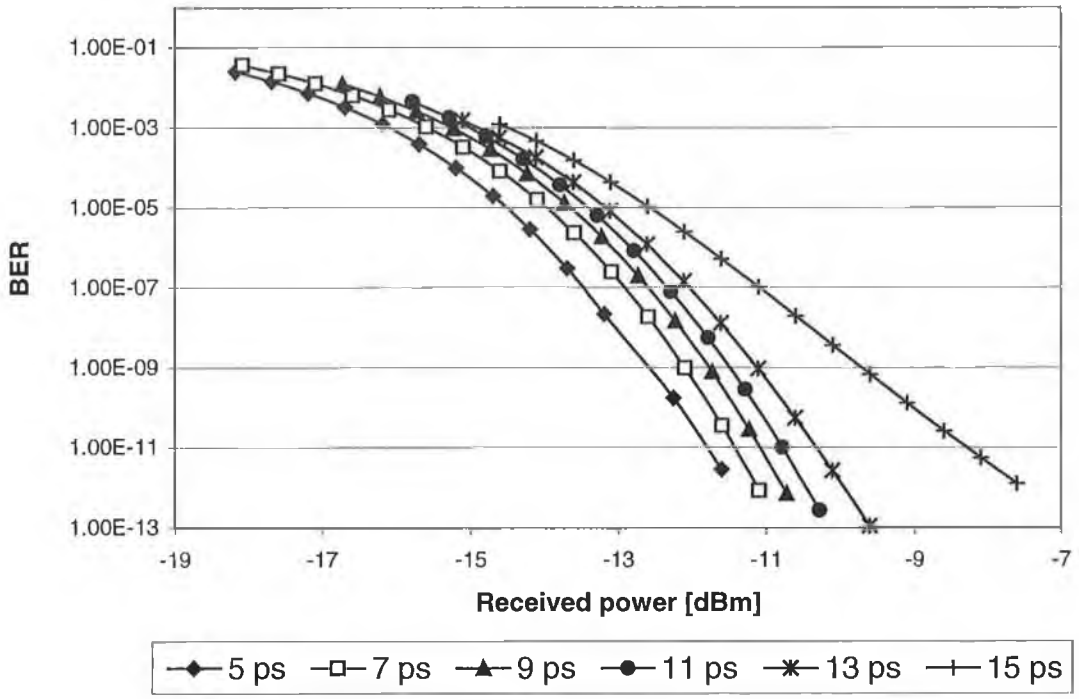

Figure 5-14: Power penalty with various pulsewidths for 200 GHz channel spacing

5.3.2.4 Simulation results with channel spacing set to 100 GHz

This was the final scenario involving the sweep with the afore-mentioned range of pulsewidths. Here the optimum value for the WDM demultiplexing filter bandwidth was 60 GHz. As in the previous simulation, the other simulation settings were left unchanged.

As the pulsewidths were once again varied from 5 ps to 15 ps using a 2 ps step interval, the performance was characterized by plotting the acquired power penalty (Figure 5-15). The result obtained here reflects a few interesting facts, which are analyzed in ascending order with the increase in the pulsewidth. First of all we can see that the when employing 5 ps pulsewidths with a 100 GHz channel spacing, the performance achieved is totally unsatisfactory. Increasing the power falling on the detector hardly changes the BER (shows a gradual improvement). Each of the pulse sources generating the 5 ps pulses would require a spectral width of about 90 GHz (at the 3 dB point) and with the channel

spacing set to 100 GHz major overlapping would occur. The overlapping results in the performance being degraded due to the spectral interference between the channels.

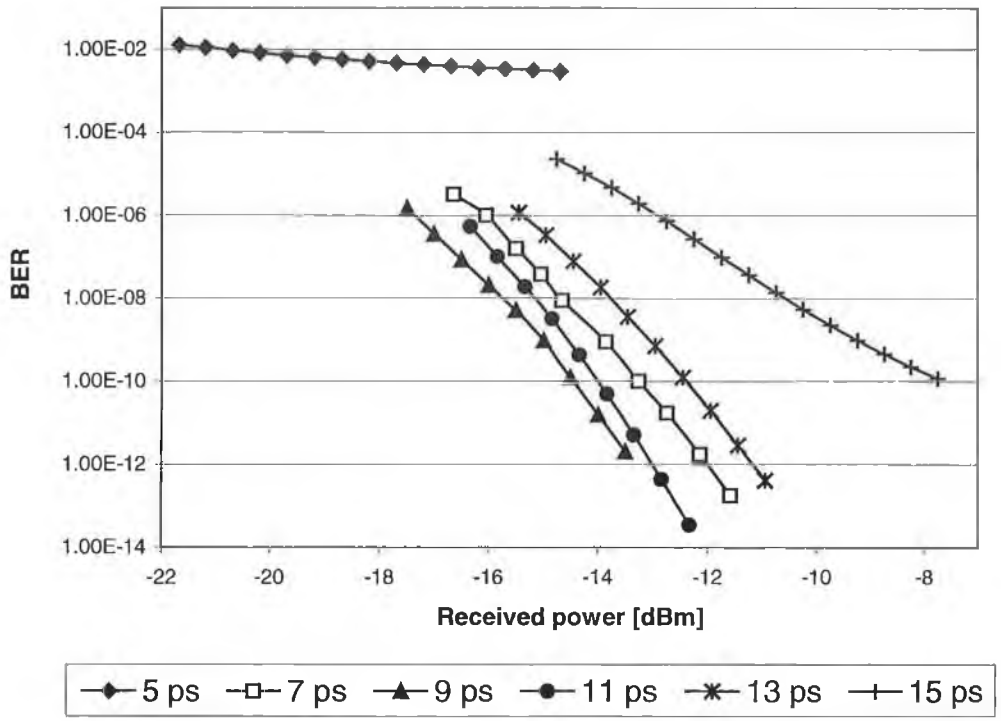

Figure 5-15: Power penalty with various pulsewidths for 100 GHz channel spacing

The improvement in performance as the pulsewidth is increased to 7 ps can be clearly seen from Figure 5-15. This improvement is due to the spectral width (~ 63 GHz) of the pulse source becoming narrower than the previous case, thereby resulting in less spectral interference[49]. The performance gets even better when the pulsewidth is increased to 9 ps. The associated spectral width of the 9 ps transform limited Gaussian pulses is about 49 GHz. Hence with the filter set to 60 GHz, a reasonable rejection ratio is achieved, thereby minimizing the spectral interference.

As the width of the pulses is further increased, the performance is seen to get gradually worse. At this juncture the temporal interference starts to have an influence on the system performance. It is important to note that the performance with the 11 ps pulse is better (less spectral interference) than the 5 and 7 ps pulses but worse (more temporal

[49] Less spectral overlapping.

interference) than the 9 ps pulse. When the pulsewidth is set to 15 ps, temporal interference leading to ISI degrades the performance to unacceptable levels. It is important to note that in the 100 GHz spaced system the spectral interference might exist for the whole range of pulsewidths used. However the result here categorically shows that, an optimum pulsewidth exists in terms of minimal temporal and spectral interference. Performance degradations are experienced when drifting above or below this optimum value. The optimum pulsewidth relative to the case here is 9 ps, and going by the results obtained any value below this would result in spectral interference while any value above this would cause temporal interference. The spectrum of the channel filtered out and its received eye are shown in Figure 5-16 (a) and (b) respectively. It is also important to note that by setting the channel spacing to 100 GHz a spectral efficiency of 0.4 bps/Hz is achieved.

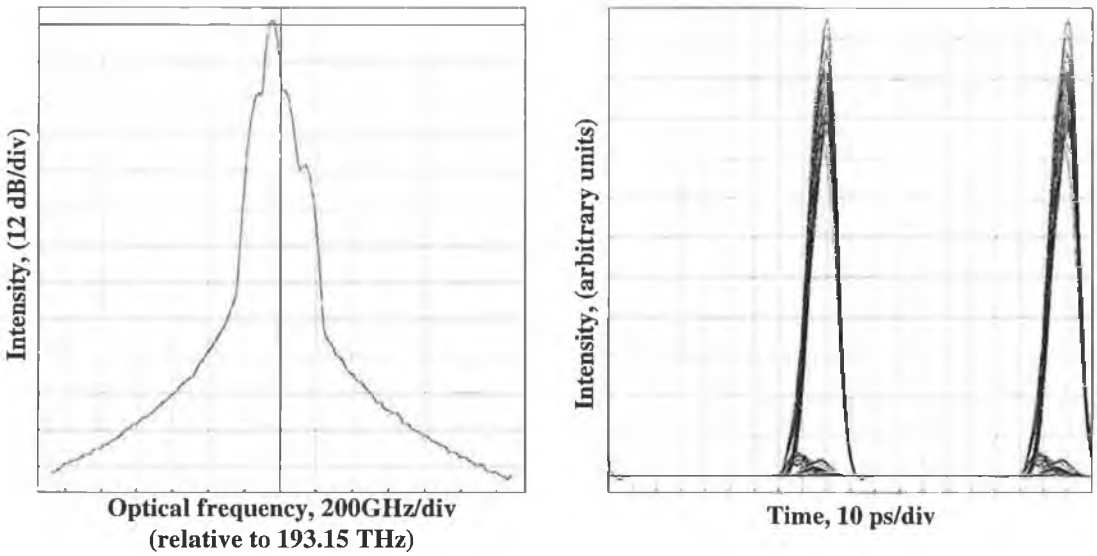

Figure 5-16: (a) Spectrum of demultiplexed channel (b) Received eye

The power penalties incurred at a BER of 10^{-9} relative to the case where the width of the pulses is set to 9 ps, is tabulated below (Table 5-1). The power penalty curve related to the 5 ps pulse was extrapolated in order get a rough estimation of the power penalty incurred.

Width of Pulses (ps)	Power Penalty Introduced (dB)
5	20-30 !!!!
7	1.2
11	0.3
13	2
15	5.8

Table 5-1: Power penalties incurred relative to the 9 ps pulsewidth

5.3.2.5 Simulation results with channel spacing set to 50 GHz

This case is mainly shown as an illustration, since intuitively it is fairly obvious that a channel spacing of 50 GHz is inadequate for four different channels multiplexed together in wavelength domain, each carrying 40 Gb of data.

The passband of the filter bandwidth was set to 40 GHz. The rest of the simulation parameters were unchanged. The width of the pulses was set at either extreme (5 and 15 ps). The results achieved are shown below in Figure 5-17.

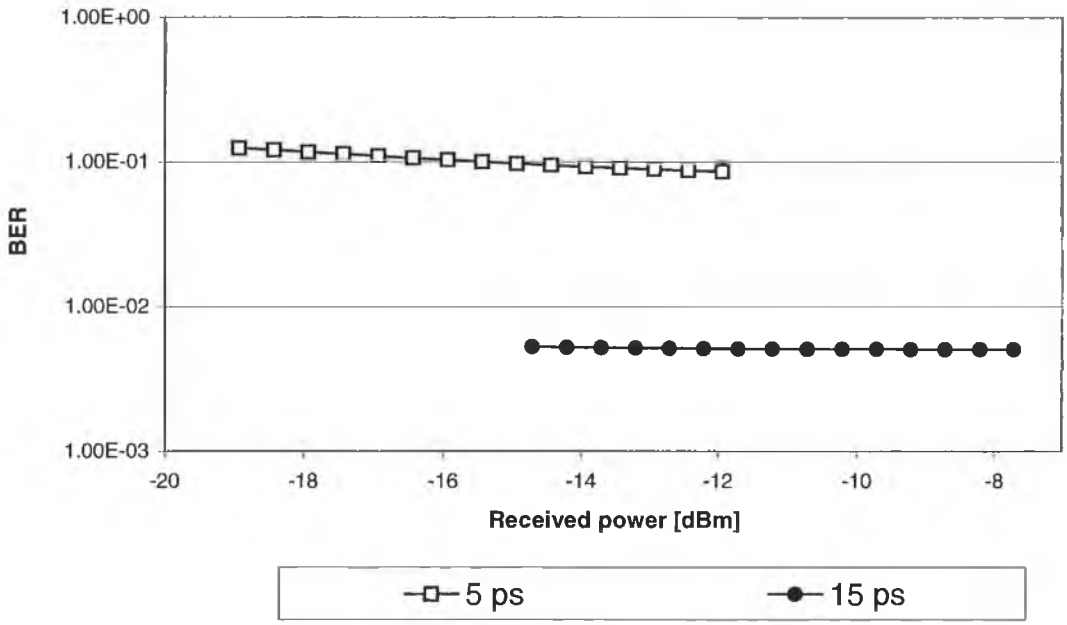

Figure 5-17: Power penalty with 5 and 15 ps pulsewidths for 50 GHz channel spacing

From the results obtained, it can be seen that a channel spacing of 50 GHz is not feasible for the proposed system.

5.4 Conclusion

In this section, system level modeling of high-speed hybrid WDM/OTDM networks has been carried out mainly to verify the efficiency of such systems based on the employed pulsewidth and channel spacing. These simulations show that the system parameters of a hybrid WDM/OTDM system should be carefully chosen so as to ensure that a balance is struck between the performance and efficiency. From the initial simulations carried out we can conclude that by employing very wide channel spacings and short pulsewidths, more than satisfactory performance as regards spectral and temporal interference could be obtained. However this enhanced performance is achieved at the cost of relinquishing spectral efficiency.

For the specific case of the simulated 4x4 (160 Gb/s) hybrid WDM/OTDM model, optimum performance and efficiency was achieved when the pulsewidth was set to 9 ps. The associated spectral width[50] with such pulse durations would be 49 GHz thereby permitting frequency spacings of 100 GHz. With the channel spacing set to 100 GHz the spectral efficiency works out to 0.4 bps/Hz, which is acceptable for standard RZ coding schemes.

[50] For transform limited Gaussian pulses

References

[1] R. S. Tucker, G. Eisenstein and S. K. Korotky, "Optical Time Division Multiplexing for Very High Bit Transmission," *IEEE J. of Lightwave Technol.*, vol. 6, pp. 1737-1749, 1988.

[2] T. Ono and Y. Yano, "Key Technologies for Terabit/second WDM Systems With High Spectral Efficiency of Over 1 bit/Hz," *IEEE J. Quantum Electron.*, vol. 34, pp 2080-2088, 1998.

[3] S. Aisawa, T. Sakamoto, M. Fukui, J. Jani, M. Jinno and K. Oguchi, "Ultra-Wideband Long Distance WDM demonstration of 1 Tb/s 600 km Transmission Using 1550 and 1580 nm Wavelength Bands," *Electron. Lett.*, vol. 34, pp. 1127-1129, 1998.

[4] S. Kawanishi, "High Bit Rate Transmission Over 1 Tbit/s," *IEICE Trans. Commun.*, vol. E84-B, pp. 11351141, May 2001.

[5] A. Hodzic, B. Konrad and K .Peteremann, "Alternative Modulation Formats in N X 40 Gb/s WDM Standard Fibre RZ-Transmission Systems," *IEEE J. of Lightwave Technol.*, vol. 20, pp. 598-607, 2002.

[6] S. G. Park, A. H. Gnauck, J. M.Wiesenfeld, and L. D. Garrett, "40-Gb/s Transmission Over Multiple 120-km Spans of Conventional Single-Mode Fiber Using Highly Dispersed Pulses," *IEEE Photon. Technol. Lett.*, Vol. 12, pp. 1085–1087, 2000.

[7] Y. Miyamoto, A. Hirano, K. Yonenega, A. Sano, H. Toba, K. Murata and O. Mitomi, "320 Gbit/s (8_40 Gbit/s) WDM Transmission Over 367 km With 120 km Repeater Spacing Using Carrier-Suppressed Return-to-Zero Format," *Electron. Lett.*, vol. 35, pp. 2041–2042, 1999.

[8] M. Sieben, J. Conradi and D. E. Dodds, "Optical Single Sideband Transmission at 10 Gbit/s Using Only Electrical Dispersion Compensation," *J. Lightwave Technol.*, vol. 17, pp. 1742–1749, 1999.

[9] A. J. Price and N. le Mercier, "Reduced Bandwidth Optical Digital Intensity Modulation With Improved Chromatic Dispersion Tolerance," *Electron.Lett.*, vol. 31, pp. 58–59, 1995.

Chapter 6 - Conclusions

The increasing demand for new services and the growth of broadband applications (video on demand, interactive multimedia, teleconferencing etc.) has fueled a great interest and a colossal amount of research effort into high capacity transmission systems. How service providers can be assured of being able to process and transport an increasing volume of traffic with this unprecedented growth in data and internet traffic is a commonly asked question. Currently there are a few choices available. One would be to install more fibre although this proves to be very expensive[51]. Furthermore this idea brings out a lot of redundancy regarding the available bandwidth offered by optical fibres. Another solution to the question raised above, is to use higher speed electronic devices, which means that one has to use the most advanced technologies that is neither established nor cost efficient. Standard single channel rates of 10 Gb/s are well established with the current state of technology. However when moving to much higher bit rates the existing devices struggle. Using various multiplexing techniques in the optical domain seems to be the most viable of options that is available at the moment especially in terms of making better use of the available bandwidth offered by optical fibre. In this work we initially looked at already existent schemes such as Wavelength Division Multiplexing (WDM) and Optical Time Division Multiplexing (OTDM). The combination of the two techniques mentioned above, to form a hybrid WDM/OTDM system (a relatively new method) is also examined in the same section.

As optical communication systems move to line rates of 40 Gbit/s and beyond, it becomes more likely that return-to-zero (RZ) coding will be used for data transmission, as it is easier to compensate for dispersion and nonlinear effects in the fibre by employing soliton-like propagation [1]. In addition to this development, the use of wavelength tunability in optical networks is being explored as a way to provide dynamic provisioning in the next generation of photonic systems [2]. Taking into account these moves towards tunable optical systems employing RZ coding, it is obvious that the development of a wavelength tunable source of short optical pulses will be of paramount importance for

[51] Existence of dark fibres - partial reason for present glut in the optical communications industry.

future WDM, OTDM, and hybrid WDM/OTDM optical communication systems [3]. Hence one of the main areas of focus in this thesis is based upon the examination of simple and cost effective methods of generating short optical pulses. The foundation of the thesis is built upon the gain switching technique, as this was the one chosen due to its simplicity, flexibility and robustness. Experimental results obtained portray some of the problems associated with the gain switching scheme. Gain switching a DFB laser resulted in 12 ps pulses with an associated spectral width of about 130 GHz. Furthermore the SMSR of the gain switched DFB was degraded[52] down to 8 dB.

One of the most effective measures of overcoming the above-mentioned tribulations was then examined, which involved the self-seeding of the gain switched laser diode. The experimental results clearly show that impairments such as turn on jitter, loss of SMSR (in DFB) and even chirp are compensated for by self-seeding. Although the TBWP was improved the results achieved did not yield transform-limited pulses. However the SMSR of the 14 ps pulses was improved to 30 dB. Furthermore the timing jitter was reduced to about 1.4 ps. The technique of self-seeding was then extended to gain switched FP lasers since the self-seeding of a gain-switched Fabry-Perot (FP) laser has been reported as one of the most reliable techniques available to generate wavelength tunable optical pulses [4-6]. Using the SSGS technique on FP lasers, nearly transform limited pulses (TBWP of 0.59) exhibiting pulsewidths of 14.7 ps and spectral widths of 0.3 nm were successfully generated. These pulses also displayed very small timing jitters (~ 1 ps). Concentrating on the tunability, we found that self-seeding of a gain switched FP could yield nearly transform limited pulses with widths (FWHM) 29 ps that were tunable over 37 nm.

The inherent bandwidth of the laser limits the pulse train repetition rates normally obtainable with the gain switching technique. By using external light injection it has been shown in this work, that the repetition rate could be increased to thrice the free running bandwidth. Characterizations of the laser under external injection have been done and reasons for the enhancement in bandwidth have been experimentally demonstrated. Furthermore the characterization shows that by varying the injected power the laser could

[52] SMSR was 36 dB when running CW.

be used over a large range of frequencies. The same section of the thesis looks at the application of this phenomenon towards pulse generation, which has not been reported before. Results show that pulses could be generated at 20 GHz and above, which is well above the inherent bandwidth of the laser, when strong external light is injected into the gain switched laser. The pulses exhibited a FWHM of 12 ps and an associated spectral width of 40 GHz resulting in a TBWP of 0.44, which is close to the TBWP product of transform limited Gaussian pulses. Pulse shaping is another method of pulse generation that was investigated in this thesis.

The main aspect that brings novelty to this work is that even though the generation of pulses using the SSGS technique has been widely reported, their utilization and performance in an optical communication system have not been considered. Many of the previously reported wavelength tunable pulses using the SSGS technique had SMSR's that varied between 10-25 dB as the output pulse wavelength was tuned [5, 7]. Our work shows that an important characteristic of these SSGS sources is the Side Mode Suppression Ratio (SMSR). Any variation in the SMSR as the wavelength is tuned [4, 5], may ultimately affect their usefulness in optical communication systems.

We started off by demonstrating how this SMSR variation greatly affects the noise induced on a single pulse source as the pulses propagate through optical fibre and an optical filter. Then we examined the noise induced on one of the pulse sources due to a variation in SMSR of the other SSGS source by using two SSGS pulse sources at different wavelengths. The result obtained, shows that as the SMSR of one channel is reduced, the power fluctuations in its side mode, which is at the same wavelength as the selected pulse source, increases. The temporal fluctuation in power of this side mode manifests itself as noise on the filtered channel (cross channel interference). We then went on to portray the effect of the increased noise on system performance, by modulating data onto one of the channels and measuring the BER. The next stage of experimentation entailed the illustration of the difference in required SMSR[53], as the number of channels was increased. Another effect that was investigated involved

[53] Higher SMSR required to maintain the same level of performance at identical received powers.

analyzing the addition of SSGS pulse sources with different gain curves to an existing channel. Plugging in different SSGS pulse sources with the data channel and scrutinizing the received power required to maintain a BER of 10^{-9} as the SMSR of the plugged in sources was varied, enabled us to achieve the fore-mentioned analysis. Finally the cumulative effect of the SMSR (degraded) of many SSGS pulse sources on the performance of a four-channel WDM system was studied. The main results here show that, power penalties (relative to the back to back case) of 0.9, 1.3, 1.6, and 2 dB were incurred when the SMSR of the three adjacent channels was set to 30, 25, 20 and 15 dB respectively. The effect of multiplexing different pulse sources (individually) with the reference pulse source (all pulse sources having their SMSR set to 30 dB) was also achieved in the same experiment. The results exhibit that the power penalty, due to the introduction of one source, varies from 0.3 to 0.7 dB (at a BER of 10^{-9}).

Simulations carried out helped verify all the experimental configurations and results. The simulations also enabled us to examine the performance of a higher capacity system (eight channels), which we were unable to perform experimentally due to equipment limitation in the laboratory. As mentioned in the simulation section, most of the simulation results were in good agreement with the experimental results.

With the aid of the experimental results and simulations, we were able to conclude that a variation in the SMSR of wavelength tunable SSGS pulse sources will affect the performance of a WDM communication system that employs such pulse sources. If the SMSR of one or more pulse sources is degraded, the interaction of the mode partition effect with spectral filtering would result in increased noise on all the received wavelength channels. The system then experiences a penalty in power, in trying to maintain the same acceptable BER, due to the increased level of noise. Another effect that was established within the same section was the introduction of stringent measures on the minimum SMSR (of each pulse source) required, as the number of channels in a WDM system using SSGS pulse sources is increased.

The final system simulations, concerning a high capacity hybrid WDM/OTDM system, depict the essence of choosing optimized system parameters. The simulation in this section involved going through intermediary stages of building OTDM and WDM networks employing pulse sources. The hybrid simulation shows that by spacing the channels far apart with an ample tolerance to avoid any spectral interference, perfect performance could be achieved at the expense of efficiency. Similarly the choice of very narrow pulses would also achieve supreme performance in the temporal domain. When very narrow pulses are used, the spectral spacing between the channels has to be increased in order to accommodate for the larger spectral width required to support such a pulse The process of choosing ideal system parameter values finishes off this chapter. The choice of effective parameters for the spectral spacing and width of pulses is shown to be vital in regard not only to the performance of the system but also to the spectral efficiencies that could be achieved. The simulation of the 160 Gb/s hybrid system, with optimized system parameters, goes on to show that spectral efficiencies of 0.4 bps/Hz could be achieved.

References

[1] R. Ludwig, U. Feiste, E. Dietrich, H.G. Weber, D. Breuer, M. Martin and F. Küppers, "Experimental Comparison of 40 Gbit/s RZ and NRZ Transmission Over Standard Single Mode Fibre," *Electron. Lett.,* vol. 35, pp. 2216-2218, 1999.

[2] C-K. Chan, K. L. Sherman, and M. Zirngibl,"A Fast 100-Channel Wavelength-Tunable Transmitter for Optical Packet Switching," *IEEE Photon. Technol. Lett.,* vol. 13, pp. 729-731, 2001.

[3] T. Morioka, H. Takara, S. Kawanishi, O. Kamatani, K. Takiguchi, K. Uchiyama, M. Saruwatari, H. Takahashi, M.Yamada, T. Kanamori, and H. Ono, "1Tbit/s (100Gbit/s times 10 channel) OTDM/WDM Transmission Using a Single Supercontinuum WDM Source," *Electron. Lett.*, vol. 32, pp. 906-907, 1996.

[4] L.P. Barry, R.F. O' Dowd, J. Debeau, and R. Boittin, "Tunable Transform Limited Pulse Generation Using Self-Injection Locking of a FP Laser," *IEEE Photonics Technol. Lett.*, vol. 5, pp. 1132-1134, 1993.

[5] C. Shu and S.P Yam, "Effective Generation of Tunable Single- and Multiwavelength optical pulses from a Fabry Perot laser diode," *IEEE Photonics Technol. Lett.*, vol. 9, pp. 1214-1216, 1997.

[6] X. Fang and D. N. Wang, "Mutual Pulse Injection Seeding by the Use of Two Fabry-Perot Laser Diodes to Produce Wavelength-Tunable Optical Short Pulses," *IEEE Photonics Technol. Lett.*, Vol. 15, pp. 855–857, 2003.

[7] D. Huhse, M. Schell, W. Utz, J. Kassner, and D. Bimberg, "Dynamics of Single-Mode Formation in Self-Seeded Fabry-Perot Laser Diodes," *IEEE Photonics Technol. Lett.*, vol. 7, pp. 351-353, 1995.

APPENDIX A

SDH standard	SONET standard	Data rate (Mb/s)
--	OC 1	51.84
STM 1	OC3	155.52
STM 4	OC 12	622.08
STM 16	OC 48	2,488.32
STM 64	OC 192	9,953.28
STM 256	OC 768	39,813.18

Standard data rates

APPENDIX B

Modulation-Demodulation Format	Chromatic dispersion	Polarization dispersion
CPFSK (Mod. Index: 1)	0.302	0.18
MSK, FSK (Mod. Index: 0.5)	0.471	0.33
ASK non synchronous	0.591	
ASK, PSK synchronous	0.691	0.4
DPSK	0.738	0.35
IM-DD	0.792	0.5

Values of chromatic dispersion coefficient γ calculated for various modulation and demodulation formats

APPENDIX C

Pulse shape	Time-Bandwidth product ($\Delta\mu\Delta t$)
Gaussian	0.4413
Hyperbolic sech	0.3148
$Sech^2$ (t) R=3 R=6	 0.278 0.232
One sided exp e^{-t}, $t \geq 0$ 0, $t < 0$	0.1103
Symmetric two-sided exp $e^{-2\|t\|}$	0.1420
Lorentzian $1/1+t^2$	0.2206

Pulse shapes and their associated time-bandwidth products

APPENDIX D

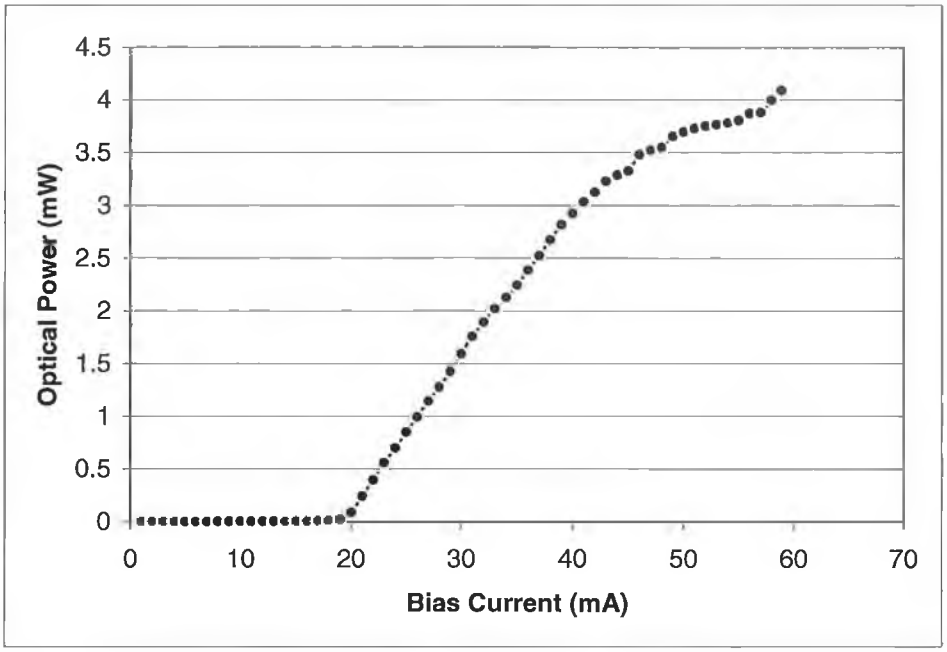

LI for 1.5 μm DFB (KELD 1551 CCC_1)

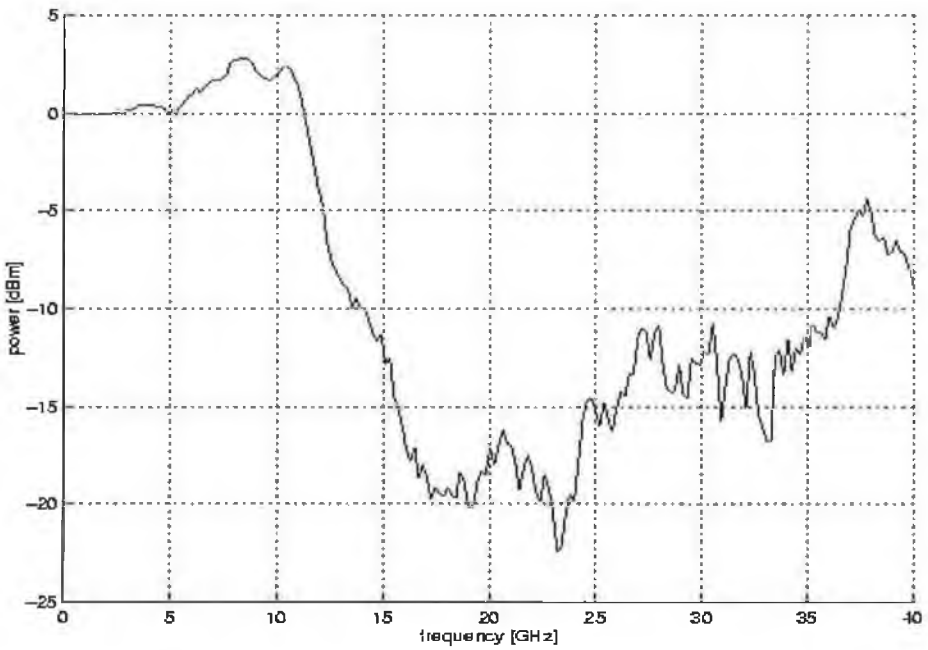

Frequency response plot for 1.5 μm DFB (KELD 1551 CCC_1)

APPENDIX E

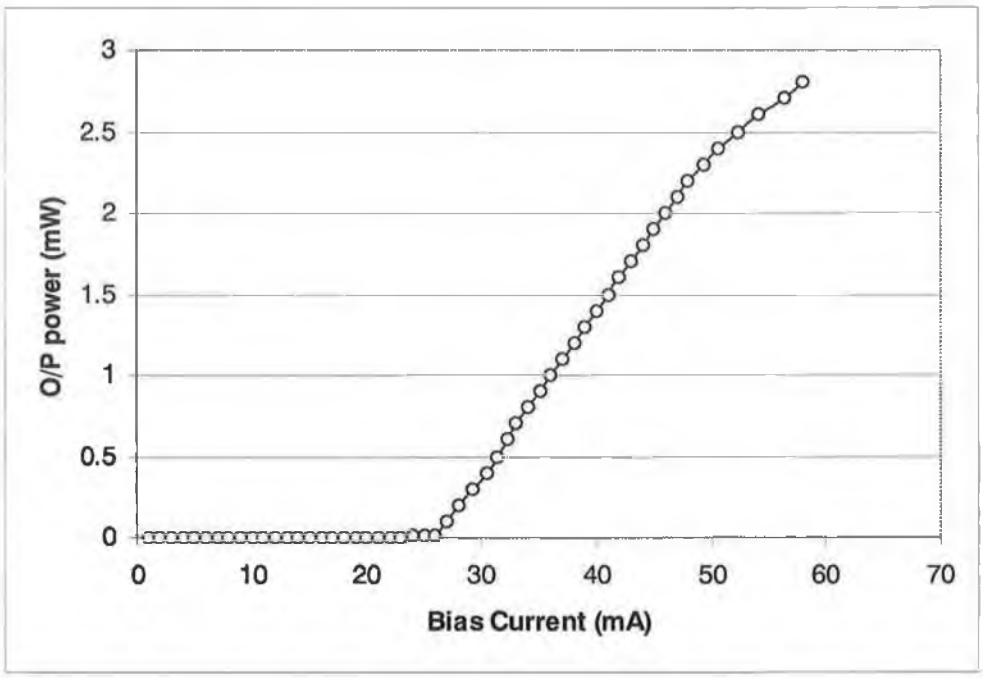

LI for 1.5 μm FP (KELD 1501R CCC_1)

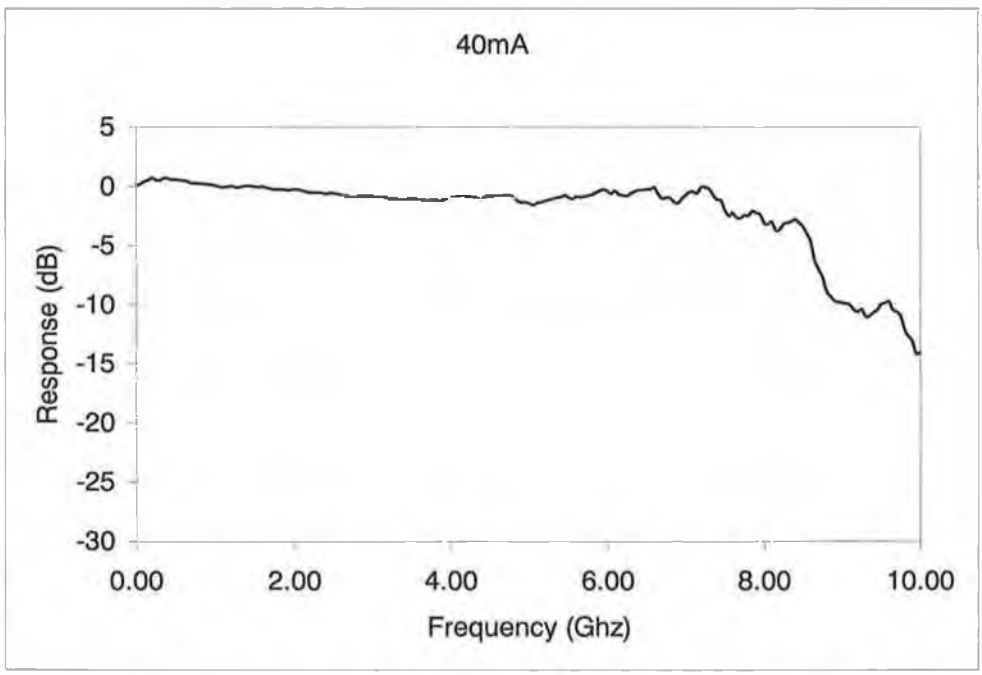

Frequency response plot for 1.5 μm FP (KELD 1501R CCC_1)

APPENDIX F

Refereed Journals

1) L. P. Barry and P. Anandarajah, "Effect of Side Mode Suppression on the Performance of Self-Seeded, Gain-Switched Optical Pulses in Lightwave Communication Systems", *IEEE Photon. Technol. Lett.*, Vol. 11, pp 1360-1362, 1999.

2) L. P. Barry and P. Anandarajah, "Cross Channel Interference due to Mode Partition Noise in WDM Optical Systems Using Self-Seeded Gain-Switched Pulse Sources", *IEEE Photon. Technol. Lett.*, Vol. 13, pp 242-244, 2000.

3) L P Barry and P Anandarajah, "Optical Pulse Generation at Frequencies up to 20 GHz Using External-Injection Seeding of a Gain-Switched Commercial Fabry-Perot Laser", *IEEE Photon. Technol. Lett.*, Vol. 13, pp 1014-1016, 2001.

4) P. Anandarajah, L. P. Barry and A. Kaszubowska, "Performance Issues Associated with WDM Optical Systems Using Self-Seeded Gain-Switched Pulse Sources Due to Mode Partition Noise Effects", *IEEE Photon. Technol. Lett.*, Vol. 14, pp 1202-1204, 2002.

5) A. Kaszubowska, P. Anandarajah and L.P. Barry, "Multiple RF Carrier Distribution in a Hybrid Radio/Fiber System Employing a Self-Pulsating Laser Diode Transmitter," *IEEE Photon. Technol. Lett.*, Vol. 14, pp 1599-1601, 2002.

Reviewed Conferences

1) P. Anandarajah A. Kaszubowska and L. P. Barry, "High frequency pulse generation using a gain switched commercial semiconductor laser with strong external injection", *IEEE High Frequency Postgraduate Student Colloquium*, Dublin, 7-8 September 2000

2) L. P. Barry, P. Anandarajah and A. Kaszubowska, "Optical pulse generation at 18GHz using external injection seeding of gain switched commercial Fabry Perot laser", *IEEE LEOS conference*, Puerto Rico, November 2000

3) P. Anandarajah, L. P. Barry and A. Kaszubowska, "Cross channel interference due to mode partition noise in WDM optical systems", *IEEE 3rd International Conference on Transparent Optical Networks*, Cracow, 18-21 June 2001

4) P. Anandarajah, L. P. Barry and A. Kaszubowska, "Cross channel interference due to mode partition noise in WDM systems", *IEEE High Frequency Postgraduate Student Colloquium*, Cardiff, 9-10 September 2001

5) P. Anandarajah and L. P. Barry, "Effect of cross channel interference on the BER of WDM optical systems using self-seeded gain-switched pulse sources *IEEE 14th LEOS Annual Meeting*, San Diego, 11-15 November 2001

6) P. Anandarajah, L. P. Barry and A. Kaszubowska, "BER measurements on WDM optical systems using self seeded gain switched pulse sources", *7th Opto-Electronics Communications Conference (OECC 2002)*, July 2002, Japan.

7) P. Anandarajah, L. P. Barry and A. Kaszubowska, "Performance issues associated with WDM optical systems using self seeded gain switched pulse sources", *SPIE's Regional Meeting on Optoelectronics, Photonics and Imaging, Opto-Ireland*, 5-6 September 2002, Galway

8) A. Kaszubowska, L. Barry, P. Anandarajah, "Self pulsating laser diode for the generation of multiple data channels in hybrid radio/fiber systems", *15th LEOS Annual Meeting*, Glasgow, 11-15 November 2002

9) L.P. Barry, P. Anandarajah, S. Del burgo, R.T. Watts, D.A Reid and J. Harvey, "Optimization of 40 Gbit/s Transmission Systems using Frequency Resolved Optical Gating Characterization Techniques", *15th LEOS Annual Meeting*, Glasgow, 11-15 November 2002

Effect of Side-Mode Suppression Ratio on the Performance of Self-Seeded Gain-Switched Optical Pulses in Lightwave Communications Systems

L. P. Barry and P. Anandarajah

Abstract— **The side-mode suppression ratio (SMSR) of self-seeded gain-switched optical pulses is shown to be an extremely important factor for the use of these pulses in optical communications systems. Experiments carried out involving pulse propagation through dispersion-shifted fiber and a bandpass optical filter demonstrate that, for SMSR values of less than 25 dB, the buildup of noise due to the mode partition effect may render these pulses unsuitable for use in optical communications systems.**

Index Terms— **Optical fiber communication, optical fiber dispersion, optical pulse generation, self-seeding, semiconductor laser.**

I. Introduction

THE DEVELOPMENT of a wavelength-tunable source of short optical pulses is extremely important for use in future wavelength division multiplexed (WDM), optical time division multiplexed (OTDM), and hybrid WDM/OTDM optical communications systems [1]. One of the simplest and most reliable techniques available to generate wavelength-tunable picosecond optical pulses involves the self-seeding of a gain-switched Fabry–Perot (FP) laser [2]–[7]. The technique basically involves gain-switching an FP laser and then feeding back one of the laser modes into the FP diode using a wavelength-selective external cavity. Provided that the optical signal reinjected into the laser arrives during the build-up of an optical pulse in the FP laser, then a single-moded output pulse is obtained. This technique has been shown to be capable of producing very low jitter optical pulses [4] with durations around 2 ps, and recent experiments have also demonstrated the generation of multiwavelength pulses suitable for use in WDM networks [7].

Although the generation of optical pulses using the self-seeding gain-switching (SSGS) technique has been widely investigated, the use of such pulses in optical communications systems has not yet been examined. In this letter, we experimentally investigate the effect of the pulse side-mode suppression ratio (SMSR) on the performance of SSGS pulses in optical communications systems. This is achieved by simply examining the propagation of these pulses through two key components of any optical network (i.e., optical fiber and an optical filter), as a function of the SMSR. Our results show that, although many of the previous reported wavelength-tunable pulse sources using the SSGS technique had SMSR's which varied between 10–25 dB as the output pulse wavelength was tuned [6], [7], in practice, such pulses may be unsuitable for use in either WDM or OTDM systems. The reason for this lies in the buildup of noise on the optical pulses due to the mode partition effect [8], [9]. It is thus vital that any wavelength-tunable pulse source based on the SSGS technique retains a large enough SMSR, at all operating wavelengths, to prevent the accumulation of mode partition noise.

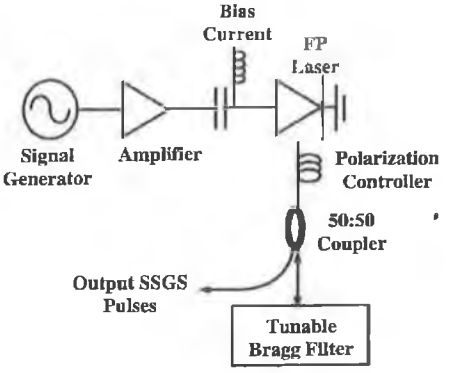

Fig. 1. Experimental setup for SSGS pulse generation.

II. Experimental Setup

Fig. 1 shows our experimental setup. The FP laser used was a commercial 1.5-μm InGaAsP device, with a threshold current of 26 mA and a longitudinal mode spacing of 1.12 nm. Gain switching of the laser was carried out by applying a dc bias current of 17 mA, and a sinusoidal modulation signal with a power of 29 dBm, to the laser diode. The sinusoidal modulation signal had a frequency around 2.6 GHz. Self-seeding of the gain-switched laser diode was achieved by using an external cavity containing a polarization controller (PC), a 3-dB coupler, and a tunable fiber Bragg grating with a bandwidth of 0.4 nm.

To achieve optimum SSGS pulse generation, the central wavelength of the fiber grating was initially tuned to one of the longitudinal modes of the gain-switched laser. The frequency of the sinusoidal modulation was then varied to

Manuscript received May 21, 1999; revised July 28, 1999.

The authors are with the School of Electronic Engineering, Dublin City University, Dublin 9, Ireland.

Publisher Item Identifier S 1041-1135(99)08661-9.

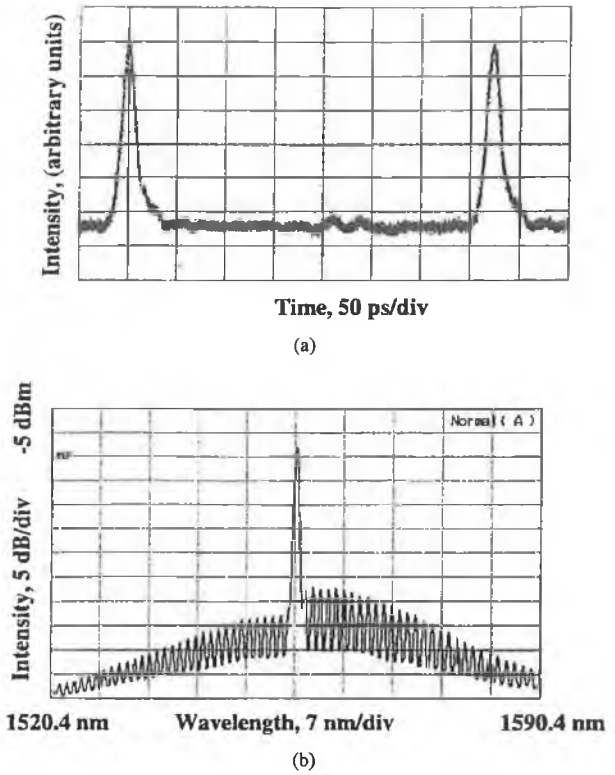

Fig. 2. (a) Optical pulses generated from the SSGS setup. (b) Optical spectrum of SSGS pulses.

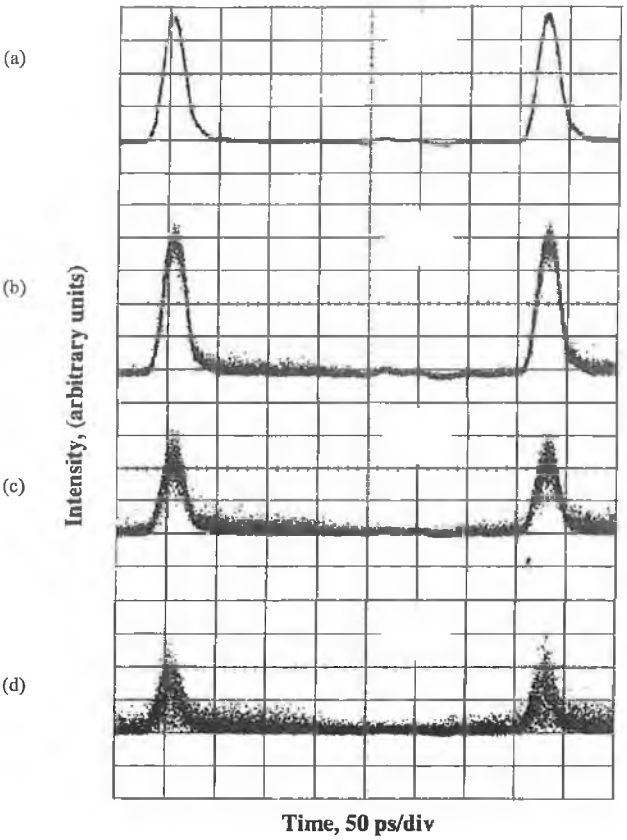

Fig. 3. Output optical pulses after propagation through 10 km of DSF with the input SMSR of the pulses set to: (a) 25 dB, (b) 20 dB, (c) 15 dB, and (d) 10 dB. Persistence of the digitizing oscilloscope display was set to 3 s.

ensure that the signal, reinjected into the laser from the external cavity, arrives as an optical pulse is building up in the laser. An operating frequency of 2.654 GHz was found to be suitable. In addition to tuning the fiber grating and the modulation frequency, we could also vary the amount of light reinjected, and, hence, the SMSR of the output optical pulses, by adjusting the PC. The output pulses after the 50 : 50 fiber coupler were characterized in the temporal domain using a 50-GHz photodiode in conjunction with a 50-GHz HP digitizing oscilloscope. Pulse characterization in the spectral domain was carried out using an optical spectrum analyzer.

III. Results and Discussion

With the PC adjusted to maximize the feedback into the FP device, the resulting output pulses from the SSGS set-upwere as shown in Fig. 2. Assuming a total response time of about 9 ps for the combination of the photodiode and the oscilloscope, we can deconvolve the output pulse duration to be around 15 ps. From the spectral output, we can determine that the FP mode selected using the Bragg grating was at a wavelength of 1555.4 nm. In addition, the SMSR of the signal was 30 dB, and the 3-dB spectral width was about 0.6 nm. To vary the SMSR of the generated optical pulses from 30 dB down to 10 dB, we simply had to adjust the PC in order to reduce the amount of light fed back into the laser diode. The reduction in feedback and SMSR also resulted in a slight decrease in the pulse duration and a slight increase in the spectral width, as expected from previous work [10], [11].

The optical pulses from the SSGS were initially propagated through 10 km of dispersion-shifted fiber (DSF), and the effect of a varying SMSR on the pulse propagation was investigated. With the SMSR set to 30 dB, the only effect of the fiber transmission was a slight broadening of the pulses due to the fiber dispersion [$D = 1.8$ ps/(km.nm) at 1555 nm]. However, as the SMSR was reduced, the noise level on the transmitted signal began to increase. Fig. 3(a)–(d) shows the output pulses after fiber propagation corresponding to input SMSR's of 25, 20, 15, and 10 dB, respectively. From this figure, we can see the noise level on, and between, the transmitted pulses beginning to appear as the SMSR was reduced from 25 to 20 dB. When the SMSR was set to 15 and 10 dB, the noise on the optical pulses after transmission became even more obvious. This noise would clearly make the use of these pulses unfeasible in optical communication systems.

The increase in noise as the SMSR is reduced is associated with the mode partition effect of the FP laser [8]. The mode partition effect is basically a fluctuation of the energy in each laser mode with time, due to a constant transfer of energy between the laser modes. When an optical pulse with a multimoded spectrum propagates in a dispersive fiber medium, the laser modes travel at different speeds and, hence, spread out in the temporal domain. The spectral fluctuation in the laser modes will thus manifest itself as an intensity fluctuation

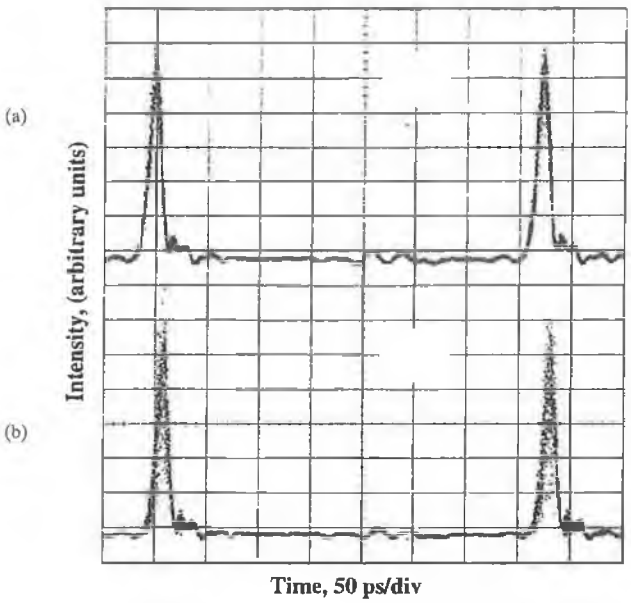

Fig. 4. Optical pulses at output of an FP filter with the SMSR of the input signal set to: (a) 20 dB and (b) 15 dB. Persistence of the digitizing oscilloscope display was set to 3 s.

(noise) on the transmitted optical signal after fiber propagation. To eliminate this noise, it is necessary to use a single-moded laser pulse in which the total power in the side modes is negligible. From our experiment, we have seen that, with a SMSR of 25 dB or greater, the noise on the optical pulse after propagation is essentially negligible, because the total pulse power in the side modes is negligible. However, as the SMSR is reduced and the power in the side modes becomes nonnegligible, the energy fluctuation of the modes results in an increasing noise level on the transmitted pulses.

We then investigated the effect of a varying SMSR on the propagation of the optical pulses through a tunable FP filter with a 3-dB bandwidth of 0.8 nm. The filter was tuned to select out the main operating mode from the SSGS pulse spectrum. With the input pulse SMSR at 30 dB, the only effect on the optical pulse was a slight reduction in its duration. However, as the SMSR was reduced, the pulse after the optical filter developed a large amount of amplitude noise. Fig. 4 displays the output pulses when the SMSR of the input signal was 20 and 15 dB, respectively. The amplitude noise on the pulses is once again due to the mode partition effect [9]. Since only the main mode is transmitted through the optical filter, any temporal fluctuations in the energy level of this mode will result in amplitude noise on the transmitted pulse. Clearly as the SMSR is reduced, the energy in the side mode increases and the fluctuation of the energy in the main mode increases, resulting in additional amplitude noise on the transmitted pulse.

IV. Conclusion

We have examined the effect of SMSR on the propagation of SSGS optical pulses through optical fiber and an optical filter. Our results show that the performance of SSGS pulses in WDM and OTDM communications systems is highly dependent on the SMSR of the generated pulses. If the SMSR is not large enough, then the interaction of the mode partition effect with either fiber dispersion, or spectral filtering, results in a large amount of amplitude noise on the transmitted optical pulses. This noise will render such pulses totally unsuitable for data transmission in optical communications.

References

[1] T. Morioka, H. Takara, S. Kawanishi, O. Kamatani, K. Takiguchi, K. Uchiyama, M. Saruwatari, H. Takahashi, M. Yamada, T. Kanamori, and H. Ono, "1Tbit/s (100Gbit/s times 10 channel) OTDM/WDM transmission using a single super continuum WDM source," *Electron. Lett.*, vol. 32, pp. 906–907, 1996.

[2] M. Cavelier, N. Stelmakh, J. M. Xie, L. Chusseau, J. M. Lourtioz, C. Kasmierski, and N. Bouadama, "Picosecond (<2.5 ps) wavelength tunable (~20 nm) semiconductor laser pulses with repetition rates up to 12 GHz," *Electron. Lett.*, vol. 28, pp. 224–226, 1992.

[3] L. P. Barry, R. F. O'Dowd, J. Debeau, and R. Boittin, "Tunable transform limited pulse generation using self-injection locking of a FP laser," *IEEE Photon. Technol. Lett.*, vol. 5, pp. 1132–1134, 1993.

[4] M. Schell, W. Utz, D. Huhse, J. Kassner, and D. Bimberg, "Low jitter single mode pulse generation by a self-seeded, gain-switched Fabry-Perot semiconductor laser," *Appl. Phys. Lett.*, vol. 65, pp. 3045–3047, 1994.

[5] Y. C. Lee and C. Shu, "Optimized operation of self-seeded gain-switched laser diode for electrically wavelength-tunable singlemode pulses," *IEEE Photon. Technol. Lett.*, vol. 7, pp. 275–277, 1995.

[6] D. Huhse, M. Schell, W. Utz, J. Kassner, and D. Bimberg, "Dynamics of single-mode formation in self-seeded Fabry–Perot laser diodes," *IEEE Photon Technol. Lett.*, vol. 7, pp. 351–353, 1995.

[7] C. Shu and S. P. Yam, "Effective generation of tunable single- and multiwavelength optical pulses from a Fabry–Perot laser diode," *IEEE Photon Technol. Lett.*, vol. 9, pp. 1214–1216, 1997.

[8] N. H. Jensen, H. Olesen, and K. E. Stubkjaer, "Partition noise in semiconductor lasers under CW and pulsed operation," *IEEE J. Quantum Electron.*, vol. QE-23, pp. 71–79, 1987.

[9] D. Curter, P. Pepeljugoski, and K. Y. Lau, "Noise properties of electrically gain-switched 1.5 μm DFB lasers after spectral filtering," *Electron. Lett.*, vol. 30, pp. 1418–1419, 1994.

[10] L. P. Barry, B. C. Thomsen, J. M. Dudley, and J. D. Harvey, "Characterization of 1.55 μm pulses from a self-seeded gain-switched Fabry–Perot laser diode using frequency-resolved optical gating," *IEEE Photon. Technol. Lett.*, vol. 10, pp. 935–937, 1998.

[11] S. Bouchoule, N. Stelmakh, M. Cavelier, and J.-M. Lourtioz, "Highly attenuating external cavity for picosecond-tunable pulse generation from gain/Q-switched laser diodes," *IEEE J. Quantum Electron.*, vol. 29, pp. 1693–1700, 1993.

Cross-Channel Interference Due to Mode Partition Noise in WDM Optical Systems Using Self-Seeded Gain-Switched Pulse Sources

L. P. Barry, *Member, IEEE*, and P. Anandarajah, *Student Member, IEEE*

***Abstract*—The sidemode suppression ratio of self-seeded, gain-switched optical pulses is shown to be a vital parameter in determining the usefulness of these pulses in wavelength-division-multiplexed communications systems. Experiments carried out on a two-channel wavelength multiplexed setup using tunable self-seeded gain-switched pulse sources at 10 GHz, have demonstrated the cross-channel interference effects that may be encountered if the sidemode suppression ratio of one of the sources becomes degraded.**

***Index Terms*—Gain-switching, optical fiber communications, optical pulse generation, self-seeding, semiconductor laser, wavelength-division-multiplexing.**

I. Introduction

THE DEVELOPMENT of a wavelength-tunable source of short optical pulses operating at 10 GHz is vital for use in wavelength-division-multiplexed (WDM), optical time-division-multiplexed (OTDM), and hybrid WDM/OTDM optical communication systems [1]. One of the most reliable techniques available to generate wavelength-tunable, picosecond optical pulses involves the self-seeding of a gain-switched Fabry–Perot (FP) laser [2]–[4]. One important characteristic of these sources is the variation in the sidemode suppression ratio (SMSR) as the wavelength is tuned [2]–[4], as this may ultimately affect their usefulness in optical communication systems. In a recent letter [5], we demonstrated how this SMSR variation greatly affected the noise induced on a single 2.5-GHz pulse source as the pulses propagated through optical fiber and an optical filter.

In this letter, we experimentally investigate the effect of the pulse SMSR on the performance of 10-GHz self-seeded gain-switched (SSGS) pulse sources in a two-channel WDM-type system. We examine the noise induced on one of the pulse sources due to a variation in SMSR of the other SSGS source. Our results show that although many of the reported wavelength-tunable pulse sources using the SSGS technique had SMSRs that varied between 10 and 25 dB as the output pulse wavelength was tuned [2]–[4], in practice, such pulses may be unsuitable for use in high-speed WDM communication systems due to cross-channel interference caused by the mode partition effect [6], [7].

Manuscript received June 28, 2000; revised November 13, 2000.

The authors are with the School of Electronic Engineering, Dublin City University, Dublin 9, Ireland (e-mail: barryl@eeng.dcu.ie).

Publisher Item Identifier S 1041-1135(01)01997-8.

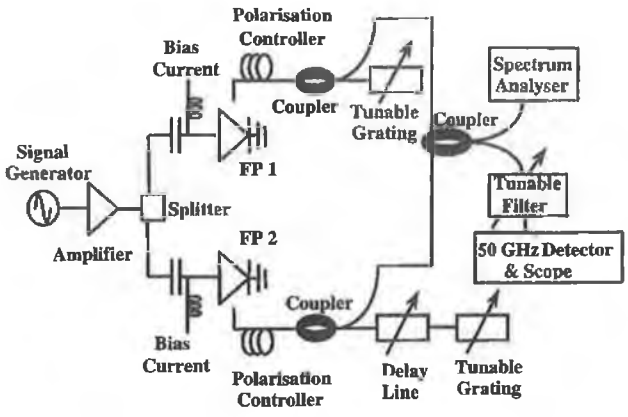

Fig. 1. Experimental setup for examining the effects of SMSR variation in a WDM-type system using two SSGS pulse sources.

II. Experimental Setup

Fig. 1 shows our experimental setup. The FP lasers used were commercial 1.5-μm InGaAsP devices, with threshold currents around 25 mA and longitudinal mode spacings of 1.1 nm. The two lasers used had central frequencies of 1556 nm. Gain switching of the lasers was carried out by applying dc bias currents of around 45 mA, and 10-GHz sinusoidal modulation signals with powers of 24 dBm, to each device. Self seeding of the diode FP1 was achieved by using an external cavity containing a polarization controller (PC), a 3-dB coupler, and a tunable Bragg grating with a bandwidth of 0.4 nm. The external cavity for self-seeding FP2 contained an additional tunable optical delay line.

To achieve optimum SSGS pulse generation from FP1, the grating was tuned to reflect one of the laser modes (at 1556 nm), and the frequency of the sinusoidal modulation was then varied ($\sim$9.987 GHz) to ensure that the signal reinjected into the laser arrives at the correct time. For SSGS operation of FP2, the Bragg grating was tuned to reflect a laser mode at 1546 nm, and the optical delay line was varied to ensure that the signal fed back from the grating arrives at the correct time. It should also be noted that the wavelength of each source may be tuned using the fiber grating, but the tuning range was limited to about 5 nm by the tunability of the grating. In addition to tuning the grating, and adjusting the sinusoidal frequency, the feedback can be adjusted, (and thus the SMSR on the output pulses varied), by using the polarization controllers (PC).

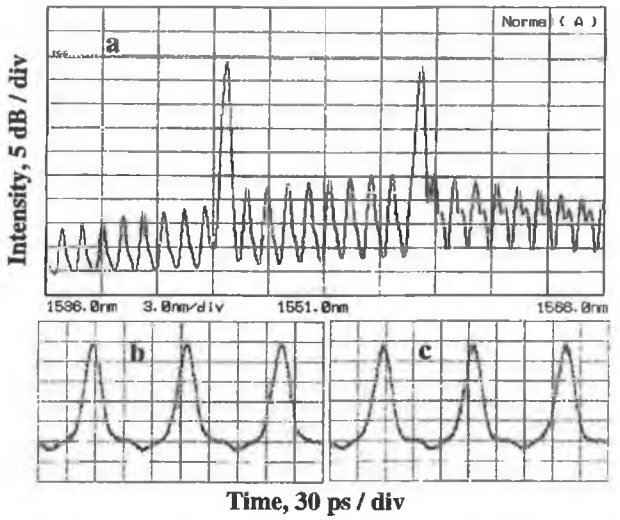

Fig. 2. (a) Optical spectrum of the two 10-GHz pulse sources after fiber coupler. (b) and (c) 10-GHz pulse trains of the 1546- and 1556-nm sources (nonaveraged).

III. Results

Fig. 2(a) displays the optical spectrum of the two pulse sources after being combined together using a fiber coupler, (with the feedback from the gratings optimized using the polarization controllers). The 3-dB bandwidths of the 10-GHz pulse sources were both around 0.25 nm, and the SMSR of the sources at 1546 nm and 1556 nm were 27 dB and 25 dB, respectively [these SMSR values have been obtained by examining the spectral output from each source independently, and not from the composite signal shown in Fig. 2(a)]. Fig. 2(b) and (c) displays the two pulse waveforms from the sources when they were subsequently filtered out from the composite signal using a tunable FP filter with a bandwidth of 0.7 nm. This particular filter bandwidth is chosen as it is narrow enough to select only a single mode from the optical signal, but large enough such that it does not affect the shape of the optical pulses passing through it. The pulses were detected and measured using a 50-GHz pin photodiode in conjunction with a 50-GHz digitizing oscilloscope. The output pulse duration was 18 ps for the 1546-nm source, and 19 ps for the 1556-nm source.

To determine the effect of SMSR on the filtered signals, we initially varied the SMSR of the 1556-nm pulses using the PC, and examined the noise added to the filtered signal at 1546 nm (which had its SMSR maintained at 27 dB). We should point out that the pulses from the two sources are temporally overlapped, thus the interference from one source is directly on top of the adjacent source in our results. Fig. 3(a), (b), and (c) displays the nonaveraged waveform of the filtered 1546-nm signal with the SMSR of the 1556-nm pulse train set to 20, 15, and 10 dB. We can clearly see that when the SMSR was reduced to 15 dB, the noise on the pulse train after the optical filter became noticeable, and as the SMSR was reduced further, the noise on the signal greatly increased. We then examined the effect of varying the SMSR of the 1546-nm source using the PC, when the FP optical filter was tuned to select out the 1556-nm pulse train (which had its SMSR maintained at 25 dB). Fig. 4(a) and (b) displays the

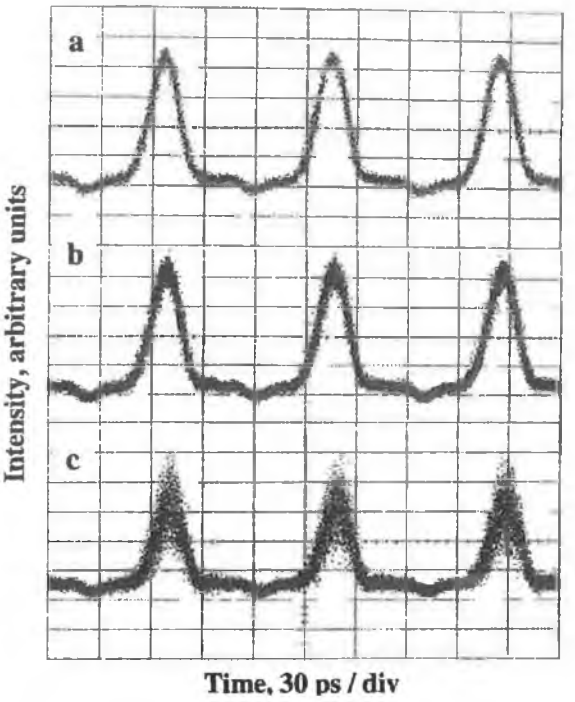

Fig. 3. (a), (b) and (c) 1546-nm pulses after FP filter with the SMSR of the 1556-nm pulse source set to (a) 20, (b) 15, and (c) 10 dB.

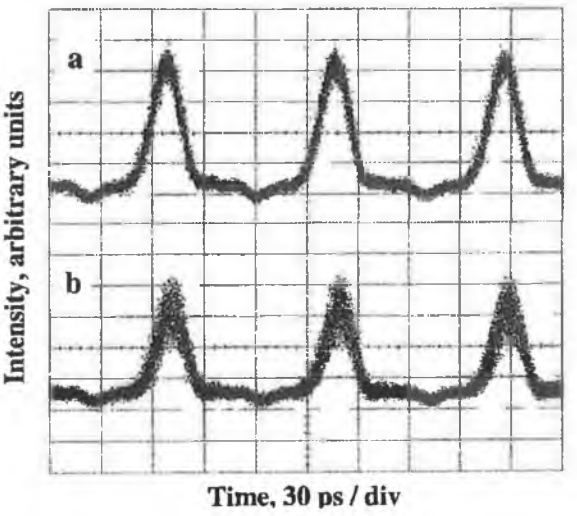

Fig. 4. (a) and (b) 1556-nm pulses after FP filter with the SMSR of the 1546-nm source set to (a) 20 dB, and (b) 15 dB.

filtered 1556-nm pulse train when the SMSR of the 1546-nm signal was set to 20 and 15 dB. We can clearly see that the noise level on the signal increases as the SMSR of the 1546-nm source was reduced.

We subsequently investigated how the mode-partition-noise was affected by varying the spectral spacing between the two sources. In this case, the amplitude noise on the detected pulse was characterized by measuring its rms noise voltage using the digitizing oscilloscope. Fig. 5 displays the results when the SSGS source using FP2 was tuned from 1543.8 to 1548.2 nm

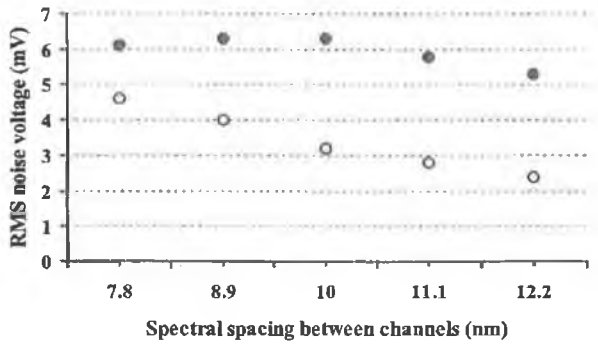

Fig. 5. Rms noise voltage (due to cross-channel interference) on detected pulses from FP1 (•) and FP2 (○), as their wavelengths are tuned over 5 FP modes, with the SMSR of the adjacent pulse source (fixed wavelength) set to 15 dB.

(with its SMSR kept constant around 27 dB), and the SMSR of the SSGS at 1556 was set to 15 dB. We can see that as the spectral spacing decreases, the noise level on the filtered out signal from FP2 increases. We then tuned the pulse source from FP1 between 1553.8 and 1558.2 nm (with its SMSR kept constant around 25 dB), and examined the interference due to the 1546-nm SSGS source from FP2 (with its SMSR set to 15 dB). These results are also shown in Fig. 5, and demonstrate that in this case the noise level on the filtered out pulse is actually maximum when it is at 1556 nm (approximately 10-nm spacing between the SSGS sources), and decreases slightly as the source is tuned to higher or lower wavelengths.

IV. Discussion and Conclusion

The noise acquired on a filtered pulse source as the SMSR of the other SSGS pulse source is reduced, is due to the mode partition effect [6], [7]. This effect is basically a fluctuation of the energy in each laser mode with time, due to a constant transfer of energy between the modes. For a single-mode laser with a large SMSR, the power in the side modes is negligible, thus the power fluctuation of the main mode is negligible. However, as the SMSR decreases, the power fluctuation of the main mode, and the side modes, may become nonnegligible. When the optical filter is tuned to select out either the 1546- or 1556-nm signal, the noise on the pulse train will be negligible provided the SMSRs of both sources is large [as shown in Fig. 2(b) and (c)]. If the SMSR of the filtered signal is reduced, then the noise level on that pulse source would clearly increase due to the mode partition effect, as already demonstrated and explained in [5]. However, in this experiment we have demonstrated the increased noise induced on one filtered pulse source due to a reduction in SMSR of a second SSGS source. This noise is also due to the mode partition effect, because as the SMSR of one SSGS pulse source is reduced, the power (and the power fluctuation) in its side mode, which is at the same wavelength as the second pulse source selected by the FP filter, increases. The temporal fluctuation in power of this side mode can thus manifest itself as noise on the filtered source.

In order to explain the variation in amplitude noise as the spectral spacing between the sources is varied, it is necessary to understand that the cross-channel interference (caused by mode-partition-noise) on channel 1 due to channel 2 is determined by the power in the side mode of channel 2, which is at the same wavelength as channel 1. The power in the side mode of any SSGS pulse source (using an FP laser) is determined by the spacing between the side mode and the peak of the FP gain curve. Thus, as the wavelength of channel 1 is varied, the cross-channel interference due to channel 2 is determined by the position (wavelength) of channel 1 relative to the gain curve of the FP laser used to generate the SSGS pulses for channel 2.

In conclusion, we have shown that the SMSR of wavelength-tunable SSGS pulse sources at 10 GHz is extremely important for determining their usefulness in WDM communication systems. If the SMSR of one source in a WDM system becomes degraded, then the interaction of the mode partition effect with spectral filtering can result in a large amount of noise on all the wavelength channels in the communications system. This noise could clearly lead to an unacceptable error rate in the communication system. It is thus vital that any WDM transmission system based on tunable SSGS pulse sources maintains a large SMSR (preferably greater than 30 dB) at all wavelengths.

References

[1] T. Morioka, H. Takara, S. Kawanishi, O. Kamatani, K. Takiguchi, K. Uchiyama, M. Saruwatari, H. Takahashi, M. Yamada, T. Kanamori, and H. Ono, "1Tbit/s (100Gbit/s times 10 channel) OTDM/WDM transmission using a single supercontinuum WDM source," *Electron. Lett.*, vol. 32, pp. 906–907, May 1996.

[2] L. P. Barry, R. F. O' Dowd, J. Debeau, and R. Boittin, "Tunable transform limited pulse generation using self-injection locking of a FP laser," *IEEE Photon. Technol. Lett.*, vol. 5, pp. 1132–1134, Oct. 1993.

[3] M. Schell, W. Utz, D. Huhse, J. Kassner, and D. Bimberg, "Low jitter single mode pulse generation by a self-seeded, gain-switched Fabry–Perot semiconductor laser," *Appl. Phys. Lett.*, vol. 65, pp. 3045–3047, 1994.

[4] C. Shu and S. P. Yam, "Effective generation of tunable single- and multi-wavelength optical pulses from a Fabry–Perot laser diode," *IEEE Photon. Technol. Lett.*, vol. 9, pp. 1214–1216, Sept. 1997.

[5] L. P. Barry and P. Anandarajah, "Effect of side mode suppression ratio on the performance of self-seeded, gain-switched optical pulses in lightwave communications systems," *IEEE Photon. Technol. Lett.*, vol. 11, pp. 1360–1363, Nov. 1999.

[6] N. H. Jensen, H. Olesen, and K. E. Stubkjaer, "Partition noise in semiconductor lasers under CW and pulsed operation," *IEEE J. Quantum Electron.*, vol. QE-23, pp. 71–79, 1987.

[7] D. Curter, P. Pepeljugoski, and K. Y. Lau, "Noise properties of electrically gain-switched 1.5 μm DFB lasers after spectral filtering," *Electron. Lett.*, vol. 30, pp. 1418–1419, 1994.

Optical Pulse Generation at Frequencies up to 20 GHz Using External-Injection Seeding of a Gain-Switched Commercial Fabry–Pérot Laser

L. P. Barry, *Member, IEEE*, P. Anandarajah, *Student Member, IEEE*, and A. Kaszubowska, *Student Member, IEEE*

***Abstract*—We demonstrate that by using strong external-injection seeding of gain-switched Fabry–Pérot (FP) lasers, it is possible to generate optical pulses at repetition rates far in excess of the laser bandwidth. Experimental results illustrate the generation of optical pulses at frequencies up to 20 GHz from a FP laser with a 3-dB bandwidth of only 8 GHz. The optical pulses generated have a duration around 12 ps, and a spectral width of 40 GHz.**

***Index Terms*—External injection, gain-switching, optical communications, optical pulse generation, semiconductor lasers, ultrafast optics.**

I. Introduction

THE DEVELOPMENT of optical pulse sources at high repetition rates (>10 GHz) is extremely important for use in future high-speed optical communications systems [1]. One of the simplest and most reliable techniques available to generate high-quality, single-mode, optical pulses involves self- or external-injection seeding of a gain-switched Fabry–Pérot (FP) laser [2]–[7]. This technique has been shown to be capable of producing very low-jitter optical pulses [3], [6] that can be tuned over wavelength ranges approaching 40 nm. As for the repetition rate, at which pulses can be generated using a gain-switched laser diode, it is essentially limited by the bandwidth of the device. In order to achieve gain-switched operation at frequencies in excess of 10 GHz, it is usually necessary to have specially developed laser diodes with bandwidths greater than 10 GHz [5], [7]. However, by using strong external-injection of light into a laser, it has also been shown that the laser bandwidth can be significantly enhanced [8], [9]. This bandwidth improvement should thus be useful for increasing the frequency at which pulses can be generated using the gain-switching technique with commercial lasers. In this letter, we experimentally demonstrate how strong external-injection into a gain-switched FP diode increases the bandwidth of the laser such that pulses can be generated at frequencies up to 20 GHz, which is far beyond what would be possible with the laser's inherent bandwidth of 8 GHz. The optical pulses generated have pulsewidths around 12 ps and spectral widths of 40 GHz.

Manuscript received September 29, 2000; revised March 9, 2001.

The authors are with the School of Electronic Engineering, Dublin City University, Dublin 9, Ireland (e-mail: barryl@eeng.dcu.ie).

Publisher Item Identifier S 1041-1135(01)07523-1.

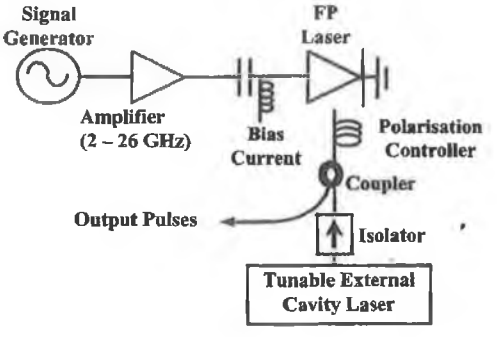

Fig. 1. Experimental setup for external-injection seeding of gain-switched FP laser.

II. Experimental Setup and Results

Fig. 1 shows our experimental setup. The FP laser used was a commercial 1.5-μm InGaAsP device from NTT Electronics, with a threshold current of 26 mA and a longitudinal mode spacing of 1.25 nm. The laser is manufactured for use in 10-Gb/s systems and has a specified bandwidth of around 8 GHz at an injection current level of 50 mA. Gain-switching was carried out by applying a dc bias current in conjunction with a sinusoidal modulation to the laser, and the optical signal from the laser was then coupled into fiber using a GRIN lens fiber pigtail, which is antireflection coated (to prevent reflections back into the laser). External-injection seeding of the gain-switched laser was carried out by injecting light from a tunable external cavity laser (ECL) into the gain-switched laser diode via an isolator, a fiber coupler, and a polarization controller. The optical pulses generated from the experimental arrangement were then characterized in the spectral and temporal domains. The optical spectra were examined using an optical spectrum analyzer with a resolution of 0.07 nm, and the temporal measurements were conducted using a 50-GHz pin detector followed by an Agilent 50-GHz sampling oscilloscope. The total time resolution of our measurement system is 12 ps; this has been measured with the use of a subpicosecond optical pulse source [10].

Before gain-switching the laser, we initially measured its modulation response with and without external injection, using a 40-GHz network analyzer. Fig. 2 shows the response when the free-running laser was biased at 40 mA. The relaxation frequency was 7.3 GHz, and the 3-dB bandwidth was around 8.4 GHz in this case. We then injected light from the ECL into the FP laser, as shown in Fig. 1, and tuned the wavelength of

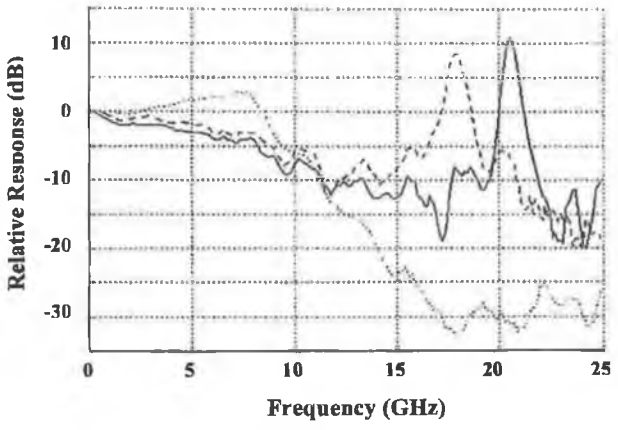

Fig. 2. Modulation response of free running FP laser diode with applied bias current of 40 mA (dotted line), and response of laser diode with external injection levels of 3 mW (solid line) and 1.5 mW (dashed line) from tunable ECL.

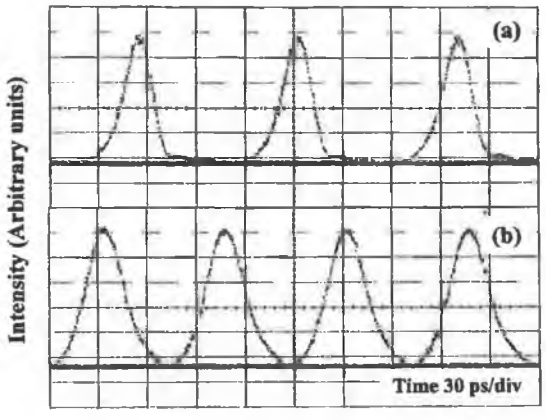

Fig. 3. Optical pulse train from gain-switched FP laser without external-injection at frequencies of (a) 10 GHz and (b) 13 GHz. The zero optical power level is also shown in the figure.

the injected light to one of the longitudinal modes of the FP laser. The polarization controller was varied to maximize the sidemode suppression ratio (SMSR) of the output spectrum from the laser, in order to ensure maximum coupling of light from the ECL laser into the FP diode. The output power from the ECL was then set to 4 dBm (maximum possible), and its wavelength was tuned slightly to obtain the maximum relaxation frequency. The resulting response of the laser (biased at 40 mA) was as shown in Fig. 2, and we can see that the relaxation frequency was greatly enhanced to 21 GHz. By gradually reducing the output power from the external cavity laser, we were also able to reduce the relaxation frequency from 21 GHz to any frequency down to 10 GHz. The modulation response when the output power from the ECL was set to 1 dBm is also shown in Fig. 2.

The laser was then initially gain-switched at a frequency of 10 GHz without external injection, and optimum operation (minimum output pulsewidth) was achieved with a bias current of 42 mA and a sinusoidal modulation power of 28 dBm. Fig. 3(a) displays the optical pulses generated from the FP laser; the pulsewidth (after deconvolving the time resolution of

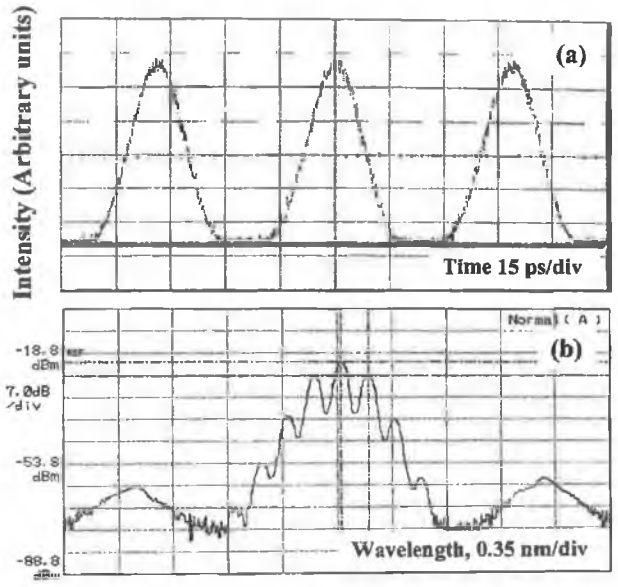

Fig. 4. (a) 20 GHz optical pulse train (with zero optical power level shown) and (b) associated optical spectrum, from gain-switched laser with external-injection level of 4 dBm from ECL.

the measurement system) was around 18 ps. We then proceeded to increase the frequency of the modulation signal applied to the laser diode, and adjust the bias current to obtain optimum pulses from the setup. At frequencies around 13 GHz, it became increasingly difficult to properly gain switch the laser [as shown in Fig. 3(b)], due to the limited bandwidth displayed in the dashed line of Fig. 2, and at frequencies beyond 15 GHz, the modulated optical signal from the laser became negligible. We then injected light from the continuous-wave (CW) external cavity laser into the gain-switched FP laser, as shown in Fig. 1, and tuned the wavelength of the injected light, and the polarization controller as explained earlier. The output power from the CW laser was set to 4 dBm, and taking into account the attenuation of the isolator and the fiber coupler, and the coupling loss between the GRIN lens and the laser diode, we estimate the external injection level into the FP laser to be around −4 dBm. The laser was subsequently gain-switched at 10 GHz as before with a modulation power of 28 dBm; however, this time the optimum bias current required was 29 mA. The frequency of the applied modulation signal was then increased, and the bias current adjusted to optimize the laser gain-switching. Fig. 4 displays the optical output pulses and associated spectrum when the laser was gain-switched using a bias current of 48 mA, and a modulation signal power of 26 dBm at 20 GHz. The pulse duration (after deconvolving the measured pulsewidth with the resolution of the measurement system) and spectral width were 12 ps and 40 GHz, respectively, giving a time-bandwidth product of 0.48, which is close to the time-bandwidth product of transform-limit Gaussian pulses (0.44). We can also see from Fig. 4(b) that the SMSR of the pulse source was nearly 40 dB. By subsequently tuning the wavelength from the ECL to different modes of the FP laser diode, we were also able to successfully tune the high-frequency pulse train over a range of around 12 nm. Fig. 5 displays the temporal output from the

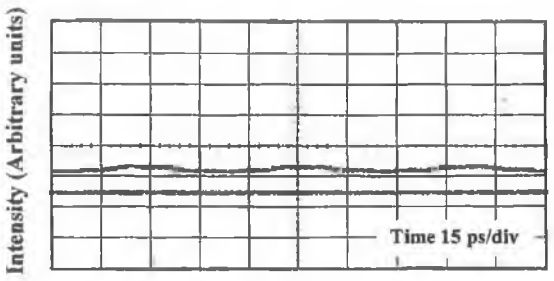

Fig. 5. Output signal from laser diode when injection level from ECL was reduced to 1 dBm (with the zero optical power level also displayed) with 20-GHz modulation applied.

laser under the same conditions as those used for Fig. 4, except that the injected power from the ECL was set to 1 dBm. As we can see, the reduced injection level alters the response of the laser (see Fig. 2) such that it cannot be gain-switched at 20 GHz.

III. Discussion

Previous studies on the bandwidth enhancement of lasers diodes under the influence of external-injection have shown that it is possible to increase the bandwidth by a factor of around three [8], [9]. In our experiment, we use a laser with a free running bandwidth of around 8 GHz, and we have managed to achieve a resonance frequency of beyond 20 GHz by using the strong external-injection. This bandwidth enhancement thus makes it possible for us to gain-switch the laser at far higher frequencies than what would be possible with the lasers inherent bandwidth. It should also be noted that the optical pulses generated from the setup are nearly transform limited (time-bandwidth product of 0.48). This is because the external injection is not only responsible for the bandwidth enhancement, but also results in significant chirp reduction on the output signal [7], [8], [11].

The resulting optical pulsewidth due to injection seeding, as the wavelength of the injected light is varied, has been studied in [7]. It was found that for negative frequency detuning, the distortion in the pulse waveform can result in shorter optical pulses than would be obtained without injection seeding. In addition, from [8], the optimum improvement in relaxation frequency is obtained by external injection at frequencies which are negatively detuned. Since our ECL is tuned to optimize the relaxation frequency, this is therefore consist with the slight reduction in pulsewidth obtained between the 10-GHz pulses without injection-seeding, and the 20-GHz gain-switched pulses with external injection. In addition, the pulsewidth generated under gain-switching conditions will normally decrease as the frequency of the electrical modulation applied increases (laser will turn off faster, resulting in a reduced fall time on the pulse).

In conclusion, we have demonstrated the generation of optical pulses at frequencies up to 20 GHz by using strong external-injection into a gain-switched laser. The commercial FP laser used has an inherent bandwidth of 8 GHz, but the external-injection increases the bandwidth sufficiently to generate near transform-limit pulses at repetition rates well in excess of the lasers free-running bandwidth. By employing this technique with higher speed lasers, it should thus be feasible to develop optical pulse sources suitable for use in optical systems with single-channel bit rates of 40 Gb/s.

References

[1] S. Kawanishi, "Ultrahigh-speed optical time-division-multiplexed transmission technology based on optical signal processing," *IEEE J. Quantum Electron.*, vol. 34, pp. 2064–2079, Nov. 1998.

[2] L. P. Barry, R. Dowd, J. Debeau, and R. Boittin, "Tunable transform limited pulse generation using self-injection locking of a FP laser," *IEEE Photon. Technol. Lett.*, vol. 5, pp. 1132–1134, Oct. 1993.

[3] M. Schell, W. Utz, D. Huhse, J. Kassner, and D. Bimberg, "Low jitter single mode pulse generation by a self-seeded, gain-switched Fabry–Pérot semiconductor laser," *Appl. Phys. Lett.*, vol. 65, pp. 3045–3047, 1994.

[4] I. Y. Khrushchev, I. H. White, and R. V. Penty, "High quality laser diode pulse compression using a dispersion imbalanced loop mirror," *Electron. Lett.*, vol. 34, pp. 1009–1010, May 14, 1998.

[5] Y. Matsui, S. Kutsuzawa, S. Arahira, and Y. Ogawa, "Generation of wavelength tunable gain-switched pulses from FP MQW lasers with external injection seeding," *IEEE Photon. Technol. Lett.*, vol. 9, pp. 1087–1089, Aug. 1997.

[6] D. S. Seo, H. F. Liu, D. Y. Kim, and D. D. Sampson, "Injection power and wavelength dependence of an external-seeded gain-switched Fabry–Pérot laser," *Appl. Phys. Lett.*, vol. 67, pp. 1503–1505, 1995.

[7] Y. Matsui, S. Kutsuzawa, S. Arahira, Y. Ogawa, and A. Suzuki, "Bifurcation in 20 GHz gain-switched 1.55-mm MQW lasers and its control by CW injection seeding," *IEEE J. Quantum Electron.*, vol. 34, pp. 1213–1223, July 1998.

[8] G. Yabre, "Effect of relatively strong light injection on the chirp-to-power ratio and the 3 dB bandwidth of directly modulated semiconductor lasers," *J. Lightwave Technol.*, vol. 14, pp. 2367–2373, Oct. 1996.

[9] X. J. Meng, T. Chau, and M. C. Wu, "Experimental demonstration of modulation bandwidth enhancement in distributed feedback lasers with external light injection," *Electron. Lett.*, vol. 34, pp. 2031–2032, Oct. 15, 1998.

[10] L. P. Barry, B. C. Thomsen, J. M. Dudley, and J. D. Harvey, "Optimised design of a fibre-based pulse compressor for gain-switched DFB laser pulses at 1.5 μm," *Electron. Lett.*, vol. 35, pp. 1166–1168, July 8, 1999.

[11] S. Mohrdiek, H. Burkhard, and H. Walter, "Chirp reduction of directly modulated semiconductor lasers at 10 Gbit/s by strong CW light injection," *J. Lightwave Technol.*, vol. 12, pp. 418–424, Mar. 1994.

Performance Issues Associated With WDM Optical Systems Using Self-Seeded Gain Switched Pulse Sources Due to Mode Partition Noise Effects

P. Anandarajah, *Student Member, IEEE*, L. P. Barry, *Member, IEEE*, and A. Kaszubowska, *Student Member, IEEE*

***Abstract*—Bit-error-rate measurements have been carried out on a four-channel wavelength division multiplexed setup using tunable self-seeded gain-switched pulse sources. These measurements demonstrate the degradation in overall system performance, due to mode partition noise, as the sidemode suppression ratio of the self-seeded gain-switched optical pulse sources is reduced. The results also show that the constraints on the minimum sidemode suppression ratio required increase with the number of channels in the system.**

***Index Terms*—Optical fiber communications, optical pulse generation, mode partition noise, semiconductor laser, wavelength-division multiplexing.**

I. Introduction

As OPTICAL communication systems move to line rates of 40 Gb/s and beyond, it becomes more likely that return-to-zero (RZ) coding will be used for data transmission, as it is easier to compensate for dispersion and nonlinear effects in the fiber by employing soliton-like propagation [1]. In addition to this development, the use of wavelength tunability in optical networks is being explored as a way to provide dynamic provisioning in the next generation of photonic systems [2]. Taking into account these moves toward tunable optical systems employing RZ coding, it is obvious that the development of a wavelength tunable source of short optical pulses will be of paramount importance for future WDM, optical time division multiplexed (OTDM), and hybrid WDM/OTDM optical communication systems [3].

Self-seeding of a gain-switched Fabry–Pérot (FP) laser is one of the most reliable techniques available to generate wavelength tunable optical pulses [4], [5]. An important characteristic of these self-seeded gain-switched (SSGS) sources is the variation in the sidemode-suppression-ratio (SMSR) as the wavelength is tuned [4], [5], as this may ultimately affect their usefulness in optical communication systems. Recent work has demonstrated how this SMSR variation greatly affects the noise induced on a single pulse source as the pulses propagate through optical fiber and an optical filter [6]. In addition, by using two SSGS pulse sources at different wavelengths, we have examined the noise induced on one of the pulse sources due to a variation in SMSR of the other SSGS source [7].

Manuscript received February 12, 2002; revised April 11, 2002.

The authors are with the School of Electronic Engineering, Dublin City University, Dublin 9, Ireland (e-mail: anandara@eeng.dcu.ie).

Publisher Item Identifier S 1041-1135(02)06086-X.

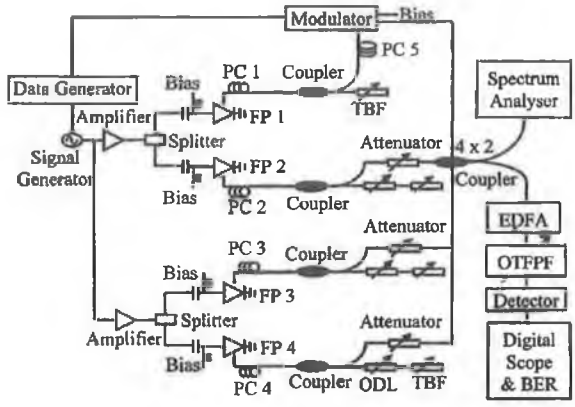

Fig. 1. Experimental setup for examining the effects of SMSR variation in a WDM system using self-seeded gain-switched pulse sources.

In this paper we experimentally investigate the system performance, by using bit-error-rate (BER) measurements, of a four-channel WDM system employing SSGS pulse sources, as the SMSR of the sources is varied. The cross channel interference due to mode-partition-noise results in significant power penalties in the system as the SMSR of the pulse sources are degraded. Our results also demonstrate that as the number of channels in a WDM system using SSGS pulse sources increases, the specifications on the required SMSR become more stringent.

II. Experimental Setup

Fig. 1 shows our experimental setup. The FP lasers used were commercial 1.55-μm InGaAsP devices, with threshold currents around 20 mA, and longitudinal mode spacings of 1.1 nm. The four lasers were gain-switched by applying dc bias currents of around 25 mA in conjunction with 2.5-GHz electrical sinusoidal signals (with powers of 24 dBm), to each diode. Self-seeding of the diode FP1 was achieved by using an external cavity containing a polarization controller (PC), a 3-dB coupler, and a tunable Bragg grating with a bandwidth of 0.4 nm. The external cavities for self-seeding FP2, FP3 and FP4 contained additional tunable optical delay lines (ODL) [7].

To achieve optimum SSGS pulse generation from FP1, the grating was tuned to reflect one of the laser modes (at 1552.6 nm), and the frequency of the sinusoidal modulation was then varied ($\sim$ 2.4836 GHz) to ensure that the signal re-injected into the laser arrives at the correct time. For SSGS operation of all the other FPs 2-4, each of the Bragg gratings

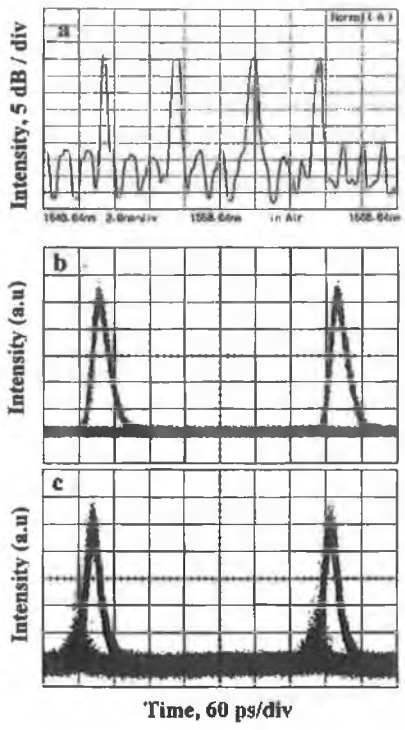

Fig. 2. (a) Optical spectrum of the composite wavelength signal after fiber coupler. (b) Back-to-back eye diagram for 1552.6 nm data channel. (c) Received eye diagram of 1552.6-nm data channel with SMSR of other pulse sources in the WDM signal set to 20 dB.

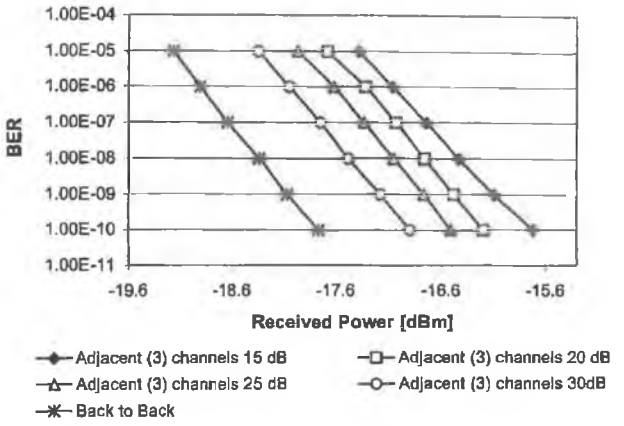

Fig. 3. BER versus received power for back-to-back case, and when the SMSR of adjacent pulse sources were set to 30, 25, 20, and 15 dB.

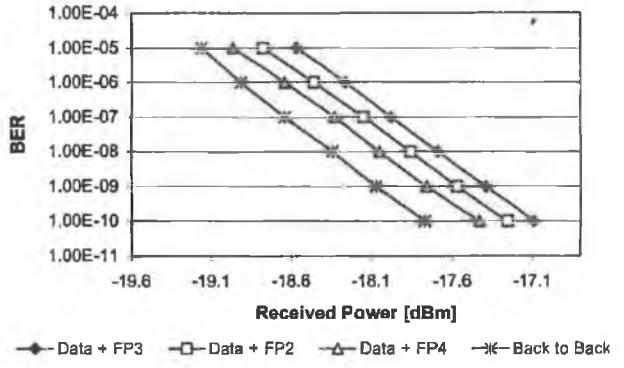

Fig. 4. BER versus received power for back-to-back case, and when data signal was multiplexed individually with each pulse source (SMSR maintained at 30 dB).

were tuned to reflect laser modes at 1544.1, 1548.1, 1556.3 nm, respectively. The ODL was varied to ensure that the signals fed back from the gratings arrive at the correct time. In addition to tuning the grating, the feedback can be adjusted, (and thus, the SMSR on the output pulses varied), by using the polarization controllers (PC) at the laser output.

A $2^{11} - 1$ pseudorandom data signal from a pattern generator, at a bit rate of 2.5 Gb/s, was then used to modulate the 1552.6-nm pulse train. The resulting 2.5-Gb/s RZ data signal from the modulator was then coupled together with the other three pulse trains with the aid of a 4×2 fiber coupler. The other three pulse train signals were attenuated before the coupler to ensure that the power level in each wavelength signal was the same after the coupler. The composite signal was then amplified before the 1552.6-nm data signal was filtered out using a tunable filter with a bandwidth of 0.7 nm. The received data signal was then detected using a 50-GHz p-i-n photodiode, before a 50-GHz oscilloscope was used to examine the received eye diagrams, and an error analyzer was used for BER measurements.

III. Results

Fig. 2(a) displays the optical spectrum of the composite signal after being combined together using the fiber coupler, (with the feedback from the gratings optimized using the polarization controllers). The 3-dB bandwidth of the 2.5-GHz pulse sources varied from 0.2 to 0.3 nm, and the pulse width varied from about 18 to 26 ps (measured using oscilloscope and deconvolution with response time of measurement setup). The optimized SMSR of each source was about 30 dB.

Fig. 2(b) displays back-to-back eye diagram of the 1552.6-nm data signal (when the three adjacent pulse sources were momentarily turned off). To determine the effect of SMSR variations on the four-channel WDM system, we proceeded to vary the SMSR of the adjacent pulse sources using the PCs, while the optical filter was tuned to select out the 1552.6-nm data channel (which had maximum SMSR $\sim$ 30 dB maintained throughout). Fig. 2(c) displays one of the results, and is the received eye diagram (of 1552.6-nm data channel) when the SMSR of the three pulse sources were set to 20 dB. The increased noise of the eye diagram in comparison with Fig. 2(b) can be clearly seen.

As the SMSR of the three pulse sources were varied in the experimental arrangement, measurements of the BER versus received optical power, for the 1552.6-nm data channel were recorded. Fig. 3 displays BER vs. received power curves for the back-to-back case, and when the SMSR of the three pulse sources in the WDM signal, were set to 30, 25, 20, and 15 dB. The power penalty introduced by each of these settings was 0.9, 1.3, 1.6, and 2 dB, respectively. We then examined the effect of multiplexing the 1552.6-nm data channel with each one of the pulse sources individually, with the SMSR of the pulse source maintained at 30 dB. As we can see from Fig. 4, the power penalty presented due to the introduction of one source, with a SMSR of 30 dB, can vary from 0.3 to 0.7 dB, for a BER of 10^{-9}.

IV. Discussions and Conclusion

The degradation in BER of the 1552.6-nm data signal as we introduce additional wavelength channels, and reduce the SMSR of these pulse sources, is due to the mode partition effect [8], [9]. This effect is basically a fluctuation of the energy in each laser mode with time, due to a constant transfer of energy between the modes. For a single-mode laser with a large SMSR, the power in the sidemodes is negligible, thus the power fluctuation of the main mode is negligible. However, as the SMSR decreases the power fluctuation of the main mode, and the sidemodes, may become nonnegligible.

With the optical filter tuned to select out the 1552.6-nm data signal, if the SMSR of the adjacent pulse soures is so large that the fluctuation in power of their sidemodes (around 1552.6 nm) is negligible, then there will be no power penalty for the received data signal. However, as the SMSR of the adjacent channels is degraded, the system performance decreases, due to the increased fluctuation in power of the sidemodes (as presented in Fig. 3). The overall power penalty experienced for the WDM system is due to the cumulative effect of the power fluctuation in the sidemodes, which are at the same wavelength as the filtered data signal. Table I displays the power penalties introduced (relative to back-to-back measurement) as the 1552.6-nm data channel is multiplexed with the various combinations of the three pulse sources (which have their SMSR maintained at 30 dB). Clearly as the number of channels increases, so does the power penalty, however the increase in power penalty is determined by which of the sources are multiplexed with the data channel. This is because the FP lasers used to generate the pulses have different gain curves. The result of this is that even though the SMSR of all the sources is maintained at 30 dB, the powers in the sidemode, which lies at the same wavelength as the data signal (and cause the power penalty), are different for each pulse source. This effect is clearly seen by examining the system performance introduced when the data signal is multiplexed with just one source (Fig. 4). The degradation in system perfomance in this case is dependent on which pulse source is multiplexed with the data (due to the different gain curves of the lasers). By examining the spectra from the three different pulse sources, we can determine the difference in power levels between the sidemode of each source at the wavelength of the data signal (1552.6 nm), and the power level in the data signal. The relative differences are 31.9 dB, 33.6 dB, and 35.3 dB for sources FP3, FP2, and FP4 respectively. We can thus see from these values, and from Fig. 4, that as the difference in power level between the data signal and the sidemode of the multiplexed source at the data signal wavelength decreases, the power penalty in the system increases, as expected.

In conclusion, we have shown how the SMSR of wavelength tunable SSGS pulse sources affects the performance of WDM communication systems which employ such sources. As the SMSR of one or more sources in a WDM system becomes degraded, then the interaction of the mode partition effect with spectral filtering will result in increased noise on all the received wavelength channels in the system. This additional noise introduces a power penalty into the overall system performance. In addition, as the number of channels in a WDM system using SSGS sources increases, the minimum required SMSR of each source, such that it does not affect system performance, will increase.

TABLE I
Power Penalties Relative to Back-to-Back Measurement, as 1552.6 nm Data Channel is Multiplexed With all Combinations of the Three Pulse Sources (SMSR Maintained at 30 dB).

Data Signal Multiplexed with pulse source :	Power Penalty Introduced (dB)
FP2	0.5
FP3	0.7
FP4	0.3
FP2 + FP3	0.8
FP3 + FP4	0.7
FP2 + FP4	0.6
FP2 + FP3 + FP4	1.0

References

[1] R. Ludwig, U. Feiste, E. Dietrich, H. G. Weber, D. Breuer, M. Martin, and F. Küppers, "Experimental comparison of 40 Gbit/s RZ and NRZ transmission over standard single mode fiber," *Electron. Lett.*, vol. 35, pp. 2216–2218, 1999.

[2] C.-K. Chan, K. L. Sherman, and M. Zirngibl, "A fast 100-channel wavelength-tunable transmitter for optical packet switching," *IEEE Photon. Technol. Lett.*, vol. 13, pp. 729–731, July 2001.

[3] T. Morioka, H. Takara, S. Kawanishi, O. Kamatani, K. Takiguchi, K. Uchiyama, M. Saruwatari, H. Takahashi, M. Yamada, T. Kanamori, and H. Ono, "1 Tbit/s (100 Gbit/s times 10 channel) OTDM/WDM transmission using a single supercontinuum WDM source," *Electron. Lett.*, vol. 32, pp. 906–907, 1996.

[4] L. P. Barry, R. F. O' Dowd, J. Debeau, and R. Boittin, "Tunable transform limited pulse generation using self-injection locking of a FP laser," *IEEE Photon. Technol. Lett.*, vol. 5, pp. 1132–1134, Oct. 1993.

[5] C. Shu and S. P. Yam, "Effective generation of tunable single- and multi-wavelength optical pulses from a Fabry–Pérot laser diode," *IEEE Photon Technol. Lett.*, vol. 9, pp. 1214–1216, Sept. 1997.

[6] L. P. Barry and P. Anandarajah, "Effect of side mode suppression ratio on the performance of self-seeded, gain-switched optical pulses in lightwave communications systems," *IEEE Photon Technol. Lett.*, vol. 11, pp. 1360–1363, Nov. 1999.

[7] ——, "Cross-channel interference due to mode partition noise in WDM optical systems using self-seeded gain-switched pulse sources," *IEEE Photon Technol. Lett.*, vol. 13, pp. 242–244, Mar. 2001.

[8] N. H. Jensen, H. Olesen, and K. E. Stubkjaer, "Partition noise in semiconductor lasers under CW and pulsed operation," *IEEE J. Quantum Electron.*, vol. 23, pp. 71–79, Jan. 1987.

[9] D. Curter, P. Pepeljugoski, and K. Y. Lau, "Noise properties of electrically gain-switched 1.5 μm DFB lasers after spectral filtering," *Electron. Lett.*, vol. 30, pp. 1418–1419, 1994.

Multiple RF Carrier Distribution in a Hybrid Radio/Fiber System Employing a Self-Pulsating Laser Diode Transmitter

A. Kaszubowska, L. P. Barry, and P. Anandarajah

***Abstract*—A self-pulsating laser diode is used to generate a multicarrier microwave optical signal for use in a hybrid radio/fiber system. The self-pulsation frequency of the laser is controlled by external light injection, and can be varied between 14–24 GHz. The hybrid radio/fiber system, employing the self-pulsation laser, is used to distribute two 155–Mb/s data signals on two radio frequency (RF) carriers (at 18.5 and 18.9 GHz). Experimental results show the overall system performance for both RF channels, and demonstrate that the performance is improved by around 17 dB compared with the case when the laser is used without external injection, and thus, does not self-pulsate.**

***Index Terms*—External light injection, microwave photonics, optical communications, optical systems, self-pulsation, semiconductor laser diode.**

I. Introduction

HIGH CAPACITY mobile networks of the future will probably use high-frequency microwave signals as the access medium (15–60 GHz), as this offers a large bandwidth for data transfer. These high-capacity microwave systems are likely to employ an architecture in which signals are generated at a central location and then distributed to remote base stations using optical fiber, before being transmitted over small areas using microwave antennas [1], [2]. Such an architecture should prove to be highly cost efficient, since it allows sharing the transmission and processing equipment (remotely located in the central control station) between many base stations. It is also expected that these broad-band mobile networks will divide the available transmission bandwidth into a number of RF channels for broadcasting data "over the air." This use of multiple carrier distribution is normally required in high-capacity multipath environments in order to overcome multipath fading effects.

On the transmission side of a radio-over-fiber distribution network it is necessary to generate the microwave optical data signal using semiconductor laser diodes. The simplest technique available to generate optical microwave signals involves direct modulation of the laser with the microwave data carriers. However, the limited bandwidth of laser diodes means that we are normally unable to use high frequency RF carriers (>10 GHz). One possible solution is to use active mode locking of a laser diode cleaved to an appropriate length such that resonant enhancement of the microwave signals may be achieved with direct modulation [3]. However, this technique requires specially designed devices that only operate at specific frequencies. Another technique to overcome the limited bandwidth of laser diodes is to employ external optical injection into the laser, as this can greatly increase the intrinsic modulation bandwidth of the diode [4], [5]. In addition, at high injection levels, the laser can start to self-pulsate at frequencies that are suitable for RF transmission, thus making the device useful for the generation of microwave optical signals in hybrid radio/fiber networks [6], [7]. In a previous letter, we showed that the performance of a single channel radio-over-fiber system can be enhanced by using this external injection technique [8]. In this letter, we characterize the self-pulsation in the laser under external injection locking conditions, and demonstrate how the injection-locked commercial laser may be employed in a hybrid radio/fiber system for the distribution of multiple-carrier RF data signals.

Manuscript received May 23, 2002; revised July 17, 2002.

The authors are with the School of Electronic Engineering, Dublin City University, Dublin 9, Ireland (e-mail: liam.barry@dcu.ie).

Digital Object Identifier 10.1109/LPT.2002.803318.

II. Self-Pulsating Laser Characteristics

The laser diode used for the experiments is a standard multiple-quantum-well distributed-feedback (DFB) device from NEL. The laser has a threshold current of 26 mA, and an intrinsic modulation bandwidth of around 8 GHz. By injecting light from a wavelength tunable external cavity laser, at the same wavelength as the DFB emission wavelength, we significantly alter the modulation response of the device, and can achieve excellent response at frequencies from 14 to 25 GHz. The enhanced response at these frequencies is caused by the external injection inducing instability in the laser diode. The instability, in turn, results in the output power from the laser undergoing strong oscillations due to beating between the optical field components in the laser cavity [6]. Fig. 1 displays the optical spectrum from the laser when it is biased at 60 mA and the externally injected power from the external cavity laser is 5 mW. We can clearly see the modulation on the spectrum at a frequency of around 20 GHz. To further investigate the oscillation from the laser, the optical output from the laser under external injection was detected with a 50–GHz photodiode and displayed on a 50-GHz oscilloscope. Triggering was achieved by splitting the electrical signal after the detector in two, and using one of the outputs as the trigger. Fig. 1(b) displays the detected signal. We can clearly see the oscillation at a frequency of around 20 GHz, and also the significant level of noise and jitter on the signal. This noise and jitter on the oscillation from the laser is also evident in the detected electrical spectrum [Fig. 1(c)], and the broad linewidth is caused by the jitter between the DFB laser diode and the tunable cavity

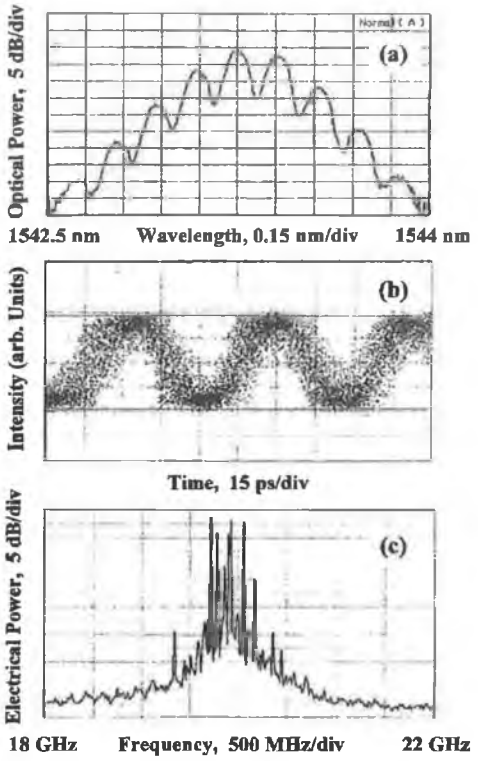

Fig. 1. (a) Optical spectrum. (b) Detected output power oscillation. (c) Electrical power spectrum of DFB laser biased at 60 mA with external injection level of 5 mW.

laser. The frequency of the oscillation from the injection-locked laser depends on the strength of the injected optical signal [6], and Fig. 2 displays how the oscillation frequency varies as a function of the injected power level. In addition, by measuring the peak-to-peak voltage of the oscillation on the oscilloscope, we have been able to determine that the optical output from the laser is 100% modulated.

III. Multicarrier Radio-Over-Fiber Setup

As we have stated in the introduction, future broad-band RF networks will require multicarrier microwave systems to overcome multipath fading. It will be necessary for optically fed microwave systems employing self-pulsing laser diodes to be capable of handling multiple RF carrier data signals. To demonstrate this, we have used the experimental arrangement described in Fig. 3. A 155-Mb/s nonreturn-to-zero (NRZ) data stream from an Anritsu pattern generator is initially passed through a 117-MHz low-pass filter to minimize the bandwidth of the electrical data signal, and then split in an RF coupler. The two signals are subsequently propagated through cables with a length difference of 1.5 m in order to ensure that there is no correlation between the two data channels. One of the two data streams is then mixed with an 18.5-GHz RF carrier, and the second data stream is mixed with an 18.9-GHz RF carrier, resulting in two binary phase-shift keyed (BPSK) data signals. The RF data signals are then combined together, and the resulting multicarrier microwave data signal is used to directly modulate the DFB laser diode described above. The

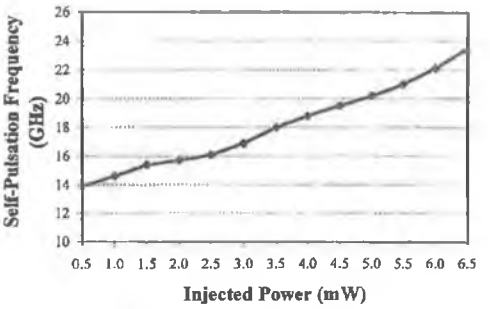

Fig. 2. Self-pulsation frequency from externally injected DFB laser as a function of injected power level.

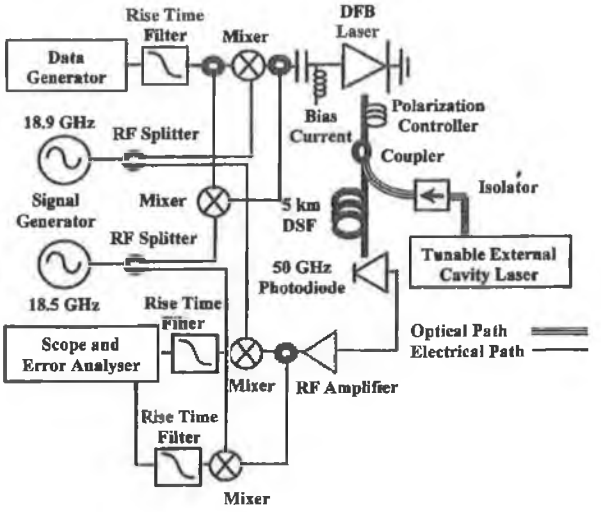

Fig. 3. Experimental set up for multicarrier hybrid radio/fiber system using self-pulsating laser diode.

data signal comprising two RF carriers can be applied either to the free-running laser or to the laser diode into which light is injected from the tunable external cavity laser. In both cases, the RF data signal is combined with a dc bias current of 60 mA. The resulting optical microwave data signal from the laser is then passed through 5 km of dispersion-shifted fiber before being detected with a 50-GHz p-i-n photodiode. In a complete radio/fiber system, the detector output would be transmitted through an RF antenna to the mobile stations, however, in our experiment we have concentrated on the optical part of the system. Hence, the down conversion of the two RF carrier data signals takes place after the photodiode. To recover the two data channels simultaneously, the detected signal is split in two. One of the signals is then down converted by mixing it with the 18.5-GHz local oscillator, and the second signal is down converted by mixing it with the 18.9-GHz local oscillator. The two down-converted signals are subsequently passed through low-pass filters to ensure that only the required baseband signal is examined using the 50-GHz oscilloscope and error analyzer. Using the oscilloscope, we are able to characterize the received eye diagrams of the two 155-Mb/s data signals, and with the Anritsu error analyzer we can determine the bit-error rate (BER) of the received signals.

Fig. 4(a) displays the received eye diagrams (displayed simultaneously on the oscilloscope) of the two down-converted

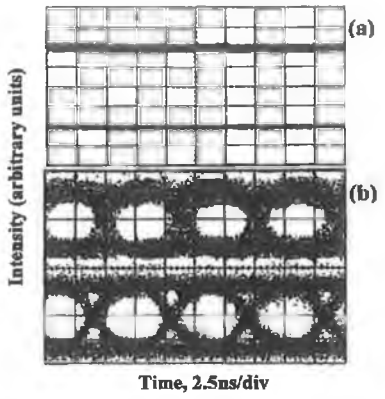

Fig. 4. Received eye diagrams of the two 155-Mb/s data signals from the optically fed microwave system using (a) free running laser diode and (b) laser diode with the external injection level of 4 mW. Received optical power (before photodiode) was −9 dBm in both cases.

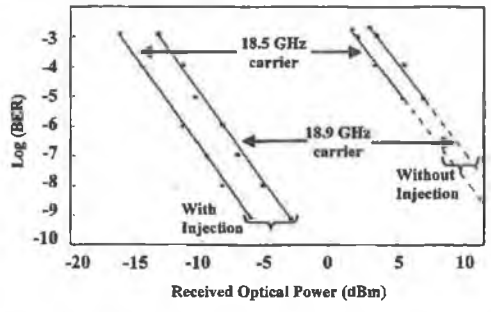

Fig. 5. BER versus received optical power for the two RF data channels using directly modulated laser with and without external injection.

155-Mb/s data signals after propagation through the optical microwave link using the DFB laser with no external light injection. The detected average optical power is −9 dBm. As we can see, because the response of the laser is so poor at frequencies around 18 GHz, the received eye diagrams are completely closed. We then proceeded to inject light into the DFB laser from the wavelength tunable external cavity laser at the same wavelength as the DFB emission wavelength. The injection level is set to around 4 mW, as this is the power level that optimizes the modulation response of the laser at the frequencies of the microwave data signal. Fig. 4(b) displays the simultaneously received eye diagrams with a detected optical power of −9 dBm. The eyes are clearly open for both data channels, demonstrating good system performance. By varying the detected optical power level using an optical attenuator, and measuring the BER of the received signals, we can plot system performance against received optical power, both with and without the external injection. Fig. 5 shows that the external injection improves the overall performance of the system by around 17 dB for each RF data channel. The difference in performance for the two RF data channels is mainly due to the different synthesizers used for the 18.5 and 18.9-GHz carriers.

The RF powers in the two data signals applied to the laser are around −12 dBm. At these low power levels, the laser does not tend to completely lock to either of the data signals applied. However, the small-signal modulation response of the self-pulsating laser does show greatly enhanced performance over a significant bandwidth [similar to that shown in Fig. 1(c)], and it is this enhanced response that improves the performance of the multicarrier system. On the issue of crosstalk, interchannel crosstalk between the data signals is negligible, as the 400-MHz channel spacing is sufficiently larger than the 117-MHz bandwidth of the data signals. In addition, crosstalk due to fiber nonlinearity, which is predominantly caused by four-wave-mixing in subcarrier multiplexing (SCM) systems with low data-rate per channel and narrow channel spacing [9], can be neglected thanks to the small number of channels and low optical power launched in the fiber (−4 dBm). However, as the channel spacing is further reduced to improve spectral efficiency, and the number of channels and launched power is further increased, it will be important to investigate degradations in system performance due to crosstalk in more detail.

IV. Conclusion

We have demonstrated the use of a self-pulsating laser diode (achieved using external injection into a commercial DFB laser) for the distribution of multicarrier RF data signals in a hybrid radio/fiber communication system. As the frequency of the self-pulsation is determined by the external injection level, we can vary the set up to operate in different frequency bands. Our results show that we can successfully modulate the self-pulsating laser with two RF data signals simultaneously, giving us a 17-dB improvement in system performance, for each RF data channel, above what would be achieved using the laser diode without external light injection. In future work, we intend to investigate how intermodulation distortion will effect the performance of a multicarrier hybrid radio/fiber system using self-pulsating laser transmitters, however, our initial work has demonstrated that such a scheme may be feasible for the development of broad-band microwave communication systems.

References

[1] R. P. Braun, G. Grosskopf, H. Heidrich, C. von Helmolt, R. Kaiser, K. Kruger, U. Kruger, D. Rohde, F. Schmidt, R. Stenzel, and D. Trommer, "Optical microwave generation and transmission experiments in the 12- and 60-GHz region for wireless communications," *IEEE Trans. Microwave Theory Tech.*, vol. 46, pp. 320–330, Apr. 1998.

[2] Z. Ahmed, D. Novak, R. B. Waterhouse, and H.-F. Liu, "37-GHz fiber-wireless system for distribution of broad-band signals," *IEEE Trans. Microwave Theory Tech.*, vol. 45, pp. 1431–1435, Aug. 1997.

[3] J. B. Georges, M.-H. Kiang, K. Heppell, M. Sayed, and K. Y. Lau, "Optical transmission of narrow-band millimeter-wave signals by resonant modulation of monolithic semiconductor laser," *IEEE Photon. Technol. Lett.*, vol. 6, pp. 568–570, Apr. 1994.

[4] G. Yabre, "Effect of relatively strong light injection on the chirp-to-power ratio and the 3 dB bandwidth of directly modulated semiconductor lasers," *J. Lightwave Technol.*, vol. 14, pp. 2367–2373, 1996.

[5] X. J. Meng, T. Chau, and M. C. Wu, "Experimental demonstration of modulation bandwidth enhancement in distributed feedback lasers with external light injection," *Electron. Lett.*, vol. 34, pp. 2031–2032, 1998.

[6] T. B. Simpson and F. Doft, "Double locked laser diode for microwave photonic applications," *IEEE Photon. Technol. Lett.*, vol. 11, pp. 1476–1478, Nov. 1999.

[7] O. Frazao, P. Tavares, J. F. da Rocha, and L. B. Ribeiro, "Tunable optical oscillator based on a DFB-MQW laser and a fiber loop reflector," *IEEE Trans. Ultrason., Ferroelect., Freq. Contr.*, vol. 46, pp. 1341–1342, Nov. 1999.

[8] A. Kaszubowska, P. Anandarajah, and L. P. Barry, "Hybrid radio/fiber distribution system based on a directly modulated laser transmitter with external injection," *IEEE Photon. Technol. Lett.*, vol. 14, pp. 233–235, Feb. 2002.

[9] R. Hui, B. Zhu, R. Huang, C. T. Allen, K. R. Demarest, and D. Richards, "Subcarrier multiplexing for high-speed optical transmission," *J. Lightwave Technol.*, vol. 20, pp. 417–427, 2002.